KUVEMPU UNIVERSITY

ELECTROCHEMICAL INVESTIGATION OF SOME BIOACTIVE MOLECULES AT CHEMICALLY MODIFIED ELECTRODE

A Thesis submitted to the Faculty of Science
Kuvempu University

For the award of Degree of

DOCTOR OF PHILOSOPHY

In

CHEMISTRY

By

Mr. DEEPAK M. P. M.Sc.,
Research Scholar
Department of Post Graduate Studies and Research in Chemistry,
Kuvempu University, Shankaraghatta-577451, Shimoga
Karnataka, India

Guide
Dr. G. P. Mamatha M.Sc., Ph.D.,
Professor
Department of Pharmaceutical Chemistry
Kuvempu University,
P.G. Centre Kadur-577 548,
Karnataka, India

OCTOBER - 2015

Dedication

I dedicate this thesis to my beloved parents, brothers, sister and Teachers for their love, support, encouragement and understanding throughout my Ph.D. work

KUVEMPU UNIVERSITY

Deepak M. P. M.Sc.
Research Scholar

Department of Post Graduate Studies and Research in Chemistry
Shankaraghatta-577 451,
Shimoga, Karnataka, India
Email: mpdeepak1988@gmail.com
Phone- 8197719862

DECLARATION

I hereby declare that the matter embodied in the thesis entitled "**ELECTROCHEMICAL INVESTIGATION OF SOME BIOACTIVE MOLECULES AT CHEMICALLY MODIFIED ELECTRODE"** is the result of investigations carried out by me, under the supervision of **Dr. G. P. Mamatha,** Department of Pharmaceutical Chemistry, Kadur, P.G. Centre, Kuvempu University.

I further declare that the results presented in the thesis or any part there of has not been submitted for the award of any degree/associateship/fellowship of this University or any other higher education institution. To the best of my knowledge and belief, the thesis contains no materials previously published or written by another person except where due reference is made.

Date: 05.10.2015
Place: Shankaraghatta

KUVEMPU UNIVERSITY

Dr. G.P.Mamatha M.Sc, Ph.D.
Professor
Department of Pharmaceutical Chemistry
Email: mamatha_gp2005@rediffmail.com
Kuvempu University,
P.G. Centre, Kadur – 577 548
Karnataka, India

Phone: +91 9448422903(Cell)
+91 8267 231512 (Off)

CERTIFICATE

This is to certify that the thesis entitled "**Electrochemical Investigation of Some Bioactive Molecules at Chemically Modified Electrode"** submitted by **Mr. Deepak M.P.** to the Faculty of Science, Kuvempu University, Shankaraghatta 577451, Shimoga, Karnataka, India for the award of the degree of **Doctor of Philosophy in Chemistry** is the result of the original work carried out by him under my guidance. I further declare that the work embodied in this thesis has not previously formed the basis for the award of same degree /associateship/fellowship of this University or any other higher education institution.

Date: 5/10/2015
Place:

(Dr. G.P.Mamatha)
Dr. MAMATHA G. P., M.Sc.,Ph.D.
Professor
Dept. of Pharmaceutical Chemistry
Kuvempu University
P.G. Centre, Kadur-577 548

Acknowledgements

I strongly believe that the completion of this thesis was possible because of my Parent's and my guide. This thesis would never have materialised without the contribution of many individuals to whom I have the pleasure of expressing my appreciation and gratitude. I apologize in advance for any omissions for any they are purely unintentional.

I oblige my deepest sense of gratitude to my respected guide **Dr. G.P. Mamatha**, Professor, Department of Pharmaceutical Chemistry, Post Graduate Centre, Kuvempu University, Kadur, for accepting me as part of her research group and introducing me to this research field which made my Ph.D. work a memorable experience, for her academic guidance, support in organizing my ideas and putting together a very fine piece of work throughout my research work. Her passion for Chemistry and an enthusiastic vision of the world helped to shape my academic interests and positively influenced other aspects of my life as a Research Scholar. Without her, I would never have reached this point! Thanks a lot for making my dreams come true! I am really beholden for her invaluable suggestions and timeless advice and support throughout my Ph.D. work. Words cannot express how much I appreciate your guidance and support

I am highly grateful to **Prof. Jogan Shankar,** Vice-Chancellor, Kuvempu University for giving me, an opportunity to pursue my dreams. His encouragements and constant support especially for providing the necessary facilities helped me to make this thesis a better one. Thank you sir for the opportunity given to me to do research in Kuvempu University.

I would like to show my gratitude to **Prof. Y. Arthob Naik,** Chairman, Department of Chemistry, Kuvempu University, Shankaraghatta, for undertaking the unenviable task of serving on my thesis committee, I am indebted for his valuable contributions and suggestions that shaped this thesis and helped to make it better.

I am very thankful to the Faculty members of the Department of Chemistry, Kuvempu University, Shankaraghatta, Shimoga, Karnataka, India, **Prof. J. Keshavayya, Prof. T.V. Venkatesha, Prof. K.M. Mahadevan, Prof. V.P. Vaidya, Prof. P. Vasudeva Nayak,** Department of Chemistry, Kuvempu University**, Dr. Ashok R. Lambani, Prof. H.S. Jayanna, Dr. J. Sannappa,** Department of Physics, Kuvempu University, **Dr. N.D. Satyanarayana,** Department of Pharmaceutical Chemistry, P.G. Kadur, Kuvempu University with whom I had an opportunity to interact with during my research work. Their guidance and support helped me, to mature as a researcher and influenced the work I did in this thesis. Thanks a lot for your unconditional support and a never ending patience.

I am also grateful to my friend **Mr. G. Pradeep,** for his unrestricted support in my Ph.D. work. You made my research work simple by providing well-timed help throughout my Ph.D. work, thank you very much.

I must thanks to **Mrs. Madhuramma**, HOD, Department of Chemistry, AVK Woman's College, Davangere, Karnataka, India for affording me the use of their equipment and lab facilities to carry out my research work and their loyal attitudes as well as the practical support helped me to feel comfortable in the lab.

I would like to express my sincere thanks to all my brothers and friends past and present in particular **Mr. M.P. Rajeeva, Mr. C.S. Naveen, Mr. S. Chaturmukha, Mr. B.S. Avinash, Mr. D.R. Rangaswamy, Mr. T.O. Shrungesh Kumar, Mr. D. Thippeswamy, Mr. Vasanth Kumar and Mr. H.M. Santhosh** for the input they provided during numerous formal and informal discussions we had. Their continuous interest in my research, their jokes and occasional criticism provided a fresh perspective on my work, helped me to keep a positive outlook and reinstated my confidence when it was needed. Thanks a lot for your countless help and support during my Research work in Kuvempu University.

I would like to thank my beloved parents **Mr. Puttaswamy** and **Mrs. Savithramma** for teaching me the value of education, supporting and

believing in me for the entire period of my studies. I sincerely appreciate their efforts and sacrifices that they made so that I could have the education. They, along with my dear brothers and my sister have been there for me when I was stressed, worn out, and needing encouragement. The love, patience, and encouragement they showed through my entire life and throughout the period of my Research work have brought me a long way in my life. They always believed in me and stood by me. This thesis would never have been completed without the continuous support I received from them. With all my love I thank you all for your patience and encouragement.

I would like to thank the non-teaching staffs of the Department of Chemistry for their support and encouragement throughout my research work. I am also very grateful to Kuvempu University library for providing me with the library facilities during the course of my research work.

Lastly, I offer my regards and blessings to all of those who supported me in any respect during the completion of my thesis.

Deepak M. P……✍

List of Abbreviation

AA	=	Ascorbic acid
ABS	=	Acetate buffer solution
AE	=	Auxiliary electrode
ASV	=	Anodic stripping voltam
AgCl	=	Silver Chloride
BCPE	=	Bare carbon paste electrode
CE	=	Counter electrode
CPE	=	Carbon paste electrode
CMEs	=	Chemically modified electrodes
CMCPEs	=	Chemically modified carbon paste electrode
CNS	=	Central nervous system
CE	=	Chemical-Electrochemical
C_o^*	=	Concentration
C_{ox}	=	Concentration of oxidised species
C_{red}	=	Concentration of reduced species
CIP	=	Ciprofloxacin hydrochloride
CV	=	Cyclic voltammetry
DA	=	Dopamine
DCE	=	Dropping carbon electrode
DME	=	Dropping mercury electrode
DICY	=	Dicyclomine hydrochloride
D_0	=	Diffusion coefficient
DPV	=	Differential pulse voltammetry
E_i	=	Initial applied potential
E_v	=	Vertex potential
E_f	=	Final potential
E_{pa}	=	Anodic peak potential
E_{pc}	=	Cathodic peak potential
E^o	=	Formal potential

ENRO	=	Enrofloxacin
FUR	=	Furosemide
F	=	Faraday Constant
INH	=	Isoniazid
I_{pa}	=	Anodic peak current
I_{pc}	=	Cathodic peak current
Ed(s)	=	Editors
Ed(ed)	=	Edition
ENRO	=	Enrofloxacin
ET	=	Electron Transfer
FSCV	=	Fast scan cyclic voltammetry
G	=	Gibb's free energy
GC	=	Glassy carbon
GI	=	Gastrointestinal
HOPG	=	Highly oriented pyrolytic graphite
5-HT	=	5-hydroxytryptamine
IPE	=	Ideally polarisable electrode
K_0	=	Heterogeneous rate constant
LSV	=	Linear sweep voltammetry
LTY	=	L-Tyrosine
MCPE	=	Modified carbon paste electrode
MWNT	=	Multiwall carbon nanotube
MSNMCPE	=	Manganese tin (IV) oxide nanoparticles modified carbon paste electrode
µA	=	Microampere
mM	=	Millimolar
mV	=	Millivolt
mVs^{-1}	=	Millivolt per second
NPP	=	Pulse polarographic techniques
NTs	=	Neurotransmitters
NSNMCPE	=	Nickel tin (IV) oxide nanoparticles modified carbon paste electrode

Ox	=	Oxidised species
PBS	=	Phosphate buffer solution
PC	=	Personal computer
PMEs	=	Polymer modified electrodes
Pt	=	Platinum
R	=	Gas Constant
RE	=	Reference electrode
Rs	=	Solution resistance
S	=	Entropy
SCE	=	Saturated calomel electrode
SEM	=	Scanning electron microscope
SHE	=	Standard hydrogen electrode
SIDS	=	Sudden infant death syndrome
SWV	=	Square wave voltammetry
TEA	=	Tetra-ethyl ammonium
TBA	=	Tetra-n-butyl ammonium
TBS	=	Terbutaline Sulphate
UA	=	Uric acid
UV/VIS	=	Ultra/Visible Spectrophotometer
υ	=	Scan rate
$\upsilon^{1/2}$	=	Square root of scan rate
WE	=	Working electrode
XRD	=	X-ray diffraction

SUMMARY OF THE THESIS

The focus of the work covered in this thesis was to study the electrochemical properties of Bioactive molecules such as Dicyclomine hydrochloride (DICY), L-Tyrosine (LTY), Ciprofloxacin hydrochloride (CIP), Dopamine (DA), Uric acid (UA), Ascorbic acid (AA) and Enrofloxacin (ENRO) at bare carbon paste electrode and at modified carbon paste electrode (MCPE) by voltammetric techniques. This thesis also discusses the different types of modifications. The following aspects like, number of electrons involved in the electrochemical reaction, reaction mechanisms and nature of electrode processes were observed.

The work carried out in this thesis is divided and described into seven chapters.

Chapter-1

Introduction, Review of Cyclic Voltammetry and Theoretical Considerations

This chapter involves the introduction, a brief historical preview of voltammetry and voltammetric techniques basics and fundamental principles and theoretical aspects and application of voltammetry. A brief review of cyclic voltammetric investigation of some bioactive molecules has been presented. Objective and scope of the present work is included in this chapter.

Chapter-2

Experimental

This chapter describes the basic equipment need for electrochemistry such as potentiostat, a recording device and an electrochemical cell. This chapter also includes the basic experimental setup of voltammetry, Instrumentation, devices, the electrode systems with special emphasis on carbon paste electrode, experimental techniques and procedures used in the present work, modified and unmodified carbon paste electrode some practical aspects of preparation of modified carbon paste electrode and its characterization were described in detail.

Chapter - 3

This Chapter is subdivided into two parts: Part 3A and Part 3B

Part - 3A:

Electrochemical Investigation of Dicyclomine Hydrochloride at Poly (Terbutaline sulphate) Modified Carbon Paste Electrode

In this chapter, a poly (Terbutaline Sulphate) modified carbon paste electrode (PTBSMCPE) was fabricated by electropolymerisation method to investigate the electrochemical behavior of dicyclomine hydrochloride (DICY) in phosphate buffer solution by cyclic voltammetric technique. The surface morphology of PTBSMCPE studied by scanning electron microscope (SEM). The modified electrode showed very good sensitivity. Well defined and discrete voltammetric oxidation peak was observed compare to bare CPE. The effect of pH, concentration and scan rate was also studied. Increase of dicyclomine hydrochloride concentration showed linear increase in oxidation peak currents. The linear relationship between oxidation peak current and DICY concentration was obtained in range 0.01mM to 1mM with correlation coefficient of 0.9944. The low detection limit (LOD) and low detection quantification (LOQ) were 0.12 µM and 0.406 µM respectively. The differential pulse voltammetric technique (DPV) was also shows the linear increase in current with increase in concentration of DICY. The preparation of the modified electrode is very easy, renewed by simple polishing gives very good reproducibility, high stability in its voltammetric response and low detection limit for dicyclomine hydrochloride.

Part - 3B:

Electrochemical Behavior of L-Tyrosine at Poly (Dicyclomine Hydrochloride) film Modified Carbon Paste Electrode: A Cyclic Voltammetric Study

In this chapter an electrochemical method for the determination of L-tyrosine (LTY) was developed using a dicyclomine hydrochloride (DICY) polymer film modified carbon paste electrode. The surface morphology of poly (dicyclomine hydrochloride) film modified carbon paste electrode was characterized by SEM. The

modified electrode showed excellent electro catalytic activity towards the oxidation of LTY compare to bare carbon paste electrode (BCPE) in 0.1 M phosphate buffer solution of pH 6.5. The effect of pH, concentration and scan rate were studied at the bare CPE and PDICYMCPE was investigated. Increase of LTY concentration shows linear increase in oxidation peak current. The linear relationship was obtained between the anodic peak current (I_{pa}) and concentration of LTY in range 2×10^{-5} M to 1×10^{-3} M with correlation coefficient of 0.9984. The low detection limit (LOD) and low quantification limit (LOQ) of LTY were 0.638 µM, 2.128 µM respectively. The cyclic voltammetric studies indicated that the oxidation of LTY at the modified electrode surface was irreversible; adsorption controlled and undergoes one electron transfer process at the poly (dicyclomine hydrochloride) film modified carbon paste electrode. The modified electrode showed high sensitivity, detection limit, high reproducibility, easy preparation and regeneration of the electrode surface.

Chapter - 4

Cyclic Voltammetric Studies of Ciprofloxacin Hydrochloride at Poly (L-Tyrosine) SnO_2 nanoparticles Modified Carbon Paste Electrode

This chapter explain the influence of poly (L-Tyrosine) SnO_2 nanoparticles modified carbon paste electrode (PLTSNMCPE) for the electrochemical investigation of ciprofloxacin hydrochloride (CIP) by cyclic voltammetric (CV) and differential pulse voltammetric techniques (DPV). Before modification the SnO_2 nanoparticles were synthesized by gel combustion method, then synthesized SnO_2 nanoparticles were characterized by XRD and SEM. Then the carbon paste electrode is modified with the synthesized SnO_2 nanoparticles and L-Tyrosine by electropolymerisation method using cyclic voltammetric technique. The surface morphology of poly (L-Tyrosine) SnO_2 nanoparticles modified carbon paste electrode confirmed by scanning electron microscope (SEM). The electrochemical response of CIP was confirmed from the remarkable oxidation peak current enhancement. The electrode process of CIP was examined with all the experimental parameters such as pH, scan rate and concentration.

A linear relationship was obtained between the anodic peak current and CIP concentration in the range of 1×10^{-5} M to 1×10^{-4} M with correlation coefficient of 0.9923. The low detection limit (LOD) and low quantification limit (LOQ) at poly (L-Tyrosine) SnO_2 nanoparticles modified carbon paste electrode were found to be 0.10×10^{-7} M and 0.33×10^{-6} M respectively by cyclic voltammetric techniques. The anodic peak current of CIP increases linearly with increases in concentration of CIP by differential pulse voltammetric technique (DPV). This method was successfully applied for investigation of CIP in commercial tablet sample. Finally a sensitive and simple voltammetric method was developed for the determination of ciprofloxacin hydrochloride for pharmacological practical application.

Chapter - 5

The Simultaneous Electrochemical Determination of Dopamine and Uric acid at $Ni_{0.02}Sn_{0.98}O_2$ Nanoparticles Modified Carbon Paste Electrode by Cyclic Voltammetric Technique

This chapter describes the electrochemical method using $Ni_{0.02}Sn_{0.98}O_2$ nanoparticles modified carbon paste electrode (NSNMCPE) for the determination of dopamine (DA) and uric acid (UA). The $Ni_{0.02}Sn_{0.98}O_2$ nanoparticles were synthesized by gel combustion method. These synthesized $Ni_{0.02}Sn_{0.98}O_2$ nanoparticles were characterized by XRD and SEM. Then the carbon paste electrode is modified with the synthesized $Ni_{0.02}Sn_{0.98}O_2$ nanoparticles by grinding method. The surface morphology of NSNMCPE was confirmed by SEM. The NSNMCPE was successfully used to study the electrochemical investigation of DA and UA in 0.1 M phosphate buffer solution (PBS) of pH 7.0 and pH 6.0 by cyclic voltammetric technique (CV). DA has revealed redox peaks reversibly, whereas UA has showed only oxidation peak at bare carbon paste electrode. The nature of voltammograms obtained at bare CPE was compared with NSNMCPE.The low detection limit (LOD) of DA and UA were found to be 0.831×10^{-5} M and 1.11×10^{-5} M and the low quantification limit (LOQ) of DA and UA were 2.77×10^{-6} M and 0.371×10^{-6} M respectively. The NSNMCPE was used for the

simultaneous determination of DA and UA, the separation of the overlapping voltammograms of dopamine and uric acid at modified electrode in a mixture is successfully carried by using cyclic voltammetric technique. The proposed method was successfully applied for the determination of DA and UA due to its good sensitivity, lower detection limit and ease of preparation of the NSNMCPE allows the development of a highly sensitive voltammetric sensor for the determination of DA and UA.

Chapter - 6

Electrochemical Behavior of $Mn_{0.02}Sn_{0.980}O_2$ Nanoparticles Modified Carbon Paste Electrode and Its Application for the Determination of Dopamine, Uric acid and Ascorbic acid

In the present chapter, the $Mn_{0.02}Sn_{0.98}O_2$ nanoparticles synthesized by the gel combustion method. The synthesized $Mn_{0.02}Sn_{0.980}O_2$ nanoparticles were characterized by XRD and SEM. The $Mn_{0.02}Sn_{0.980}O_2$ nanoparticles modified carbon paste electrode (MSNMCPE) was developed by known procedure. The surface morphology of MSNMCPE was confirmed by SEM. The MSNMCPE has been optimized for the determination of dopamine (DA), uric acid (UA) and ascorbic acid (AA) at MSNMCPE by cyclic voltammetric technique in 0.1 M phosphate buffer solution of pH 7.0, pH 6.5 and pH 5.5 respectively. The effect of pH, concentration and scan rate were studied. The MSNMCPE showed very good sensitivity for DA, UA and AA compare to bare CPE. The results suggest that the nature of electrode reaction was diffusion controlled at both bare CPE and MSNMCPE. Increase of DA, UA and AA concentration shows linear increase in redox peak currents and oxidation peak current respectively. The linear relationship was obtained between the anodic peak current (I_{pa}) and concentration of DA, UA and AA in the of range 1×10^{-5} M to 1×10^{-3} M with correlation coefficient of 0.993, 0.99707 and 0.99622 respectively. The low detection limit (LOD) and low quantification limit (LOQ) of DA, UA, AA were 1.316, 0.848, 0.965 µM and 0.4389, 2.825, 3.216 µM respectively. The simultaneous determination of dopamine, uric acid and ascorbic acid, uric acid, were carried out by both cyclic voltammetric and

differential pulse voltammetric techniques. The preparation of the modified electrode was easy, renewed by simple polishing gives very good reproducibility, high stability in its voltammetric response and low detection limit for DA, UA and AA.

Chapter - 7

This Chapter is subdivided into Part 7A and Part 7B

Part – 7A:

Simultaneous Determination of Ciprofloxacin Hydrochloride and Enrofloxacin at Poly (Furosemide) Modified Carbon Paste Electrode by Cyclic Voltammetry

In this chapter, a poly (furosemide) modified carbon paste electrode (PFURMCPE) was used for the sensitive voltammetric determination of ciprofloxacin hydrochloride (CIP) and Enrofloxacin (ENRO). The surface morphology of PFURMCPE was characterized by SEM. It was found that the electrochemical behavior of the polymer film modified electrode depended on the film thickness of the polymer film. The electrochemical response of CIP and ENRO were investigated by cyclic voltammetric (CV) and differential voltammetric techniques (DPV). The effect of pH, concentration and sweep rate has been studied. The modified electrode was used for the simultaneous determination of CIP and ENRO in the PBS of pH 7.2 by CV and DPV techniques. The linear relationship was obtained between the anodic peak current (I_{pa}) and concentration of ENRO and CIP in the range of 8×10^{-5} M to 1×10^{-3} M with correlation coefficient of 0.993, 0.9915 respectively. The low detection limit (LOD) and low quantification limit (LOQ) of ENRO and CIP were 4.526, 1.335 µM and 0.4451×10^{-5} M, 1.508×10^{-5} M respectively. This modified electrode was successfully used for the simultaneous determination of CIP and ENRO by resolving the overlapped voltammetric peaks by using cyclic voltammetric technique. The modified electrode showed high sensitivity, detection limit, high reproducibility, easy preparation and regeneration of the electrode surface.

Part – 7B:

Electrochemical Investigation of Uric acid at Poly (Isoniazid) film Modified Carbon Paste Electrode

This chapter involves the electrochemical investigation of uric acid at poly (isoniazid) film modified carbon paste electrode (PINHMCPE) by cyclic voltammetry in 0.2 M phosphate buffer solution of pH 5 has been carried out. The carbon paste electrode (CPE) was modified by isoniazid showed very good sensitivity for uric acid compare to carbon paste electrode. The effect of scan rate at PINHMCPE has been studied. The linear relationship between oxidation peak current and UA concentration was obtained in range from 0.01 mM to 1 mM with correlation coefficient of 0.99442. The low detection limit (LOD) and low detection quantification (LOQ) were found to be 1.173 µM and 3.910 µM. The preparation of the modified electrode was very easy, renewed by simple polishing gives very good reproducibility, high stability in its voltammetric response and low detection limit for UA.

TABLE OF CONTENTS

CHAPTER – I

INTRODUCTION, REVIEW OF CYCLIC VOLTAMMETRY AND THEORETICAL CONSIDERATIONS

CHAPTER - II

EXPERIMENTAL

CHAPTER – III (PART - A)

ELECTROCHEMICAL INVESTIGATION OF DICYCLOMINE HYDROCHLORIDE AT POLY (TERBUTALINE SULPHATE) MODIFIED CARBON PASTE ELECTRODE

CHAPTER – III (PART - B)

ELECTROCHEMICAL BEHAVIOR OF L-TYROSINE AT POLY (DICYCLOMINE HYDROCHLORIDE) FILM MODIFIED CARBON PASTE ELECTRODE: A CYCLIC VOLTAMMETRIC STUDY

CHAPTER – IV

CYCLIC VOLTAMMETRIC STUDIES OF CIPROFLOXACIN HYDROCHLORIDE AT POLY (L-TYROSINE) SnO_2 NANOPARTICLES MODIFIED CARBON PASTE ELECTRODE

CHAPTER – V

THE SIMULTANEOUS ELECTROCHEMICAL DETERMINATION OF DOPAMINE AND URIC ACID AT $Ni_{0.02}Sn_{0.98}O_2$ NANOPARTICLES MODIFIED CARBON PASTE ELECTRODE BY CYCLIC VOLTAMMETRIC TECHNIQUE

CHAPTER – VI

ELECTROCHEMICAL BEHAVIOR OF $Mn_{0.02}Sn_{0.98}O_2$ NANOPARTICLES MODIFIED CARBON PASTE ELECTRODE AND ITS APPLICATION FOR THE DETERMINATION OF DOPAMINE, URIC ACID AND ASCORBIC ACID

CHAPTER – VII (PART - A)

SIMULTANEOUS DETERMINATION OF CIPROFLOXACIN HYDROCHLORIDE AND ENROFLOXACIN AT POLY (FUROSEMIDE) MODIFIED CARBON PASTE ELECTRODE BY CYCLIC VOLTAMMETRY

CHAPTER – VII (PART - B)

ELECTROCHEMICAL INVESTIGATION OF URIC ACID AT POLY (ISONIAZID) FILM MODIFIED CARBON PASTE ELECTRODE

LIST OF RESEARCH PAPERS PRESENTED AT INTERNATIONAL AND NATIONAL CONFERENCES / SEMINARS / SYMPOSIA / WORKSHOPS

PUBLICATIONS

Chapter-1

INTRODUCTION, REVIEW OF CYCLIC VOLTAMMETRY AND THEORETICAL CONSIDERATIONS

Ralph N.Buss Adams-Inventor of Carbon Paste Electrode

1.1 Introduction

Electrochemistry involves chemical reactions associated with charge transfer. Atoms and molecules consist of a heavy nucleus with electrons swirling around it; these electrons are the same electrons that carry electrical currents and detection of this current is the basis of the measurement method. But the electron movement happens within an extremely short distance and can't be measured unless the two parts of the reaction, the oxidation and the reduction are separated by a large (atomically speaking) distance and the two reaction sites are connected by a wire for the electrons to travel, which is the essential feature of electrochemistry. This can be achieved by two electrodes, anode and cathode separated by at least one electrolyte phase, which is merely a phase through which charge is carried by the movement of ions. At the anode, oxidation occurs, in which electrons are removed from oxidizable solution components and enter the electrode. Simultaneously, the cathode, in reduction processes, gives up electrons to reducible solution components [1]. Hence, electrochemistry can be seen as the relationship between electricity and chemistry, namely the measurement of electric quantities, such as current, potential and charge and their relationship to chemical parameters. These chemical reactions involving the transfer of electrons to and from a molecule or ion are often referred to as redox (reduction/oxidation) reactions. The use of electrochemistry for analytical purposes has found a wide range of applications in industrial quality control, metallurgy, geology, pharmacy, medical chemistry, biomedical analysis and environmental monitoring [2].

Electrochemical processes by their nature are all heterogeneous reactions which occur in the interfacial region either in solution or immobilized at the electrode surface. Since one is dealing with a very small amount of material on the electrode surface, the kinetics of this heterogeneous process can be significantly affected by the microstructure and roughness of the electrode surface, the blocking of active sites on the electrode surface by adsorbed materials, and the nature of the functional groups (e.g., oxides) present on the electrode surface [3, 4]. Hence the study of the chemically modified electrodes (CMEs) has evolved as a field of high activity. In detail, the chemically modified electrodes comprise an approach to

electrode system design that finds the use in a wide spectrum of basic electrochemical investigations, including a better insight into the nature of charge transfer and charge transport processes in thin films and the design of electrochemical devices and systems for applications in chemical sensing, energy conversion and storage, molecular electronics, electrochromic displays and electro-organic synthesis. The applicability of these CMEs is wide-ranging, in the field of bioactive active molecules of biological interest.

Electrode surfaces may be modified in many ways to get better catalytic effects or some other desirable effect not obtainable at the classical electrode materials. Modified electrodes can be prepared by several different methods such as polymer-coated, electropolymerised, physically adsorb, covalently attached to the electrode surface and functionalized electrodes. Carbon was the chosen surface, for the modification as it is highly conducting with a wide potential window, structurally stable, relatively inexpensive and stable layers of modifiers can attach to the surface in a controllable manner. There are many different forms of conducting carbon materials including glassy carbon (GC), highly oriented pyrolytic graphite (HOPG), pyrolysed photoresist film (PPF), carbon nanotubes, carbon powder, screen printed carbon, carbon fibres, carbon nanocapsules, fullerene and carbon composites [5]. Carbon paste electrodes (CPEs) belong to a special group of heterogeneous electrodes [6-8]. CPEs are represented by carbon paste, i.e. a mixture prepared from carbon (graphite) powder and a suitable liquid binder packed into a suitably designed electrode body [9, 10].

The focus of the work covered in this thesis was to study the electrochemical properties of bioactive compounds such as Dicyclomine Hydrochloride (DICY), Ciprofloxacin Hydrochloride (CIP), L-Tyrosine (LTY), Dopamine (DA), Uric acid (UA), Ascorbic acid (AA), Enrofloxacin (ENRO) at modified carbon paste electrodes (CPEs) by voltammetric techniques.

1.2. Voltammetry

Electrochemical methods are classified into 3 general classes viz. Voltammetry, Potentiometry and Coulometry. Voltammetry is a class of

electroanalytical methods used in analytical chemistry wherein, information about an analyte is obtained by the measurement of current that result from the application of potential. The potential is varied arbitrarily either step by step or continuously. The beginning of voltammetry was facilitated by the discovery of polarography in 1922 by the Nobel Prize winning chemist Jaroslav Heyrovsky. Polarography is a special case of voltammetry wherein a dropping mercury electrode (DME) serves as the microelectrode. Usually it is in form of dropping mercury electrode. Polarography provided a strong base for developing various voltammetric techniques. Early voltammetric techniques had many problems, limiting their viability for everyday use in analytical chemistry. Unlike potentiometric measurements, which employ only two electrodes, voltammetric measurements utilise a three electrode electrochemical cell. The use of three electrodes (working, auxiliary and reference) along with the potentiostat instrument allows accurate application of potential functions and measurement of the resultant current.

Voltammetry is a versatile technique for research purposes, it allow to search into several aspects of the electrochemical reactions, namely those quantitative determination of a variety of dissolved inorganic and organic substances. Voltammetric techniques provide useful information concerning its physical and chemical properties such as oxidation potentials, diffusion coefficients, electron transfer rates and electron transfer numbers, reaction mechanisms, kinetics of electron transfer processes and thermodynamic properties of solvated species *etc*.

Potentiometry, the electrochemical potential of one electrode (the reference electrode - RE) is usually fixed, so the measured cell potential can be interpreted in terms of an equilibrium half-cell reaction involving an analyte species in contact with the other electrode (the working electrode -WE).

Coulometry measures the current passed through an indicator electrode while it is held at a fixed potential. By appropriate choice of potential for a selected species, quantitative determinations are achieved by simply integrating the current over time in order to calculate charge passed. The integrated current gives a direct measure of the number of ions that have been oxidized or reduced.

1.2.1. Types of voltammetry

The different voltammetric techniques used in the voltammetry were distinguished from each other primarily by the potential function that is applied to the working electrode to drive the reaction, and by the material used as the working electrode. These can be described as follows.

- ✓ Linear Sweep Voltammetry (LSV)
- ✓ Staircase Voltammetry (SV)
- ✓ Square Wave Voltammetry (SWV)
- ✓ Anodic Stripping Voltammetry (ASV)
- ✓ Cathodic Stripping Voltammetry (CSV)
- ✓ Normal Pulse Voltammetry (NPV)
- ✓ Differential Pulse Voltammetry (DPV)
- ✓ Fast Scan Cyclic Voltammetry (FSCV)
- ✓ Cyclic Voltammetry (CV)

✓ **Linear Sweep Voltammetry (LSV)**

Linear sweep voltammetry is a voltammetric method where the current at a working electrode is measured while the potential between the working electrode and a reference electrode is swept linearly in time. Oxidation or reduction of species is registered as a peak or trough in the current signal at the potential at which the species begins to be oxidized or reduced. It is the simplest voltammetric method where the current at a working electrode is measured while the potential between the working electrode and a reference electrode is swept linearly in time. Oxidation or reduction of species is registered as a limiting current signal at the potential at which the species begins to be oxidized or reduced may be used to quantitatively determine the concentration of that species in solution.

✓ **Staircase Voltammetry**

Staircase voltammetry is a derivative of linear sweep voltammetry. In linear sweep voltammetry the current at a working electrode is measured while the potential between the working electrode and a reference electrode is swept linearly in time. Oxidation or reduction of species is registered as a peak or trough in the current signal at the potential at which the species begins to be oxidized or reduced.

✓ **Square Wave Voltammetry (SWV)**

Square wave voltammetry (SWV) is a further improvement of staircase voltammetry which is itself a derivative of linear sweep voltammetry. It's a differential technique in which potential waveform composed of a symmetrical square wave of constant amplitude is superimposed on a base staircase potential [11, 12]. The differential current is then plotted as a function of potential, and the reduction or oxidation of species is measured as a peak current. Due to the lesser contribution of capacitive charging current SWV shows excellent peak separation and therefore the detection limits for SWV are on the order of nanomolar concentrations.

✓ **Anodic Stripping Voltammetry (ASV)**

Anodic stripping voltammetry is a voltammetric method for quantitative determination of specific ionic species. The analyte of interest is electroplated on the working electrode during a deposition step, and oxidized from the electrode during the stripping step. The current is measured during the stripping step. The oxidation of species is registered as a peak in the current signal at the potential at which the species begins to be oxidized. The stripping step can be either linear, staircase, square wave, or pulse.

✓ **Cathodic Stripping Voltammetry (CSV)**

Cathodic stripping voltammetry is a voltammetric method for quantitative determination of specific ionic species. It is similar to the trace analysis method anodic stripping voltammetry, except that for the plating step, the potential is held at an oxidizing potential, and the oxidized species are

stripped from the electrode by sweeping the potential positively. This technique is used for ionic species that form insoluble salts and will deposit on or near the anodic, working electrode during deposition. The stripping step can be either linear, staircase, square wave, or pulse.

- ✓ **Normal Pulse Voltammetry (NPV)**

In this technique working electrode is held at a base potential at which negligible electrolysis occurs. After a fixed waiting period, the potential is changed abruptly by applying a pulse for a short period. This potential pulse is ended by returning back to the original base potential value. The current is tested after a fixed time after the application of the pulse and a signal proportional to this sampled value is compared with the current at a constant base potential. The voltammogram is obtained by plotting the measured current vs. the potential to which the step occurs. Normal pulse voltammogram has the typical shape of a sigmoid. After the initial potential step, the capacitive current decays exponentially while the faradaic current decays as the square root of time.

- ✓ **Differential Pulse Voltammetry (DPV)**

In this technique a slowly varying potential ramp is applied to the working electrode. DPV can provide greater sensitivity and more efficient resolution and differentiation of various species. This technique differs from NPV because each potential pulse is fixed, of small amplitude. Current is measured at two points from each pulse, just before the application of the pulse and at the end of the pulse. The difference between the current measurements at these points for each pulse is determined and plotted against the base potential. When the ramp potential is close to the potential where faradaic current starts to rise, the sudden application of the pulse increases the potential of the electrode which results in the higher mass transfer (diffusion). The current response is therefore a symmetric peak. For a reversible system, the peak current, which is proportional to the concentration of the electroactive species, is about 10 times larger than the normal pulse voltammetry.

Pulse and differential pulse voltammetry can be carried out in the presence of more dilute supporting electrolytebthan other electroanalytical methods. For trace

analysis, it is highly desirable to keep the concentration of the supporting electrolyte as low as possible, in order to avoid any introduction at trace levels of impurity.

- ✓ **Fast Scan Cyclic Voltammetry (FSCV)**

Fast Scan Cyclic Voltammetry is a linear sweep voltammetric technique in which the background substracted voltammogram gives additional information about the electro analyzed species. The current response over a range of potentials is measured, making it a better technique to discern additional current contributions from other electro active species. It is relatively fast technique with signal scans typically recorded every 100 ms, however, the fast scan rate decrease the signal to noise ratio.

- ✓ **Cyclic Voltammetry (CV)**

Cyclic voltammetry (CV) is an electroanalytical technique which provides the means to examine the nature or pathway, information on the thermodynamics and kinetics of redox processes in an electrochemical reaction in detail. It not only provides basis for control of the reaction but also elucidates nature of reactive intermediates and the fundamental chemistry that underlies the reaction system of interest. It was first reported in 1938 and described theoretically by Randles [13]. Because of its relative experimental simplicity, Cyclic voltammetry is perhaps more readily applied and often the first experimental approach performed in the electrochemical studies of new systems, since it offers rapid location of redox potentials of the electroactive species, and has proved as a sensitive tool for obtaining information about fairly complicated electrode reactions [14-17].

CV is a technique, wherein a species that undergoes a reduction during a cathodic polarization of the working electrode in an unstirred solution is reoxidized by applying a reverse (i.e. anodic) scan. The correlation of the cathodic and anodic peak currents and of differences in cathodic and anodic peak potentials with the voltage scan rates has been studied mathematically for different electrochemical reactions [18 - 20].

1.3. Theory and basic principles of Cyclic Voltammetry

Cyclic voltammetry is modified form of the rapid scan technique. In cyclic voltammetry voltage is linearly scanned beyond peak potential. After traversing the potential region, the direction of the linear scan is reversed, registering the voltammogram of both cathodic and anodic electrode processes occurring at the test electrode [21, 22].

Cyclic voltammetry is a versatile electro analytical technique for the study of electro active species for acquiring qualitative information in electrochemical research. It is used in the study of electro active compounds particularly biological molecules to investigate coupled chemical reactions particularly to determine reaction mechanisms, rates of oxidation/reduction reactions and also study of electrode surfaces. The electrode potential at which a drug, a metal ion or complex or some other compounds undergoes reduction (addition of electrons) or oxidation (removal of electrons) can be rapidly located by cyclic voltammetry. The most useful aspect of this technique is its ability to generate a new redox species during the first potential scan and then probe the species fate on the second and subsequent scans. Cyclic voltammetry makes possible the elucidation of the kinetics of electrochemical reactions taking place at electrode surfaces [23, 24], information on the thermodynamics of redox process and the kinetics of heterogeneous electron transfer reactions and on coupled chemical reactions or adsorption process.

In typical cyclic voltammetry, a solution component is electrolyzed (oxidized or reduced) by placing the solution in contact with an electrode surface, and then making that surface sufficiently positive or negative in voltage to force electron transfer. In simple cases, the surface is started at a particular potential with respect to a reference electrode and the electrode potential is changed to a higher or lower potential at a linear rate and finally, the potential is changed back to the original value at the same linear rate. When the surface becomes sufficiently negative or positive, a solution species may gain electrons from the surface or transfer electrons to the surface. This results in a measurable current in the electrode circuit.

Cyclic voltammetry is an electrolytic method that uses microelectrodes and an unstirred solution so that the measured current is limited by analyte diffusion at the electrode surface. CV consists of linearly cycling (i.e. the electrode potential is scanned linearly to a more negative potential, and then ramped in reverse back to the starting potential) the potential of an electrode immersed in an unstirred solution while measuring the current. Thus a voltammogram is a display of current vs. potential.

A three electrode system design is an essential feature of all cyclic voltammetry system. One of the electrodes is a reference electrode, and the three electrode design locks the potential of an auxiliary electrode to the reference electrode using a potentiostat. Most of the actual current flows between the auxiliary and working electrodes, leaving the reference electrode essentially unchanged.

1.4. Fundamentals of Cyclic Voltammetry

1.4.1. Circuit

Voltammetric analysis circuits one of which is a polarizing circuit that applies the potential to the cell and the other is a measuring circuit that monitors the cell current. The working electrode is potentiostatically controlled. The potential is varied in some systematic manner and resulting current vs. potential plot is known as voltammogram.

1.4.2. Scan rate

A simple potential waveform that is used often in electrochemical experiments is the linear waveform i.e., the potential is continuously changed as a linear function of time. The rate of change of potential with time is called scan rate.

1.4.3. Switching potentials and the excitation signal

Cyclic voltammetry involves the cycling of potential of an electrode between two designated values called the Switching potentials in an unstirred solution and measuring the resulting current. The controlling potential applied across the working electrode (WE) and the reference electrode (RE) is called the excitation signal which

is a linear potential scan with a triangular waveform as shown in **Fig. 1.1**. The potential axis is also a time that is related to scan rate [25]. The excitation signal causes the potential to scan negatively from +0.8 V to –0.2 V vs. SCE, at which point the scan direction is reversed causing a positive scan back to the original potential of +0.8V. Single or multiple cycles can be used.

1.4.4. Potential control

The potential control of the external point is done using a potentiostat and a three electrode system in which the potential of the WE is controlled relative to the RE, saturated calomel electrode (SCE) or Silver-Silver chloride (Ag/AgCl) electrode. The current passes between WE and the auxiliary electrode (AE).

Because of its greater experimental simplicity, CV has become a very popular technique for electrochemical studies of new systems and has proved as a sensitive toll for obtaining information about fairly complicated electrode reactions.

CV is a technique, where in a species that undergoes a reduction during a cathodic polarization of the WE in an unstirred solution is reoxidized by applying a reverse (i.e., anodic) scan. The correlation of the cathodic and the anodic peak currents and differences in cathodic and anodic potentials with the voltage scan rates has been studied mathematically for different electrochemical reaction [26, 27]. The sweep rates in the CV can be about the same as in single sweep voltammetry.

1.4.5. CV- an active electrochemical method

CV can describe as ‘active’ electrochemical method because the experiment drives an electrochemical reaction by incorporating the chemistry in to a circuit and then controlling the reaction by circuit parameter such as voltage.

1.4.6. Characteristic parameters of a cyclic voltammogram

The cyclic voltammogram is characterized by several important parameters. Four of these observables, the two peak currents and two peak potentials, provide the basis for the diagnostics developed by Nicholson and shain [28] for analysing the cyclic voltammetric response. There are two peaks associated with the redox

reaction and accordingly we have the anodic peak potential (E_{pa}) and cathodic peak potential (E_{pc}) and the corresponding current associated are anodic peak current (I_{pa}) and cathodic peak current (I_{pc}) respectively.

In cyclic voltammetry, the electrode ramps linearly vs. time. This ramping is known as the experiment's scan rate (V/s). The potential is measured between the reference electrode and working electrode and the current is measured between the working electrode and the counter electrode. This data is then plotted as current (i) vs. potential (E). The basic shape of the current vs. potential response for a cyclic voltammetry experiment is as shown in **Fig. 1.2** for a reversible process (a reversible wave is when an analyte is reduced or oxidized on a forward scan and is then reoxidized or rereduced in a predictable way on the return scan). As the figure shows, the forward scan produces a current peak for any analytes that can be reduced (or oxidized depending on the initial scan direction) through the range of the potential scanned. The scan shown starts at a slightly negative potential, i.e. the initial potential (E_i), there is no net conversion of oxidized species (O) into reduced species (R) (point A). As redox potential is approached, the current is first observed to peak at E_{pa} (with value i_{pa}) (point B) indicating that an oxidation is taking place and then drops due to depletion of the reducing species from the diffusion layer. During the reverse scan i.e. switching potential, E_{switch}, (point C) reduction occurs and a peak current is observed at E_{pc} (with value i_{pc}) (point D). Providing that there is no surface interaction between the electrode and the reagents, and the redox products are stable (at least in the time frame of the experiment). The situation is very different when the redox reaction is not reversible, when chemical reactions are couple to the redox process or when adsorption of either reactants or products occurs. In fact, it is these non-ideal situations which are usually of greatest chemical interest and for which the diagnostic properties of cyclic voltammetry are particularly suited. This is helpful in understanding the fundamentals of the technique. As shown in **Fig.1.3**, scanning the potential in the negative direction makes the electrode a stronger reductant, whereas scanning the potential in the positive direction makes it a better oxidant.

1.5. Solvent

Electrochemical measurement are commonly carried out in a medium which consist of solvent containing a supporting electrolyte. A number of physicochemical properties must be considered while choosing a solvent for electrochemical work [29] like being in a liquid state at room temperature, capable of dissolving electro active species of interests, having a large potential window and having required acid-base properties. The dielectric constant is the most important parameter for a solvent.

The cheapest solvent is water, which possesses many physico-chemical properties. It can dissolve ionic components and form highly conducting solutions. Water, deionized and repeatedly distilled with alkaline $KMnO_4$, is usually considered as pure. The purity is checked by conductivity measurements. The volatile and organic impurities [30] are removed by passing the distilled water vapour through a column containing Pt catalyst at about 800°C over which oxygen also simultaneously passed.

Dimethyl formamide (DMF) is one of the aprotic solvents, which has very good dissolving power of ionic species. It has a cathodic limit up to –3.0 V for anion radicals. Hence, this is the solvent of choice for studies on anion radicals and dianinons. In the positive potential regions above +1.0 V, the solvent itself decomposes. Cation radicals are less stable in this medium.

Acetonitrile is perhaps a solvent with inert electrochemical properties. It has +3.0 V (versus SCE) anodic and –3.0 V cathodic limits. However, this solvent has very poor solubility for ionic species. Salts containing organic ions such as tetra-alkyl ammonium salts must be employed.

Methylene chloride is the solvent of choice for organic oxidation studies. It is stable up to +3.0 V as acetonitrile. Cation radicals and dications are quite stable in this medium. Electrolytes are easily soluble in methylene chloride. However, at negative potentials of –1.0 V, the solvent decomposes. The anionic species are less stable in this medium.

Dimethyl sulphoxide has electrochemical properties similar to DMF in the cathodic region. Since it is not as basic as DMF, cation radicals are somewhat stable in this medium.

Even totally non-polar solvents such as benzene and other hydrocarbons may be used to study the solution phase [31] as well as surface processes [32, 33-36]. Water, deionized and repeatedly distilled with alkaline $KMnO_4$, is usually considered as pure. The main impurity present in non-aqueous solvents is water. Refluxing with anhydrous copper sulphate, alumina, aluminum chloride, P_2O_5 etc., and distilling under reduced pressure many times and collecting the proper fraction usually remove this. Vacuum lines are employed during purification, storage and dehydrating agent such as anhydrous alumina is added as an internal addition [37].

1.6. Supporting electrolytes

Electrolyte usually added to the test solution in voltammetric techniques to ensure sufficient conductivity i.e. it is a phase through which charge is carried by the movement of ions. All ionic salts or ionizable compounds in a solvent are defined as the supporting electrolytes. This electrolyte is added at high concentration to the sample and could be liquid solutions (a simple salt solution, acid, base or also a buffer solution), fused salts or they may be ionically conducting salts such as sodium β-alumina which as mobile sodium ions. It is very important to realize that they can influence the electrochemical processes in a number of ways.

i. These electrolytes impart conductivity to the solvent and hence enable the continuous current flow in solution.
ii. They must remain electro-inactive in the potential region of interest, if any useful voltammetric study is to be conducted.
iii. If the concentration of the supporting electrolyte should be very high, they can form a space charge near the surface and the space charge potential can influence the charge transfer kinetics.
iv. If the ions of the supporting electrolyte are adsorbed on the surface, they can catalyze or inhibit other reactions.

v. Small cations may form ion pairs with the anion radicals formed in the electrode process and the properties of the ion pairs can be very different from those of the free anion racial.

vi. Some ions may form complexes with the reactants and products.

vii. The supporting electrolyte generally controls the acidity of the ionic solution.

viii. The liquid electrolyte melts and solid electrolyte acts as the medium for the ionic phase.

Relating to the influence of supporting electrolyte on the electrochemical processes, the choice of the supporting electrolyte has to be made on the basis of the following characteristics:

i. Be chemically inert.
ii. Do not interfere with diffusion and with the electrons exchange on the electrode surface.
iii. Have a different discharge potential.
iv. Have a high ionic conductivity and a low electrical resistance.

H_2SO_4, $HClO_4$ and HCl are normally employed for studies in acidic aqueous solutions and NaOH or KOH are employed for alkaline media. In neutral region, if buffering is important, acetate, citrate and phosphate buffers are usually employed. B-R buffer is used over a wide pH range. If the redox process does not involve acid-base reactions, no buffers are needed and any electrolyte may be used.

Solubility is the main consideration in selecting supporting electrolyte for aprotic solvent. A number of Tetra-Alkyl Ammonium (TAA) salts show good solubility in aprotic media. Tetra-ethyl ammonium (TEA) salts and more recently Tetra-n-Butyl Ammonium (TBA) salts are widely employed for this purpose.

Most of the inorganic acids, bases or salts are commercially available in the high purity grade. TAA salts are frequently available in the form of halides. The perchlorates or fluroborates may be easily obtained by double decomposition of

these salts with the corresponding sodium salts. The precipitated $TAAClO_4$ or $TAABF_4$ may be recrystallized twice or thrice [38].

Some electrolytes may be hygroscopic. Dehydration may be done in an oven. Dehydrated samples should be stored in desiccators. Care must be exercised in handling explosives salts such as $NaClO_4$. They must neither be overheated nor ground in mortars with force and contact with organics should scrupulously be avoided.

1.7. Electrodes

In the present work three electrode system is used i.e. WE/ AE/ REs. RE used is standard calomel electrode (SCE) which is often isolated from the solution by a salt bridge to prevent contamination by leakage from the RE. The platinum foil as AE and WEs are carbon paste electrode, or Modified carbon paste electrode.

1.7.1. Working Electrode (WE)

Electrode is a metallic conductor immersed in an electrolyte solution through which charge is carried by electronic movement i.e. at the surface of the electrode dissolved electroactive ions change their charges by exchanging the electrons with the conductor and the electrode at which this charge transfer occurs is called the working (or indicator) electrode. The response of a species in an electrochemical reaction is strongly influenced by the material of the working electrode. Electrodes can be metals or semiconductors, and they can be solid or liquid like noble metals, carbon or mercury. These electrodes are generally encased in a rod of inert insulator made from Teflon, glass or epoxy with a disk exposed at one end. Having a controlled surface area with a defined shape is important for interpreting cyclic voltammetry results. The working electrode should possess numerous characteristics such as:

- High signal-to-noise ratio
- Reproducible response
- No interfering reactions in a certain potential window

- High electrical conductivity
- Low surface capacitance
- Mechanical and chemical stability
- Low cost and easily available and
- Low toxicity and long term stability.

In electrochemical reaction both the reduced and oxidizing ions remain in solution and the working electrode which is chemically inert acts as a source or sink of electrons in the interfacial region.

1.7.1.1. Mercury Electrode (Liquid electrode)

Mercury drop electrodes are an example for liquid electrodes and are a very attractive choice of electrode material because of its high hydrogen overvoltage that greatly extends the cathodic potential window (compared to solid electrode materials) and possesses a more reproducible, readily renewable, smooth surface, more negative potentials can be obtained in aqueous systems and amalgamation with heavy metals. Therefore, mercury drop electrodes are used for determination of trace metals. The simplest mercury electrode is the Dropping mercury electrode (DME), which consists of a mercury drop at the end of the capillary and the other end of the capillary is attached to a reservoir of mercury and control of the flow of mercury from the reservoir is controlled by a valve and is held open throughout the experiment. An alternative mercury electrode is the Static Mercury Drop Electrode (SMDE), for which the valve is held open for a set length of time. In the Controlled Growth Mercury Electrode (CGME), the drop is grown incrementally using a user-defined valve. Disadvantages of the use of mercury are its limited anodic range (due to the oxidation of mercury) and its toxicity.

1.7.1.2. Solid electrodes

The limited anodic potential range of mercury electrodes has precluded their utility for monitoring oxidizable compounds. Accordingly, solid electrodes with extended anodic potential windows have attracted considerable analytical interest.

Of the many different solid materials that can be used as working electrodes, the most often used are platinum, gold and carbon in several different forms. Silver, nickel, and copper can also be used for specific applications. New materials such as graphite, vitreous carbon and boron carbide have been developed.

Carbon Electrodes are the most widely used solid working electrodes [39, 40] due to its broad potential window in both the positive and negative directions with low background current, high temperature resistance, hardness, low density, low electrical resistance, low friction, low thermal resistance, extreme resistance to chemical attack and impermeability to gases and liquids, rich surface chemistry, low cost, and suitability for various sensing and detection applications. The most popular carbon electrode materials are those involving glassy carbon, carbon paste, graphite pencil electrode, carbon fiber, screen-printed carbon strips, carbon films, or other carbon composites (e.g., graphite epoxy, wax-impregnated graphite, Kelgraf). Carbon paste electrodes are the less expensive and most commonly used carbon electrodes because the paste can be squeezed inadvertently after being polished.

While all common carbon electrode materials share the basic structure of a six-membered aromatic ring and sp^2 bonding, they differ in the relative density of the edge and basal planes at their surfaces. Electron transfer rates observed at carbon surfaces are often slower than those observed at metal electrodes. The electron-transfer reactivity is strongly affected by the origin and history of the carbon surface [41, 42]. Although carbon electrode suffers from high residual currents, different forms of carbon such as wax impregnated graphite, pyrolytic graphite, carbon paste etc have been used to minimize high residual currents. A variety of electrode pretreatment procedures have been proposed to increase the electron transfer rates. The type of carbon, as well as the pretreatment method, thus has a profound effect upon the analytical performance.

Platinum Electrode is one of the most widely used materials for fabricating working electrodes. Platinum has the advantage of being an easily machined metal that is electrochemically inert despite the expense associated with this precious metal. In aqueous solvent systems, the platinum working electrode is a good choice when working with positive potentials, but at negative potentials, interference from

the reduction of hydronium ion is a problem. In rigorously anhydrous organic solvent systems.

There are large diameter platinum macro electrodes generally fabricated by welding a thick platinum disk to the end of a brass rod and small diameter platinum disk electrodes and platinum microelectrodes, usually fabricated by shrouding a short length of platinum wire in soft glass. The platinum surface is then ground to a mirror quality finish using a polishing paste that contains sub-micron alumina particles.

Gold Electrodes are designed along the same lines as platinum working electrodes. Gold is usually less expensive than platinum, but it is not as electrochemically inert. The surface of a gold electrode is subject to oxidation at moderately positive potentials, and so it is not as generally useful as platinum. Gold electrodes are better suited for cathodic processes (reduction) than platinum.

Rotating disk electrode (RDE) is a hydrodynamic working electrode used in a three electrode system. The electrode rotates during experiments inducing a flux of analyte to the electrode. These working electrodes are used in electrochemical studies when investigating reaction mechanisms related to redox chemistry, among other chemical phenomena. The more complex rotating ring-disk electrode can be used as a *rotating disk electrod*e if the ring is left inactive during the experiment. The electrode includes a conductive disk embedded in an inert non-conductive polymer or resin. The disk, like any working electrode, is generally made of a noble metal or glassy carbon, however any conductive material can be used based on specific needs. The more complex **rotating ring-disk electrode (RRDE)** can be used as a rotating disk electrode if the ring is left inactive during the experiment. The cell contents are open to the air, making oxygen removal difficult therefore strong flow of inert gas is required to blanket the solution whenever a rotating electrode is being used to study an air-sensitive electrochemical system.

Potential sweep reversals as used in cyclic voltammetry are not possible for a RDE system since the products of the potential sweep are continually swept away

from the electrode. In contrast, the rotating ring-disk electrode is well suited to investigate this further reactivity.

1.7.2. Reference Electrode (RE)

Choosing a reference electrode the purpose of the reference electrode is to provide a stable, well-known half-reaction on which to reference the redox process occurring at the working electrode. Reference electrodes however are so called because the potential of a working electrode in a voltammetry experiment is always controlled with respect to this. The high stability of the electrode potential is usually reached by employing a redox system with constant (buffered or saturated) concentrations of each participants of the redox reaction [43].

There are many ways reference electrodes are used. The simplest is when the reference electrode is used as a half cell to build an electrochemical cell. This allows the potential of the other half cell to be determined. The selection of a proper reference electrode is equally vital in voltammetry especially when accurate and precise data on the formal potentials of the redox couples under examination are needed. While the thermodynamic scale of half-reaction potentials found in most textbooks measures electrode potentials against the "standard hydrogen" reference electrode (SHE), in actual practice the SHE is much too cumbersome to use. For this reason, a number of other reference electrodes have been developed.

One of the most generally available reference electrodes for work in aqueous solutions is the saturated calomel electrode (SCE) i.e. mercury (Hg) in direct contact with solid calomel (Hg_2Cl_2) paste with saturated KCl solution. The half reaction that occurs inside of an SCE reference is given below.

$$Hg_2cl_{2(s)} + 2e^- \longrightarrow 2Hg_{(l)} + 2Cl^-_{(aq)}$$

Electrical contact is made by immersing a platinum wire into the liquid mercury, and the potassium chloride solution which in turn contact with the test solution. The electrode potential depends on Cl^- ion concentration. The $Hg/HgSO_4$, Ag/AgCl and Hg/Hg_2O electrodes also belong to this group.

Other useful reference electrodes are based on Ag/AgCl. Used in aqueous systems, the half reaction for this reference electrode is as follows:

$$AgCl_{(s)} + e^{-} \longrightarrow Ag_{(s)} + cl^{-}_{(aq)}$$

The metal/metal ion electrodes may also be employed as reference electrodes, example Cu/Cu^{+2}.

1.7.3. Counter/Auxiliary Electrode (AE)

The counter electrode, alternatively referred to as the auxiliary electrode, act as source or sink for electrons in the electrochemical circuit formed with the working electrode. The auxiliary or counter electrode, is an electrode used in a three electrode electrochemical cell in which an electrical current is expected to flow [43 - 45]. This electrode provides an alternative route for the current to follow i.e. current flows between working electrode and auxiliary electrode so that only a very small current flows through the reference electrode i.e. the auxiliary electrode functions as a cathode whenever the working electrode is operating as an anode and vice versa. The auxiliary electrode often has a surface area much larger than that of the working electrode to ensure that the half-reaction occurring at the auxiliary electrode can occur fast enough so as not to limit the process at the working electrode. The potential of the auxiliary electrode is usually not measured and is adjusted to so as to balance the reaction occurring at the working electrode. This configuration allows the potential of the working electrode to be measured against reference electrode without compromising the stability of that reference electrode by passing current over it.

The auxiliary electrode can be made from just about any material using any desired electrode geometry. Design choices are usually based on finding a material that is chemically inert in the particular test solution being studied. In most cases, a coil of platinum wire is used but stainless steel, copper or aluminum wire may work in non-corrosive solutions where metal cation interference is not a concern. If the electrochemical cell is made of metal, then the cell itself might be used as the auxiliary. In most cases the auxiliary electrode can be placed right in the test solution along with the reference and working electrodes. But if current flows at the

auxiliary electrode, electrochemical process will also occur here and the products generated at the auxiliary diffuse to the working electrode and may interfere with the experimental measurement. When this is a problem, the auxiliary electrode is placed in a separate compartment containing an electrolyte solution that is in ionic contact with the main test solution via a glass frit.

1.8. Residual Currents in Voltammetry

When a potential scan is applied to an electrode system, immersed in supporting electrolyte solution, before the charge transfer takes place, the current that flows through the cell is called the residual or background current. It is primarily composed of the following components [46].

1.8.1. Charging / Non Faradaic Current

This current also called the capacity current as it results from the charging and discharging of the electrode double layer (which acts like a capacitor) associated with the electrode-solution interface. There is no charge transfer across the double layer, and hence it is not governed by Faraday's laws and, therefore, it is named as non-faradic current. The charging current is directly proportional to the true area of the electrode. Since the solid electrode surface is rough and full of edges, the true area of the electrode is much greater than geometric area.

1.8.2. Faradaic Current

The electric current flowing through the working electrode has two components. The First, the faradic current, follows the faraday laws and is due to the discharge of the electroactive compound (A_{ox}).

The second, the capacitive current, is produced by the growth of a double electrical layer on the interface between the electrode and solution. This double layer is due to the high concentration of the supporting electrolyte in the solution and act as a condenser and the faradic current.

The capacitive current acts as a non-specific background interference of the faradic current and sometimes can be higher than the latter, when the depolarizer is

present at low concentration in solution. In this case the measure of the faradic current is difficult and some electronic adjustment has to be used. Therefore Polarography and voltammetry is growth, as analytical technique, only after the progress in the electronic field, so affirm that the development of this technique is strictly linked to the tentative to electronically overcome problems due to capacitive current.

1.9. Polarisable and Non-Polarisable Interface

All electrode-solution interfaces can be classified as polarisable or non-polarisable. An electrode for which an electron can pass easily across the interface is called non-polarisable. In this case, external application of a change of potential may result in more electrons passing rapidly across the interface. Thus, there is a negligible build-up of excess charge in the electrode surface, i.e., the interface does not polarise. Platinum in contact with hydrochloric acid is a non-polarizable interface. In contrast when the transfer of electrons is difficult, a potential change from outside will induce a substantial build-up of excess charges at the interface, hence, the electrodes is termed polarisable. When a potential is applied externally to the electrode, the transfer of electrons through this is negligible. That is, a small change in current flow causes a large change in electrode potential. An ideally polarisable interface is one which can allow the passage of current without causing a change in the potential difference across it. In addition, when the current associated with charging the electrode-electrolyte interface arises purely from capacitive effect; such an interface is termed an ideally polarisable electrode. while no real electrode behaves ideally over the entire potential rage, some electrode-solution system, over limited potential ranges, can show behaviour which is approximately, ideal for instance, a mercury electrode in contact with a de-aerated potassium chloride solution which behaves as an ideal polarisable electrode at potential in excess of 1.5V.

1.10. Electrode Processes

For a complete comprehension of the mechanism on which the voltammetric technique is based on within the solution, between the electrode surface and species

that causes the conversion of the dissolved oxidised species (O) to reduced species (R) and/or vice-versa.

The individual rates of each process affect overall rate of reaction. Therefore it is important to study the various processes taking place at the electrode and electrode-electrolyte interface which affects the reaction rate such as:

i. Mass transfer
ii. Electron transfer
iii. Chemical reactions preceding or following the electron transfer which could be homogeneous such as protonation or dimerization or heterogeneous ones like catalytic decompositions on the electrode surfaces.
iv. Other surface reactions such as adsorption, desorption, crystallization etc.

The simplest reaction involves only mass transfer of reactant to the electrode, heterogeneous electron transfer involving non adsorbed species and the mass transfer of the product to the bulk solution. More complex reaction sequence involving a series of electron transfer, protonations, branching mechanisms, parallel paths or modifications of the electrode surfaces are quite common. When a steady state current is obtained, the rates of all reactions steps are the same. The magnitude of this current is often limited by the inherent sluggishness of one or more reactions called rate determining steps. The more facile reactions are then held back from maximum rates by the slowness with which such steps disposes of their products or create their participants [47, 48].

1.10.1. Mass Transfer Processes

The rate of transport to the surface can also effect or even dominate the overall reaction rate apart from applied voltage. The exponential relationship between applied voltage and reaction rates predicts that as the voltage is increased the current will increase exponentially. This would mean that it is possible to pass unlimited quantities of current. In reality this does not happen. For a fixed electrode area (A) the reaction can be controlled by two factors. First the rate constant k_{red} and second the surface concentration of the reactant. If the rate constant is large, such that any reactant close to the interface is immediately converted into products then

the current will be controlled by the amount of fresh reactant reaching the interface from the bulk solution. Thus movement of reactant in and out of the interface (mass transport) is important in predicting the current. There are three forms of mass transport which can influence an electrolysis reaction:

Mass transfer in electrochemistry is the movement of electroactive species from one location to another in solution arising from the differences in electrical or chemical potential. During the charge transfer process, the electroactive material gets depleted at the surface of the electrode and hence a concentration gradient is set up. Under such conditions the reactant diffuses towards the electrode surface and the corresponding product of the electrode reaction diffuses away from the electrode surface. The three modes of mass transport principally considered are [**Fig.1.4**]:

a) Diffusion

b) Migration and

c) Convection

1.10.1a. Diffusion

Diffusion occurs in all solutions and arises from local concentration gradient of reagents. Diffusion is particularly significant in an electrolysis experiment since the conversion reaction only occurs at the electrode surface. Consequently, there will be a lower reactant concentration at the electrode than in bulk solution. Similarly a higher concentration of product will exist near the electrode than further out into solution. Movement of material by diffusion can be predicted mathematically by Fick's laws [49]. First Law states that:

$$J_0 = -D_0 \frac{\partial c_0}{\partial_x}$$

This relates the diffusional flux $'J_0'$(i.e. the rate of movement of material by diffusion) to the concentration gradient and the diffusion coefficient $'D_0'$. The negative sign simply signifies that material moves down a concentration gradient i. e. from regions of high to low concentration. However, in many measurements we

need to know how the concentration of material varies as a function of time and this cannot be predicted from the first law.

The second law states:

$$\frac{\partial c_0}{\partial t} = -\frac{\partial J_0}{\partial_x}$$

The rate of change of the concentration $'c_0'$ as a function of time't' can be seen to be related to the change in the concentration gradient. So the steeper the change in concentration the greater the rate of diffusion. In practice diffusion is often found to be the most significant transport process for many electrolysis reactions.

1.10.1b. Migration

This is essentially an electrostatic effect which arises due the application of a voltage on the electrodes. This effectively creates a charged interface (the electrodes). Any charged species near that interface will either be attracted or repelled from it by electrostatic forces. Due to ion solvation effects and diffuse layer interactions in solution, migration is very difficult to calculate accurately for real solutions. Consequently most voltammetric measurements are performed in solutions which contain a background electrolyte - this material is a salt (e.g., KCl) that does not undergo electrolysis itself but helps to shield the reactants from migratory effects. By adding a large quantity of the electrolyte (relative to the reactants) it is possible to ensure that the electrolysis reaction is not significantly effected by migration. The purpose of introducing a background electrolyte into a solution is not however solely to remove migration effects as it also acts as a conductor to help the passage of current through the solution.

To gain a quantitative model of the current flowing at the electrode we must account for the electrode kinetics, the 3 dimensional diffusion, convection and migration, of all the species involved **(Fig.1.4)**. This is very computation intensive and requires very large processing power [49].

1.10.1c. Convection

Convection results from the action of a force on the solution. This can be a pump, a flow of gas or even gravity. There are two forms of convection the first is termed natural convection and is present in any solution. This natural convection is generated by small thermal or density differences and acts to mix the solution in a random and therefore unpredictable manner. In the case of electrochemical measurements these effects tend to case problems if the measurement time for the experiment exceeds 20 seconds. It is possible to drown out the natural convection effects from an electrochemical experiment by deliberately introducing convection into the cell. This form of convection is termed forced convection [49].

1.10.2. Electron Transfer

The electron transfer process is also known as charge transfer process. The electroactive species after moved from the bulk of the solution, either by diffusion or under forced convection (using a rotating electrode or stirring the solution by a magnetic stirrer) enters the electrical double layer, which is under direct influence of the electrode. On entering the double layer the species undergoes a structural orientation so that it can take up or give up electrons from or to the electrode surface respectively with the least activation energy when a suitable potential is applied and simultaneously we observe current. This state of reactant species is known as transition state. Being unstable the species converts itself to the final product by release of activation energy and gets reduced or oxidized. This final product after undergoing suitable reorientation either gets deposited on the electrode surface or move away from the electrode surface into the bulk solution. The electrode process are three types:

a) Reversible process

b) Irreversible process

c) Quasi-reversible process

1.10.2a. Reversible Electron Transfer Process

A reversible process is one in which the electron transfer process is rapid, and the electro active oxidized (or reduced) species in the forward scan in equilibrium with the electroactive reduced (oxidized) species in the reverse scan.

$$\mathbf{Red \rightleftharpoons Ox + ne^-}$$

For a reversible process, redox peak is observed as shown in **Fig.1.5**. Reversibility can be defined as chemical or electrochemical. In an electrochemically reversible process the electron transfer is not rate limiting. For a chemically reversible process, both forms of redox couple (O for oxidized form and R for reduced form) are stable in the time scale of measurement. The value of rate constant k_s, in case of reversible reaction exceeds 2×10^{-2} cm/sec. For the reactions that are fast i.e. reversible electron transfer reactions, the voltage applied will result in the generation of the concentrations, C_{ox} and C_{red} of oxidized and reduced forms of the redox couple respectively at the electrode surface is predicted by the Nernst equation

$$E = E^o + RT/ nF \ln C_{ox} / C_{red} \text{ ……..} \quad (1.1)$$

Where, n is no. of electrons transferred, F is Faraday constant, R is Gas constant and T is temperature. If the system is diffusion controlled then the Fick's law of diffusion holds for both oxidation and reduction. Under these conditions the peak current for a reversible couple (25^oC) is given by Randles-Sevcik equation;

$$i_p = (2.69 \times 10^5)\, n^{3/2} A D^{1/2} C_o^* \nu^{1/2} \text{ ……} \quad (1.2)$$

Where n is the stoichiometric number of electrons involved in the electrode reaction, A is the area of electrode in cm^2, D_o is the diffusion coefficient of the species O in cm^2/s, C_o is the concentration of the species O in mol/cm^3 and ν is the scan rate in V/s.

The current peaks are commonly measured by extrapolating the preceding baseline current. The position of the peaks on the potential axis (E_p) is related to the formal potential of the redox process. The formal potential (E^0) is centered between E_{pa} and E_{pc} and separation between the peak potentials (ΔE_p) is the difference of the

potentials E_{pa} and E_{pc} for a reversible couple. It is possible to relate the half-peak potential ($E_{p/2}$, potential at which the current is half of the peak current) to the half-wave potential, $E_{1/2}$.

Diagnostic tests for cyclic voltammograms of reversible system at 25º C

i. $E^0 = (E_{pa} + E_{pc})/2$

ii. $\Delta E_p = E_{pa}-E_{pc} = 59/n$ mV, where n is number of electrons change

iii. $i_{pc}/i_{pa} = 1$

iv. $i_p \; \alpha \; \nu^{1/2}$

v. E_p (E_{pa} and E_{pc}) is independent of ν

vi. $E_{p/2} = E_{1/2} \pm 29$ mV/n

1.10.2b. Irreversible Electron Transfer Process

For an irreversible process, only forward oxidation or reduction peak is observed but at times with a weak reverse peak (**Fig. 1.6)** and individual peaks are reduced in size and widely separated due to slow electron exchange. Totally irreversible systems are characterized by a shift of the peak potential E_p with scan rate because the current takes more time to respond to the applied voltage than in the reversible reaction and is given by:

$$E_p = E^0 - (RT/\alpha n_a F)\,[0.78 - \ln (k^0/(D)^{1/2}) + \ln (\alpha n_a F\nu/RT)^{1/2}] \quad \ldots\ldots\ldots (1.3)$$

Where α is the charge transfer coefficient, a measure of asymmetry of electron transfer and n_a is the number of electrons involved in the charge transfer step. Thus E_p occurs at potentials higher than E^0, with the over potential related to k^o and a. Independent of the value k^0, such peak displacement can be compensated by an appropriate change of the scan rate. The peak potential and the half-peak potential (at 25^0C) will differ by

$$47.7/\alpha n_a \text{ mV} \quad \ldots\ldots (1.4)$$

Hence the voltammogram becomes more drawn-out as αn_a decreases. For an Irreversible reaction, the peak current is given by [50]

$$i_p = (2.99 \times 10^5)\, n\, (\alpha n_a)^{1/2}\, A\, D_0^{1/2}\, \nu^{1/2}\, C_o^{*} \quad \text{.....(1.5)}$$

The value of E_p, the difference between the cathodic and anodic peak is of the order of 59 mV/n is given by equation. The peak separation E_p is a factor determining the reversibility or irreversibility of an electrode reaction. The equation by Nicholson is normally used to calculate electron transfer rate constants.

Diagnostic tests for cyclic voltammograms of irreversible system at 25° C

i. no reverse peak

ii. $i_p \alpha \nu^{1/2}$

iii. E_p shifts = $30/\alpha n_a$ mV, where α is charge transfer coefficient

iv. $[E_p - E_{p/2}] = 47.7/\alpha n_a$ mV

1.10.2c. Quasi Reversible Electron Transfer process.

Unlike the reversible process in which the current is purely mass-transport controlled, current due to quasi- reversible process are controlled by mixture of mass transported and charge transfer kinetics [2, 17]A quasi reversible electron transfer is a class of electrode reactions in which the rates of charge transfer and mass transfer are comparable or competitive. Quasi-reversible process is intermediate between reversible and irreversible systems (**Fig.1.7**). The current due to quasi-reversible processes is controlled by both mass transport and charge transfer kinetics [51]. The shape of the cyclic voltammogram is a function of the ratio $k_0/(\pi\, \gamma\, nFD/RT)^{1/2}$. As the ratio increases, the process approaches the reversible case. Overall, the CV of quasi-reversible system is more drawn out and exhibits a larger separation in peak potentials compared to a reversible system. The process occurs when the relative rate of electron transfer with respect to that of mass transport is insufficient to maintain Nernst equilibrium at the electrode surface. In the quasi-reversible region both forward and backward reactions make a contribution to the observed current.

Diagnostic tests for cyclic voltammograms of quasi-reversible system at 25° C

i. i_p increases with scan rate (ν), but is not proportional to scan rate.

ii. $i_{pc}/i_{pa} = 1$, provided $\alpha_c=\alpha_a = 0.5$

iii. ΔE_p may approach 59/n mV at a low ν but increases with increasing scan rate

iv. E_{pc} shifts negatively with increasing ν

1.10.3. Coupled Chemical reaction.

In addition to charge transfer and mass transfer processes, electrode process can also be complicated by parallel homogeneous chemical reaction. The coupling of chemical reactions to the electron transfer reactions can lead to changes in the peak potentials and/or the peak currents, and the effect of chemical reactions is often expressed in terms of changes in the peak current ratio and/or peak potentials. The most commonly occurring reaction mechanisms are given as:

Following Chemical reactions (EC): In this case the product of the electron transfer undergoes a homogeneous chemical reaction.

Preceding Chemical reactions (CE): In this case, the electrode process (E) is preceded by a chemical reaction (C) whereby an electroactive substance undergoes a homogeneous chemical reaction to liberate an electroactive substance.

1.11. Applications of Cyclic Voltammetry

Cyclic voltammetry (CV) is the most effective and versatile electroanalytical technique available for the mechanistic study of redox systems [52-58]. CV has become increasingly popular in all fields of chemistry as a means of studying redox states. The method enables a wide potential range to be rapidly scanned for reducible or oxidizable species. This capability together with its variable time scale and good sensitivity make this the most versatile electro analytical technique. It enables the electrode potential to be rapidly scanned in search of redox couples. Once the redox couple located, it can then be characterized from the potential of peaks on the cyclic

voltammogram and from changes caused by variation of the scan rate. As the peak current is proportional to concentration, this method can be used for the estimation of a number of inorganic, organic and organometallic compounds.

CV has its ability to generate a species during one scan and then probe its fate with subsequent scans. The power of CV results from its ability to rapidly provide information about:

1. Rapid location of redox potentials of the electroactive species present in new drugs.
2. Number of electrons involved in each of the observed redox processes.
3. Reaction mechanism, rate constants, transfer coefficients and diffusion coefficients of redox processes and the kinetics of electron-transfer reactions and detection of chemical reactions coupled to electron transfer or adsorption processes.
4. Analysis of the organic compounds, neuroactive compounds in pharmaceutical preparations.
5. In vivo analysis of biologically significant molecules.
6. Relative surface area and roughness.
7. Whether the redox behaviour is affected by a change in the concentration of the electroactive species, solvent system, or the electrode surface.
8. Reaction intermediates and their identification in the electrode reaction.
9. Whether the redox process is kinetic or diffusion controlled.
10. Products formed in the electrochemical reaction.
11. Charge storage capacity.
12. Surface contamination.

1.12. A Brief Literature Survey

Electron transfer plays a fundamental role in governing the pathway of chemical reactions. Measurement of speed of electron transfer process and the number of electrons involved are different in traditional experimental method spectroscopy. Consequently our knowledge of the driving force for many reactions remains exclusive. Electrochemical methods offer the potential to investigate this by the determination of the number of electrons involved. Electrochemical techniques have been used in analytical chemistry for more than 50 years. Emeritus Professor I.M Kolthoff is a maker and also is a scientific ancestor of generations of electroanalytical chemists. Faraday, Arrhenius, Vant Hoff and Ostwald made substantial contribution to either electrochemistry or kinetics. The discovery of polarography has further enhanced the analytical potentialities of voltammetric methods. In the 60's modern organic, inorganic and biological electroanalytical chemistry flourished rapidly with the advent of cyclic voltammetry, differential pulse polarography, pulsed chronoamperometry, rotating disc electrodes and the use of ESR and optical measurements coupled with electrochemical experiments.

1.12.1. Literature Survey of Carbon Paste Electrode: Invention and its Modification

In the second half of the 60's, electrodes other than mercury began to draw more serious attention because of the potential range being studied is more positive than the potential for the oxidation of mercury. New electrode materials such as platinum, gold, glassy carbon and pyrolytic carbon with extended anodic potential windows have attracted considerable analytical interest. Silver, nickel and copper were also used for specific applications. These electrodes require precise electrode pretreatment and polishing to obtain reproducible results. New materials such as carbon paste, boron carbide have been extensively developed.

In 1958, shortly before Professor Jaroslov Heyrovsky received the Nobel Prize for chemistry and his polarographic method became known worldwide, Adams reported on a new type of electrode [59]. The proper material of this sensor was formed by a mixture of carbon powder and a nonelectroactive liquid binder prepared

in thicker consistency and simply called it as “carbon paste”. The original idea of the inventor behind carbon paste was to develop “dropping carbon electrode” similar to that of dropping mercury electrode (DME), that is, from a reservoir with suspension of carbon powder in a liquid and connected to a capillary, allowing one to obtain periodically renewable droplets of “carbon electrode”. The inventor however hoped that this set-up could serve as a certain analogy to the DME for anodic oxidations of organic compounds where mercury-based electrodes were inapplicable.

Carbon paste electrodes (CPEs) were mainly employed in studying the mechanisms of electrode reactions of various organic compounds [60, 61].

The composite nature of carbon pastes and their easy preparation were undoubtedly stimulating factors for altering the properties of CPEs. The deliberate and controlled modification of the electrode surface can produce electrodes with new and interesting properties that may form the basis of new applications of electrochemistry and novel devices. Electrode surfaces are modified in a quest to render an electrochemical function either not possible or difficult to achieve using conventional electrodes. Targeted improvements include increased selectivity, sensitivity, chemical and electrochemical stability, as well as a larger usable potential window and improved resistance to fouling. Furthermore, electrodes with tailored surfaces enhance fundamental studies of interfacial processes. Therefore, the need for improved electrode performance and logically designed interfaces is rapidly growing in many areas of science.

The definition of a chemically modified electrode (CME) is a conducting or semiconducting material that has been coated with a monomolecular, multi-molecular, ionic, or polymeric film (termed adlayer) which alter the electrochemical, optical, and other properties of the interface. Recent improvements in surface characterization techniques enable a molecular-level understanding of modified interfaces. These techniques, coupled with electrochemical characterizations, not only provide a means to verify the function, but also serve as a basis for refinements of the modification strategy to further enhance its performance.

The first modification was done in 1964 in which an organic substance was dissolved in a binder [62] and served to study the electrode behaviour of the

substance itself was considered as a pioneering step in the field of carbon paste electroactive electrode. In 1965, the second modification of CPE, prepared by rubbing a modifier into the paste had represented the first case when direct modification of a CPE had resulted which was aimed at improving of the electrode performance [63]. In 1974, the replacement of common non-electroactive pasting liquids by electrolyte solutions [64] opened the avenue for a specific branch of the electrochemistry of carbon paste electroactive electrodes, allowing one to investigate the redox behaviour as well as various structural and morphological changes of inorganic compounds dissolved directly in the electrolyte. At present, studies of this kind usually belong to a special field of the so-called solid state electrochemistry [65].

In the era of chemically modified carbon pastes for the preparation of a new generation of sensors culminated at the beginning of the 1980s Modification of a carbon paste by impregnating the carbon particles with methanolic solution of dimethylglyoxime [66] It was a first attempt when classic analytical reagent had served as selective modifier, thus initiating a very successful role of chemically modified carbon paste electrodes (CMCPEs) in electrochemical analysis. Biologically modified carbon pastes as enzymatic biosensors were introduced in 1988 to monitor some enzymatically catalysed reactions of biologic substances. The priority in this area can be attributed to Matuszewski and Trojanowicz [67] who have reported on a CPE with glucose oxidase blended into the carbon paste. This way of anchoring enzymes to an electrode material immediately attracted biochemists and carbon paste-based enzymatic biosensors had rapidly come to the fore. More detailed discussions of CMCPEs are contained in review articles covering the period from 1981 to 2000 [68−71].

1.13. Objectives and Scope of the Thesis.

Bioactive molecules are very well suited for analysis using CPE. The reason for it is the active ingredient in it is generally electrochemically active. This is not only an advantage for analysis of pharmaceutical formulations of bioactive molecules, but also for the analysis of pharmaceuticals or their metabolites in body fluids acting as desired sensors. The application of the chemically modified

electrodes in electroanalysis offer several advantages due to their unique electrode surface properties. Therefore, there has been an increasing interest in the creation of chemically modified electrode surfaces that differ from the corresponding bare surfaces. These chemically modified electrodes can lower the over potential, increase the reaction rate and improve the selectivity of some bioactive molecules. With this much of scope it was thought worthwhile to investigate some bioactive molecules of pharmaceutical formulations by using the cyclic voltammetry and differential pulse voltammetric techniques.

The focus of the work covered in this thesis is to controllably alter the properties of carbon surfaces by different modification techniques such as electropolymerisation, chemisorption, grind modification, immobilisation of surfactants and modification using nanoparticles by cyclic voltammetric technique, so that the surfaces are useful for desired sensor applications. Beside the primary goal, the research carried out promotes knowledge at many levels relevant to the interests of the academic community in the field of sensor fabrication, such as preparation, characterisation and application to pharmaceutical and real samples.

The present work is aimed at investigating that the electrode process near the electrode surface is reversible/irreversible or coupled, nature of electron transfer, number of electrons involved, kinetic and diffusion controlled processes, effect of concentration of electroactive species on the redox pathways, effect of pH, nature of the products formed when compounds are reduced or oxidised electrochemically, electrochemical studies and elucidation of the sequence of electron transfer and chemical reactions that occur at or near the electrode surface etc.

More importance has been given not only to the electrochemical behaviour of bioactive molecules but also the versatility of use of carbon paste. The preparation and characterisation of bare and chemically modified carbon paste electrode surface has been studied. Thorough characterisation of carbon paste electrode before and after modification has been studied. The electrochemical properties, carbon composition and surface roughness of both the surfaces are examined.

Present work is also aimed at the development of voltammetric sensors for the detection of bioactive molecules such as UA, DA, AA and which are also neurotransmitters present in the extracellular fluid of the central nervous system, Dicyclomine Hydrochloride is an antibacterial potential of an antispasmodic drug, L-Tyrosine is a bioactive amino acid, Ciprofloxacin hydrochloride is a fluoroquinolone antibiotic, Enrofloxacin is a synthetic fluroquinoline antimicrobial agent. These bioactive molecules at bare electrodes are generally undergoes redox reactions at very similar potentials and often suffers from pronounced fouling effects Hence there is need for the development of modified electrodes because of its high selectivity and sensitivity due to the film homogeneity in electrochemical deposition, strong adherence to the electrode surface and chemical stability of the film. In addition to analytical aspects the electrochemical studies of these biologically active species serve to elucidate their biological process and their interrelationship that are involved in living organisms. CV has been used to establish the electrochemical behaviour of the given molecules through mechanistic studies. Because the biological electrons transfer reactions are complicated, though they have many things in common. Both involves essentially heterogeneous electron transfer process, pH and temperature dependent and occur at electrode/electrolyte interface or membrane/solution interface. Hence, explanations based on electrochemistry have played an important role in interpreting and understanding the biological phenomena.

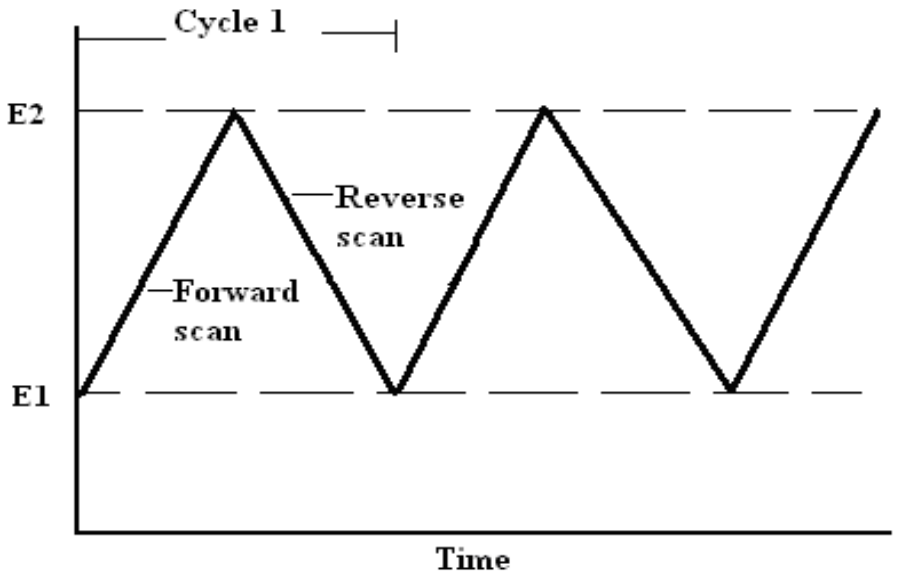

Fig.1.1. Variation of the applied potential as a function of time in a cyclic voltammetry experiment.

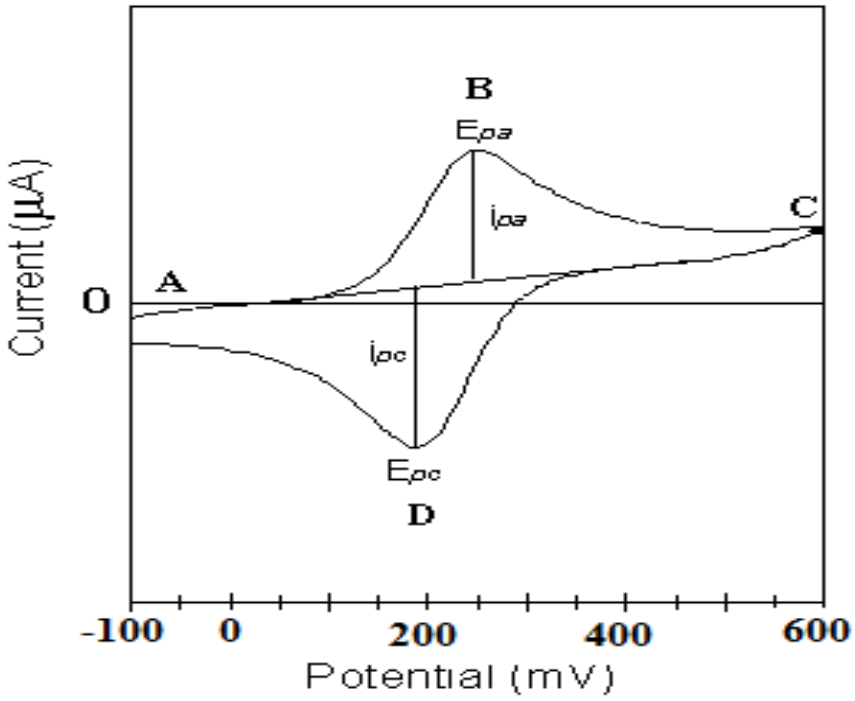

Fig.1.2. A typical cyclic voltammogram of current verses potential

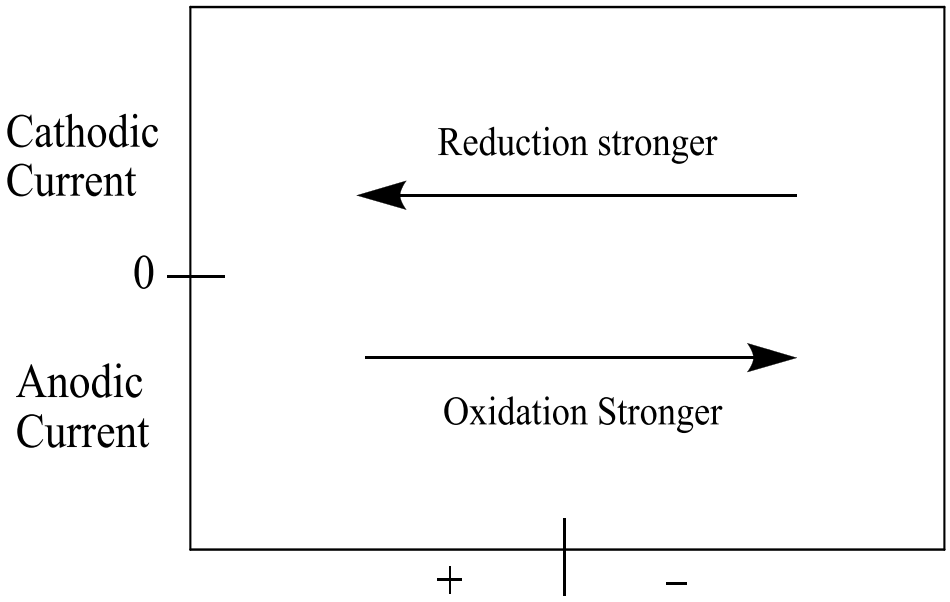

Fig. 1.3: Potential-Current axes for Cyclic Voltammetry

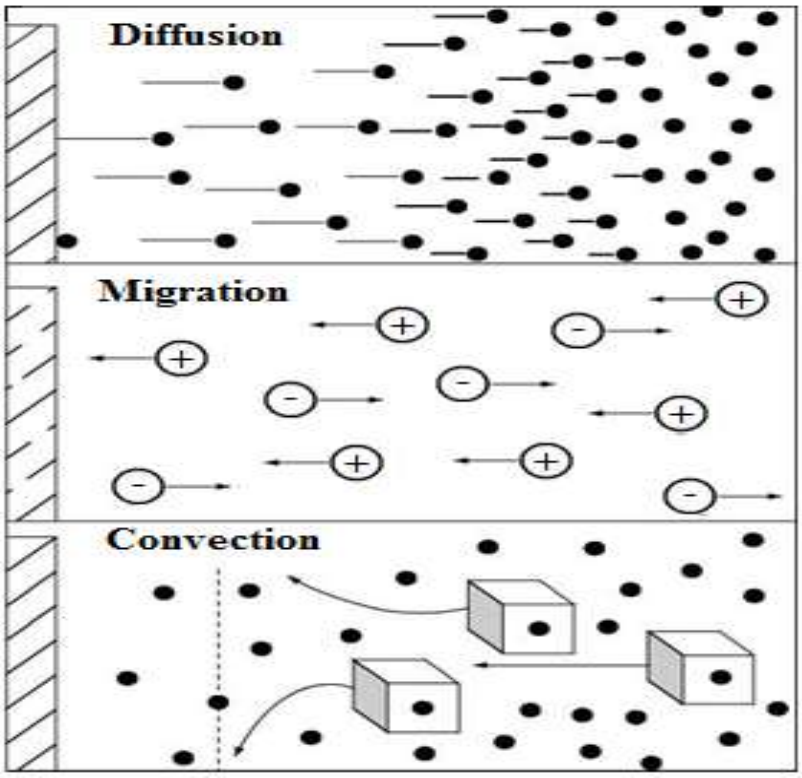

Fig. 1.4: Modes of mass transport

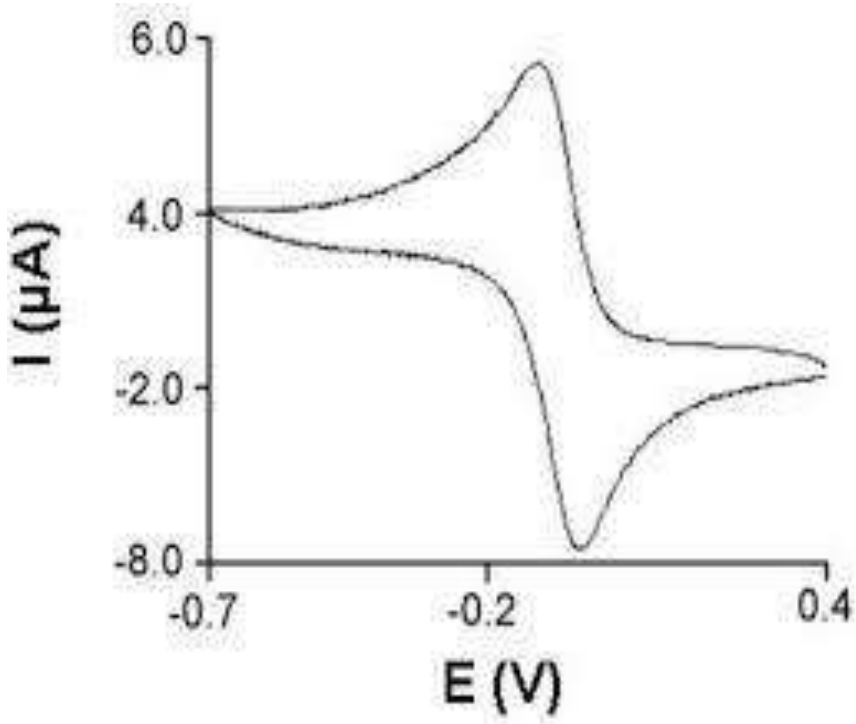

Fig. 1.5: Typical voltammogram for a reversible process

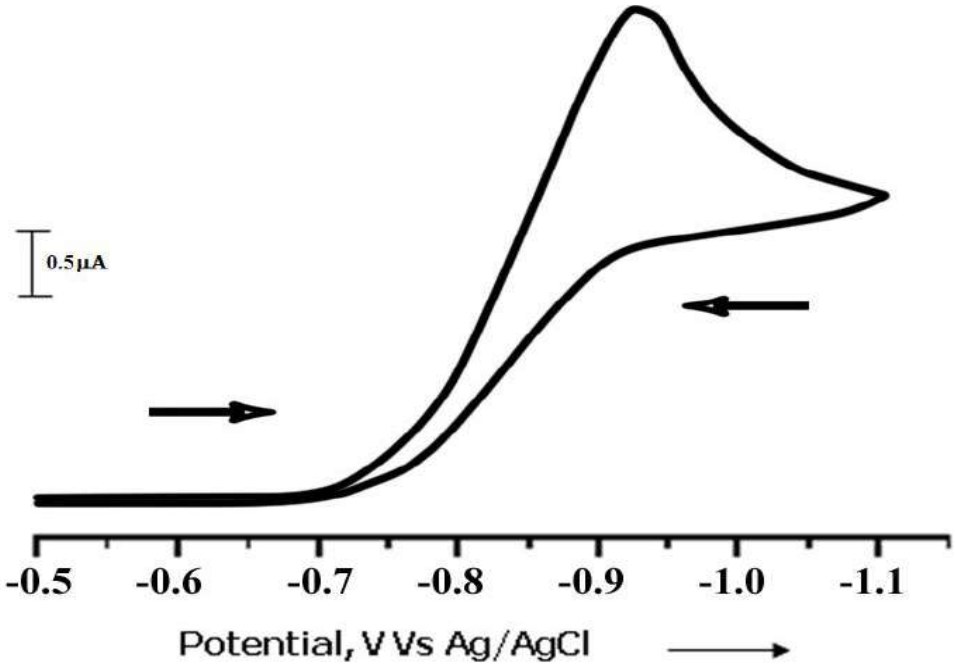

Fig. 1.6: Typical voltammogram for an irreversible process.

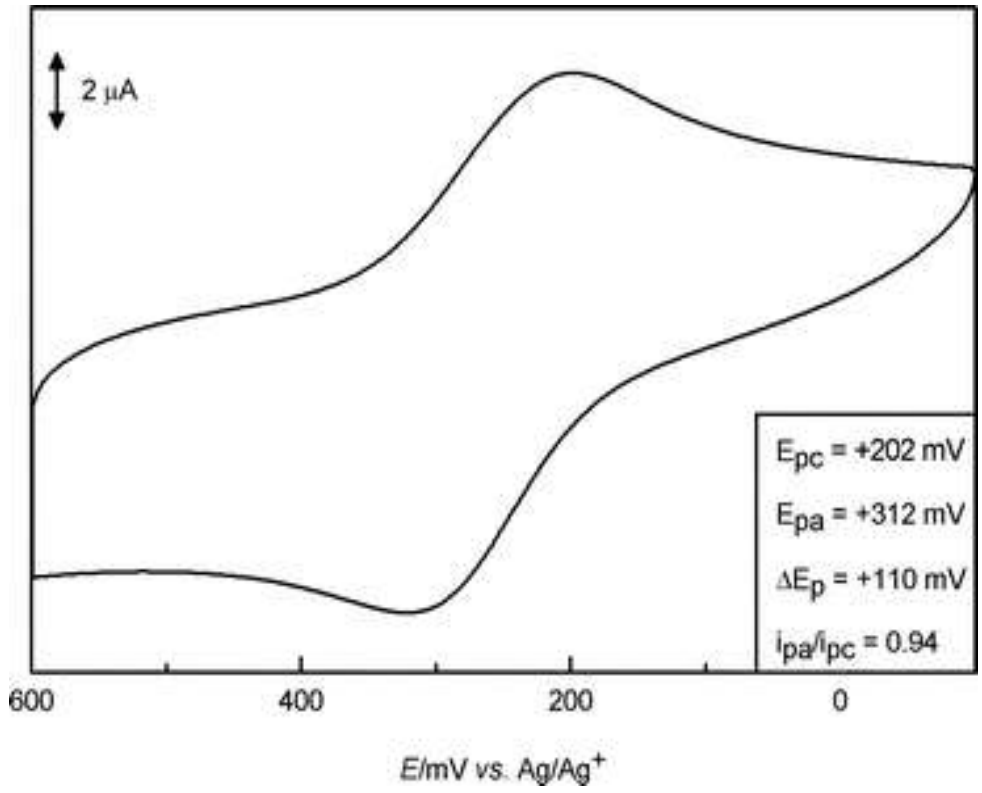

Fig. 1.7: Typical voltammogram for a quasi-reversible process

1.14. References

[1] A.J. Bard and L.R. Faulkner, *Electrochemical Methods*, (Jon Wiley, New York), 1980.

[2] J. Wang, *Analytical Electrochemistry*, (VCH Published Inc. New York), 1994.

[3] R.L. McCreery and K.K. Kline, *Laboratory Techniques in electroanalytical chemistry*, 2nd Edition (P.T. Kissinger, and W.R. Heineman eds) Dekker, New York, 1995 Chap.10.

[4] R.L. McCreery, *Electroanalytical chemistry*, (A.J. Bard ed.) Dekker, New York, **17** (1991) 221.

[5] R.L. McCreery, M. Callstrom, T. Neenan, D. Alsmeyer and Y. Wang, *Front. Chem.*, **2** (1990) 27.

[6] K. Kalcher, *Electroanalysis*, **2** (1990) 419.

[7] K. Kalcher, J.M. Kauffmann, J. Wang, I. Svancara, K. Vytras, C. Neuhold and Z. Yang, *Electroanalysis*, **7**(1995) 5.

[8] K. Kalcher, X. Cai, G. Kolbl, I. Svancara and K. Vytras, *Sb. Ved. Pr, Vys. Sk, Chemickotechnol, Pardubice*, **57** (1995) 5.

[9] I. Svancara, K. Vytras, F. Renger, M.R. Smyth and G. Kolbl, *Sb. Ved. Pr, Vys. Sk, Chemickotechnol, Pardubice*, **56** (1992).

[10] I. Svancara, K. Vytras, *Chem. Listy.*, **88** (1994) 138.

[11] J. Wang, *Analytical Electrochemistry*, (VCH Publishers Inc., New York), 1994.

[12] J. Wang, D.B. Luo, P.A.M. Farias and J.S. Mahmoud, *Anal. Chem.*, **57**(1985)158.

[13] J. Randles, *Trans. Far. Soc.*, **44** (1948) 327.

[14] A.E. Kaifer and M. Gomez-Kaifer, *Supramolecular Electrochemistry*, (Willey, VCH, New York), 1999.

[15] A.J. Bard and L.R. Faulkner, *Electrochemical Methods: Fundamentals and Applications*, (John Willey & Sons), 1996.

[16] D.G. Davis, in D. Dolphin, Ed., *Physical Chemistry: The porphyrins*, Part A, Vol. **III**. Academic Press, NY, 1978, Ch. 4.

[17] E.R. Brown and R.F. Large, *Physical Methods of Chemistry*, Vol.1-Part IIA: Electrochemical Methods, eds. A. Weissberger and B. Rossiter, (Willey-Interscience, New York), 1971.

[18] S. Ono, M. Takagi, T. wasa, *J. Am. Chem. Soc.*, **31** (1958) 356.

[19] S.P. Perone, W.J. Kretlow, *Anal. Chem.*, **38** (1966) 1760.

[20] A. Aldaz, R. Jimenez, C. Piazza and J.L. Vazquez, *Anal. Quim.*, **70** (1974) 410.

[21] D.H. Evans, K.M. O'Connell, R.A. Petersen and M.J. Kelly, *J.Chem.Educ*., **60** (1983) 290.

[22] G.A. Mabbott, *J.Chem.Educ*., **60** (1983) 697.

[23] C.M.A. Brett and A.M.O. Brett, *Electrochemistry: Principles Methods and Applications*, (Oxford University Press), 1993.

[24] J. Bockris and S.U.M. Khan, *Surface Electrochemistry*: *A Molecular Level Approach*, Plenum Press, (New York and London), 1993.

[25] J.P. Renault, A. Bernard, A. Bietsh, B. Michel, H.R. Bosshard, E.B. Dalamarche, M. Kleiter, B. Hecht and U.P Wild, *J. Phys. Chem. B.*, **107** (2003) 703.

[26] R.S. Nicholson, *Anal. Chem.*, **37** (1965) 1351.

[27] R.S. Nicholson, I. Shain, *Anal. Chem.*, **37** (1965) 190.

[28] R.S. Nicholson, I. Shain, *Anal. Chem.*, **36** (1964) 706.

[29] M. Noel, K.I. Vasu, *Cyclic Voltammetry and the Frontiers of Electrochemistry*, 1st ed. (Oxford & IBH Publishing Co.Pvt.Ltd. New Delhi) 1990, p 174.

[30] R. Lines, V.D. Parker, *Acta Chem.Scand. B*., **31** (1977) 368.

[31] E. Peled, A. Mitavski, A. Reger and E. Gileadi, *J.Electroanal.Chem*. **75** (1977) 677.

[32] M. Elam, I. Eahatt, E. Peled and E. Gileadi, *J.Phys.Chem*., **88** (1984) 1609.

[33] D.T. Sawyer, J.E. Roberts, *Jr. Experimental Electrochemistry for Chemists*, (Wiley Interscience, New York), 1974.

[34] C.K. Mann, *Electroanal.Chem*., **3** (1969) 57.

[35] H. Lund, *Organic Chemistry*, (M.M. Baizer and H. Lund Eds, mercel, Dekker, New York), 1983, p 161.

[36] B.E. Conway, H. Angerstein-Kozlowska, W.B.A Sharp and E.Criddle, *Anal. Chem*., **45** (1973) 1331.

[37] O. Hammerich, V.D. Parker, *Electrochim.Acta*, **18** (1973)537.

[38] L. Meites, *Polarographic Techniques*, 2nd ed, Wiley intersceince, New York (1958).

[39] R.E. Panzer, P.J. Elving, *Electrochica Acta*, **20** (1975) 635.

[40] J.P. Randin, *Encyclopedia Electrochem. Elements*, **5** (1976) 1.

[41] L. Gorton, J. Chem. Soc. *Faraday Trans.*, **82** (1986) 1245.

[42] M. Lobo, A. Miranda, P. Tunon, *Electroanalysis*, **9** (1997) 191.

[43] A.J. Bard, L.R. Faulkner, R. Larry, 2nd ed, Wiley, 2000.

[44] P. Kissinger, R. William, Heineman 2nd ed, Rev, *CRC.*, 1996.

[45] Zoski, G. Cynthia, *Elsevier Science*., 2007.

[46] R. Parsons, *Surface Science*, **2** (1964) 418.

[47] D.K. Grosser, *Cyclic voltammetry, simulation and analysis of reaction mechanisms*, (VCH Publishers, Inc.,), 1993.

[48] A.J. Bard and L.R. Faulkner, *Electrochemical methods fundamentals and applications*, 2nd ed, (John Wiley& Sons Inc.,), 2001.

[49] J. Cooper and T. Cass, *Biosensors*, 2nd ed, (Oxford University Press Inc.,) New York, 2004.

[50] S. Hou, N. Zheng, H. Feng, X. Li and Z. Yuan, *Anal.Biochim.*, **179** (2008) 179.

[51] X. Lin, G. Kang, L. Lu, *Bioelectrochem.*, **70** (2007) 235.

[52] R.S. Nicholson, I. Shain, *Anal. Chem.*, **36** (1964) 706.

[53] J.J.V. Benschoten, J.Y. Lewis, W.R. Heineman, D.A. Roston and P.T. Kissinger, *J. Chem. Educ*., **60** (1983) 772.

[54] A.W. Bott, *Current Separations*, **16** (1997) 61.

[55] D.H. Evans, *Acc.Chem.Res.*, **10** (1997) 313.

[56] W.R. Heineman, P.T. Kissinger, *Am. Lab.*, **14** (1982) 29.

[57] D.H. Evans, K.M.O. Connell, R.A. Peterson and M.J. Kelly, *J. chem. Edu*., **60** (1983) 290.

[58] P.T. Kissenger, W.R. Heinmen, *J. chem. Edu*., **60** (1983) 702.

[59] R.N. Adams, *Anal. Chem.*, **30** (1958) 1576.

[60] P.T. Kisinger, *Electroanalysis*, **11** (1999) 292.

[61] R.N. Adams, *Rev. Polarog (Japan).,* **11** (1963) 71.

[62] T. Kuwana, W. G. French, *Anal. Chem*., **36** (1964) 241.

[63] L.S. Marcoux, K.G. Prater, B.G. Prater and R.N. Adams, *Anal. Chem.,* **37** (1965) 1446.

[64] D. Bauer, M. P. Gaillochet, *Electrochim. Acta*, **19** (1974) 597.

[65] F. Scholz, B. Meyer, *Chem. Soc. Rev.,* (1994) 341.

[66] K. Ravinchandran, R. P. Baldwin *J. Electroanal. Chem*., **126** (1981) 293.

[67] W. Matuszewski, M. Trojanowicz, *Analyst*, 1**13** (1988)735.

[68] K. Kalcher, *Electroanalysis*, **2** (1990) 419.

[69] N.A. Ulakhovich, E.P. Medyantseva, G.K. Budnikov, *Zh. Anal. Kh.,* **48** (1993) 980.

[70] K. Kalcher, J.M. Kauffmann, J. Wang, I. Svancara, K. Vytras, C. Neuhold and Z. Yang, *Electroanalysis*, **7** (1995) 5.

[71] K. Kalcher, K. Schachl, I. Svancara, K. Vytras and H. Alemu, *Sci. Pap. Univ. Paradubice, Ser. A.,* **3** (1997) 57.

Chapter-2

EXPERIMENTAL

2.1. Introduction

This chapter describes the experimental techniques and instruments used for the detection of electrochemical behaviour of bioactive molecules at modified electrodes. The electrode system with special emphasis the carbon paste electrodes used in this research is outlined. The method of preparation and characterization of modified carbon paste electrode, polymer film modified carbon paste electrode has been described.

2.2. Experimental Techniques

The chief electrochemical / analytical techniques used throughout this study were cyclic voltammetry, differential pulse voltammetry, and scanning electron microscope (SEM), X-ray diffraction (XRD) and ultraviolet visible (UV/Vis) spectrophotometer. A brief overview of each technique is given below.

2.2.1. Cyclic Voltammetry (CV)

It consists of cycling the potential of an electrode which is immersed in an unstirred solution of the electro active species and then measuring the resulting current. A potential of this working electrode is controlled versus a reference electrode like as a saturated calomel electrode (SCE) or a silver/silver chloride electrode (Ag/AgCl). A controlling potential that is applied across these two electrodes can be considered as excitation signal. The excitation signal for CV is a linear potential scan with a triangular waveform as shown in **Fig.2.1**. This triangular potential excitation signal sweeps the potential of the electrode between two values, many times known as the switching potentials. The excitation signal in Figure causes the potential first to scan negatively from +0.80 (initial potential) to -0.20 V (E_f final potential) versus SCE at which point the scan direction is reversed, resulting a positive scan back to the original potential of +0.80 V (E_i). The scan rate as reflected by the slope is 50 mV per second as shown in **Fig.2.1**. A second cycle is indicated by the darked line. One or multiple cycles can be used. Cyclic voltammetry or CV is a type of potentiodynamic electrochemical measurement. In a cyclic voltammetry experiment the working electrode potential is ramped linearly

versus time. Unlike in linear sweep voltammetry, after the set potential is reached in a CV experiment, the working electrode's potential is ramped in the opposite direction to return to the initial potential. These cycles of ramps in potential may be repeated as many times as desired. The current at the working electrode is plotted versus the applied voltage (i.e., the working electrode's potential) to give the cyclic voltammogram trace. Cyclic voltammetry is generally used to study the electrochemical properties of an analyte in solution [1 - 3].

2.2.2. Differential Pulse Voltammetry (DPV)

An electrochemical technique where the cell current is measured as a function of time and as a function of the potential between the indicator and reference electrodes. The potential is varied using pulses of increasing amplitude and the current is tested before and after each voltage pulse. Pulse voltammetry was developed to improve the sensitivity of voltammetric measurements. This is achieved by reducing the double layer capacitance to zero so that the current recorded is totally faradaic. In differential pulse voltammetry, the base potential is incremented and increased at a fixed rate. The pulses applied are of the same magnitude each time. The current is measured shortly before the pulse is applied and at the end of the pulse. The difference between these two values is recorded and plotted as a function of the applied potential.

2.2.3. Scanning Electron Microscope (SEM)

A scanning electron microscope (SEM) is a type of electron microscope that produces images of a sample by scanning it with a focused beam of electrons. The electrons interact with atoms in the sample, producing various signals that can be detected and that contain information about the sample's surface topography and composition [4-9]. SEM can achieve resolution better than 1nm. The most common SEM mode is detection of secondary electrons emitted by atoms excited by the electron beam. In this study a model JEOI-SEM 6360 was employed to study the size and structure of the polymer modified carbon paste electrode.

2.2.4. X-ray diffraction (XRD)

When an electron from the inner shell of an atom is excited by the energy of a photon, it moves to a higher energy level, which is shown as an outer shell; the difference in energy is emitted as a photon which has a wavelength that is characteristic for the element (there could be several of characteristic wavelengths per element). Analysis of the X-ray emission spectrum produces qualitative results about elemental composition of the specimen. Comparison of spectrum of the specimen with spectra of standards of known composition produces quantitative results (after some mathematical corrections for absorption, fluorescence and atomic number). X-rays can be excited by a high-energy beam of charged particles such as electrons (as in electron microscope) or protons (see PIXE), or a beam of X-rays (see X-ray fluorescence, or XRF). These methods enable elements from the entire periodic table to be analyzed, with the exception of H, He and Li. In electron microscopy electron beam excites X-rays; there are two main techniques for analysis of spectrum of characteristic X-ray radiation. In a wavelength dispersive X-ray spectrometer the single crystal diffracts the photons (Bragg's law) which are collected by a detector. Without any motion there will be just one wavelength detected. By moving crystal and detector, a wide region of spectrum is observed (to collect all parts of spectrum three of four different single crystals may be needed). In contrast to EDS, WDS method is a method of sequential spectrum acquisition. While WDS is slower than EDS and more sensitive to positioning specimen in the spectrometer, it has superior spectral resolution and sensitivity. WDS is widely used in microprobes (where X-ray microanalysis is the main task) and in XRF. It is widely used in the field of x ray diffraction to calculate various data such as interplaner spacing, wavelength of incident x ray by using Bragg’s law.

2.2.5. UV-Visible Spectrophotometer

UV-Vis Spectrophotometer is also used in the semiconductor industry to measure the thickness and optical properties of thin films on a wafer. UV-Vis spectrometers are used to measure the reflectance of light, and can be analyzed via the Forouhi-Bloomer dispersion equations to determine the Index of Refraction (n) and the Extinction Coefficient (k) of a given film across the measured spectral

range. The method is most often used in a quantitative way to determine concentrations of an absorbing species in solution, using the Beer-Lambert law:

$$A = \log (I_0 / I) = \varepsilon c L$$

Where A is the measured absorbance, in **A**bsorbance **U**nits (**AU**), I_0 is the intensity of the incident light at a given wavelength, I is the transmitted intensity, L is the path length through the sample, and c the concentration of the absorbing species. For each species and wavelength, ε is a constant known as the molar absorptivity or extinction coefficient. This constant is a fundamental molecular property in a given solvent, at a particular temperature and pressure, and has units of 1/M ∗ cm or often AU/M ∗ cm. The absorbance and extinction ε are sometimes defined in terms of the natural logarithm instead of the base-10 logarithm. The Beer-Lambert Law is useful for characterizing many compounds but does not hold as a universal relationship for the concentration and absorption of all substances.

2.3. Instrumentation and Basic Equipment

2.3.1. Potentiostat

Potentiostat is one of the most widely used instrument in electrochemical studies and makes possible the performance of techniques such as cyclic voltammetry. The principal function of a potentiostat is to control potential and measure current. The conventional three-electrode potentiostat is connected to the working, reference, and auxiliary electrodes immersed in the test solution. The potentiostat operates with a three electrode system in an analytical cell. The three electrode system function is to maintain the potential of working electrode at a desired level with respect to a fixed reference electrode (RE). While simultaneously measuring the current flowing between the WE and the auxiliary electrode (AE) **(Fig.2.2)**. The potentiostat performs the following functions:

- Controls the applied potential, which is potential difference between the WE and RE (the applied potential controls what half reactions occur at the WE).

- Allows to pass current between the WE and AE without passing current through the RE (which would change its potential if current did pass through it) and

- Converts the cell current to a voltage for recording devices.

2.3.1.1. Potentiostat employed in the present work for CV and DPV experiments

The electrochemical experiments were carried out using potentiostat provided with the Data Acquisition PC interface Card Model EA-201 Electro analyser fabricated by Chemi Link Systems, Trombay, Mumbai, India; compatible with an IBM PC and coupled to a printer (**Fig. 2.3).** This instrument is capable of performing more than six electro analytical techniques. The instrument incorporates a high speed, high accuracy and an electrolysis mode that consists of high-gain operational amplifier with circuits for controlled potential.

The WE current signal is handled a bit differently. This signal line is also presented as a voltage signal, but the voltage level is actually proportional to the current flowing at the WE. The potentiostat has an internal 'current converter' circuit that performs the necessary current-to-voltage conversion automatically. The current converter has a number of ranges and the operator is expected to choose the range most appropriate for the experiment being performed. Each range is associated with a particular proportionality constant, such as '100 mA/V' or '1 mA/V'.

2.3.2. Recording Device

Computers entered into electroanalytical instrumentations in 1967 [10] or even earlier. Computers applications in stationary electrode voltammetry [11] and CV [12-14] were reported. Computers can be used to apply potential programmes to the working electrode through the potentiostat. The initial potential, final potential, sweep rate, nature of the pulse; current sensitivity etc. may be instructed to the computer in the digital form. Computers can be used very effectively in data acquisition. The applied potential values and the resulting current values may be converted to the digital information by A/D converter and this improves the signal to

noise ratio of the experimental cyclic voltammograms. Computers can repeat each experiment under identical conditions. Computers are used for the data analysis. It measures peak current or peak potential very accurately [15, 16], by subtracting of background current [12]. Voltammetric curves may be differentiated to obtain peak potentials with greater precision [17]. The information thus obtained such as peak current, peak potential, and peak width at various concentrations may then be correlated with theoretical predictions for establishing the nature of process and for evaluating the rate parameters.

2.3.3. Electrochemical Cell

The electrochemical cell is a single piece of glassware capable of holding an appropriate volume of a test solution (i.e. an electrolyte through which charge transfer can take place by the movement of ions) containing one or more electroactive analytes. Immersed in this solution are three electrodes (working, reference and auxiliary) that are also electrically connected to a potentiostat. An electrode may be considered to be an interface at which the mechanism of charge transfer changes between electronic (movement of electrons) and ionic movement of ions. The electrode in the cell are positioned using an appropriate cell top made of chlorotrifluoroethylene (CTFE) plastic material and appropriate CTFE o-rings. The cell top also provides space for the incorporation of nitrogen line to purge nitrogen gas to remove any dissolved oxygen in solutions.

A standard three-electrode electrochemical cell configuration employed for all electrochemical experiments in the present work is as shown in **Fig. 2.4**. The WE used is a bare carbon paste electrode (CPE) / modified carbon paste electrode. The RE was a saturated calomel electrode (SCE) and the AE consisted of a platinum wire. This cell was then connected to a potentiostat and the results were recorded by a computer in the manner shown in **Fig 2.2**. In general, the potential is measured between the RE and the WE and the current is measured between the WE and the CE. The electrochemical cell consisted of these three electrodes, unless otherwise stated.

2.3.4. pH Meter

A pH meter is an electronic instrument used to measure the pH (acidity or alkalinity) of a liquid (though special probes are used to measure the pH of semi-solid substances). A typical pH meter consists of a special measuring probe (a glass electrode) connected to an electronic meter that measures and displays the pH reading. A pH meter manufactured by Systronics digital pH Meter 335 was used for measuring and adjusting pH of the solution making use of a combination of glass and saturated calomel electrode.

2.4. Working Electrodes

In the present work three electrode system is used i.e. WE / AE / REs. The RE used is standard calomel electrode (SCE) which is often isolated from the solution by a salt bridge to prevent contamination by leakage from the RE. The platinum foil as AE and WEs are carbon paste electrode, and modified carbon paste electrode. The performance of the voltammetric procedure is strongly influenced by the working electrode material. The working electrode should provide high signal-to-noise characteristics, as well as a reproducible response.

Solid electrodes based on carbon are currently in widespread use in electroanalysis, primarily because of their broad potential window, low background current, chemical inertness, low cost and suitability for various sensing and detection applications. In contrast, electron transfer rates observed at carbon surfaces are slower than those observed at metal surfaces. The electron transfer activity is affected by the carbon surface structure. A variety of electrode pre-treatment procedures have been proposed to increase the electron transfer rates. The type of carbon, as well as the pre-treatment method, has a profound effect upon the analytical performance. The most popular carbon-electrode materials are glassy carbon, carbon paste, carbon fibre, carbon films, or carbon composites.

2.4.1. Carbon paste as electrode material

2.4.1.1. Unmodified Carbon Paste

Some carbon pastes may not be totally compact immediately after homogenization but the required consistency can be achieved by pressing such mixtures into electrode holders. Binary mixtures prepared from carbon powder and organic liquid of non-electrolytic character are known as unmodified (bare or virgin) carbon pastes [18]. The proper electroactive moiety in carbon pastes is still graphite powder with micrometric particles of high purity and distribution uniformity. Such materials are now commonly available on the market as spectroscopic graphites. Non-electrolytic binders such as Nujol [19-21] and Silicone oil [22] are non-polar pasting liquids fulfil all the important criteria; both are sufficiently insulating, chemically inert, water-immiscible non-volatile, and forming paste mixtures of fine consistency. Silicone oil could be used in non-aqueous solvents also.

2.4.1.2. Modified Carbon Pastes

In recent years electrochemists have become interested in modifying an electrode by, coating, adsorbing or attaching specific molecules to the surface. This deliberate and controlled modification of the electrode surface can produce electrodes with new and interesting properties that may form the basis of new applications and novel devices. The base of modified carbon pastes is usually a mixture of powdered graphite and non-electrolytic binder [18, 20, 23]. Another important constituent in the mixture is then a modifier itself. Modifying agent is usually one substance; but, the pastes can also be modified with two or even more components, which is the case of carbon paste-based biosensors containing enzyme (or its carrier) together with appropriate mediator [21] or chemically modified carbon paste electrode (CMCPEs) with a mixture of two modifiers [24] The amount of modifier in the paste usually varies between 10-30% (w/w), depending on the character of modifying agent and its capability of forming enough active sites in modified paste e.g., functional groups immobilised at the electrode surface [25] or molecules of an extractant in the bulk [26]. In general, the main reason for

modifying an electrode is to obtain qualitatively new sensor with desired, often pre-defined properties like:

- ✓ To reduce the over potential
- ✓ To get better catalytic effects
- ✓ Increase the reaction rate
- ✓ A better insight into the nature of charge transfer and charge transport processes in thin films.
- ✓ Improve the selectivity of some bioactive molecules
- ✓ For the new applications like chiral induction or other desired groups.
- ✓ Design of electrochemical devices and systems for applications in chemical sensing, energy conversion and storage.
- ✓ Molecular electronics, electrochromic displays and electro-organic synthesis.

In this thesis various modifiers were adopted are Terbutaline Sulphate, Dicyclomine hydrochloride, Tin (IV) oxide nanoparticles, Nickel tin (IV) oxide nanoparticles, Manganese tin (IV) oxide nanoparticles, Furosemide, Isoniazid and the modified electrodes were prepared by several different techniques like:

- ✓ Electropolymerisation
- ✓ Grind modification
- ✓ Surface modification by Immobilization and mobilization

Macrocyclic-modified electrode surfaces can be prepared by **electropolymerization** of monomeric species bearing suitable functional groups onto the surface. In recent year's polymer-film modified electrodes has become a preferred method for the construction of chemically modified electrodes (CMEs) because of their good stability, reproducibility, three dimensional distribution of mediators compared to monolayer's and their wide applications in the fields of

chemical sensors and biosensors. Polymer layers can be produced by inducing the polymerisation of monomers at the electrode surface by electrochemical means. Several types of polymer electrodes have been studied [27-30]. In some, the polymer itself is electroactive and can undergo redox reactions. In others the polymer acts as polyelectrolyte that is a material which contains ionic groups, which can extract charged ions from the solution and hold them by electrostatic binding.

In **grind modification** the modifier is mixed mechanically to the paste during its homogenisation [31, 32]. The modifier might combine with the substrate in certain forms and strengthen their adsorption on the electrode surface, which facilitated the electron or substance transfer between the electrode and the solution and alter the properties of the electrode/solution interface and finally influence the electrochemical process of electroactive species [33-36].

Surface modification by Immobilization and mobilization is the simplest method and consists of the adsorption due to electrostatic, hydrophobic or dispersive forces on the electrode surface. Surface modification forms an insulating layer which is much more stable. This can be achieved by immersing or immobilising the electrode with the required molecules in solution. e.g., Surfactants [37-41].

2.4.2. Construction and Design of Carbon Paste Electrodes

The proper selection of both carbon powder and pasting liquid along with construction and design of CPE influences the resultant behaviour of CPE [18, 23].The proper construction and design of CPE is based on short Teflon rod (shaped as a robust plug) with a well drilled in and a Pt-wire which provides electrical contact with the external circuit. New portions of carbon paste can be easily re-filled into the end-hole of Teflon rods each time [32, 37-40 and 42]. Various glasses, PVC tubes, simple constructions equipped with a piston for extrusion of the paste [22, 42] are also frequently employed. For common CPEs, the actual diameter of the end-hole forming the proper carbon paste surface is being chosen from 2 to 10 mm, which is convenient for a majority of electrochemical measurements. Both above-mentioned construction variants of CPEs for batch measurements allows to utilise fully one of the most valuable property of carbon pastes easy and quick surface

renewal or, in necessary cases, even removal and renewing of a larger portion of the paste. Practically immediate surface renewal can be achieved by wiping some paste off using a wet filter paper. If being performed carefully [22, 24] this procedure provides surface reproducibility nearly comparable to that attained by rather time-consuming circle-like polishing of the electrode surface upon a paper pad [43].

2.4.3. Choice of carbon (graphite) powder

The carbon powders with uniformity of size distribution, high purity and more or less suppressed adsorption capabilities [18, 44] are preferred in current based measurements techniques like voltammetry, coulommetry or amperometry as the main component which ensures the proper function of an electrode or a sensor in electrochemical measurements. Suitable carbonaceous materials should obey the following criteria:

i) Particle size in micrometers

ii) Uniform distribution of the particles

iii) High chemical purity and

iv) Low adsorption capabilities.

Naturally, the type and quality of graphite used, as well as its overall amount in the carbon paste mixture, are reflected in all typical properties of the respective mixture. From the early era of CPEs up until now, the most often selected carbon powder is spectroscopic graphite with particles in the low micrometric scale (typically, 5 – 20 mm).

2.4.4. Choice of binders (Pasting Liquids)

The chief function of binder or pasting liquid is to link mechanically the individual graphite particles. However, beside this main function, the binder as the second main purpose i.e. binders give rise to hydrophobic character of the carbon paste surface, which is in principle the main reason for different behaviour of carbon paste electrode compared to carbon solid electrodes [18, 23, 44]. The presence of

pasting liquid at the surface decreases the transfer rate (slower kinetics) causing the higher over potential compared to homogeneous electrodes [45]. The increasing lipophility of the pasting liquid enhances the electrode over potential (irreversibility). This is due to the marked hydrophobicity of the liquid which hinders the access of analyte towards the surface. Typical parameters required for pasting liquids should be:

i) Non conducting non volatile

ii) Minimal solubility in aqueous solutions

iii) Chemical inertness and electro inactivity

iv) High viscosity and low volatility and

iii) Immiscibility with organic solvents.

iv) The most popular binding agents used for preparation of carbon pastes are mineral (paraffin) oils such as Nujol oil and various silicone oils [37]. Also room-temperature ionic liquids (R ILs or ILs, respectively) have soon come into the fore of research interest, which is also reflected in the electrochemistry with carbon pastes [46 - 53].

2.4.5. Preparation of Carbon Paste Electrode

Carbon pastes can be done by simply hand mixing the graphite powder with an appropriate amount of mineral oils such as Nujol or various silicone oils. A clean glass rod is used to mix both the components carefully. A homogeneous carbon paste is thus prepared by thorough hand mixing in a mortar and pestle by rubbing and intensive pressing with the pestle for effective homogenization. The paste is scrapped off the wall with a spatula and ultimately homogenized again and this step is repeated several times. The paste is kept for 24 hours for self-homogenization. The ready prepared paste is then packed into the well (hole) in the electrode body. Its filling is made in small portions when each of them being pressed intimately before adding the next one.

The bare carbon-paste electrode in the present study was prepared by mixing graphite powder (70%) with an appropriate amount of silicone oil (30%) and thorough hand mixing in a mortar and pestle to produce a homogenous paste. The portion of the mixture was packed into the end of Teflon rod (i.e. 3 mm) and then smoothened on a weighing paper. Electrical contact was made by a copper wire provided at the end of the tube **(Fig.2.5**).

2.4.6. Physicochemical and Electrochemical Characteristics of Carbon Pastes

2.4.6.1. Surface Renewal of the Carbon Pastes

Mechanical renewal of CPE is one of the quickest and effective method Easy and quick surface renewal is one of the key advantages of carbon pastes both in bare and modified forms [21]. Practically Immediate surface renewal is achieved by wet filter paper or wiping of the used carbon paste layer with a soft tissue or simple mechanical removal and renewing it with a fresh paste. If being performed carefully [22, 43], this procedure provides surface reproducibility in few seconds nearly comparable to that attained by rather time-consuming circle-like polishing of the electrode surface upon a paper pad and with other solid electrodes [54].

2.4.6.2. Ageing of Carbon Pastes

Bare carbon pastes containing silicone oils or paraffin, are reported to be stable for months or, if stored properly, even some years [55]. Nevertheless, some special mixtures made of more volatile binders (e.g., organic esters [56, 57]) may dissociate within a few weeks only.

2.4.6.3. Paste composition and surface states on electron transfer rate and ohmic Resistance of Carbon Pastes

Dry graphite gives electron transfer rates which give an almost Nernstian response and approach those obtained with platinum. The addition of typically insulating pasting liquid or binders such as paraffin and silicone oils are decreases these rates. But despite the presence of these pasting liquids carbon paste mixtures exhibit a very low ohmic resistance. These carbon pastes made of paraffin oil had

the average resistances of 20 – 50 Ω, whereas some silicon oil-based CPEs were reported to have the resultant values even below 10 Ω [22]. It seems that minimal resistance of carbon pastes can be due to the tightest systematic arrangement of spherical particles [58].

2.4.6.4. Potential range and background currents of the Carbon Pastes

The polarizability of carbon paste electrode for both anodic and cathodic potential ranges, as well as the background level, can be controlled effectively via the quality of graphite and the binder as well as their ratio [18, 23, 44].

In faradic measurements with common types of carbon paste electrode and chemically modified carbon paste electrode, the background currents are typically below 1μA [59] which could be used for definition of both anodic and cathodic limits and of the resultant potential range (window). If so, the operational range is normally between -1.0V and 1.0V vs. SCE, varying in dependence of the actual pH and concentration of the solution chosen.

2.4.6.5. Storage of Carbon Paste Electrode

The carbon paste electrode could be placed in a beaker containing distilled water and the tip filled with the paste is completely dipped down to the water level. Such storage prevents the desiccation of carbon paste. The CPE stored in this manner exhibits very stable behaviour.

2.5. Chemicals and Solutions

The chemicals used throughout this study were purchased from Sigma-Aldrich (Bangalore India), Himedia chemicals (Mangalore, India) and spectroscopically pure graphite powder was obtained from SDFC Chemie. All chemicals were used as supplied. All stock solutions were prepared freshly before each experiment. The electrolytes used were all buffer solutions like phosphate buffer except HCl. The pH of the solutions was adjusted using orthophosphoric acid and NaOH. Further details regarding chemicals and reagents used are discussed in the respective working chapters.

2.6. Removal of Dissolved Oxygen

It is essential to eliminate the dissolved oxygen from the test solution whenever moderate to quite negative potentials are applied to the working electrode since oxygen is capable of dissolving in aqueous solution in millimolar levels at room temperature and pressure. Therefore the solution in the electrochemical cell was deoxygenated by vigorously bubbling an inert gas such as nitrogen using a purge tube. Oxygen undergoes reduction in the potential range approximately between –0.05 V and -0.9 V as given below in one of the two steps:

$$O_2 + 2H^+ + 2e^- \rightarrow H_2O_2 \quad \text{or} \quad O_2 + 4H^+ + 4e^- \rightarrow 2H_2O$$

2.7. Procedure used to Record Voltammograms

The solutions were taken into the electrochemical cell. The electrodes were inserted into the arms of the cell. The supporting electrolyte was taken in solvent without adding the analyte in order to record the voltammogram of the blank. Before the voltammetric measurements the solution was purged with pure (99.9%) nitrogen for 20 minutes to remove the dissolved oxygen and stream of nitrogen gas was blanketed over the solution. The potentiostat is programmed for sweep rates for measurements. Voltammograms of blank was recorded. A fixed volume of the solution analyte was taken in supporting electrolyte and the same procedure was repeated to record the voltammogram. The electrode surface was renewed by scoping some paste off and filling the new one, and then polishing the electrode on a wet filter paper or transparent polishing paper before conducting any experiments. The experiments were performed in unstirred solutions using cyclic voltammetry and differential pulse voltammetric techniques.

2.8. Model system for Basic Characterization of Carbon Paste Electrode in Voltammetry

2.8.1. Potassium Ferrocyanide System.

To evalutate interfacial electrochemical properties of the carbon paste, $[Fe(CN)_6]^{3-}$/ $[Fe(CN)_6]^{4-}$ model system was used as the electrochemical redox probe [60, 61]. Usually modification of electrodes with charged species has remarkable effects on the rate of electron transfer kinetics are known to be sensitive to the state of the surface. These effects depend on charge of both electrode surface and redox probe. More reversible behavior is observed for the charged probe redox reactions at the modified electrodes with opposite charge and less reversible behavior for the charged probe redox reactions at the modified electrodes with similar charge [62, 63].

2.8.2. Surface Area calculation of the CPE

The surface area of CPE was determined using potassium ferrocyanide (1mM) in 1 M KCl. The effect of scan rate on cyclic voltammograms of 1mM solution of ferrocyanide has been studied from 50 to 200 mVs^{-1}. For a reversible redox couple, the number of electrons transferred in the electrode reaction can be determined by the separation between the peak potentials ΔE_p $(E_{pa}-E_{pc})/n \sim 0.059$ V. The value found to vary from 0.061 V and 0.066 V which corresponds to one electron transfer. It is found that the separation of the peak potentials is independent of the scan rate. Also the ratio of i_{pa} / i_{pc} was found to be close to one (0.9953) which is a typical behaviour, exhibited by a reversible electrochemical transfer. The surface area of electrode can be measured by given equation

$$i_p = 2.65\times10^5\, n^{3/2}\, A\, C_O^*\, D_o^{1/2}\, \upsilon^{1/2}$$

Where, i_p is the peak current in A (ampere), A is the area of the electrode in cm^2, n is the number of electrons, C_O^* is the concentration in moles dm^{-3}, D_o diffusion coefficient in cm^2s^{-1} and υ is the scan rate in Vs^{-1}.

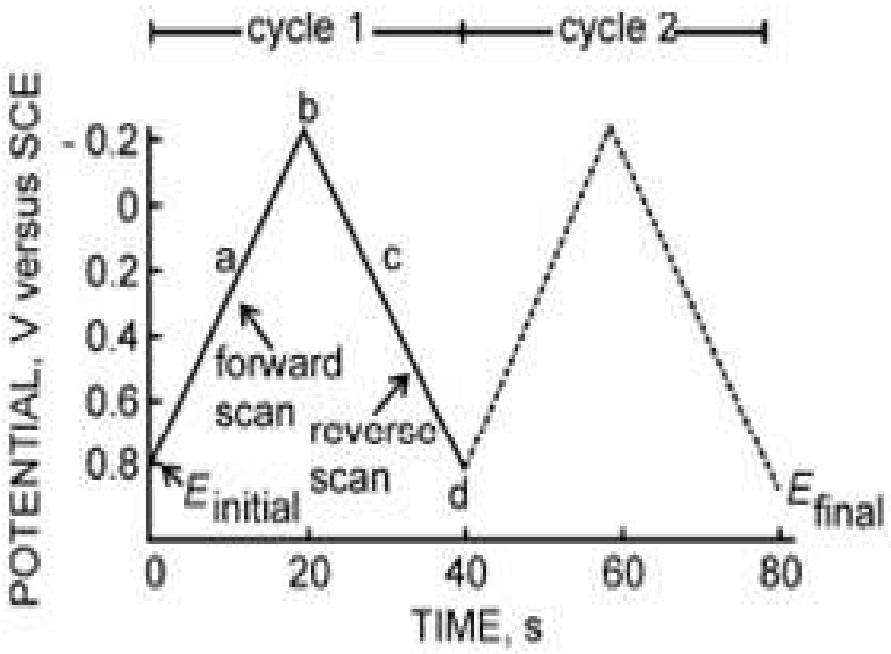

Fig. 2.1: Typical excitation signal for cyclic voltammetry- a triangular potential waveform with switching potentials at 0.8 and -0.2 V versus SCE.

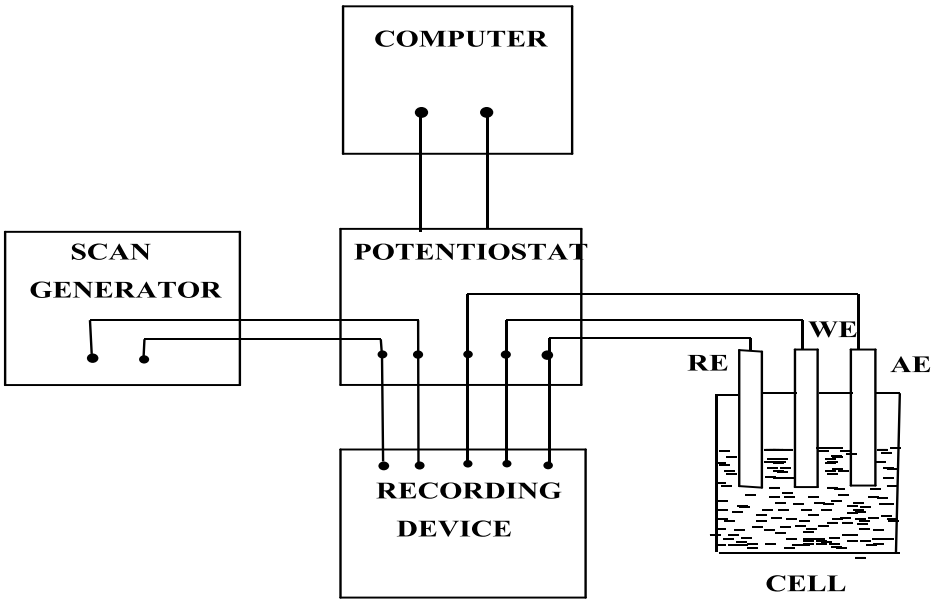

RE - Reference Electrode
WE - Working Electrode
AE - Auxiliary Electrode

Fig. 2.2: Schematic representation of the experimental setting consisting of an external control voltage source, a potentiostat and the electrochemical cell.

Fig. 2.3. Experimental set set-up used to record all electrochemical measurements

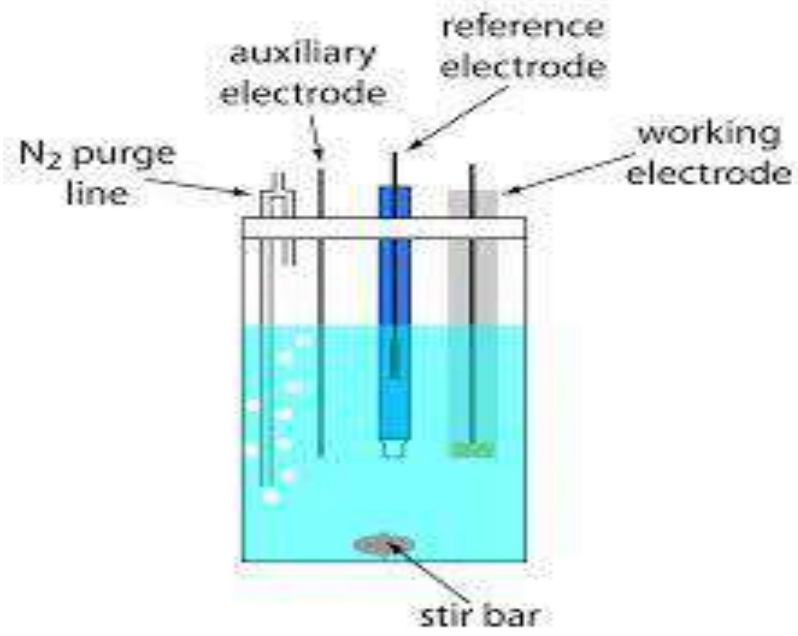

Fig. 2.4: Schematic representation of an assembled electrochemical cell containing an electrolyte solution, N_2 purge line and the three electrodes (WE, RE and CE) for cyclic voltammetric experiments.

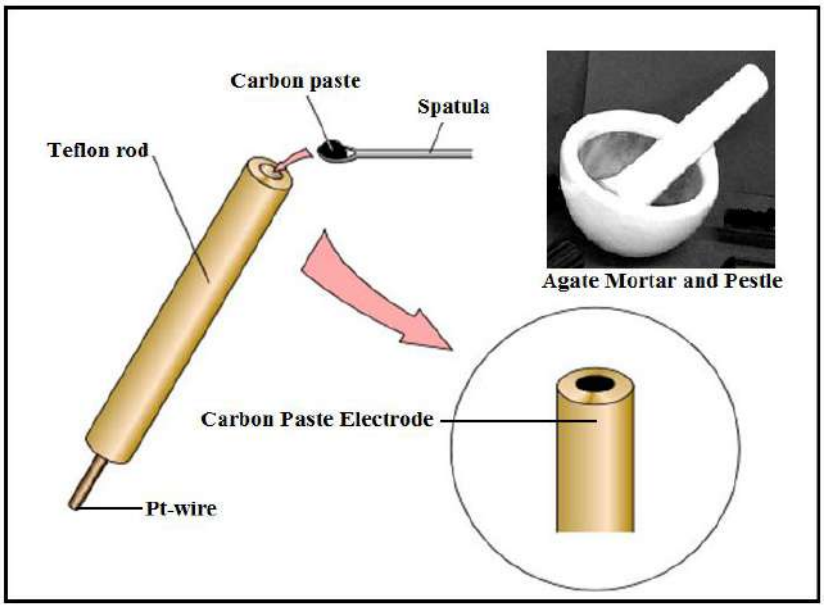

Fig. 2.5: Carbon Paste electrode, Preparation and Filling

2.9. Reference

[1] Bard, J. Allen and Larry R. Faulkner, *Electrochemical Methods: Fundamentals and Applications* (2 ed.), Wiley, 2000.

[2] R.S. Nicholson and Irving. Shain, *"Theory of Stationary Electrode Polarography. Single Scan and Cyclic Methods Applied to Reversible, Irreversible, and Kinetic Systems*", *Analytical Chemistry*, **36**(4): 706.

[3] Heinze and Jurgen, *"Cyclic Voltammetry-"Electrochemical Spectroscopy"*, *New Analytical Methods* (25)", *Angewandte Chemie International Edition in English*, **23** (1984) 831.

[4] Boyde, A. *Proc. 3rd ZZTRZ, Symposium on Scanning Electron Microscopy, Chicago,* 1970, p.105.

[5] V.E. Cosslett and W.C Nixon, 1960 *X-ray microscopy*. Cambridge University Press.

[6] A.V. Crewe, *Proc. Reg. European Con$ on E.M.,* Rome: Tipogr. Poligl. Vat., 1968, p77

[7] H. E. Hinton, *Micron,* 1 (1969) 84.

[8] T. Mulvey, *Focusing of chargedparticles* (ed. A. Septier), Academic Press, vol. I (1967) p 469.

[9] W.C. Nixon, Ph.D. Dissertation, Cambridge University, 1952.

[10] G. Lauer, R.Abel, F.C.Anson, *Anal.Chem*., **48** (1976) 1616.

[11] S.P. Perone, J.E. Harrar, F.B. Stephens and R.E. Anderson, *Anal.Chem*., **40** (1968) 899.

[12] S.P. Perone, J.W. Frazer, A. Kray, *Anal.Chem*., **43** (1971) 1485.

[13] S.C. Creason, R.J. Loyd, D.E. Smith, *Anal.Chem*., **44** (1972) 1159.

[14] P.E. Whitson, H.W.V. Born, D.H. Evans, *Anal.Chem*., **45** (1973) 1298.

[15] B. Aalstad, V.D. Parker, *J.Electroanal.Chem*., **112** (1980) 263.

[16] R. Eliason, V.D. Parker, *J.Electroanal.Chem*., **170** (1984) 347.

[17] E. Ahlberg, V.D. Parker, *J Electroanal Chem. and Interfac. Electrochem*, **121** (1981) 57.

[18] K. Kalcher, J.M. Kauffmann, J. Wang, I. Svancara, K. Vytras, C. Neuhold, and Z. Yang, *Electroanal.,* **7** (1995) 5.

[19] K. Kalcher, X.H. Cai, G. Kolbl, I. Svancara and K. Vytras, *Sb. Ved. Pr., Vys. Sk. Chemickotechnol. Pardubice,* **57 (**1994**)** 5.

[20] K. Kalcher, K. Schach, I. Svancara, K. Vytras and H. Alemu, *Sci. Pap. Univ. Pardubice, Ser A.,* **3** *(*1997) 57.

[21] L. Gorton, *Electroanal.*, **7** (1995) 23.

[22] I. Svancara, K. Schachl, *Chem. Listy.,* **93** *(*1999**)** 490.

[23] K. Kalcher, *Electroanal.,* **2** (1990) 419.

[24] Z. Q. Zhang, H. Liu, H. Zhang and Y.F. Li, *Anal.Chim. Acta*, **333** (1996)119.

[25] I. Svancara, K.Kalcher, W. Diewald and K. Vytras, *Electroanal.,* **8** (1996**)** 336.

[26] I. Svancara, J. Konvalina, K. Schachl, K. Kalcher and K. Vytras, *Electroanal.,* **10** (1998) 435.

[27] K.M. Manesh, P. Santhosh, A. Gopalan and K.P. Lee, *Talanta*, **75** (2008) 1307.

[28] W.Y. Su, S.H. Cheng, *Electrochem. Commun.,* **10** (2008) 899.

[29] W. Zheng, J. Li, Y.F. Zheng, *Biosens. Bioelectron.,* **23** (2008) 1562.

[30] A.L. Liu, S.B. Zhang, W. Chen, X.H. Lin and X.H. Xia, *Biosens. Bioelectron.,* **23** (2008) 1488.

[31] R. Metelka, K. Vytras, A. Bobrowski, *J. Solid State Electrochem*., **4** (2000) 348.

[32] R. Martinez, M.T. Ramirez, I. Gonzalez, *Electroanal.,* **10** (1998) 336.

[33] T.F. Connors, J.F. Rusling, A. Owlia, *Anal. Chem.,* **57** (1985) 170.

[34] J.F. Rusling, F.N. Alaa-Eldin, *J. Am. Chem. Soc.,* **15** (1993) 11891.

[35] M. Plavsiae, D. Krznaric, B. Cosoviae, *J. Electroanal. Chem.,* **6** (1994) 469.

[36] J. Yang, N.F. Hu, J.F. Rusling, *J. Electroanal. Chem.,* **463** (1999) 53.

[37] M. Stadlober, K. Kalcher, G. Raber and C. Neuhold, *Talanta,* **43**(1996**)** 1915.

[38] M. Stadlober, K. Kalcher, G. Raber, *Sci. Pap.Univ.Pardubice, Ser. A.,* **3 (**1997**)** 103.

[39] M. Stadlober, K. Kalcher, G. Raber, *Electroanal.,* **9** (1997) 225.

[40] M. Stadlober, K. Kalcher, G. Raber, *Anal. Chim.Acta,* **350** (1997) 319.

[41] K. Hu, A.J. Bard, *Langmuir*, **13** (1997) 5418.

[42] Q.T. Cai, S.B. Khoo, *Analyst,* **120 (**1995) 1047.

[43] Z. Navratilova, P. Kula, *J. Solid State Electrochem.,* **4** (2000) 342.

[44] I. Svancara, K. Vytras, *Chem. Listy.,* **88** (1994) 138.

[45] M. Rice, Z. Galus, R.N. Adams, *J. Electroanal. Chem.,* **143** (1983) 89.

[46] K. Kalcher, I. S.Vancara, R. Metelka, K. Vytras and A.Walcarius, *The Encyclopedia of Sensors,* (Eds:C. A. Grimes, E. C. Dickey, M. V. Pishko), American Scientific, Stevenson Ranch , Vol. 4 (2006) 283.

[47] H.T. Liu, P. He, Z.Y. Li, C.Y. Sun, L.H. Shi, Y. Liu, G.Y. Zhu and J.H. Li, *Electrochem. Commun*., **7** (2005) 1357.

[48] G. Shul, J. Sirieix-Plenet, L. Gaillon and M. Opallo, *Electrochem.Commun.*, **8** (2006) 1111.

[49] N. Maleki, A. Safavi, F. Tajabadi, *Anal. Chem.*, **78** (2006) 3820.

[50] A. Safavi, N. Maleki, O. Moradlou and F. Tajabadi, *Anal.Biochem*., **359** (2006) 224.

[51] A. Safavi, N. Maleki, F. Honarasa, F. Tajabadi and F. Sedaghatpour, *Electroanal.*, **19** (2007) 582.

[52] N. Maleki, A. Safavi, F. Tajabadi, *Electroanal.*, **19** (2007) 2247.

[53] A. Safavi, N. Maleki, F. Tajabadi, *Analyst*, **132** (2007) 54.

[54] I. Svancara, J. Zima, K.Schachl, *Sci. Pap. Univ. Pardubice, Ser. A.*, **4** (1998) 49.

[55] C. Olson, R. N. Adams, *Anal. Chim. Acta*, **29** (1963) 358.

[56] I. Svancara, K. Vytras, *Anal. Chim. Acta*, 2**73** (1993) 195.

[57] I. Svancara, B. Ogorevc, M. Novic and K. Vytras, *Anal. Bioanal. Chem.*, **372** (2002) 795.

[58] T. Mikysek, I.S. Vancara, M. Bartos, M. Galik and K. Vytras, *14th Youth Investigators Seminar on Analytical Chemistry, Proceedings* (Eds: P. C. Esla, R. Metelka, K. Vytras), University of Pardubice, Pardubice, 2007, p 107.

[59] R.N. Adams, *Electrochemistry at Solid Electrodes*, (Marcel Dekker, New York), 1969, p 26.

[60] Z. Galus, R.N. Adams, *J.Phys.Chem.*, **67** (1963) 866.

[61] P. Doderhgelm, *J.Electrochem.Chem.*, **71** (1976) 109.

[62] M. Kooshki, E. Shams, *Anal. Chim. Acta*, **587** (2007) 110.

[63] R. Karimi-Shervedani, M. Bagherzadeh, S.A. Mozaffari, *Sens. Actuators B.*, **115** (2006) 614.

Chapter-3

PART-A

ELECTROCHEMICAL INVESTIGATION OF DICYCLOMINE HYDROCHLORIDE AT POLY (TERBUTALINE SULPHATE) MODIFIED CARBON PASTE ELECTRODE

Dicyclomine Hydrochloride

3.1. Introduction

In this chapter, a poly (Terbutaline Sulphate) modified carbon paste electrode (PTBSMCPE) was fabricated by electropolymerisation method to investigate the electrochemical behavior of DICY in phosphate buffer solution by cyclic voltammetric technique. The surface of morphology of PTBSMCPE studied by scanning electron microscope (SEM). The discussion involves the chemistry, biological relevance of DICY and their oxidation behaviors at PTBSMCPE. The modified electrode showed very good sensitivity for DICY. Well defined and discrete voltammetric oxidation peak was observed compare to bare carbon paste electrode. The effect of pH, scan rate, concentration were also studied. Linear calibration plots for DICY was obtained in range 0.01 mM to 1 mM with the detection limit 0.12 µM. The differential pulse voltammetric technique (DPV) was also shows the linear increase in current with increase in concentration of DICY. The preparation of the modified electrode is very easy, renewed by simple polishing gives very good reproducibility, high stability in its voltammetric response and low detection limit for dicyclomine hydrochloride.

3.2. Chemistry and Biological Relevance of Dicyclomine Hydrochloride

Dicyclomine Hydrochloride (DICY) chemically is 2-(diethyl amino) ethyl 1 cyclohexylcyclohexane-1-carboxylate (**Scheme 3.1**), is a muscarinic antagonist used as an anti-spasmodic and in urinary incontinence. This dual mode of action provides a specific anti cholinergic effect at acetylcholine receptor and a direct effect upon smooth muscle, but rarely causes any side effect [1]. It decreases spasms of the gastrointestinal tract, biliary tract, ureter, and uterus without producing characteristic atropinic effects on the salivary, sweat, or gastrointestinal glands, the eye, or the cardiovascular system except in the large doses [2].

3.3. Review of electrochemistry of Dicyclomine Hydrochloride

The designing, fabrication and application of sensitive and selective electrochemical sensors are considerable interest in recent years. The Xiao Feng Tanga *et al*., [3] studied the simple, rapid, accurate, and sensitive spectrophotometric methods for the determination of dicyclomine hydrochloride. Savaa *et al*., [4] develop a rapid and specific nuclear magnetic resonance (NMR) spectroscopic method was developed for determining dicyclomine hydrochloride in tablet, capsule, and injection dosage forms. Leathwood *et al*., [5] prepared the carbon-paste electrode for determination of dicyclomine hydrochloride (DICY) in terms of composition, life span, usable pH range and temperature.

The electrochemical sensors based on chemically modified electrodes (CMEs) have been widely used for the detection of biologically important organic compounds. The modified electrodes using transition metal complexes [6], organic electron mediators [7] and polymer-modified electrodes [8] have attracted the most attention in this regard. One of the most important characteristics of the electron mediators, which are used in modified electrodes, is sufficient sensitivity and selectivity [9].

3.4. Chemistry and Biological relevance of Terbutaline Sulphate

Terbutaline Sulphate (TBS), *β*- [(tert-butylamino) methyl] -3, 5- dihydroxy- benzyl alcohol ($C_{12}H_{19}NO_3$) **(Scheme 3.2),** is a β_2- agonist that is widely used as a bronchodilator in acute and long-term treatment of chronic bronchitis, emphysema and other chronic obstructive pulmonary diseases [10]. Terbutaline Sulphate is widely used for the therapeutic management of chronic as well as prophylaxis of asthma and nocturnal asthma in particular. It is a drug of choice for the treatment of asthma but it has several drawbacks such as short biological half-life of about 3.6h [11]. It selectively stimulates β_2-adrenoceptors in the bronchial tree, whilst having little or no effect upon cardiac β_1-adrenoceptors. Terbutaline enhances tracheal mucus velocity when given subcutaneously to patients with airways obstruction (Mossberg *et al*., 1976a; 1976b) and to healthy subjects (Camner *et al*., 1976). However, the effect of terbutaline on

mucus transport when administered via a pressurized metered dose inhaler (MDI) is largely unknown [12].

Electropolymerisation is a good approach to immobilize polymers to prepare polymer modified electrodes (PMEs) as adjusting the electrochemical parameters can control film thickness, permeation and charge transport characteristics. Polymer-modified electrodes have many advantages in the detection of analytes because of its selectivity, sensitivity and homogeneity in electrochemical deposition, strong adherence to electrode surface and chemical stability of the film [13]. Selectivity of PMEs as a sensor can be attained by different mechanisms such as size exclusion [14], ion exchange [15], hydrophobicity interaction [16], and electrostatic interaction [17, 18].

Limited work has been done in the area of carbon paste electrode for the determination of dicyclomine hydrochloride.

This section describes the procedure that has been optimized for the determination of DICY at poly (Terbutaline Sulphate) modified carbon paste electrode by cyclic voltammetric (CV) and differential pulse voltammetric technique (DPV) in 0.2 M phosphate buffer solution of pH 6. The effect of pH, scan rate, concentration were studied. The preparation of the modified electrode is very easy, renewed by simple polishing gives very good reproducibility, high stability in its voltammetric response and low detection limit for dicyclomine hydrochloride.

3.5. Experimental Section

3.5.1. Reagents

Terbutaline Sulphate (TBS) and Dicyclomine Hydrochloride (DICY) were purchased from sigma aldrich and all other chemicals were of analytical grade. The electropolymerisation of terbutaline sulphate was performed in 0.2 M phosphate buffer solution. The phosphate buffer solution was prepared from KH_2PO_4 and K_2HPO_4 and the pH was adjusted with H_3PO_4 and 0.1 N NaOH solution. The stock solution of the dicyclomine hydrochloride (10 mM) was prepared by dissolving in water. Other

chemicals used were of analytical grade except for spectroscopically pure graphite powder. All solutions were prepared with doubly distilled water. Freshly prepared DICY solution is used prior to measurements.

3.5.2. Apparatus

Electrochemical measurements were carried out with an Electroanalyser model EA-201 chemlink system in a conventional three-electrode system. The working electrode was carbon paste electrode, having cavity of 3 mm diameter. The counter electrode was platinum electrode with a saturated calomel electrode (SCE) as a standard reference electrode for completing the circuit.

3.5.3. Modification procedure

3.5.3a. Preparation of bare carbon paste electrode

The bare carbon paste electrode was prepared by hand mixing of 70% graphite powder and 30% silicon oil to produce a homogenous carbon paste which was then packed into the cavity of a homemade carbon paste electrode and smoothed on a weighing paper.

3.5.3b. Preparation of the Terbutaline sulphate polymer film modified carbon paste electrode

The polymer film modified electrode was prepared by electrochemical polymerization of TBS in 0.2 M phosphate buffer solution of pH 6.0 containing 1 mM TBS in the potential range of 200 to 1400 mV at the scan rate 100 mVs^{-1} using cyclic voltammetric technique. After 15 cycles, the surface of the electrode was washed with double distilled water to remove the physically adsorbed material, air dried and used for the electrochemical studies.

3.6. Result and Discussion

3.6.1. Electropolymerisation of Terbutaline Sulphate (TBS) on Carbon Paste Electrode

Electropolymerization of TBS was performed on bare carbon paste electrode. The cyclic voltammograms for the electropolymerisation of 1mM of TBS in 0.2 M phosphate solution of pH 6 at bare carbon paste electrode (BCPE) as shown in **Fig 3.1,** which displays the continuous cyclic voltammetric of 1mM TBS monomer by scanning in the potential range of 200 to 1400 mV for 15 cycles. During the electropolymerisation process, indiscernible peaks started to appear after 5^{th} cycle. An anodic peak at 861 mV potential was observed due to the formation of poly (TBS). The peak descended gradually with the increase in cyclic number such decrease indicates the poly (TBS) membrane forming and depositing on the surface of the carbon paste electrode by electropolymerisation. TBS was oxidized to free radical at the surface of CPE rapidly resulting in the possible structure of electropolymerised poly (TBS). After polymerization the poly (TBS) modified CPE was carefully rinsed with distilled water to remove the physically adsorbed material. Then the film electrode was transferred to an electrochemical cell and cyclic voltammetric sweeps were carried out to obtain electrochemical steady state.

3.6.2. Effect of the poly (Terbutaline Sulphate) film thickness on the electrochemical response of Dicyclomine Hydrochloride (DICY)

The thickness of poly (TBS) film could be controlled by the cyclic number of voltammetric scans during the electrochemical modification. The effect of the thickness of poly (TBS) film on the electrochemical response was investigated by cyclic voltammetric technique. The current (I_{pa}) response of poly (TBS) films increase gradually as the number of cycles increases during film formation from 5 to 15 cycles. Afterwards I_{pa} starts to decrease by increasing the number of cycles which was examined up to 30 cycles **(Fig.3.1a)**. In order to obtain better oxidation peak and higher

sensitivity of current for the electrochemical response of DICY, 15 scans were chosen to control the thickness of the poly (TBS) film.

3.6.3. SEM Characterization of poly (Terbutaline Sulphate) modified carbon paste electrode

Fig.3.2a and **Fig.3.2b**, explain the surface morphology of bare CPE and poly (TBS) modified CPE respectively using scanning electron microscope (SEM). The surface of bare CPE was formed by irregularly shaped micrometer-sized flakes of graphite. Whereas the modified electrode had a typical uniform arrangement of TBS molecules on the surface of CPE [19].

3.6.4. Electrochemical response of potassium ferrocyanide at poly (TBS) modified carbon paste electrode

Fig.3.3. shows the electrochemical response of 1 mM potassium ferrocyanide in 1M KCl at bare carbon paste electrode (BCPE) (curve'b') and at poly (TBS) modified carbon paste electrode (curve 'a'). The curve 'b' shows the electrochemical response of BCPE having the electrochemical cathodic peak potential (E_{pc}) 36 mV with peak current (I_{pc}) of 6.23 µA and anodic peak potential (E_{pa}) 442 mV with peak current (I_{pa}) of 12.48 µA. After modification with poly (TBS) modified carbon paste electrode, the enhancement of both anodic peak current (I_{pa}) 20.76 µA and cathodic peak current (I_{pc}) 14.55 µA with corresponding anodic peak potential (E_{pa}) 262 mV and cathodic peak potential (E_{pc}) 129 mV has been observed. The surface area of bare carbon paste electrode is 0.023 cm^2. Whereas, the effective surface area of the modified electrode was found to be 0.0342 cm^2.

3.6.5. Electrochemical behavior of Dicyclomine Hydrochloride at poly (TBS) modified carbon paste electrode

Fig.3.4 shows cyclic voltammograms of 0.1 mM DICY in phosphate buffer solution of pH 6.0 at bare carbon paste electrode (curve 'b') and poly (TBS) modified carbon paste electrode (curve 'a'). The curve 'c' represents cyclic voltammogram of

blank solution at poly (TBS) modified carbon paste electrode. Above studies showed that only one oxidation peak at 1030 mV with peak current of 4.49 µA at bare CPE, whereas an oxidation peak at 992 mV with peak current of 24.88 µA at the poly (TBS) modified carbon paste electrode in the potential range of 200 to 1200 mV. No reduction peak was observed in the reverse scan, suggesting that the electrochemical reaction is a totally irreversible process and the oxidation peak at the bare CPE is broad due to slow electron transfer, while the response was considerably improved at the poly (TBS) modified carbon paste electrode and the peak potentials shifted to negative direction, the shape of the peak turns sharper and the peak current increased significantly.

3.6.6. Effect of pH

The effect of pH was investigated by cyclic voltammetric measurement at different pH values between 2.5 and 9.0 as shown in **Fig.3.5a**. The maximum response current was observed at pH 6.0. In order to obtain the maximum bioactivity and optimal sensitivity, phosphate buffer solution of pH 6.0 at scan rate 50 mVs^{-1} was selected for our experiments. The oxidation peak current increases with increase of pH from 2.5 to 6 and becomes maximum and peak potential shifted negatively. While pH beyond 6, a great decrease of the oxidation peak current could be observed, then it decreased gradually with the further increase in pH of the solution as shown in **Fig.3.5a** and the anodic peak potential decrease with increase of pH as shown in **Fig.3.5b**. A linear relationship is obtained between the anodic peak potential and pH of the solution in the range 2.5 – 9. The corresponding linear regression equation is

$$E_{pa}\ (mV) = 1138.217 - 41.367\ pH \quad (R = 0.99386) \ldots\ldots\ldots\ldots\ldots\ldots\ (3.1)$$

With a negative slope of 41.367 indicating that the number of electrons and protons are equal in the electrochemical oxidation of DICY at poly (TBS) modified carbon paste electrode. In the view of determination of DICY and also in order to carry out the reaction at physiological environment, pH 6.0 was chosen for further study.

3.6.7. Effect of scan rate

The effect of scan rates on the electrochemical response of 0.1 mM DICY at poly (TBS) modified carbon paste electrode was studied at different scan rates. Redox peak current increase linearly with the scan rate in the range 25, 50, 75, 100, 125,150, 175, 200, 225, 250, 275 and 300 mVs^{-1}. The cyclic voltammograms were shown in **Fig.3.6a**. The linearity was obtained for the plot of the anodic peak current vs. scan rate with a correlation coefficient of 0.992 is shown in **Fig.3.6b**. The corresponding linear regression equation is

I_{pa} (μA) = 0.0467 ν + 6.9081 (R = 0.992)…………………………. (3.2)

This indicates that the electrode process was controlled by rather diffusion than adsorption. Furthermore the anodic peak potential shifted towards more positive. **Fig.3.6c** shows linear relationship with a correlation coefficient of 0.9973 obtained between the peak current and square root of scan rate in the range of 25 - 300 mVs^{-1}, which revealed that a diffusion controlled process occurring at the poly (TBS) modified carbon paste electrode. The relationship between the anodic peak potential and scan rate can explained by plotting the anodic peak potentials vs. natural logarithm of scan rate **(Fig.3.6d)** by considering the relation:

E_{pa} (mV) = 0.0918 lnυ + 0.62534 R= 0.9817……………………….. (3.3)

The relationship between the anodic peak current and scan rate is explained by plotting the logarithm of anodic peak current vs. logarithm of scan rate **(Fig.3.6e)** by considering following linear regression equation:

logI_{pa} (μA) = 0.4375 logυ + 0.2135 R= 0.99672…………………… (3.4)

The slopes for the equation is 0.437 which is close to the theoretical value of 0.5 for a diffusion controlled process between scan rates 25 – 300 mVs^{-1} [20].

According to Laviron's theory [21] the slope is equal to $RT/\alpha n_\alpha F$. As for a totally irreversible electrode reaction on the basis of the above discussion, the n_α was

found to be 1.6386, which indicated that two electrons were involved in the oxidation process of DICY at the poly (TBS) MCPE. Since the equal number of electrons and protons took part in the oxidation of DICY, therefore two electrons and two protons transfer were involved in the electrode reaction process. The electrochemical reaction process for DICY at poly (TBS) modified carbon paste electrode can therefore be summarized as in **Scheme 3.3**. From the deduced mechanism of DICY, an intermediate of a free radical was formed. It may be just the free radical polymerizes and comes into being as insoluble products that deposit on the electrode surface, which agrees with the phenomena of voltammograms recorded from multi-cycles [22].

3.6.8. Effect of DICY concentration and detection limit

Under selected conditions, the effect of DICY concentration on the oxidation peak current was studied by cyclic voltammetry in 0.1 M PBS of pH 6.0 at the scan rate 50 mVs^{-1}. The oxidation peak current increases with increase in concentration of DICY. **Fig.3.7a** and **Fig.3.7b** shows the linear relationship between the anodic peak current (I_{pa}) with DICY concentration in the range from 1×10^{-5} M to 1×10^{-4} M. The corresponding linear regression equation is given by

$$I_{pa}\ (\mu A) = 195.726\ C\ (10^{-5}\ M) + 4.4108 \quad (R = 0.9944) \ldots\ldots\ldots\ldots\ldots\ (3.5)$$

The limit of detection (LOD) and limit of quantification (LOQ) of DICY were found to be 0.12 µM and 0.406 µM respectively. Related stastical data of calibration curves were obtained from five different calibration curves (n=5). The LOD and LOQ were calculated from the peak current using the following equations:

$$LOD = 3S/M \text{ and } LOQ = 10S/M$$

Where S is standard deviation and M is the slope (sensitivity) of calibration plot.

3.6.9. Dicyclomine hydrochloride studies by differential pulse voltammetric (DPV) technique

Differential pulse voltammetric technique (DPV) was used to investigate the possibility of poly (TBS) modified carbon paste electrode for determination of DICY. The current responses of this DICY changed by changing the concentrations of DICY. As illustrated in **Fig.3.8** DPV responses of the modified electrode of DICY increased linearly with increase of their concentration. The corresponding linear regression equations for DICY in the range of 1×10^{-5} to 4×10^{-5} M is given by

I_{pa} (µA) = 3.5 + 189 C (10^{-5} M) (R = 0.9957)…………………….......... (3.6)

3.7. Conclusion

- In the present study, a poly (Terbutaline Sulphate) modified carbon paste electrode based on the electropolymerisation has been prepared for the electrochemical determination of DICY.
- Results showed that the oxidation peak current of DICY was improved at poly (TBS) modified carbon paste electrode.
- The electrochemical response is diffusion controlled and irreversible in nature for DICY.
- A linear concentration range was found to occur from 1×10^{-5} to 1×10^{-4} M by CV.
- The probable reaction mechanisms involved in the oxidation of DICY were also proposed.

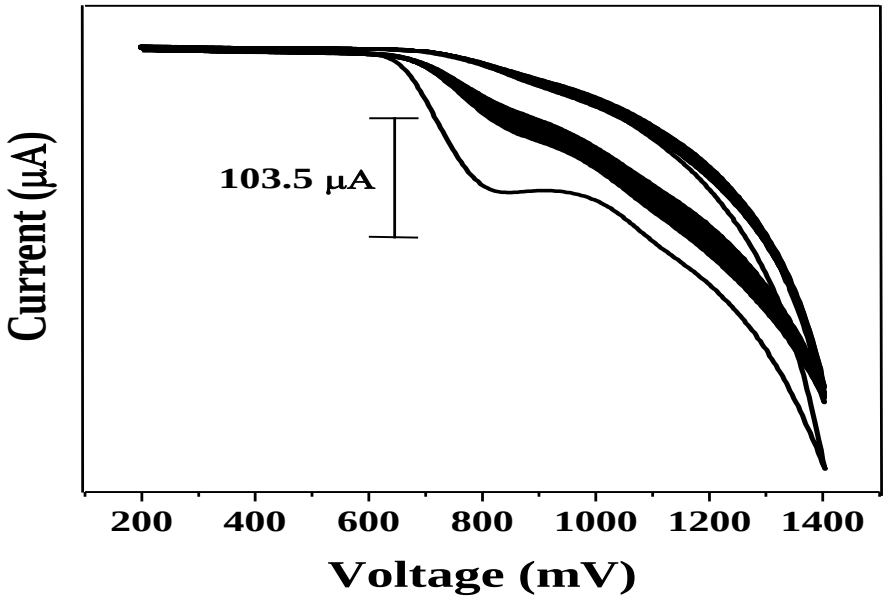

Fig. 3.1: Cyclic voltammograms for the electro polymerization of 1 mM of Terbutaline Sulphate in 0.2 M phosphate buffer solution on CPE.

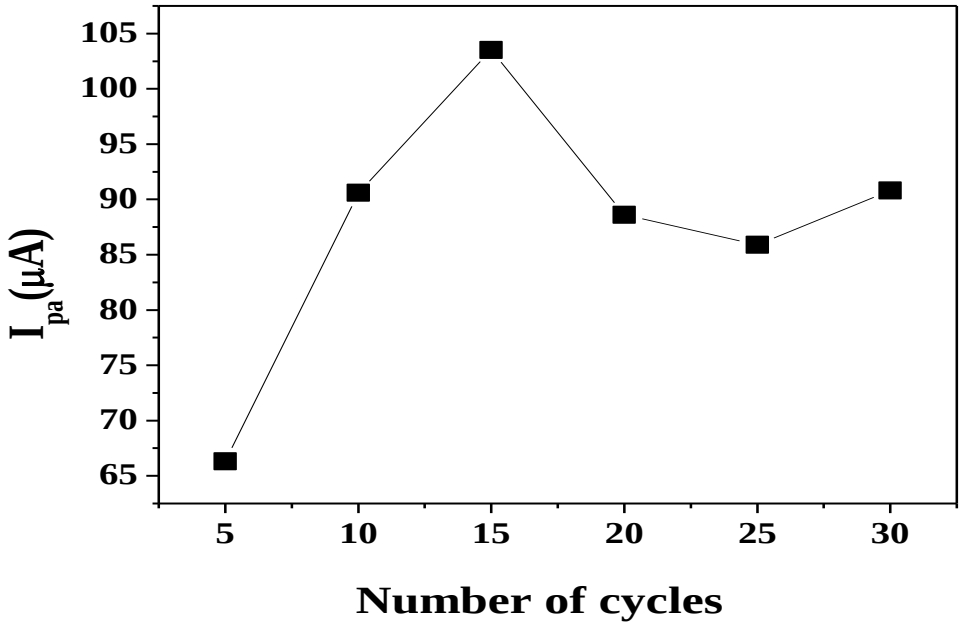

Fig. 3.1a: Plot of anodic peak current v/s. number of cycles of Terbutaline Sulphate (TBS)

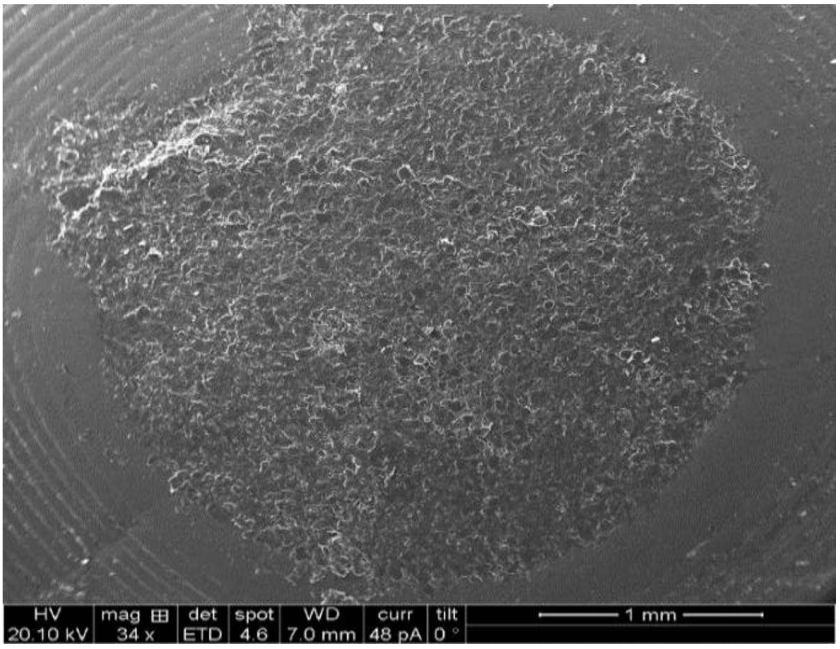

Fig. 3.2a: SEM image of bare carbon paste electrode.

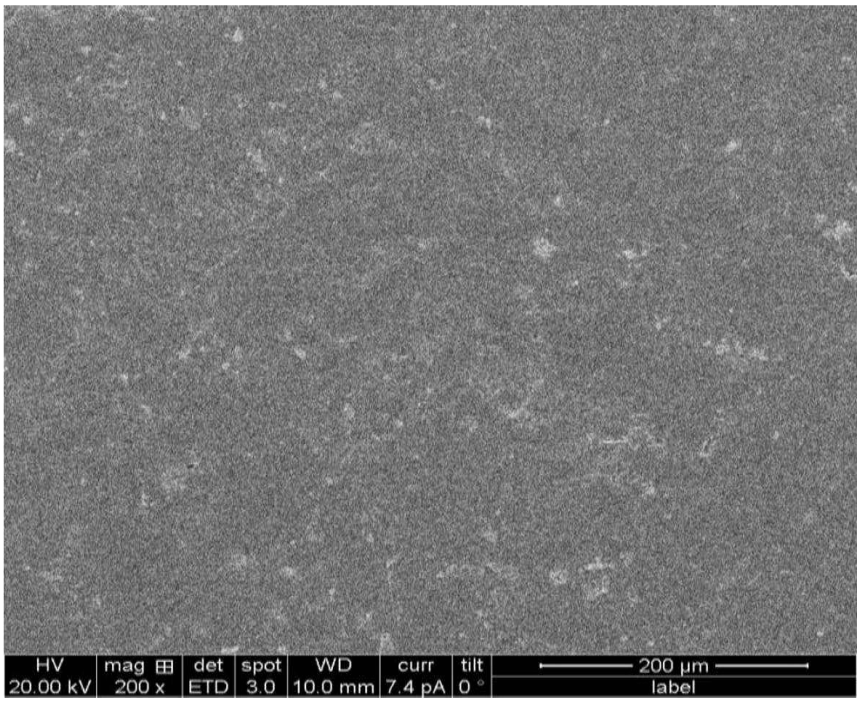

Fig. 3.2b: SEM image of poly (TBS) modified carbon paste electrode

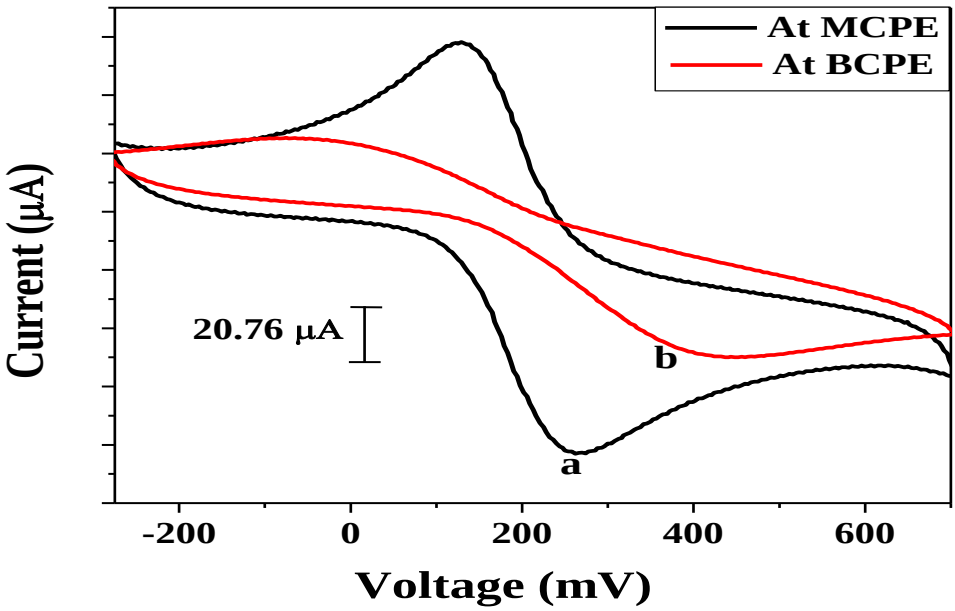

Fig. 3.3: Comparison of 1 mM $K_4[Fe(CN)_6]$ in 1 M KCl solution at poly (TBS) modified carbon paste electrode (a) and bare carbon paste electrode (b).

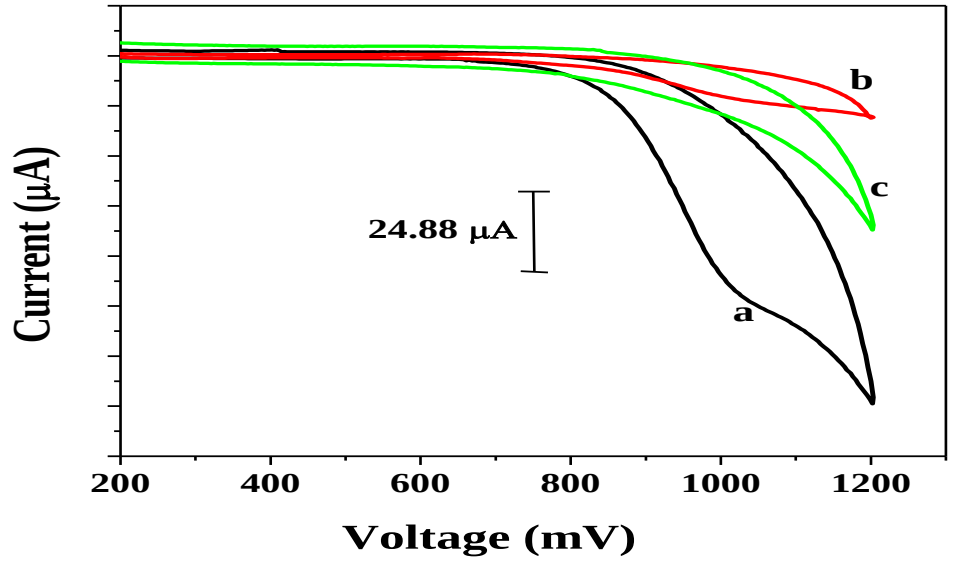

Fig. 3.4: Comparision of 0.1 mM DICY at poly (TBS) modified carbon paste electrode (a), at bare carbon paste electrode (b) and blank solution in phosphate buffer (c) of pH 6; scan rate 50 mVs^{-1}.

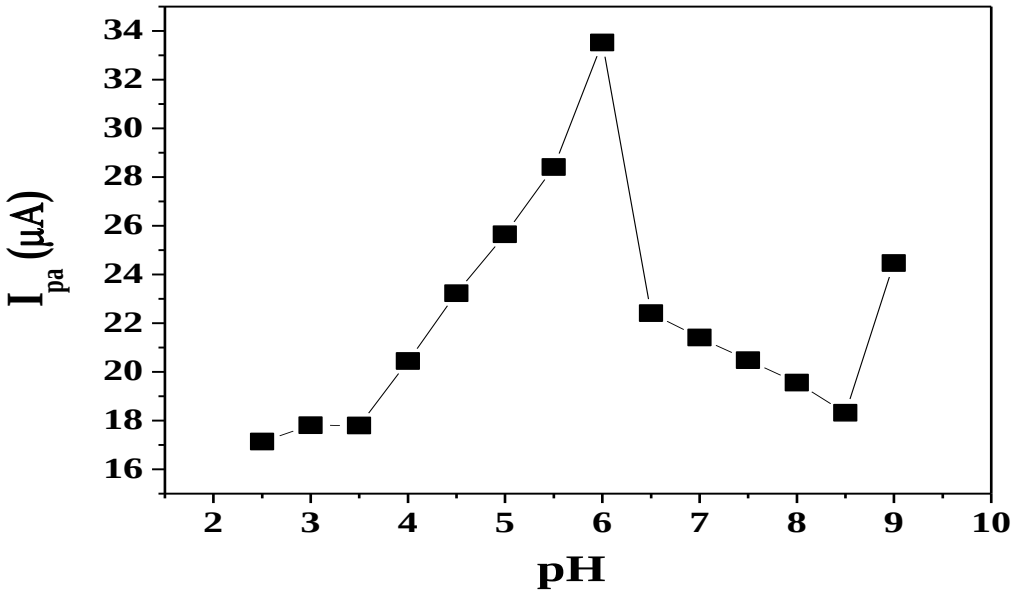

Fig. 3.5a: Plot of anodic peak current vs. pH (2.5 – 9.0) of 0.1 mM DICY at poly (TBS) modified carbon paste electrode.

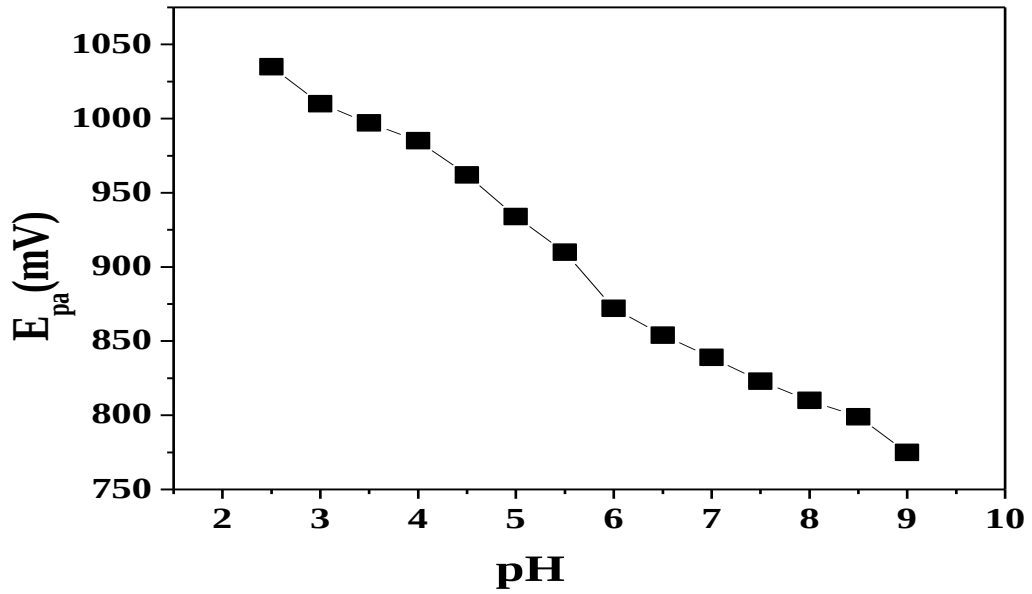

Fig. 3.5b: Plot of anodic peak potential vs. pH (2.5 – 9.0) of 0.1 mM DICY at poly (TBS) modified carbon paste electrode.

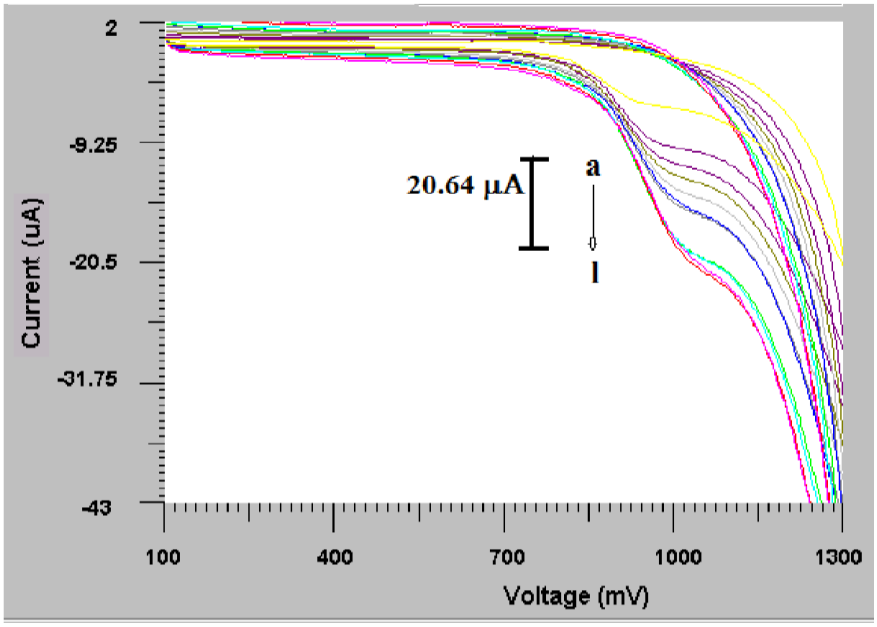

Fig. 3.6a: Cyclic voltammograms of 0.1 mM DICY at poly (TBS) modified carbon paste electrode with different scan rates (a) 25, (b) 50, (c) 75, (d) 100, (e) 125, (f) 150, (g) 175, (h) 200, (i) 225, (j) 250, (k) 275, (l) 300 mVs^{-1}.

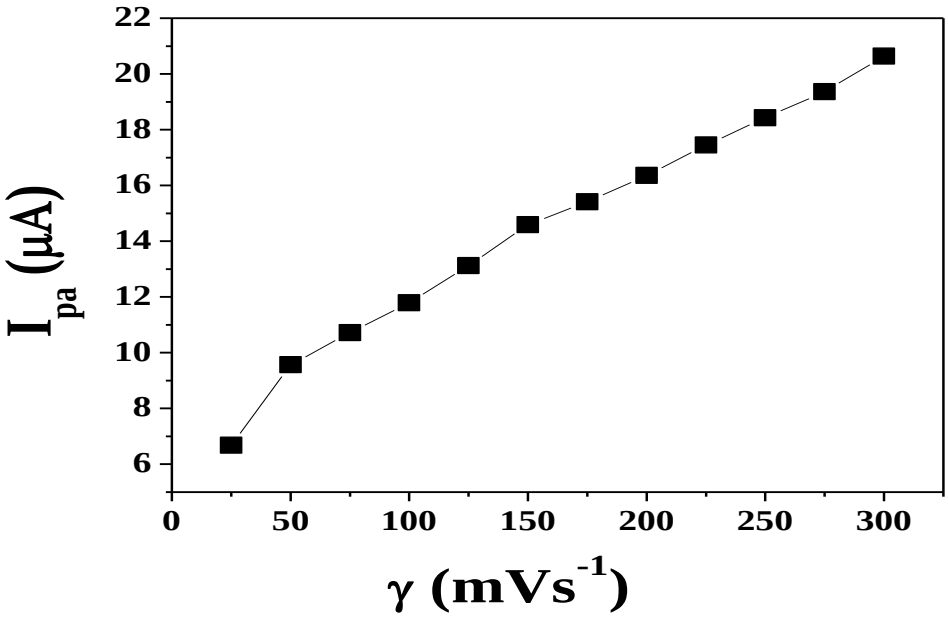

Fig. 3.6b: Plot of anodic peak current vs. scan rates of DICY at poly (TBS) modified carbon paste electrode.

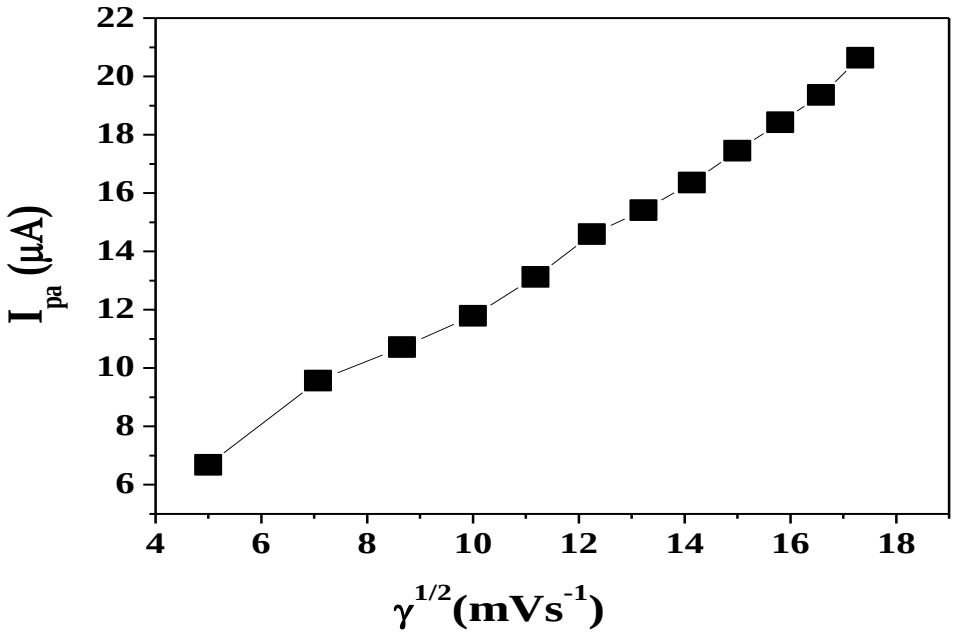

Fig. 3.6c: Plot of anodic peak current (I_{pa}) vs. square root of scan rates of DICY at poly (TBS) modified carbon paste electrode.

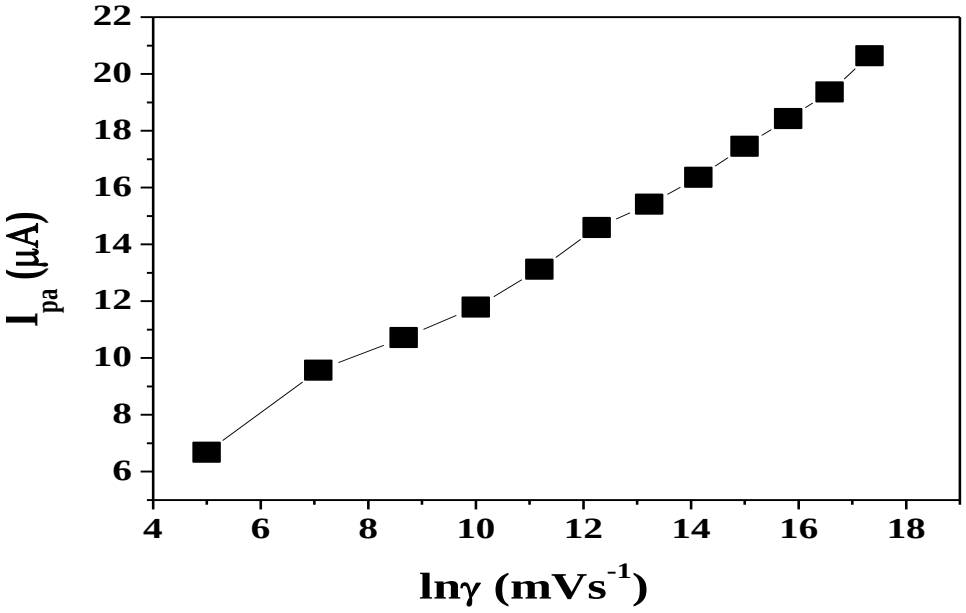

Fig. 3.6d: Plot of anodic peak potential vs. natural logarithm of scan rates of DICY at poly (TBS) modified carbon paste electrode.

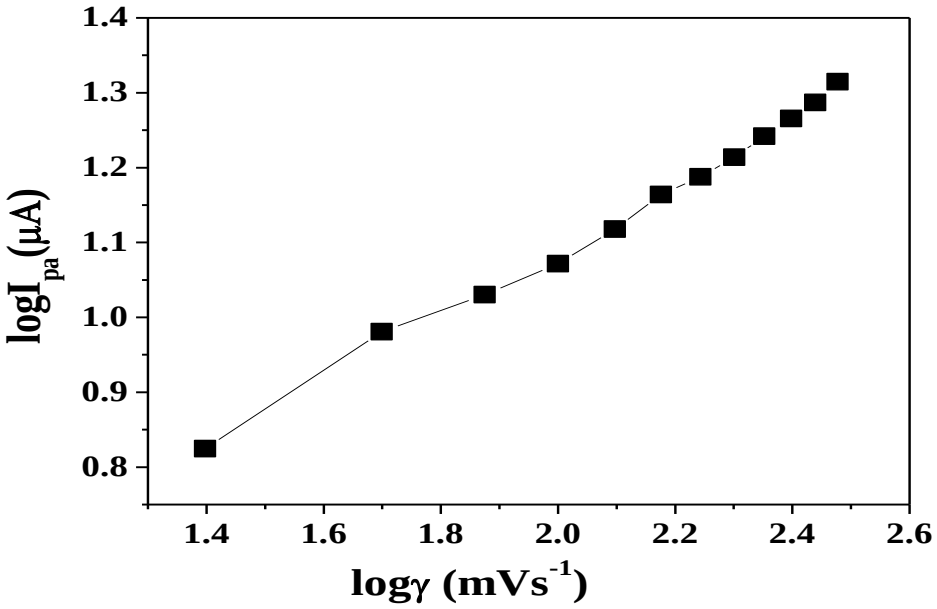

Fig. 3.6e: Plot of logarithm of anodic peak current vs. logarithm of scan rates of DICY at poly (TBS) modified carbon paste electrode.

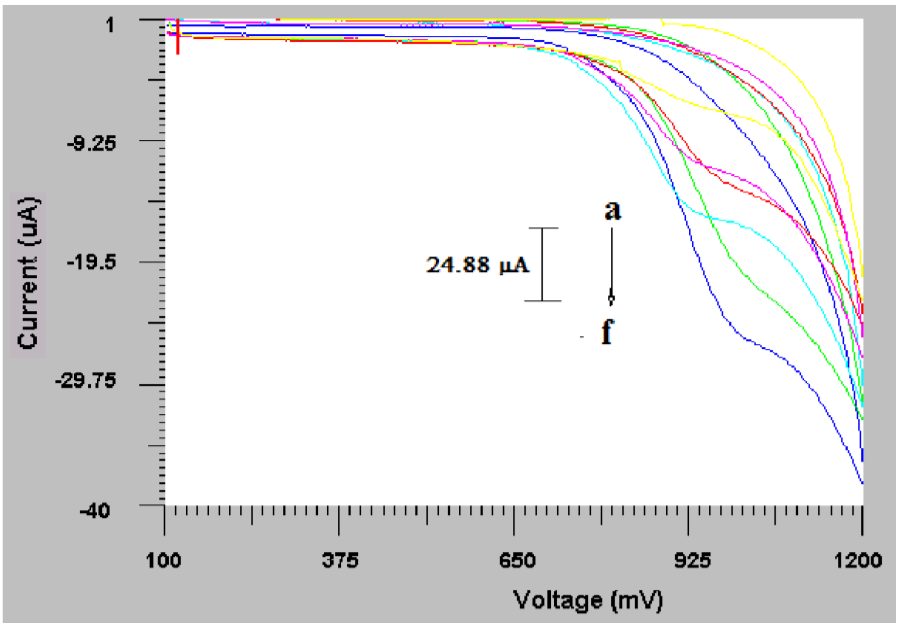

Fig. 3.7a: Effect of variation of concentration of DICY (a) 1×10^{-5} M, (b) 2×10^{-5} M, (c) 4×10^{-5} M, (d) 6×10^{-5} M, (e) 8×10^{-5} M, (f) 1×10^{-4} M on anodic peak current at poly (TBS) modified carbon paste electrode; scan rate 50 mVs^{-1}.

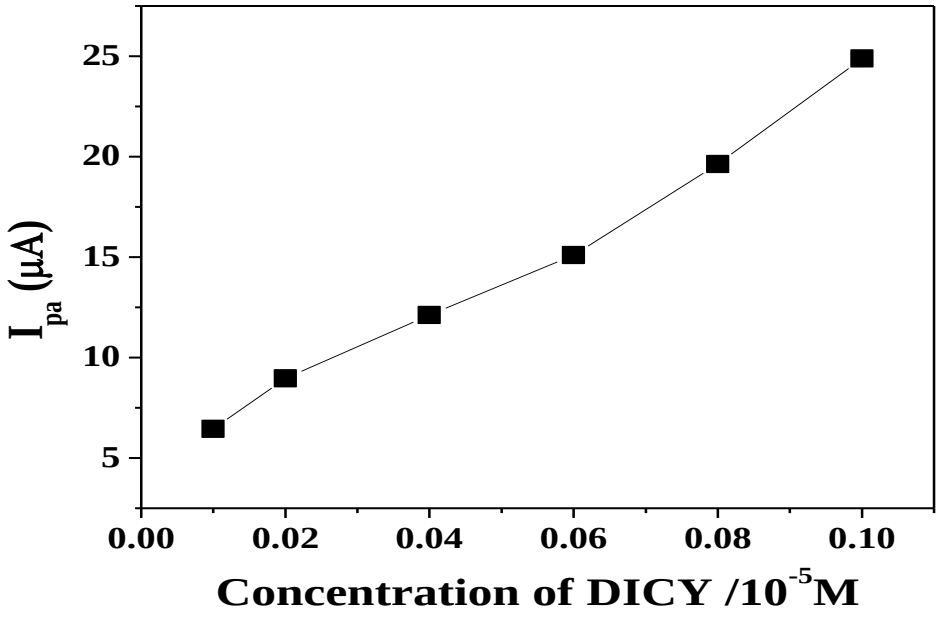

Fig. 3.7b: Plot of anodic peak current vs. DICY concentration at poly (TBS) modified carbon paste electrode.

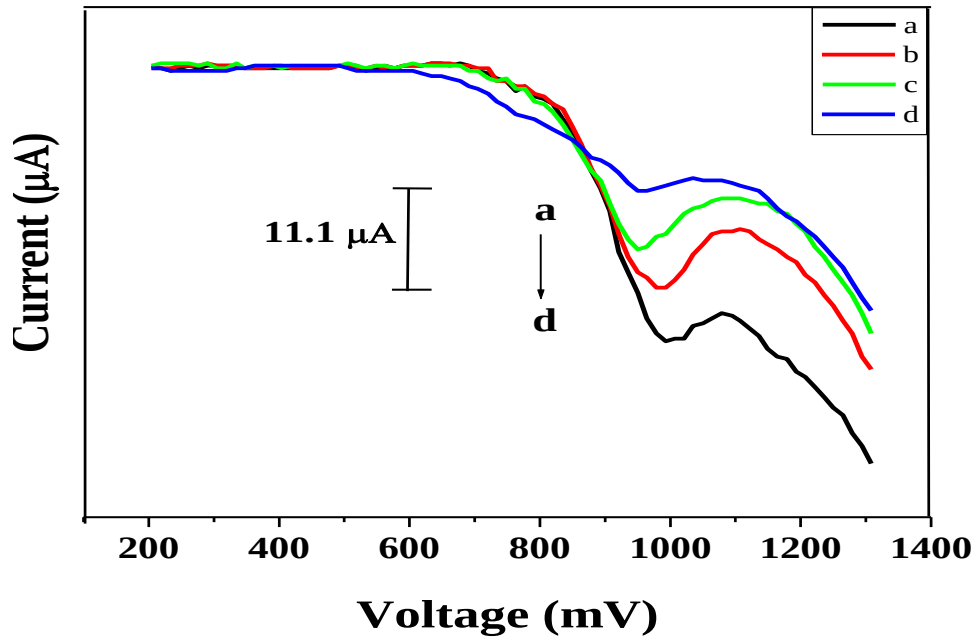

Fig. 3.8: DPV of DICY of (a) 1×10^{-5} M, (b) 2×10^{-5} M, (c) 3×10^{-5} M, (d) 4×10^{-5} M at poly (TBS) modified carbon paste electrode.

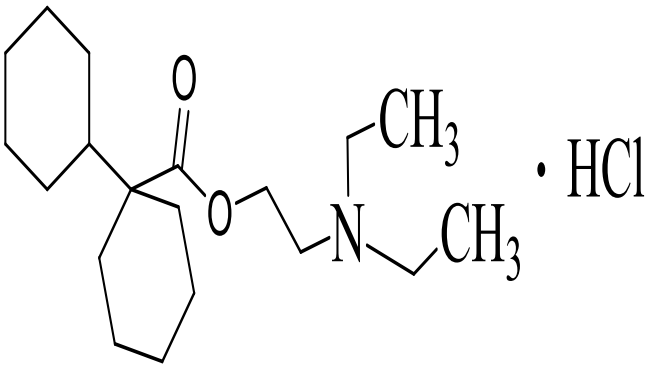

Scheme 3.1: Dicyclomine Hydrochloride.

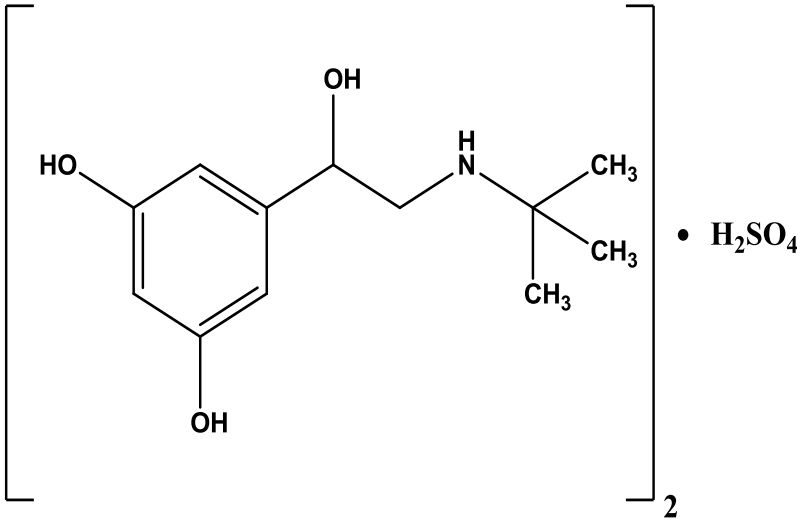

Scheme 3.2: Terbutaline Sulphate.

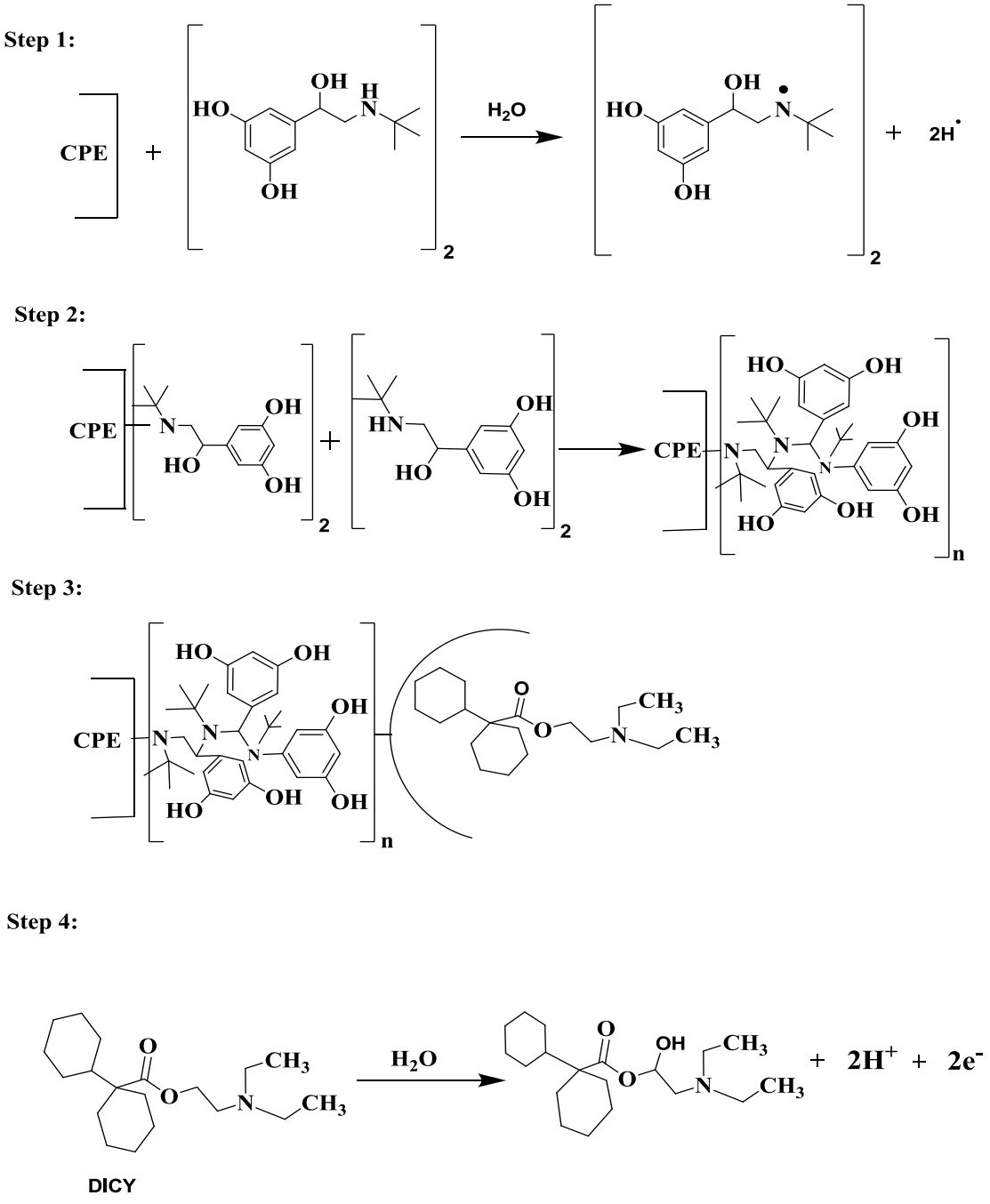

Scheme 3.3: Probable Oxidation Reaction Mechanism of DICY.

3.8. Reference:

[1] R.J. Hedpara, Vibhuti Chhatarala, Ashwin Agola, *IJPSR*, **4** (2013) 2400.

[2] Goodman and Gilman's, *The Pharmacological Basis of Therapeutics*, 7th Ed., Macmillan, New York, 1985.

[3] L.I. Bebawy, Y.M. Issa, K.M. Abdel Moneim, *J AOAC Int.*, **86** (2003) 1.

[4] G.M. Hanna, *J Assoc off Anal Chem.*, **67** (1984) 222.

[5] H. Ibrahim, Y.M. Issa, Hazem M. Abu-shawish, *Analytical sciences*, **20** (2004) 911.

[6] P. Janda, J. Weber, L. Dunsch and A.B.P. Lever, *Anal.Chem.*, **68** (1996) 960.

[7] S. Shahrokhian, M. Ghalkhani, *Electrochim Acta*, **51** (2006) 2599.

[8] R. Aguilar, M.M. Davila, M.P. Elizalde, J. Mattusch and R. Wennrich, *Electrochim. Acta*, **49** (2004) 851.

[9] B. Ursula and P E.T. Anthony, *Biosensors for Environmental Monitoring*, Harwood Academic Publishers, Amsterdam, 2000, p 428.

[10] N. Daraghmeh, M.M. Al-Omari, Z. Sara, A.A. Badwan and A.M. Jaber, *Journal of Pharmaceutical and Biomedical Analysis*, **29** (2002) 927.

[11] J.G. Leferink, W. van den Berg, I. Wagemaker-Engels, *Arzneimittel-forschung*, **32** (1982) 159.

[12] J.R.M. Bateman, D. Pavia, N.F. Sheahan, S.P. Newman and S.W. Clarke, *Br. J. clin. Pharmac.*, **15** (1983) 695.

[13] P.R. Roy, T. Okajima, T. Ohsaka, *Bioelectrochem.*, **59** (2003) 11.

[14] J. Wang, S.P. Chen, M.S. Lin, *J. Electroanal.Chem.*, **273**(1989) 231.

[15] E. Ekinci, G. Erdogdu, A.E. Karagozler, *J.Appl. Polym.Sci.*, **79** (2001) 327.

[16] M. Pontie, C. Gobin, T. Pauporte, F. Bedioui and J. Devynck, *Anal. Chim. Acta*, **411** (2000) 175.

[17] H. Zhao, Y.Z. Zhang, Z.B. Yuan, *Electroanal.*, **14** (2002) 445.

[18] H. Zhao, Y.Z. Zhang, Z.B. Yuan, *Anal. Chim. Acta*, **454** (2002) 75.

[19] J.R.B. Rodriguez, A. Costa Garcia, P.T. Blanco, *Electrochim.Acta*, **34** (1989) 957.

[20] C.A. Caro, F. Bedioui, J.H. Zagal, *Electrochim.Acta*, **47** (2002) 1489.

[21] E.J. Laviron's, *Electroanal. Chem.*, **52** (1974) 355.

[22] M.P. Deepak, G.P. Mamatha, B.S. Sherigara, *Int J Phar Chem.*, **4** (2014) 122.

Chapter-3

PART-B

Electrochemical Behavior of L-Tyrosine at Poly (Dicyclomine Hydrochloride) film Modified Carbon Paste Electrode: A Cyclic Voltammetric Study

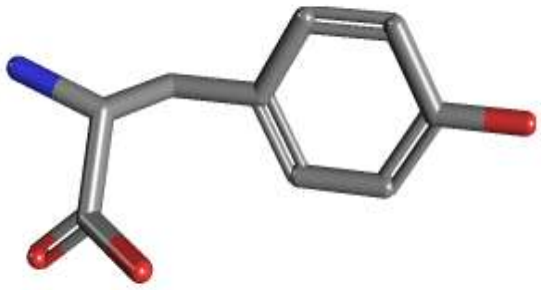

L-Tyrosine

3.9. Introduction

This chapter involves an electrochemical method for the determination of L-Tyrosine (LTY) using a dicyclomine hydrochloride (DICY) polymer film modified carbon paste electrode. The discussion involves chemistry and biological relevance of L-Tyrosine. The surface morphology of poly (DICY) modified carbon paste electrode was characterized by SEM. The modified electrode showed excellent electro catalytic activity towards the oxidation of LTY in 0.1 M phosphate buffer solution of pH 6.5. The effect of pH, concentration and scan rate were studied at the bare carbon paste electrode and poly (DICY) modified carbon paste electrode were investigated. Increase of LTY concentration shows linear increase in oxidation peak current. The linear relationship was obtained between the anodic peak current (I_{pa}) and concentration LTY in range 2×10^{-5} M to 1×10^{-3} M with correlation coefficient of 0.9984. The low detection limit (LOD) and low quantification limit (LOQ) of LTY were detected. The cyclic voltammetric studies indicated that the oxidation of LTY at the modified electrode surface was irreversible, adsorption controlled and undergoes a one electron transfer process at the poly (DICY) film modified carbon paste electrode. The modified electrode showed high sensitivity, detection limit, high reproducibility, easy preparation and regeneration of the electrode surface.

3.10. Chemistry of L-Tyrosine

L-Tyrosine (LTY, **Scheme.3.10**) or 4-hydroxyphenylalanine is one of the 22 amino acids that are used by cells to synthesize proteins. The word "tyrosine" is from the Greek *tyri*, meaning *cheese*, as it was first discovered in 1846 by German chemist Justus von Liebig in the protein casein from cheese [1, 2]. It is called tyrosyl when referred to as a functional group or side chain. Aside from being a proteogenic amino acid, tyrosine has a special role by virtue of the phenol functionality. It occurs in proteins that are part of signal transduction processes. It functions as a receiver of phosphate groups that are transferred by way of protein kinases (so-called receptor

tyrosine kinases). Phosphorylation of the hydroxyl group changes the activity of the target protein.

A tyrosine residue also plays an important role in photosynthesis. In chloroplasts (photosystem II), it acts as an electron donor in the reduction of oxidized chlorophyll. In this process, it undergoes deprotonation of its phenolic OH-group. This radical is subsequently reduced in the photosystem II by the four core manganese clusters.

3.10.1. Biological Relevance of L-Tyrosine

LTY is the precursor of dopamine, thyroxin and neurotransmitters in mammalian central nervous systems [3]. The absence of TY could cause albinism and alkaptonuria, while a high TY concentration in culture medium results in increased sister chromatid exchange. In dopaminergic cells in the brain, tyrosine is converted to levodopa by the enzyme tyrosine hydroxylase (TH). TH is the rate-limiting enzyme involved in the synthesis of the neurotransmitter dopamine. In addition, in the adrenal medulla, tyrosine is converted into the catecholamine hormones norepinephrine (noradrenaline) and epinephrine (adrenaline). Tyrosine, through its effect on neurotransmitters, is used to treat conditions including mood enhancement, appetite suppression and growth hormone stimulation. In addition, tyrosine is reported to have an antioxidant effect. Tyrosine is the precursor to the pigment melanin, tyrosine is converted by skin cells into melanin, the dark pigment that protects against the harmful effects of ultraviolet light. It occurs in proteins that are part of signal transduction and also plays an important role in photosynthesis. The study had documented that the trace level tyrosine can modulate and control acetylcholine (Ach) receptors metabolic stability in muscle cells [4]. The absence of tyrosine could cause albinism and alkaptonuria, while a high tyrosine concentration in culture medium results in increased sister chromatid exchange. Tyrosine has little effect on mood in normal circumstances [5-7], but the effect on mood is more noticeable in humans subjected to stressful conditions. A number of studies have found tyrosine to be useful during conditions of stress, cold, fatigue [8], loss of a loved one such as in death or divorce, prolonged work and sleep deprivation [9, 10], with reductions in stress hormone levels [11],

improvements in cognitive and physical performance [5, 12, 13] seen in human trials; however, because tyrosine hydroxylase is the rate-limiting enzyme, effects are less significant than those of L-dopa.

3.11. Review of electrochemistry of L - Tyrosine

There are number of electrochemical methods reported for the determination of tyrosine using various modified electrodes which include, L-serine polymer film [14], multiwall carbon nanotubes [15], poly (9-aminoacridine) [16] and gold nanoparticles [17] modified with glassy carbon electrode, FTIR spectroscopic studies at poly crystalline platinum surface [18] and polyamide modified carbon paste electrode along with tryptophan [19] and iron(III) doped zeolite modified with carbon paste electrode along with dopamine [20] amperometry and cyclic voltammetry at carbon fiber microelectrodes applied to single cell analysis along with tryptophan [21]. Numerous methods have been reported for tyrosine determination mainly spectrophotometric, fluorimetric, flow injection, chemiluminescence, liquid chromatography-tandem mass spectrometry, gas chromatography-mass spectrometry and high-performance liquid chromatography [22-28].

Limited work has been done in the area of carbon paste electrode for the determination of L-Tyrosine. Therefore in the present work we used dicyclomine Hydrochloride polymer modified CPE to study the electrochemical behavior of L-Tyrosine and polymerization of dicyclomine hydrochloride has been established for the determination of L-Tyrosine for the first time. This electrode showed excellent electrocatalytic activity towards the oxidation of L-Tyrosine, the determination and sensitivity is significantly improved compared to bare CPE.

3.12. Experimental Section

3.12.1. Reagents

Dicyclomine Hydrochloride (DICY) and L-Tyrosine (LTY) were purchased from Sigma Aldrich and all other chemicals were of analytical grade. The

electropolymerisation of dicyclomine hydrochloride was performed in 0.1 M phosphate buffer solution. The phosphate buffer solution was prepared from KH_2PO_4 and K_2HPO_4, the pH was adjusted with H_3PO_4 and 0.1 N NaOH solution. The stock solution of L-Tyrosine (10 mM) was prepared by dissolving in 0.1 N NaOH. Other chemicals used were of analytical grade except for spectroscopically pure graphite powder. All solutions were prepared with doubly distilled water. Freshly prepared LTY solution is used prior to measurements.

3.12.2. Apparatus

Electrochemical measurements were carried out with Electroanalyser model EA-201 chemlink system in a conventional three-electrode system. The working electrode was carbon paste electrode, having cavity of 3 mm diameter. The counter electrode was platinum electrode with a saturated calomel electrode (SCE) as a standard reference electrode for completing the circuit.

3.12.3. Modification procedure

3.12.3a. Preparation of bare carbon paste electrode

The Bare Carbon paste electrode was prepared by hand mixing of 70% graphite powder and 30% silicon oil to produce a homogenous carbon paste which was then packed into the cavity of a homemade carbon paste electrode and smoothed on a weighing paper.

3.12.3b. Preparation of the Dicyclomine hydrochloride polymer film modified carbon paste electrode

The polymer film modified electrode was prepared by electrochemical polymerization of DICY in 0.1 M phosphate buffer solution of pH 6.5 containing 1 mM DICY with cyclic voltammetric in the potential range 100 to 1400 mV at the scan rate of 100 mVs^{-1}. After 10 cycles, the surface of the electrode was washed with double distilled water to remove the physically adsorbed material, air dried and used for the electrochemical studies.

3.13. Result and Discussion

3.13.1. Electropolymerisation of Dicyclomine Hydrochloride (DICY) on Carbon Paste Electrode

Electropolymerization of dicyclomine hydrochloride (DICY) was performed on bare carbon paste electrode (BCPE). The cyclic voltammograms for the electropolymerisation of 1 mM of DICY in 0.1 M phosphate buffer solution on CPE is shown in **Fig.3.9**, which displays the continuous cyclic voltammetric of 1 mM DICY monomer by scanning in the potential range of 100 to 1400 mV for 10 cycles. During the electropolymerisation process, indiscernible peaks started to appear after 5^{th} cycle. An anodic peak at 861 mV potential was observed due to the formation of poly (DICY). The peak descended gradually with the increase in cyclic time; such decrease indicates the poly (DICY) membrane forming and depositing on the surface of the CPE by electropolymerisation. After polymerization the poly (DICY) modified carbon paste electrode was carefully rinsed with distilled water to remove the physically adsorbed material. Then the film electrode was transferred to an electrochemical cell and cyclic voltammetric sweeps were carried out to obtain electrochemical steady state.

The thickness of poly (DICY) film could be controlled by the cyclic number of voltammetric scans during the electrochemical modification. The effect of the thickness of poly (DICY) film on the electrochemical response was investigated by cyclic voltammetric technique. The current (I_{pa}) response of poly (DICY) films increase gradually as the number of cycles increases during film formation from 5 to 10 cycles. Afterwards I_{pa} starts to decrease by increasing the number of cycles which was examined up to 30 cycles **(Fig.3.9a).** In order to obtain better oxidation peak and higher sensitivity of current for the electrochemical response of DICY, 10 scans were chosen to control the thickness of the poly (DICY) film.

3.13.2. SEM Characterization of poly (Dicyclomine Hydrochloride) modified carbon paste electrode

Fig.3.10a and **Fig.3.10b**, explain the surface morphology of bare carbon paste electrode (BCPE) and poly (DICY) modified carbon paste electrode respectively using scanning electron microscope (SEM). The surface of bare CPE was formed by irregularly shaped micrometer-sized flakes of graphite. Whereas the modified electrode had a typical uniform arrangement of DICY molecules on the surface of CPE [29].

3.13.3. Electrochemical response of potassium ferrocyanide at poly (DICY) modified carbon paste electrode

Fig.3.11 shows the electrochemical response of 1 mM potassium ferrocyanide in 1M KCl at bare carbon paste electrode (BCPE) curve 'b' and at poly (DICY) modified carbon paste electrode curve 'a'. Anodic peak potential E_{pa} 290 mV with peak current I_{pa} of 13.38 µA and cathodic peak E_{pc} 50 mV with peak current I_{pc} of 8.23 µA respectively. After modification with poly (DICY) modified carbon paste electrode which shows enhancement of both electrochemical anodic peak potential (E_{pa}) 234 mV with peak current (I_{pa}) of 23.9 µA and cathodic peak potential (E_{pc}) 163 mV with peak current (I_{pc}) of 14.55 µA respectively were observed. The surface area of bare carbon paste electrode is 0.0258 cm^2. Whereas, effective surface area of the modified electrode was found to be 0.0365 cm^2.

3.13.4. Electrochemical behavior of L-Tyrosine at poly (Dicyclomine Hydrochloride) modified carbon paste electrode

Fig.3.12 shows cyclic voltammograms of 0.1 mM L-Tyrosine in 0.1 M phosphate buffer solution of pH 6.5 at bare carbon paste electrode (curve 'b') and at poly (DICY) modified carbon paste electrode (curve 'a'). The curve 'c' represents cyclic voltammogram of the blank solution at poly (DICY) modified carbon paste electrode. Above studies showed that only one oxidation peak at 1009 mV potential with peak current of 12.49 µA at bare CPE, whereas an oxidation peak at 991 mV

potential with peak current of 28.70 µA at the poly (DICY) modified carbon paste electrode respectively in the potential range 100 to 1300 mV. No reduction peak was observed in the reverse scan, suggesting that the electrochemical reaction is a totally irreversible process and the oxidation peak current at the bare CPE is broad due to slow electron transfer, while the response was considerably improved at the poly (DICY) modified carbon paste electrode and the peak potentials shifted to negative direction, the shape of the peak turns sharper and the peak current increased significantly.

3.13.5. Effect of pH

The pH influence was investigated by cyclic voltammetric measurement at different pH values between 3.5 and 9.0 as shown in **Fig.3.13a**. The maximum response of current was observed at pH 6.5. In order to obtain the maximum bioactivity and optimal sensitivity, phosphate buffer solution of pH 6.5 and scan rate 50 mVs^{-1} were selected for our experiments. The oxidation peak current increases with increase of pH from 4.5 to 6.5 and becomes maximum and peak potential shifted negatively. While pH beyond 6.5, a great decrease of the oxidation peak current could be observed, then it decreased gradually with the further increase in pH of the solution as shown in **Fig.3.13a** and the oxidation peak potential decrease with increase of pH as shown in **Fig.3.13b**. A linear relationship was obtained between the anodic peak potential and pH of the solution in the range 3.5 – 9. The corresponding linear regression equation is

$$E_{pa}\ (mV) = 1086 - 28.89\ pH \quad (R = 0.99149) \qquad (3.8)$$

With a negative slope of 28.89 indicating that the number of electrons and protons are equal in the electrochemical oxidation of LTY at poly (DICY) modified carbon paste electrode.

3.13.6. Effect of scan rate

The effect of scan rates on the electrochemical response of 0.1 mM LTY at poly (DICY) modified carbon paste electrode was studied at different scan rates. Redox peak current increase linearly with the scan rate in the range 10, 20, 30, 40, 50, 60, 70, 80, 90

and 100 mVs^{-1}.The cyclic voltammograms were shown in **Fig.3.14a**. However linearity obtained for the plot of the anodic peak current vs. scan rate with a correlation coefficient of 0.9943 shown in **Fig.3.14b.** The linear relationship with a correlation coefficient of 0.9988 obtained between the peak current and square root of scan rate in the range of 10 - 100 mVs^{-1} is shown in the **Fig.3.14c** which indicates the process occurring is adsorption controlled. The relationship between the anodic peak potential and scan rate is explained by plotting the anodic peak potentials vs. natural logarithm of scan rate **(Fig.3.14d)** by considering the liner regression equation given by

$$E_{pa}\,(mV) = 0.01443\ \ln\upsilon + 0.43687 \quad R= 0.99754 \ldots\ldots (3.9).$$

The relationship between the anodic peak current and scan rate is explained by plot of the logarithm of anodic peak current vs. logarithm of scan rate **(Fig.3.14e)** by considering the following equation:

$$\log I_{pa} = 0.8266\ \log\upsilon - 0.15702 \quad R= 0.9873 \ldots\ldots (3.10)$$

The slope of 0.82 is close to the theoretically expected value of 1.0 for an adsorption controlled process [30] and as a result the peak potential shifts towards positive side.

According to Laviron's theory [31] the slope is equal to $RT/\alpha n_{\alpha}F$. As for a totally irreversible electrode reaction on the basis of the above discussion, the n_{α} was found to be 0.806, which indicated that one electron was involved in the oxidation process of LTY at the poly (DICY) modified carbon paste electrode. Since the equal number of electrons and protons took part in the oxidation of LTY, therefore one electron and one proton transfer were involved in the electrode reaction process. The electrochemical reaction process for LTY at poly (DICY) modified carbon paste electrode can therefore be summarized as in **Scheme 3.12.**

3.13.7. Effect of L-Tyrosine (LTY) concentration and detection limit

The effect of LTY concentration was studied by cyclic voltammetry in 0.1 M phosphate buffer solution (PBS) of pH 6.5 at the scan rate 50 mVs^{-1}. The oxidation peak

current increases with increase in concentration of LTY. **Fig.3.15a** and **Fig.3.15b** shows the linear relationship between the anodic peak current (I_{pa}) with LTY concentration in the range from 2×10^{-5} M to 1×10^{-3} M. The corresponding linear regression equation is

$$I_{pa}\ (\mu A) = 26.5481\ C\ (10^{-5}\ M) + 2.26913 \quad (R = 0.9984)\ldots\ldots\ldots\ldots\ldots\ldots\ (3.11)$$

The limit of detection (LOD) and limit of quantification (LOQ) of LTY were found to be 0.638 µM and 2.128 µM respectively. Related stastical data of calibration curves were obtained from five different calibration curves (n=5). The LOD and LOQ were calculated from the peak current using the following equation:

$$LOD = 3S/M \text{ and } LOD = 10S/M$$

Where S is standard deviation and M is the slope (sensitivity) of calibration plot.

3.14. Conclusion

- In the present study, the poly (Dicyclomine Hydrochloride) modified carbon paste electrode based on the electropolymerisation has been prepared for the electrochemical investigation of LTY.
- Results showed that the oxidation peak current of LTY was improved at poly (DICY) modified carbon paste electrode.
- The electrochemical response is diffusion controlled and irreversible in nature for LTY.
- A linear concentration range was found to occur from 2×10^{-5} to 1×10^{-3} M by CV.
- The probable reaction mechanism involved in the oxidation of (LTY) is also proposed.

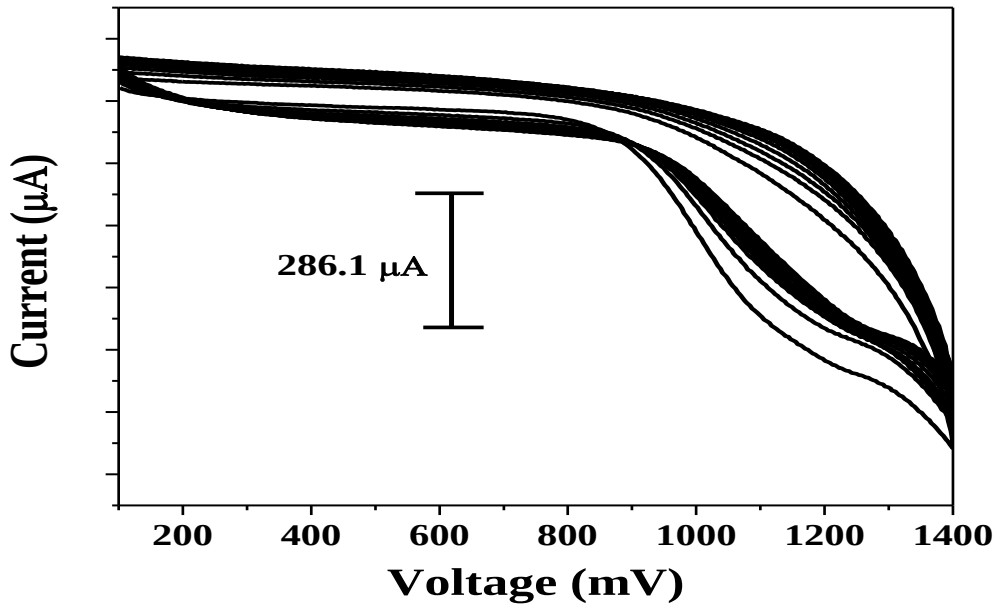

Fig. 3.9: Cyclic voltammograms for the electro polymerization of 1 mM of DICY in 0.1 M phosphate buffer solution on carbon paste electrode.

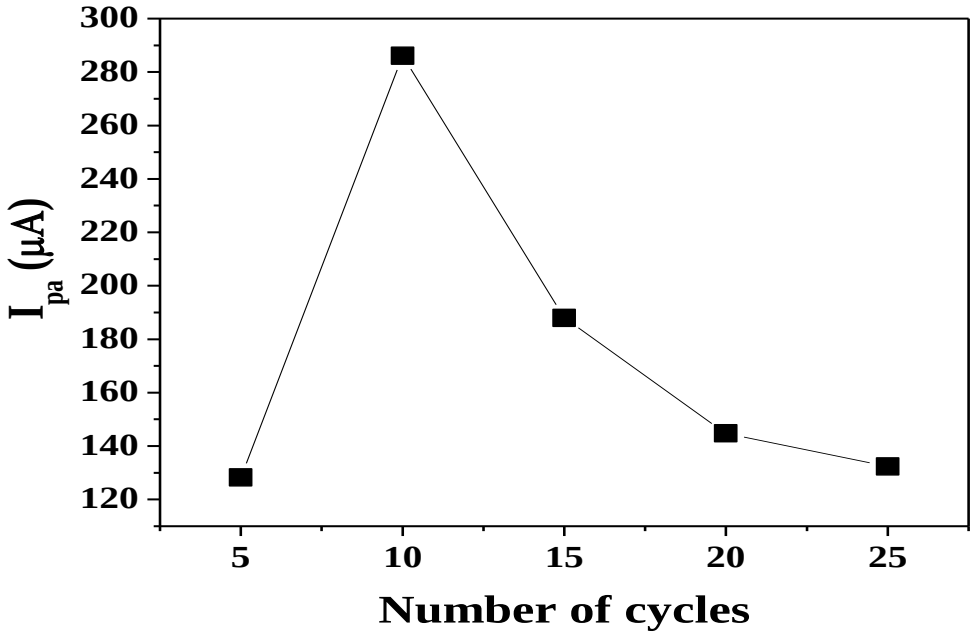

Fig. 3.9a: Plot of anodic peak current vs. number of cycles of Dicyclomine hydrochloride.

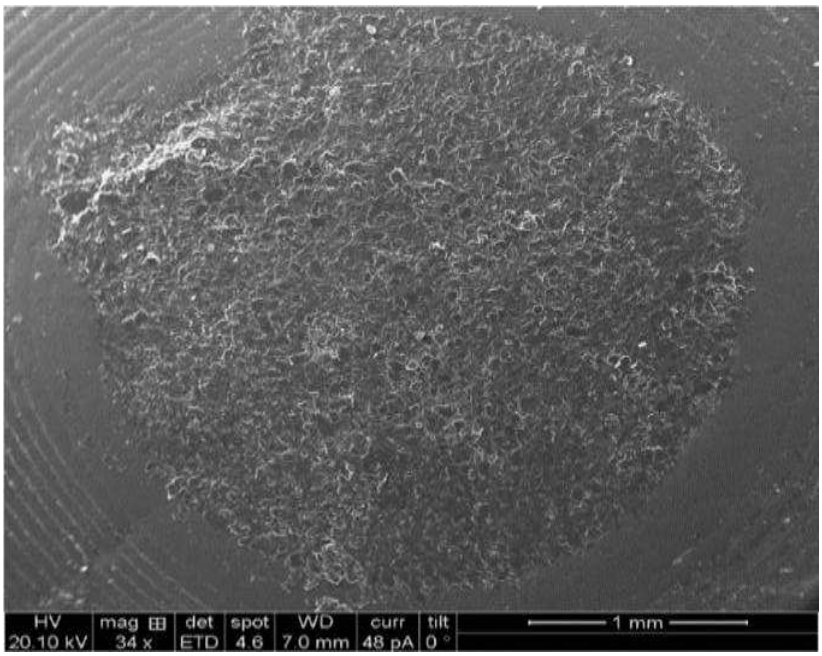

Fig. 3.10a: SEM image of bare carbon paste electrode.

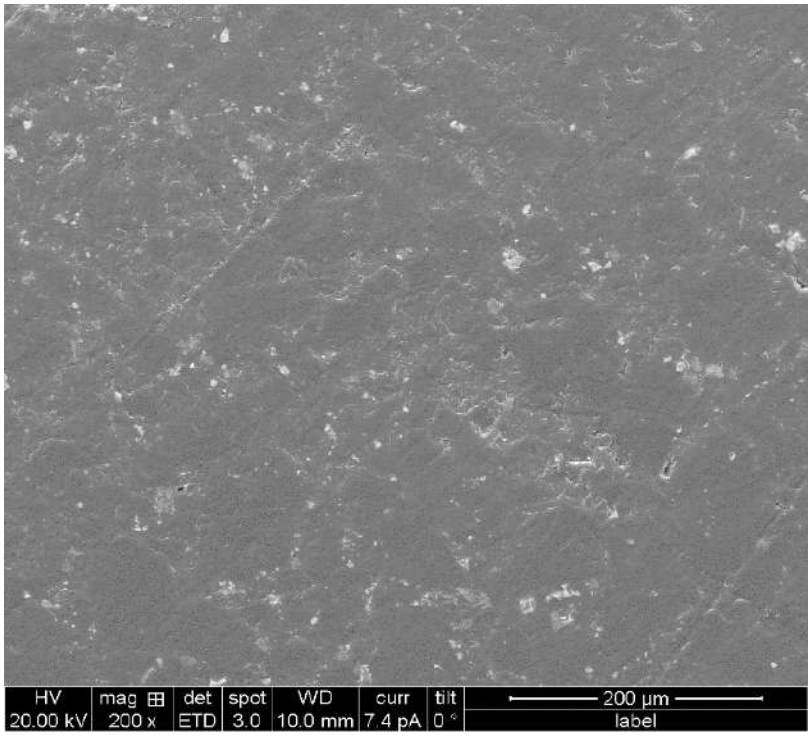

Fig. 3.10b: SEM image of poly (DICY) modified carbon paste electrode.

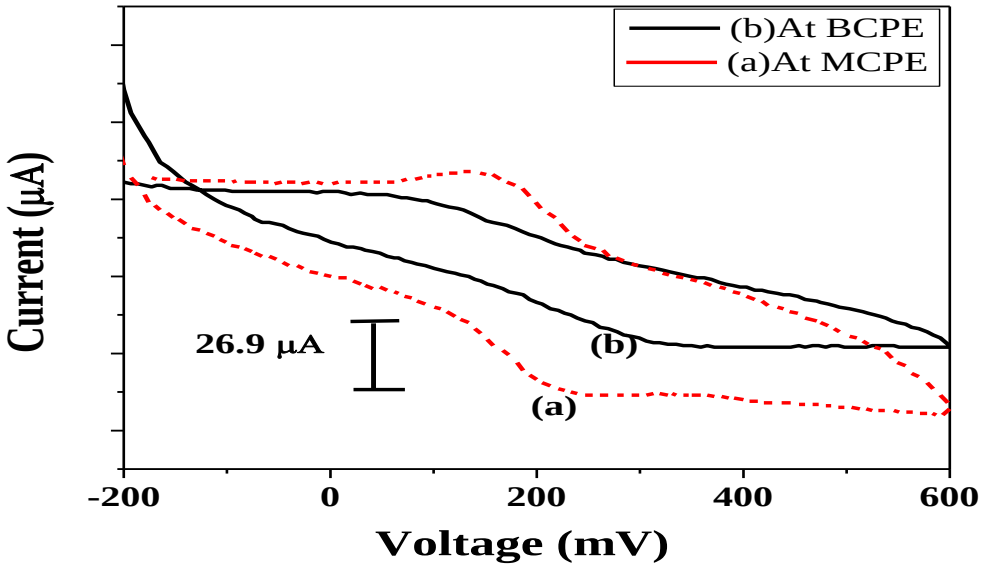

Fig. 3.11: Comparison of 1 mM $K_4[Fe(CN)_6]$ in 1 M KCl solution at poly (DICY) modified carbon paste electrode (a) and bare carbon paste electrode (b).

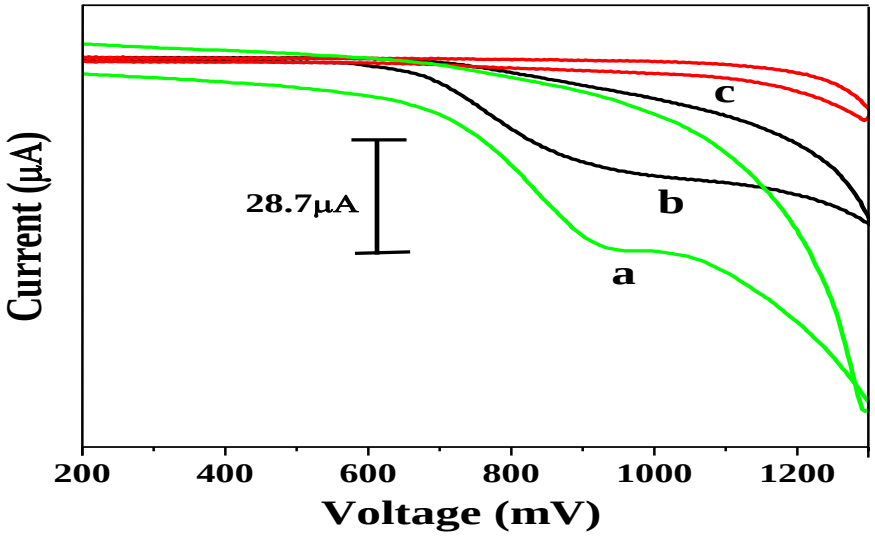

Fig. 3.12: Comparision of 1 mM LTY at poly (DICY) modified carbon paste electrode (a), bare carbon paste electrode (b) and blank solution in phosphate buffer at poly (DICY) modified carbon paste electrode (c); pH 6.5, scan rate 50 mVs^{-1}.

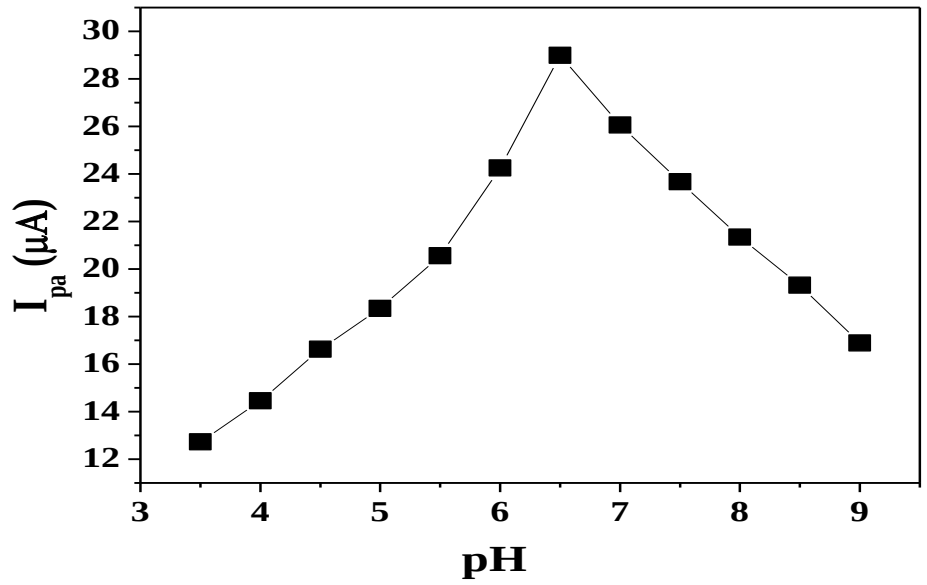

Fig. 3.13a: Plot of anodic peak current vs. pH (3.5 – 9.0) of 0.1 mM LTY at poly (DICY) modified carbon paste electrode.

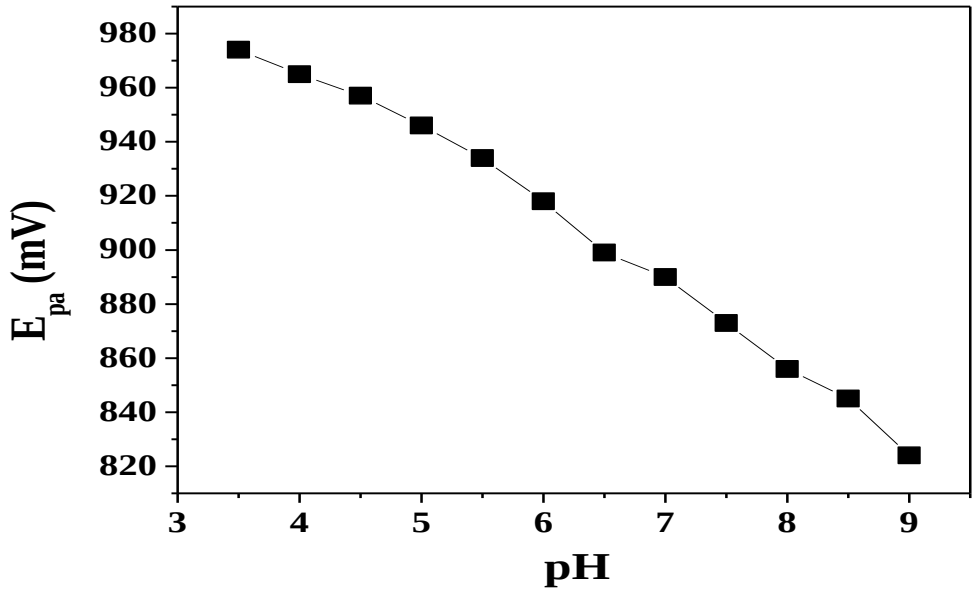

Fig. 3.13b: Plot of anodic peak potential vs. pH (2.5 – 9.0) of 0.1 mM LTY at poly (DICY) modified carbon paste electrode.

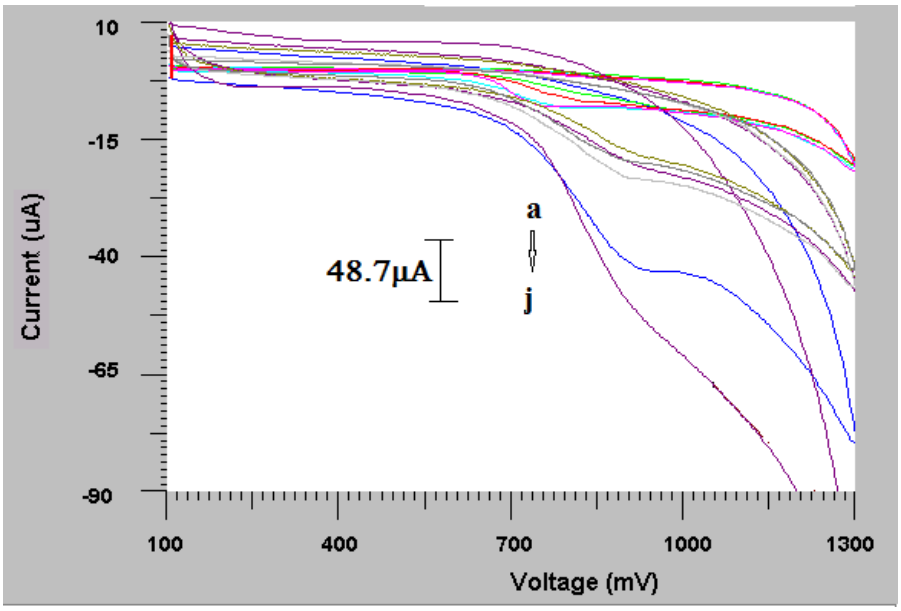

Fig. 3.14a: Cyclic voltammograms of 0.1 mM LTY at poly (DICY) modified carbon paste electrode with different scan rates (a) 10, (b) 20, (c) 30, (d) 40, (e) 50, (f) 60, (g) 70, (h) 80, (i) 90, (j) 100 mVs^{-1}.

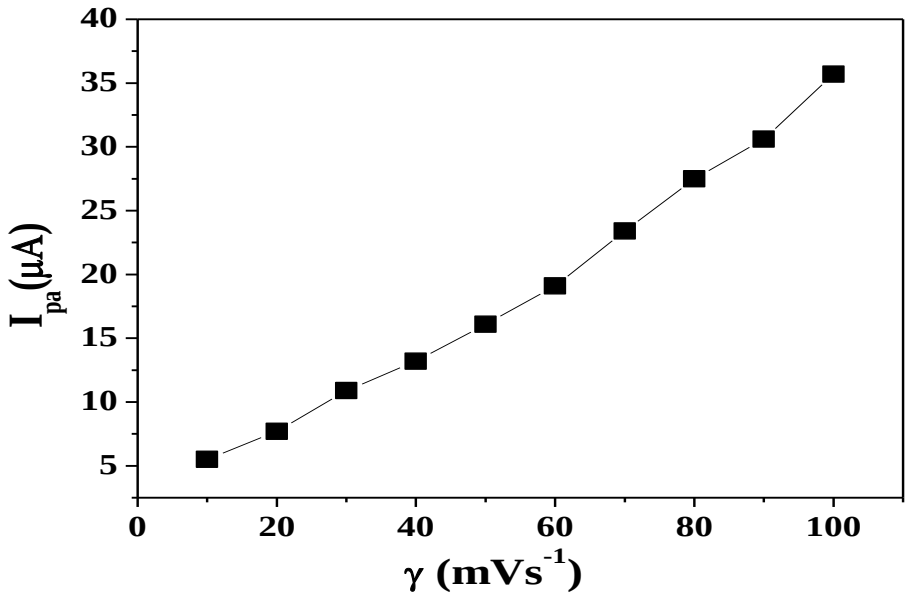

Fig. 3.14b: Plot of anodic peak current vs. scan rates of LTY at poly (DICY) modified carbon paste electrode.

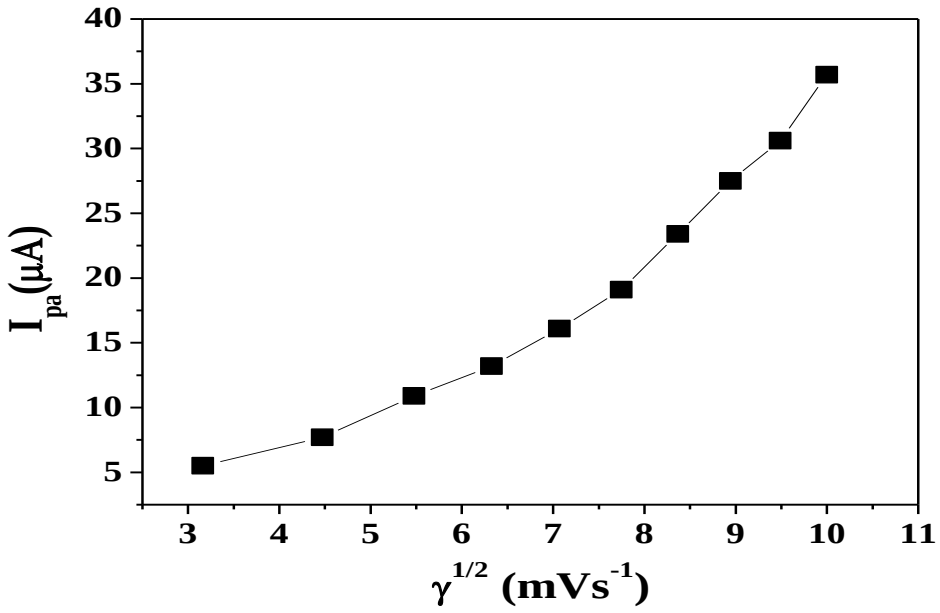

Fig. 3.14c: Plot of anodic peak current (I_{pa}) vs. square root of scan rates of LTY at poly (DICY) modified carbon paste electrode.

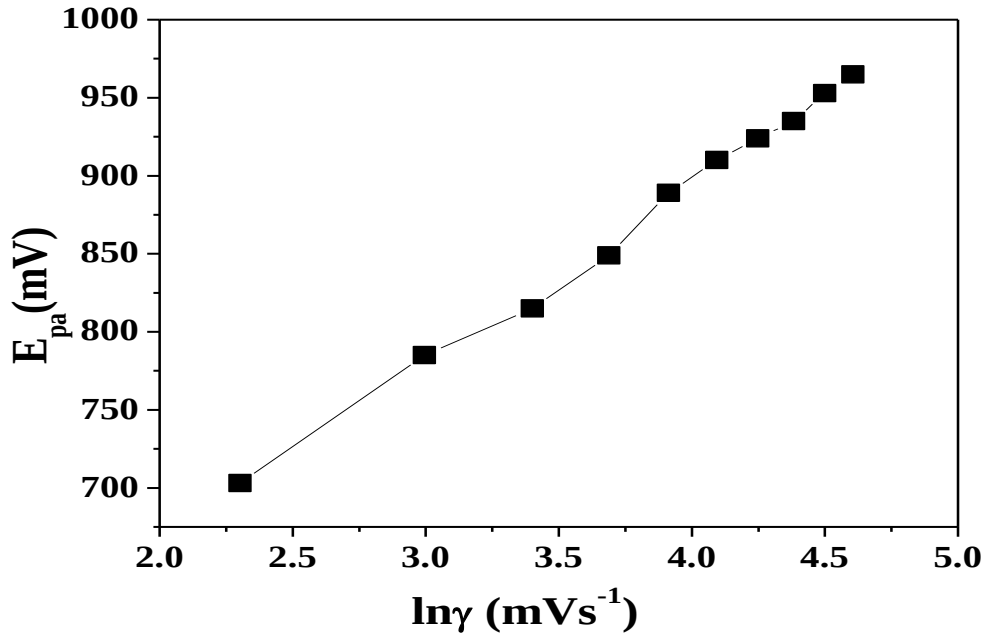

Fig. 3.14d: Plot of anodic peak potential vs. natural logarithm of scan rates of LTY at poly (DICY) modified carbon paste electrode.

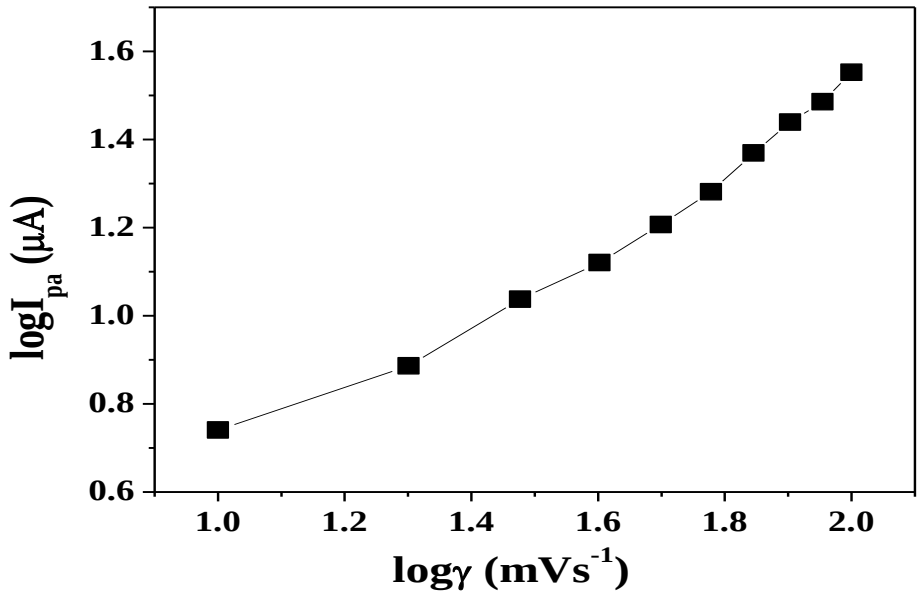

Fig. 3.14e: Plot of logarithm of anodic peak current vs. logarithm of scan rates of LTY at poly (DICY) modified carbon paste electrode.

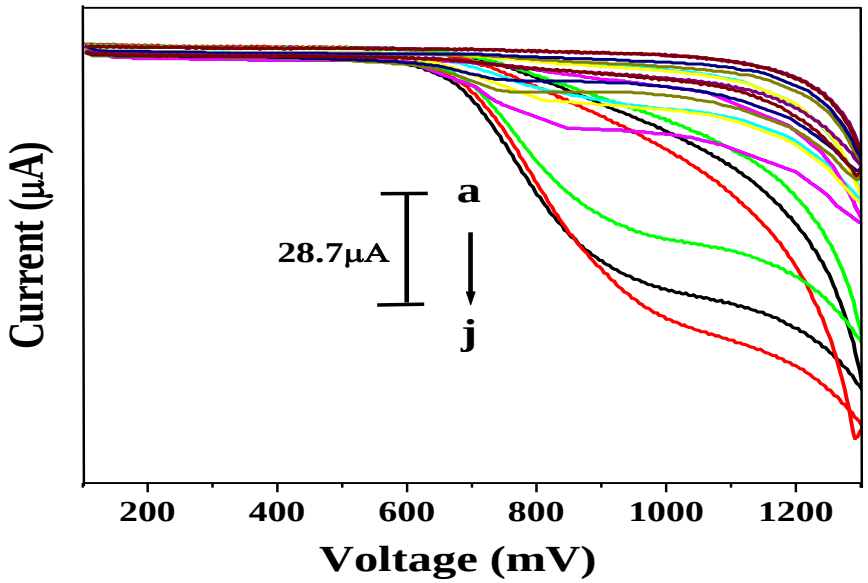

Fig. 3.15a: Effect of variation of concentration of LTY (a) 2×10^{-5} M, (b) 4×10^{-5} M, (c) 6×10^{-5} M, (d) 8×10^{-5} M, (e) 1×10^{-4} M, (f) 2×10^{-4} M, (g) 4×10^{-4} M, (h) 6×10^{-4}M, (i) 8×10^{-4} M, (j) 1×10^{-3}M on anodic peak current at poly (DICY) modified carbon paste electrode; pH 6.5, scan rate 50 mVs^{-1}.

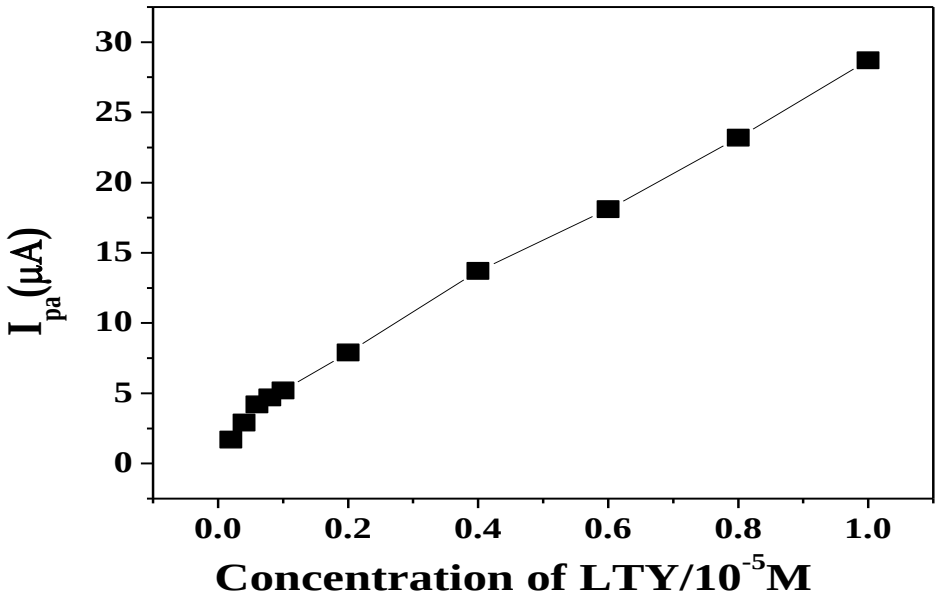

Fig. 3.15b: Plot of anodic peak current vs. LTY concentration at poly (DICY) modified carbon paste electrode.

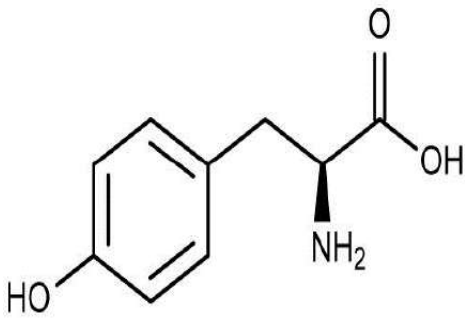

Scheme 3.10: L-Tyrosine.

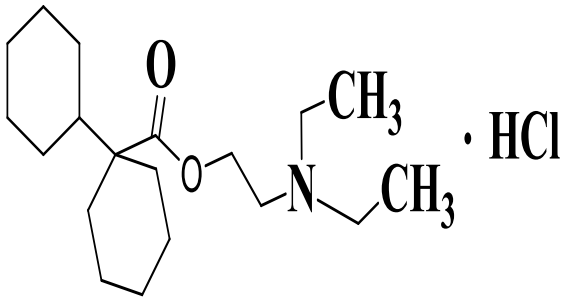

Scheme 3.11: Dicyclomine Hydrochloride.

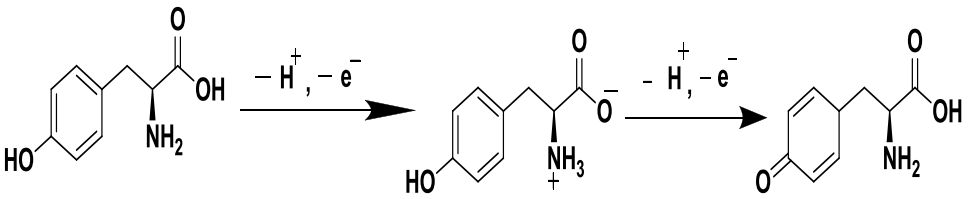

L-Tyrosine

Scheme 3.12: Probable Reaction Mechanism of L-Tyrosine.

3.15. Reference

[1] "Tyrosine". The Columbia Electronic Encyclopedia, 6th ed. Columbia University Press, 2007.

[2] D. Harper, *"Tyrosine". Online Etymology Dictionary*, 2001.

[3] Xiaofeng Tanga, Yang Liua, Haoqing Houb and Tianyan You, *Talanta*, **80** (2010) 2182.

[4] Savaa, I. Barisonea, D.D. maurob, *Neurosci. Lett.*, **313** (2001) 37.

[5] P.D. Leathwood, P. Pollet, *Journal of psychiatric research,* **17** (1982) 147.

[6] J.B. Deijen, J.F. Orlebeke, *Brain Res Bull.,* **33** (1994) 319.

[7] H.R. Lieberman, S. Corkin, B.J. Spring, R.J. Wurtman and J.H. Growdon, *Am J Clin Nutr.,* **42** (1985) 366.

[8] S. Hao, Y. Avraham, O. Bonne and E.M. Berry, *Pharmacol Biochem Behav.,* **68** (2001) 273.

[9] R.A. Magill, W.F. Waters, G.A. Bray, J. Volaufova, S. R. Smith, H.R. Lieberman, N. McNevin and D.H. Ryan, *Nutritional Neuroscience,* **6** (2003) 237.

[10] D.F. Neri, D. Wiegmann, R.R. Stanny, S.A. Shappell, A. McCardie and D.L. McKay, *Aviation, space and environmental medicine,* **66** (1995) 313.

[11] D.K. Reinstein, H. Lehnert, R.J. Wurtman, *Life Sci.,* **37** (1985) 2157.

[12] J.B. Deijen, C.J. Wientjes, H.F. Vullinghs, P.A. Cloin and J.J. Langefeld, *Brain Res Bull.,* **48** (1999) 203.

[13] C.R. Mahoney, J. Castellani, F.M. Kramer, A. Young and H.R. Lieberman, *Physiology and Behavior*, **92** (2007) 575.

[14] K. J. Huang, D.F. Luo, W.Z. Xie and Y.S. Yu, *Colloids Surf B.,* **61** (2008) 176.

[15] B. Fang, H. Liu, G. Wang, Y. Zhou, *Ann. Chim.*, **97** (2007) 1005.

[16] C.F. Zinola, J.L. Rodriguez, M.C. Arevalo, *J. Soild State Electrochem.,* **12** (2008) 523.

[17] C.D. Paras, R.T. Kennedy, *Electroanalysis*, **9** (1997) 203.

[18] H. Cheng, C. Chen, S. Zhang, *Analyt. Sci.,* **25** (2009) 1221.

[19] B. Ali, Z. Mojgan, K. Balal, A. Mohammad, *Chin. J. Chem.,* **28** (2010) 1967.

[20] C. Li, *Colloids Surf. B.,* **50** (2006) 147.

[21] Y.D. Zou, J. Wang, J.Y. Mo, R.J. Zhang, *Fenxi Ceshi Xuebao,* **18** (1999) 25.

[22] Y. Azuma, M. Maekawa, Y. Kuwabara, T. Nakajima, K. Taniguchi and T. Kanno, *Clin Chem.,* **35** (1989) 1399.

[23] F. Wang, K.Z. Wu, Y. Qing, Y.X. Ci, *Anal Lett.*, **25** (1992) 1469.

[24] J.W. Costin, P.S. Francis, S.W. Lewis, *Analytica Chim Acta,* **480** (2003) 67.

[25] Y. Huang, X.Y. Jiang, W. Wang, *Talanta,* **70** (2006) 1157.

[26] H. Orhan, N.P.E. Vermeulen, C. Tump, H. Zappey and J.H.N. meerman, *J. Chromatogr. B.,* **799** (2004) 245.

[27] C.H. Deng, Y.H. Deng, B. Wang and X.H. Yang, *J. Chromatogr. B.,* **780** (2002) 407.

[28] S. Letellier, J.P. Garnier, J. Spy, B. *J. Chromatogr B.,* **696** (1997) 9.

[29] C.A. Caro, F. Bedioui, J.H. Zagal, *Electrochim. Acta,* **47** (2002) 1489.

[30] R.N. Hegde, N.P. Shetty, S.T. Nandibewoor, *Talanta,* **79** (2009) 361.

[31] E.J. Laviron's, *Electroanal. Chem.*, **52** (1974) 355-393.

Chapter-4

Cyclic Voltammetric Studies of Ciprofloxacin Hydrochloride at Poly (L-Tyrosine) SnO_2 nanoparticles Modified Carbon Paste Electrode

Ciprofloxacin Hydrochloride

4.1. Introduction:

This chapter describes the electrochemical investigation of CIP at poly (L-Tyrosine) SnO_2 nanoparticles modified carbon paste electrode (PLTSNMCPE) by cyclic voltammetric (CV) and differential pulse voltammetric techniques (DPV). The discussion involves the chemistry, biological relevance of CIP and their oxidation behavior at PLTSNMCPE. Before modification the SnO_2 nanoparticles were synthesized by gel combustion method, this synthesized SnO_2 nanoparticles were characterized by XRD and SEM. Then the carbon paste electrode is modified with the synthesized SnO_2 nanoparticles and L-Tyrosine by electropolymerisation method using CV technique. The surface morphology of poly (L-Tyrosine) SnO_2 nanoparticles modified carbon paste electrode confirmed by scanning electron microscope (SEM). The electrochemical response of CIP at modified electrode was confirmed from the remarkable oxidation peak current enhancement. The electrode process of CIP was examined with all the experimental parameters such as pH, scan rate and concentration. This method was successfully applied for investigation of CIP in commercial tablet sample. Finally a sensitive and simple voltammetric method was developed for the determination of CIP for pharmacological practical application.

4.2. Chemistry and Biological Relevance of Ciprofloxacin Hydrochloride

The ciprofloxacin hydrochloride (CIP) chemically described as 1-cyclopropyl -6-fluoro -1, 4-dihydro -4-oxo -7- (1-piperazinyl) -3- quinoline carboxylic acid, monohydrochloride **(scheme 4.1).** CIP is used to treat or prevent certain infections caused by bacteria. CIP is also used to treat or prevent anthrax in people who may have been exposed to anthrax germs in the air [1]. CIP belongs to the family of fluoroquinolone antibacterial agents that also includes norfloxacin, ofloxacin and some other molecules. These fluoroquinolone antibacterial agents are synthetic derivatives of 6-fluoro-4-oxo-quinoline-3-carboxylic acid. They are fluorinated at position 6 and mostly bear a piperazinyl moiety at position 7. Ciprofloxacin is one of the most potent quinolone derivatives in clinical use with a very broad spectrum of antibacterial activity

and is often used as an antibacterial agent of last resort [2]. Ciprofloxacin (belonging to the second-generation fluoroquinolone) is the most potent fluoroquinolone against Gram-positive and Gram-negative bacteria through inhibition of their NAD gyrase, a critical enzyme to bacterial chromosome replication [3, 4].

4.3. Review of electrochemistry of Ciprofloxacin Hydrochloride

Literature survey reveals that the reported methods for the determination of ciprofloxacin hydrochloride. Zhang Zhuoyong *et.al.,* [5] have reported the novel flow injection chemiluminescence (CL) method for the determination of ciprofloxacin (CIP). The voltammetric behavior of ciprofloxacin was investigated using cyclic voltammetry and differential-pulse anodic stripping voltammetry at bare glassy carbon (GC) electrode and DNA modified glassy carbon (DNA-GC) electrode by Nizam Diab *et al.,* [6]. The reduction square wave voltammetric method was developed and validated for the direct determination of ciprofloxacin (CIP) in pharmaceutical formulation and biological fluid using hanging mercury dropping electrode (HMDE) by Ali F. Al Ghamdi *et al.,* [7]. Navalon *et al.,* [8] studied a method for the determination of trace amounts of ciprofloxacin, based on solid-phase spectrofluorimetry. A.C. Igboasoiyi *et al.,* [9] studied the sensitive and precise spectrophotometric method for the determination of CIP. Qun Wang *et al.,* [10] have reported the films of chitosan and polyethylene glycol (PEG), with ciprofloxacin hydrochloride as model drug incorporated at different concentrations by a casting/solvent evaporation method. As reported in the literature, several methods have been reported for the determination of CIP either separately or in the presence of other drugs in various pharmaceutical formulations including high-performance liquid chromatography (HPLC) [11-16], spectrofluorimetry [17], spectrophotometry [18-20], and voltammetric methods [21–27]. Ciprofloxacin hydrochloride was also studied by Glassy carbon electrode [28], Mercury electrode [14] and nano-SnO_2/PVS modified electrode [29].

4.4. Chemistry and Biological relevance of L-Tyrosine

L-Tyrosine (LTY, **Scheme. 4.2**) or 4-hydroxyphenylalanine is one of the 22 amino acids that are used by cells to synthesize proteins. The word "tyrosine" is from the Greek *tyri*, meaning *cheese*, as it was first discovered in 1846 by German chemist Justus von Liebig in the protein casein from cheese [30, 31]. It is called tyrosyl when referred to as a functional group or side chain. Aside from being a proteogenic amino acid, tyrosine has a special role by virtue of the phenol functionality. It occurs in proteins that are part of signal transduction processes. It functions as a receiver of phosphate groups that are transferred by way of protein kinases (so-called receptor tyrosine kinases). Phosphorylation of the hydroxyl group changes the activity of the target protein. A tyrosine residue also plays an important role in photosynthesis. In chloroplasts (photosystem II), it acts as an electron donor in the reduction of oxidized chlorophyll. In this process, it undergoes deprotonation of its phenolic OH-group. This radical is subsequently reduced in the photosystem II by the four core manganese clusters.

4.5. Brief review of Tin(II) Oxide nanoparticles

Nanotechnology is concerned with materials and systems whose structures and components exhibit novel and significantly improved physical, chemical and biological properties, phenomena and processes due to their nanoscale size [32-34]. Nano-SnO_2 possesses excellent photo electronic properties, high gas sensitivities and a short response time as well as relatively higher conductivity than TiO_2 and SiO_2 [35-37]. The nanoporous structures of these inorganic oxide films greatly enhance the active surface area available for bioactive molecules. These films facilitate direct electron transfer process between biomolecules and electrodes. SnO_2 has been synthesized by different methods such as the sol–gel method, chemical vapor deposition (CVD), magnetron sputtering and hydrothermal treatment [38].

In the present work, SnO_2 nanoparticles were synthesized by the gel combustion method. We used the SnO_2 nanoparticles to modify a CPE and this SnO_2 nanoparticles

MCPE again polymerized by L-Tyrosine and then investigated the electrochemical behavior of CIP at the poly (L-Tyrosine) SnO_2 nanoparticles modified CPE. There are no reports for quantitative determination of Ciprofloxacin hydrochloride (CIP) by using poly (L-Tyrosine) SnO_2 nanoparticles modified carbon paste electrode. This method was successfully applied for investigation of CIP in commercial tablet sample. Finally a sensitive and simple voltammetric method was developed for the determination of ciprofloxacin hydrochloride for pharmacological practical application.

4.6. Experimental section

4.6.1. Reagents and Stock Solution

Tin (II) chloride dehydrate ($SnCl_2.H_2O$, 99.99%, Merck), Nitric acid (HNO_3, 70%, Merck), Citric acid ($C_6H_8O_7$, 99.5%, Merck), Ciprofloxacin hydrochloride (CIP), L-Tyrosine and potassium chloride (KCl) were purchased from Merck and all other chemicals were of analytical grade. The electropolymerisation of L-Tyrosine was performed in 0.2 M phosphate buffer solution. The phosphate buffer solution was prepared from KH_2PO_4 and K_2HPO_4, the pH was adjusted with H_3PO_4 and 0.1 N NaOH solution. The stock solution of the ciprofloxacin hydrochloride (10 mM) was prepared by dissolving in water, 1 M potassium chloride (KCl) was used as supporting electrolyte for all analytes. Other chemicals used were of analytical grade except for spectroscopically pure graphite powder. All solutions were prepared with doubly distilled water. Freshly prepared CIP was used prior to measurements.

4.6.2. Apparatus

Electrochemical measurements were carried out with an Electroanalyser model EA-201 chemlink system in a conventional three-electrode system. The working electrode was carbon paste electrode, having cavity of 3 mm diameter. The counter electrode was platinum electrode with a saturated calomel electrode (SCE) as a standard reference electrode for completing the circuit.

4.6.3. Synthesis of SnO_2 nanoparticles

SnO_2 nanoparticles were synthesized by gel combustion method. The materials used are tin (II) chloride dehydrate, 6.2 mole of nitric acid which is used as an oxidizer and mixed in an appropriate ratio to form a tin nitrate solution, then 1.5 mole of citric acid which acts as fuel was added to solution and the solution was heated at 90°C in a pyrex vessel with constant stirring. When the temperature was raised to about 300°C, the polymeric precursor underwent a strong, self-sustaining combustion reaction occurs with evolution of large volume of gases and swelled into voluminous and foamy ashes. The entire combustion process occurs in a few seconds. The produced ashes were then calcined at 800°C (for 1 hour). The process was carried out, until the complete decomposition of the carbonaceous residues. Then the white powder SnO_2 nanoparticles were obtained [39].

4.6.4. Preparation of bare carbon paste electrode

The bare carbon paste electrode was prepared by hand mixing of graphite powder 70% and silicon oil 30% in an agate mortar for about 30 min to get homogenous carbon paste. The paste was then packed into the cavity of Teflon tube electrode (3 mm diameter). Before measurement, the modified electrode was smoothened on a piece of transparent paper to get a uniform, smooth and fresh surface.

4.6.5. Preparation of the L-Tyrosine polymer on SnO_2 nanoparticles modified carbon paste electrode

The poly (L-Tyrosine) SnO_2 nanoparticles modified carbon paste electrode was prepared by hand mixing of 70% graphite powder and 10 mg SnO_2 nanoparticle with 30% silicon oil in an agate mortar to produce a homogenous carbon paste. The paste was packed into the homemade cavity (3 mm in diameter) and then smoothed on a weighing paper. The electrical contact was provided by a copper wire connected to the paste in the end of the tube. Electrochemical polymerization of 1 mM L-Tyrosine is carried out in 0.2 M phosphate buffer solution of pH 4.0 by using cyclic voltammetry in

the potential range from 500 to 1200 mV at scan rate 50 mVs^{-1}. After 10 cycles, the surface of the electrode was washed with doubly distilled water to remove the physically adsorbed material. This modified electrode was immersed in phosphate buffer solution of pH 6.5 and electrochemical determination of CIP was carried out in a voltammetric cell in the potential range from 500 to 1200 mV. The same procedure was applied for all the sample analysis and all electrochemical measurements were carried out at room temperature.

4.7. RESULTS AND DISCUSSION

4.7.1. Characterization of prepared SnO_2 nanoparticles by XRD and SEM

Crystalline structure and crystallite size of SnO_2 nanoparticles were analyzed by Cu-K_α X-ray radiation (λ = 1.5418A˚) in 2θ range from 20º to 80° operating at 30 kV and 15 mA. The scan rate was 5°/min. XRD patterns of SnO_2 annealed at 800°C for 1h as shown in **Fig.4.1**, the average grain size was calculated using the Scherer relation,

$$d = 0.89\frac{\lambda}{\beta\cos\theta} \quad \text{..... (4.1)}$$

Where d is the crystallite size, λ is the wavelength of X-rays, β is the full width of half maximum and θ the diffraction peak angle [40]. The crystallite sizes of samples are found to be 12 nm for sample SnO_2 nanoparticles by using Scherer formula. The particles are homogeneous with the average diameter of 12 nm. **Fig.4.1** shows the X-ray diffraction patterns of the nanoparticles prepared. We could see that the 2θ peaks are in agreement with the diffraction patterns from (110), (101), (200), (111),(210), (211), (112),(220), (002), (310), (112), (301) planes. The surface morphology and shape of the nanoparticles of powdered samples were investigated by scanning electron microscope (SEM) (Hitachi Model S-3200N). **Fig.4.2** shows the typical SEM image of the SnO_2 nanoparticles.

4.7.2. UV–Visible Spectrophotometer for SnO_2 nanoparticles

The UV–visible absorption spectra of SnO_2 nanoparticles are shown in **Fig.4.3**. The absorption band of the SnO_2 nanoparticles exhibits maximum due to the quantum confinement in sample compared to bulk SnO_2 particles. This optical phenomenon indicated that these nanoparticles showed the quantum size effect [41, 42].

4.7.3. Electropolymerisation of L-Tyrosine on SnO_2 nanoparticles modified carbon paste Electrode

SnO_2 nanoparticles modified carbon paste electrode (SNMCPE) was prepared and electropolymerised by L-Tyrosine as discussed in 4.4.5 section. A solution of monomer L-Tyrosine was oxidized to an activated form that polymerizes to form a polymer film directly on the electrode surface. This procedure results in few pinholes since polymerization would be accentuated at exposed (pinholes) sites at the electrode surface. Electro catalysis at a SnO_2 nanoparticles modified carbon paste electrode is usually an electron transfer reaction between the SnO_2 nanoparticles modified carbon paste electrode and solution substrate which, when mediated by a immobilized redox couple (i.e., the mediator), proceeds at a lower over potential than would otherwise occur at the bare electrode and enhances the peak current. Electropolymerisation of 1mM L-tyrosine was fabricated in 0.2 M phosphate buffer solution on SnO_2 nanoparticles modified carbon paste electrode. The film was grown on SnO_2 nanoparticles modified carbon paste electrode by cyclic voltammetric scans between 500 to 1200 mV. The optimized scan number under the experimental conditions was determined as 10 for reaching the steady response. As shown in **Fig.4.4,** in the first cycle, with the potential scanning from 500 to 1200 mV the anodic peak was observed at 946 mV potential corresponding to the oxidation of L-Tyrosine. The peak descended gradually with the increase in cyclic number such decrease indicates the formation of poly (L-Tyrosine) membrane on the surface of the SnO_2 nanoparticles modified carbon paste electrode by electropolymerisation. L-Tyrosine was oxidized to free radical at the surface rapidly resulting in the possible structure of electropolymerised poly (L-

Tyrosine). After polymerization the poly (L-Tyrosine) SnO_2 nanoparticles modified carbon paste electrode was carefully rinsed with distilled water to remove the physically adsorbed material. Then the film electrode was transferred to an electrochemical cell and cyclic voltammetric sweeps were carried out to obtain electrochemical steady state.

4.7.4. SEM Characterization of poly (L-Tyrosine) SnO_2 modified carbon paste electrode

Fig.4.5a and **Fig.4.5b** explain the surface morphology of bare carbon paste electrode and poly (L-Tyrosine) SnO_2 nanoparticles modified carbon paste electrode respectively using scanning electron microscope (SEM). The surface of bare CPE was formed by irregularly shaped micrometer-sized flakes of graphite. Whereas the modified electrode had a typical uniform arrangement of L-Tyrosine molecules on the surface [43].

4.7.5. Electrochemical response of potassium ferrocyanide at poly (L-Tyrosine) SnO_2 nanoparticles modified carbon paste electrode (PLTSNMCPE)

Potassium ferrocyanide was used as a standard to determine the efficiency of poly (L-Tyrosine) SnO_2 nanoparticles modifier. **Fig.4.6** shows the electrochemical behavior of 0.1mM potassium ferrocyanide ($K_4[Fe(CN)_6]$) in 0.1M KCl at bare carbon paste electrode (BCPE) curve 'b' and at poly (L-Tyrosine) SnO_2 nanoparticles modified carbon paste electrode (PLTSNMCPE) curve 'a' respectively. The curve 'b' shows the cathodic peak current I_{pc} 5.1 µA of E_{pc} 119 mV and anodic peak current I_{pa} 5.18 µA of E_{pa} 241 mV at BCPE. Whereas, curve 'a' shows the cathodic peak current I_{pc} 19.56 µA of E_{pc} 123 mV and anodic peak current I_{pa} 19.85 µA of E_{pa} 237 mV at the PLTSNMCPE has been observed. The enhancement of peak current showed excellent catalytic ability of PLTSNMCPE. The surface area of bare carbon paste electrode is 0.032 cm^2. The effective surface area of the modified electrode was found to be 0.045 cm^2.

4.7.6. Electrochemical behavior of ciprofloxacin hydrochloride (CIP) at PLTSNMCPE:

The electrochemical behavior of CIP was investigated in 0.2 M phosphate buffer solution of pH 6.5 at PLTSNMCPE using cyclic voltammetric technique**. Fig.4.7a** and **Fig.4.7b** shows cyclic voltammograms of 0.1 mM CIP at bare CPE (curve 'b') and at PLTSNMCPE (curve 'a'). The curve 'c' represents the cyclic voltammogram of blank solution at PLTSNMCPE. Above studies showed that only one oxidation peak at 1046 mV potential with peak current of 3.8 µA at bare CPE, whereas an oxidation peak at 913 mV with peak current of 18.52 µA at PLTSNMCPE in the potential range 500 to 1200 mV. No reduction peak was observed in the reverse scan, suggesting that the electrochemical reaction is a totally irreversible process and the oxidation peak at the bare CPE is broad due to slow electron transfer, while the response was considerably improved at PLTSNMCPE and the peak potentials shifted to negative direction, the shape of the peak turns sharper and the peak current increased significantly.

4.7.7. Effect of pH

The electro oxidation of CIP was studied at 1 mM stock solution in 0.2 M phosphate buffer solution over pH range from 2.5 to 9.5 at a scan rate of 50 mVs^{-1} at PLTSNMCPE using cyclic voltammetric technique. The oxidation peak current increases with increase of pH from 2.5 to 6.5 and becomes maximum and peak potential shifted negatively. While pH beyond 6.5, a great decrease of the oxidation peak current has been observed, then it decreased gradually with the further increase in pH of the solution as shown in **Fig.4.8a** and oxidation peak potential decrease with increase of pH shown in **Fig.4.8b**. A linear relationship was obtained between the anodic peak potential and pH of the solution in the range 2.5 – 9. The corresponding linear regression equation was given by:

$$E_{pa}\ (mV) = 1156.94 - 25.675\ pH \quad (R = 0.9934) \ldots\ldots\ldots\ldots\ldots\ldots\ldots\ldots\ldots\ldots\ (4.2)$$

With a negative slope of 25.675. The value of this slope is in close agreement with the theoretical value of 30 mV/pH at 25^0 for a $2e^-$ transfer process which indicating that the number of electrons and protons are equal in the electrochemical oxidation of CIP at PLTSNMCPE.

4.7.8. Effect of scan rate

Useful information involving electrochemical mechanism usually can be acquired from the relationship between peak current and scan rate. The effect of scan rates on the electrochemical response of 0.1 mM CIP at PLTSNMCPE was studied at different scan rates 10, 20, 30, 40, 50, 60, 70, 80, 90, 100 mVs^{-1} and the cyclic voltammograms were shown in **Fig.4.9a.** A linear relationship with a correlation coefficient of 0.9948 was obtained between the anodic peak current and square root of scan rate in the range of 10 - 100 mVs^{-1} is shown in **Fig.4.9b** which revealed that a diffusion controlled process occurring at PLTSNMCPE. Increasing in scan rate shifts the anodic peak potentials of CIP to the more positive potential. However linearity was also obtained for the plot of anodic peak current vs. scan rate with a correlation coefficient of 0.9915 shown in **Fig.4.9c**. The corresponding linear regression equation is

$$I_{pa}\ (\mu A) = 0.1633\ \nu + 10.018 \quad (R = 0.99155) \ldots\ldots\ldots\ldots\ldots\ldots\ldots\ldots\ (4.3)$$

This indicates that the electrode process was controlled by diffusion rather than adsorption. The relationship between the anodic peak potential and scan rate can be explained by plotting the anodic peak potentials vs. natural logarithm of scan rate **(Fig.4.9d)** by considering the relation:

$$E_{pa}\ (mV) = 0.01481\ \ln\upsilon + 1.0309 \quad R = 0.99383 \ldots\ldots\ldots\ldots\ldots\ldots\ldots\ (4.4)$$

It is noted from **Fig.4.9d** that, along with an increase in the scan rate, the peak potential for the catalytic oxidation of CIP shifts to the more positive potentials, suggesting a kinetic limitation to the reaction between the modified electrode and CIP also the relationship between the anodic peak current and scan rate can be explained by

plotting the logarithm of anodic peak current vs. logarithm of scan rate **(Fig.4.9e)** by considering the relation:

$$\log I_{pa}\,(\mu A) = 0.14654 \log \upsilon + 1.01411 \quad R = 0.9938 \ldots\ldots\ldots\ldots\ldots\ldots\ldots\ldots \quad (4.5)$$

According to Laviron's theory [44] the slope is equal to $RT/\alpha n_{\alpha}F$. As for a totally irreversible electrode reaction on the basis of the above discussion, the n_{α} is 1.8032, which indicated that two electrons were involved in the oxidation process of CIP at PLTSNMCPE. Since the equal number of electron and proton took part in the oxidation of CIP, the two electrons and two protons transfer were involved in the electrode reaction process. The electrochemical reaction process for CIP at PLTSNMCPE can therefore be summarized as in **scheme 4.3**. From the deduced mechanism of CIP, an intermediate of a free radical was formed. It may be just the free radical polymerizes and comes into being as insoluble products that deposit on the electrode surface, which agrees with the phenomena of voltammograms recorded from multi-cycle [45].

4.7.9. Calibration of ciprofloxacin hydrochloride (CIP) concentration

A series of ciprofloxacin hydrochloride solution from 1×10^{-5} to 1×10^{-4} M were prepared to investigate the relationship between the anodic peak current (I_{pa}) and concentration of CIP at PLTSNMCPE at a scan rate 50 mVs^{-1}. **Fig.4.10a** shows as the concentration of CIP increases the oxidation peak current also increases. The plot of anodic peak current (I_{pa}) vs. concentration shows linear **Fig.4.10b** is described by a linear regression equation:

$$I_{pa}\,(\mu A) = 139.767\,(10^{-5}\ M) + 4.7837 \quad (R = 0.9923) \ldots\ldots\ldots\ldots\ldots\ldots \quad (4.6)$$

The limit of detection (LOD) and limit of quantification (LOQ) were found to be 0.10×10^{-7} M and 0.33×10^{-7} M respectively. The LOD and LOQ were calculated from the peak current using the following equation: LOD = 3S/M and LOD = 10S/M

Where S is standard deviation and M is the slope of calibration plot.

4.7.10. Ciprofloxacin hydrochloride (CIP) studies by differential pulse voltammetric technique (DPV)

Differential pulse voltammetry (DPV) was used to investigate the possibility of PLTSNMCPE for determination of CIP. The current responses of this CIP changed by changing the concentrations of CIP. As illustrated in **Fig.4.11a** DPV responses of the modified electrode of CIP increased linearly with increase of its concentration. The plot of anodic peak current (I_{pa}) vs. concentration of CIP shows linear **Fig.4.11b** can be described by linear regression equations for CIP in the range of 1×10^{-5} to 1×10^{-4} M is given by

$$I_{pa}\ (\mu A) = 0.953 + 18.1\ C \quad (R = 0.9928) \ldots\ldots\ldots\ldots\ldots\ldots\ldots\ldots\ldots\ldots\ (4.7)$$

The limit of detection (LOD) and limit of quantification (LOQ) were found to be 0.646×10^{-7} M and 2.15×10^{-6} M respectively.

4.7.11. Pharmaceutical determination of CIP in tablets by Cyclic voltammetry

In order to validate the proposed method the ciprofloxacin hydrochloride was determined in the commercially available as ciprodac tablets (declared content is 500 mg/tablet labeled on the sample). Ten tablets each containing 500 mg/tablet of ciprofloxacin hydrochloride were accurately weighed and the average value was determined. The tablets were then grind into a fine powder and an accurately weighed quantity of powder was dissolved in deionized water and transferred to a 100 ml volumetric flask. The resulting mixture was sonicated for 20 - 30 min to ensure that ciprofloxacin hydrochloride was completely dissolved. Then the mixture was filtered to remove the insoluble and the residue was washed several times and then diluting it to the required concentration in PBS of pH 6.5. The quantitative determination of ciprofloxacin hydrochloride was conducted according to the above mentioned experimental procedure under the optimum experimental conditions. The results of ciprofloxacin hydrochloride in commercial tablets obtained from cyclic voltammetric

determination are presented in **Table.4.1**. Voltammogram for the determination of ciprofloxacin hydrochloride in the commercial tablet confirms the one peak. A typical cyclic voltammograms for the determination of ciprofloxacin hydrochloride in commercial ciprodac tablets at bare carbon paste electrode and poly (L-Tyrosine) SnO_2 nanoparticles modified carbon paste electrode were shown in **Fig.4.12**.The detection limit obtained with several other modified electrodes using cyclic voltammetry is given in **Table.4.2**.

4.7.12. Electrocatalytic response of CIP and ENRO at poly (L-Tyrosine) SnO_2 nanoparticles modified carbon paste electrode

It is well known that Enrofloxacin (ENRO) widely coexists with CIP in chemical compounds. Therefore avoiding of ENRO interference is an important target for any CIP analytical methods. The **Fig.4.13** shows the voltammetric response of CIP and ENRO at PLTSNMCPE in pH of 6.5 at scan rate 50 mVs^{-1}. At modified electrode CIP exhibited enhanced peak current in the presence of ENRO. The Three well oxidation peaks are separated between CIP and ENRO. The electrocatalytic anodic peak potential of CIP was obtained at 1280 mV and ENRO at 850 and 936 mV potential respectively. This result shows that PLTSNMCPE acts as good sensor for the detection of CIP in the presence of ENRO.

4.8. CONCLUSION

- In the present study, a chemically modified poly (L-Tyrosine) SnO_2 nanoparticles carbon paste electrode based on the electropolymerisation has been prepared for the electrochemical determination of ciprofloxacin hydrochloride (CIP).

- Results showed that the oxidation peak current of ciprofloxacin hydrochloride (CIP) was improved at poly (L-Tyrosine) SnO_2 nanoparticles modified carbon paste electrode.

- The electrochemical response is diffusion controlled and irreversible in nature for CIP.

- A linear concentration range was found to occur from 1×10^{-5} to 1×10^{-4} M.

- The probable reaction mechanisms involved in the oxidation of ciprofloxacin hydrochloride (CIP) were also proposed.

- The applicability of the proposed voltammetric method for the assay of ciprofloxacin hydrochloride (CIP) was examined by analyzing the commercially available ciprodac tablets (declared content is 500 mg of ciprofloxacin hydrochloride in one tablet) and successfully applied for the determination of ciprofloxacin hydrochloride in pharmaceutical dosages.

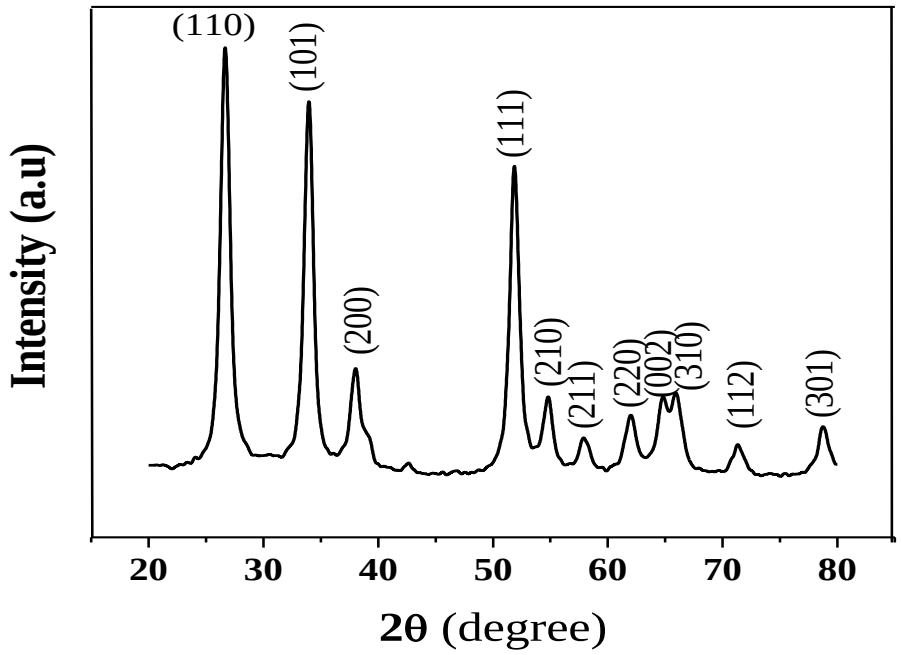

Fig. 4.1: XRD pattern of the synthesized SnO_2 nanoparticles

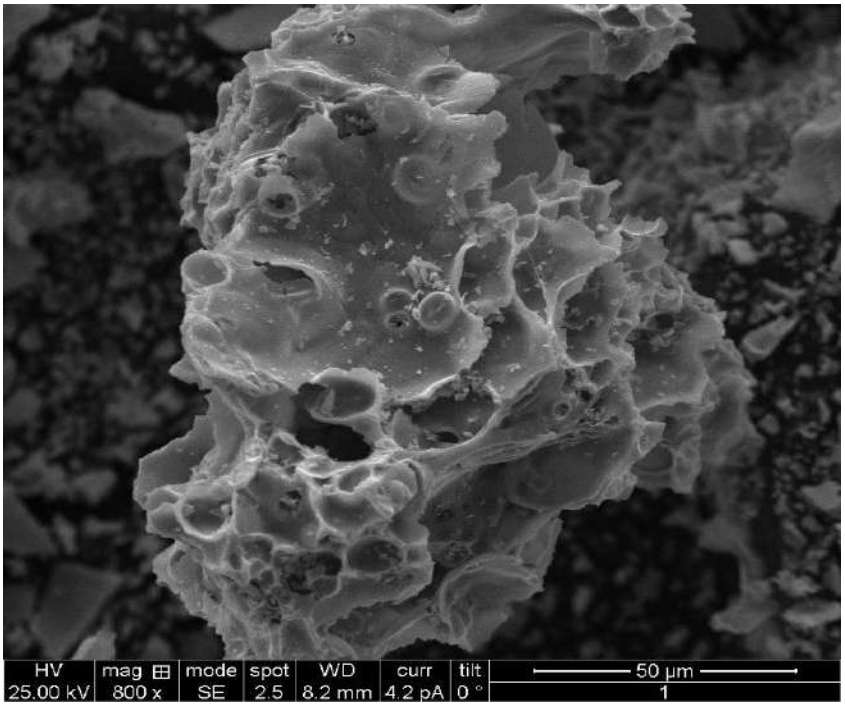

Fig. 4.2: SEM images of synthesized SnO_2 nanoparticles.

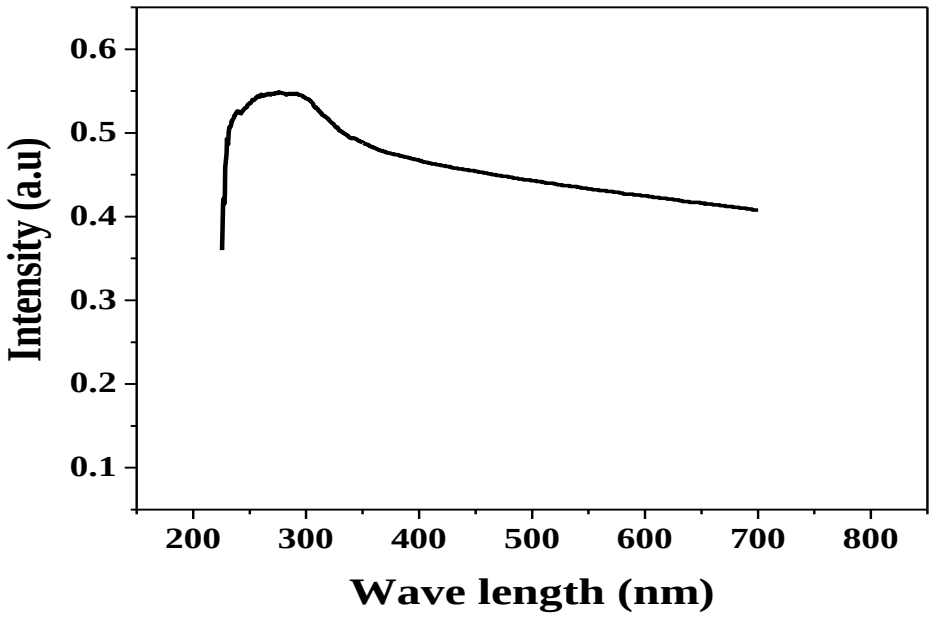

Fig. 4.3: UV-VIS spectra for SnO_2 nanoparticles; the shift occurred in ~280 nm wavelength.

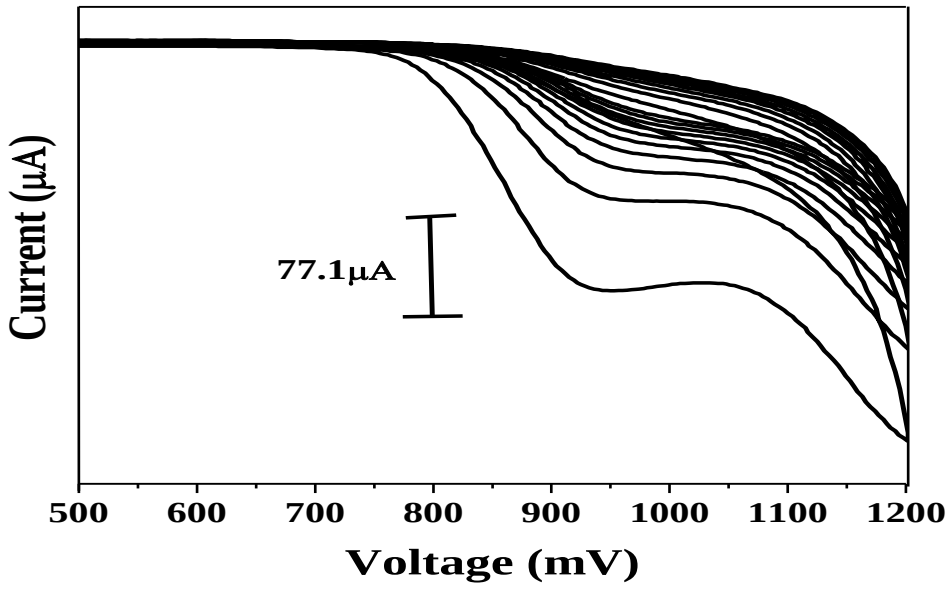

Fig. 4.4: Electropolymerisation of L-Tyrosine on SnO_2 nanoparticles modified carbon paste electrode.

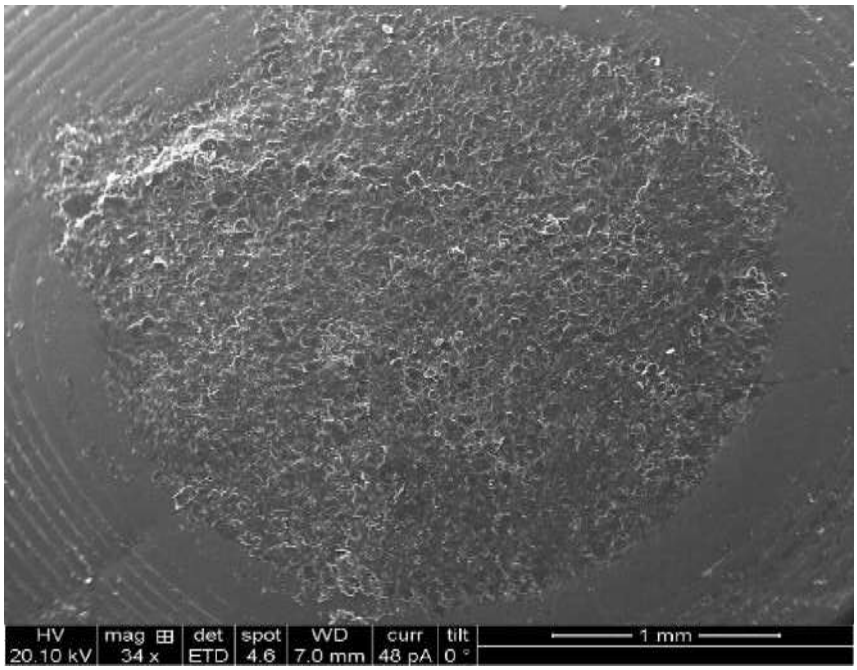

Fig. 4.5a: SEM image of bare carbon paste electrode.

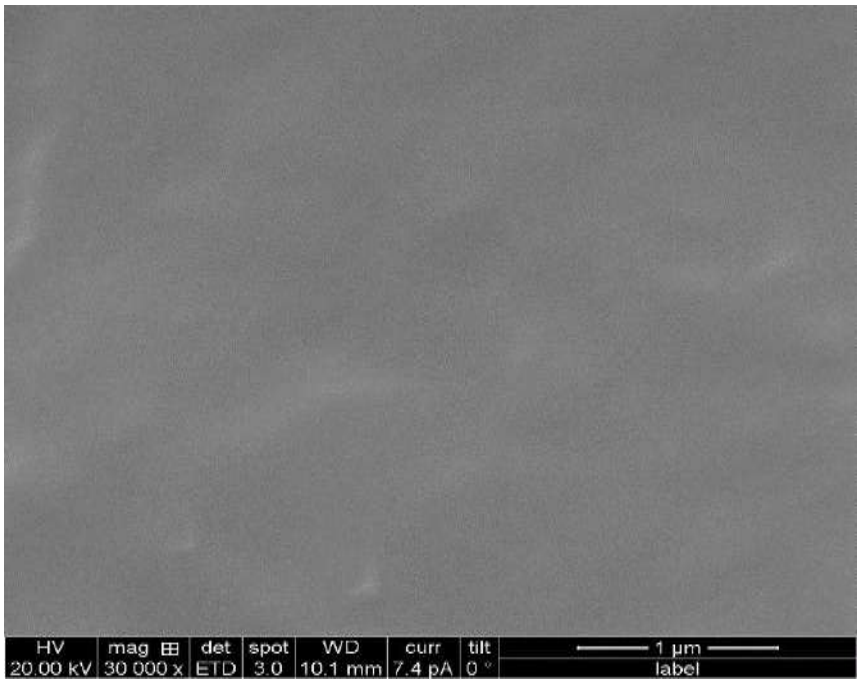

Fig. 4.5b: SEM image of poly (L-Tyrosine) SnO_2 nanoparticles modified carbon paste electrode.

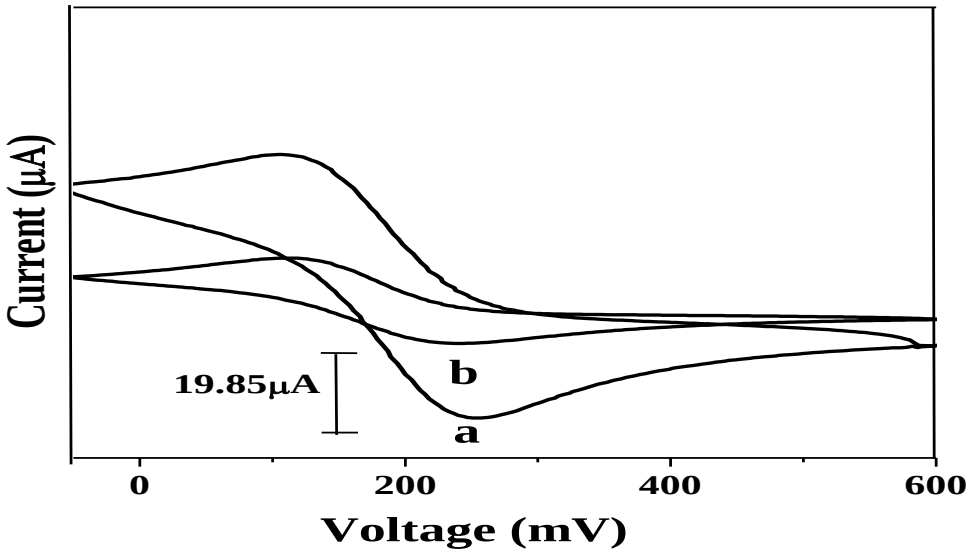

Fig. 4.6: Comparision of 0.1 mM $K_4[Fe(CN)_6]$ in 0.1 M KCl solution at poly (L-Tyrosine) SnO_2 nanoparticles modified carbon paste electrode (a) and bare carbon paste electrode (b).

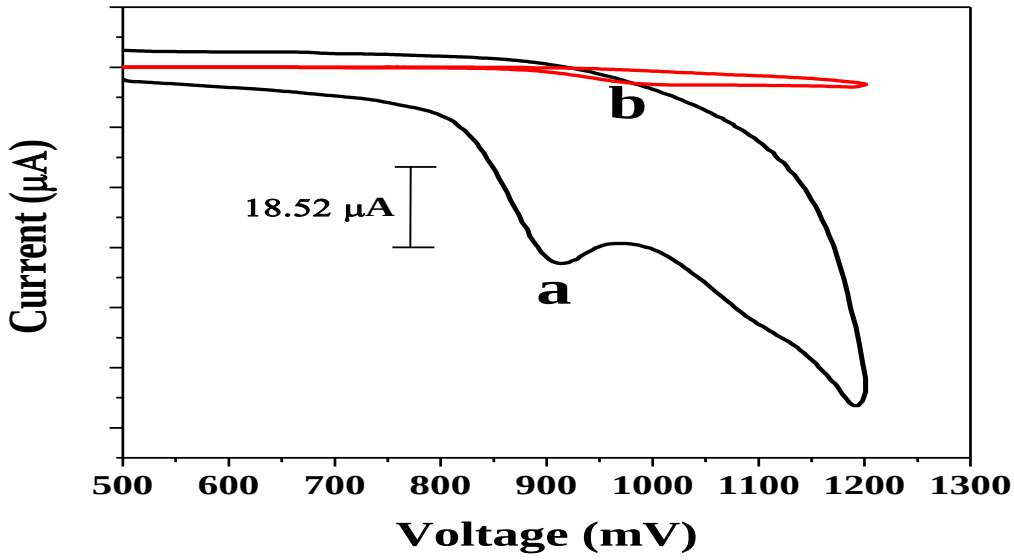

Fig. 4.7a: Comparision of 0.1 mM CIP at poly (L-Tyrosine) SnO_2 nanoparticles modified carbon paste electrode (a) and bare carbon paste electrode (b); pH 6.5, scan rate 50 mVs^{-1}.

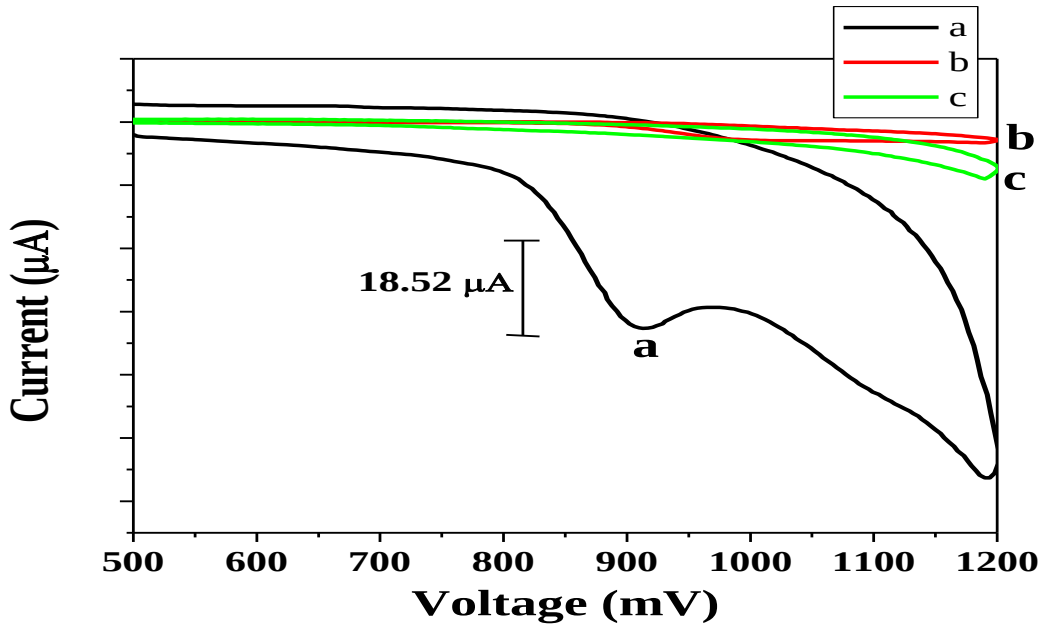

Fig. 4.7b: Comparision of 0.1 mM CIP at poly (L-Tyrosine) SnO_2 nanoparticles modified carbon paste electrode (a), bare carbon paste electrode (b) and blank solution at poly (L-Tyrosine) SnO_2 nanoparticles modified carbon paste electrode (c); pH 6.5, scan rate 50 mVs^{-1}.

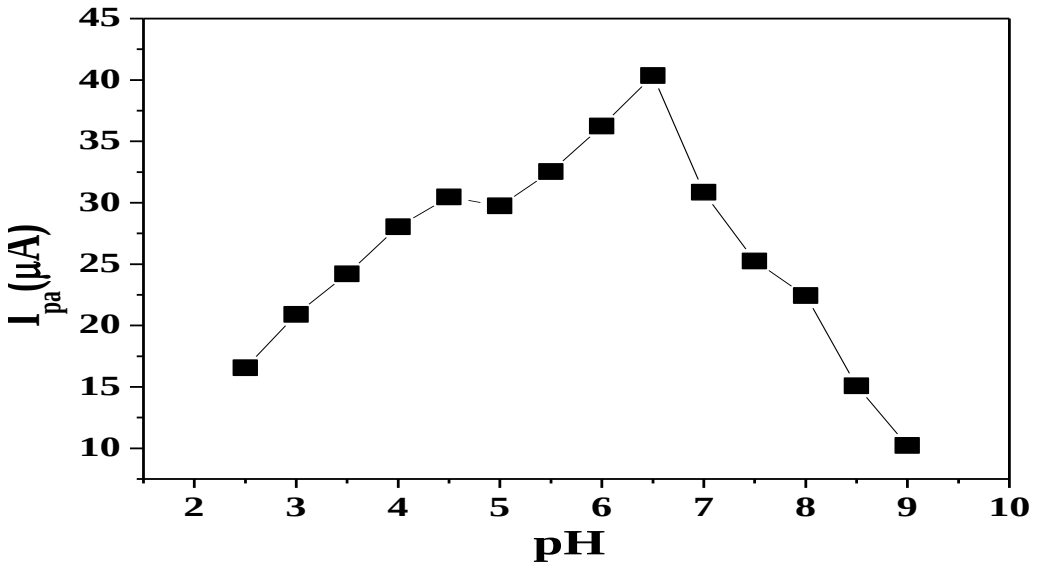

Fig. 4.8a: Plot of anodic peak current vs. pH (2.5 – 9.0) of 0.1 mM CIP at poly (L-Tyrosine) SnO_2 nanoparticles modified carbon paste electrode.

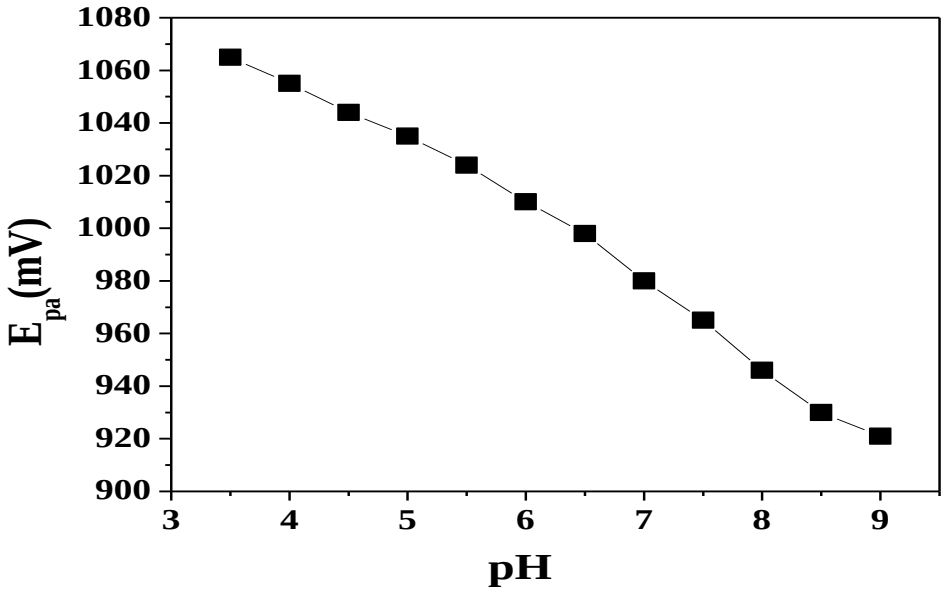

Fig. 4.8b: Plot of anodic peak potential vs. pH (2.5 – 9.0) of 0.1 mM CIP at poly (L-Tyrosine) SnO_2 nanoparticles modified carbon paste electrode.

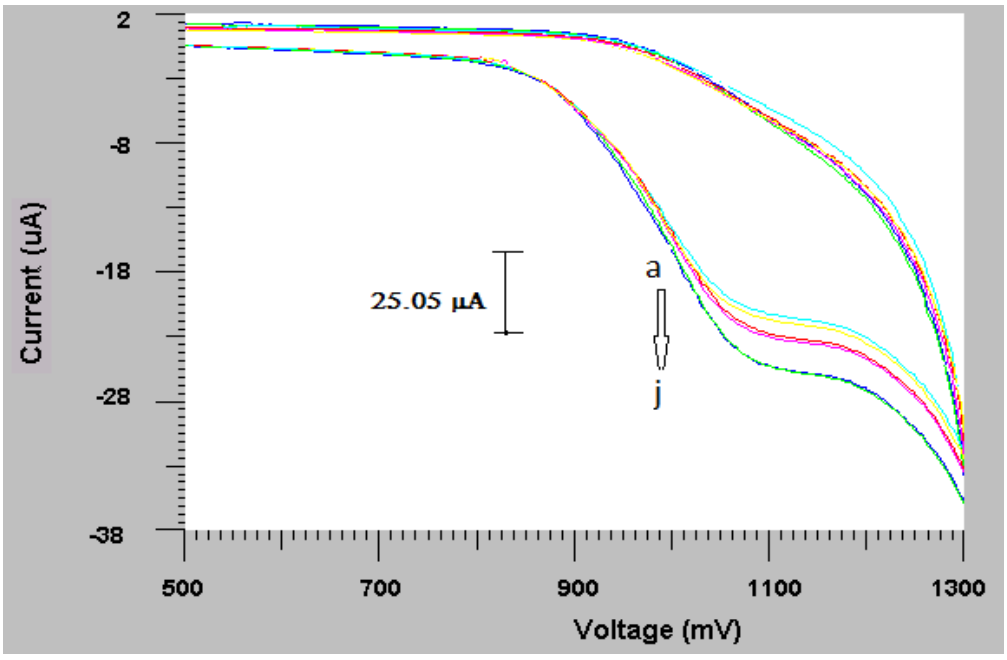

Fig. 4.9a: Cyclic voltammograms of 0.1 mM CIP at poly (L-Tyrosine) SnO_2 nanoparticles modified carbon paste electrode with different scan rates (a) 10, (b) 20, (c) 30, (d) 40, (e) 50, (f) 60, (g) 70, (h) 80 (i) 90, (j) 100 mVs^{-1}.

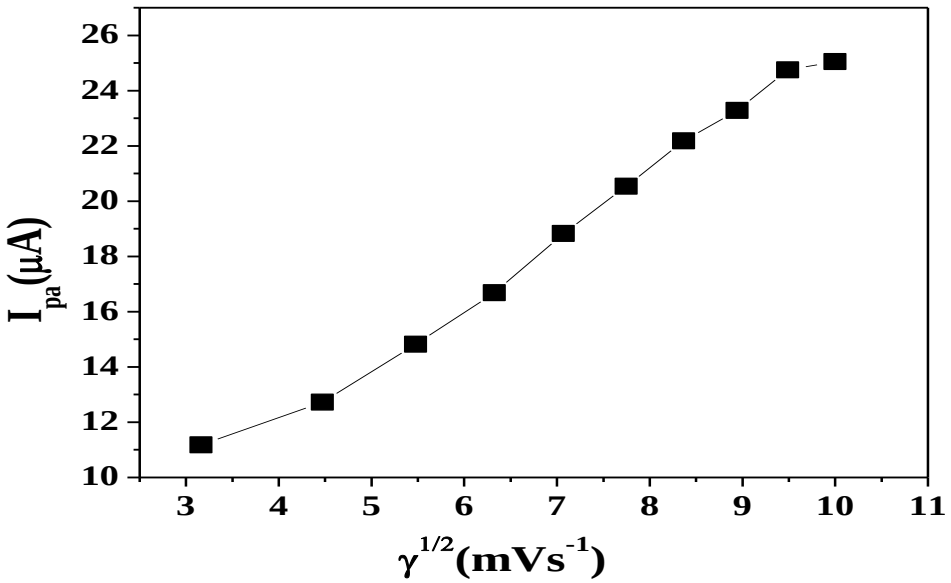

Fig. 4.9b: Plot of anodic peak current vs. square root of scan rates of CIP at poly (L-Tyrosine) SnO_2 nanoparticles modified carbon paste electrode.

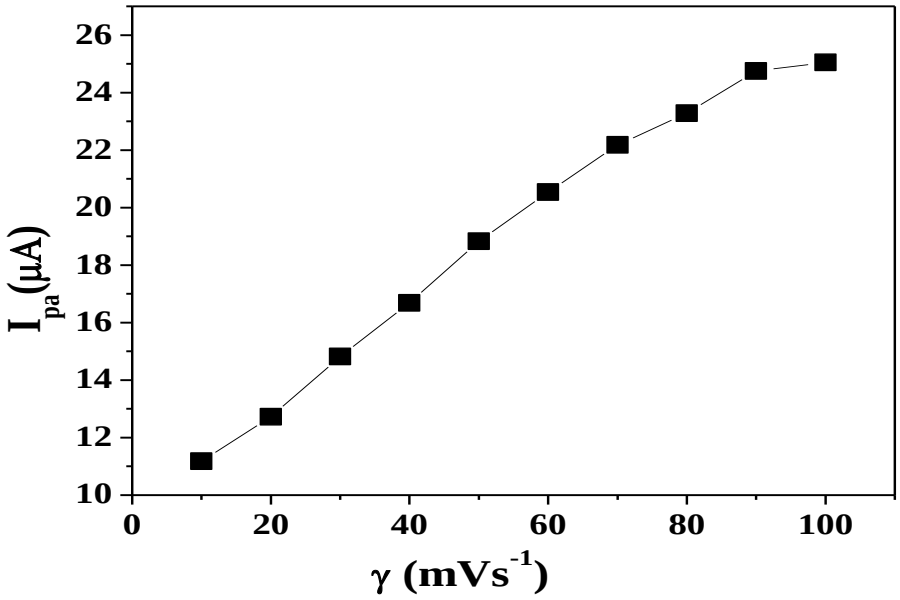

Fig. 4.9c: Plot of anodic peak current vs. scan rates of CIP at poly (L-Tyrosine) SnO_2 nanoparticles modified carbon paste electrode.

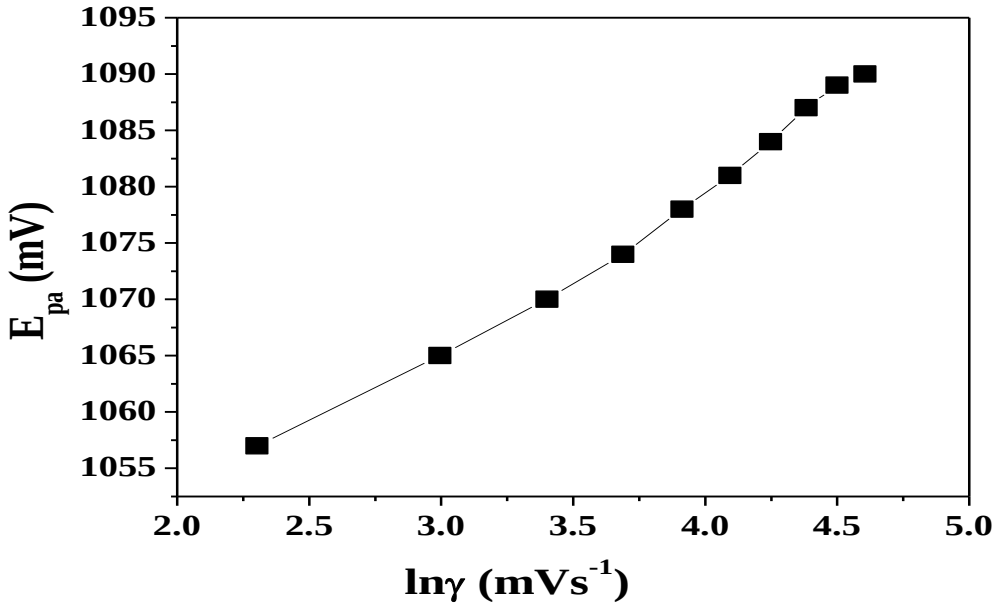

Fig. 4.9d: Plot of anodic peak potential vs. natural logarithm of scan rates of CIP at poly (L-Tyrosine) SnO_2 nanoparticles modified carbon paste electrode.

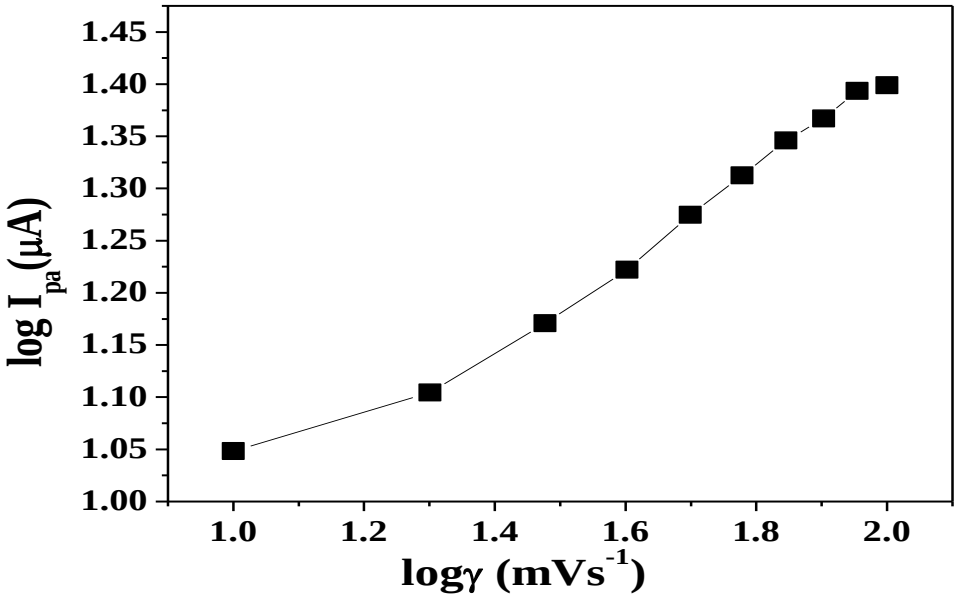

Fig. 4.9e: Plot of logarithm peak current vs. logarithm of scan rates of CIP at poly (L-Tyrosine) SnO_2 nanoparticles modified carbon paste electrode.

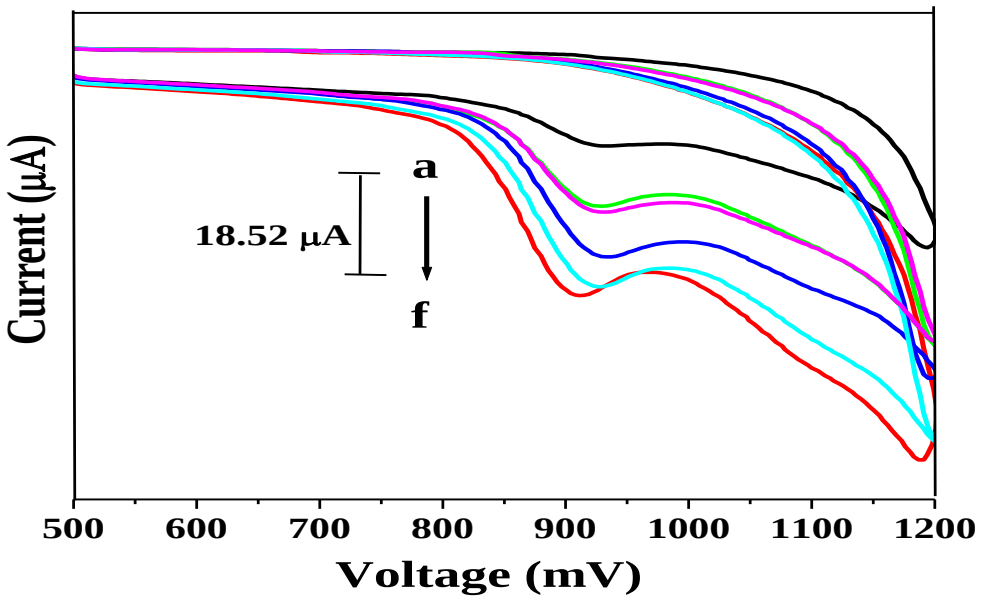

Fig. 4.10a: Effect of variation of concentration of CIP (a) 1×10^{-5} M, (b) 2×10^{-5} M, (c) 4×10^{-5} M, (d) 6×10^{-5} M, (e) 8×10^{-5} M, (f) 1×10^{-4} M on anodic peak current at poly (L-Tyrosine) SnO_2 nanoparticles modified carbon paste electrode; scan rate 50 mVs^{-1}.

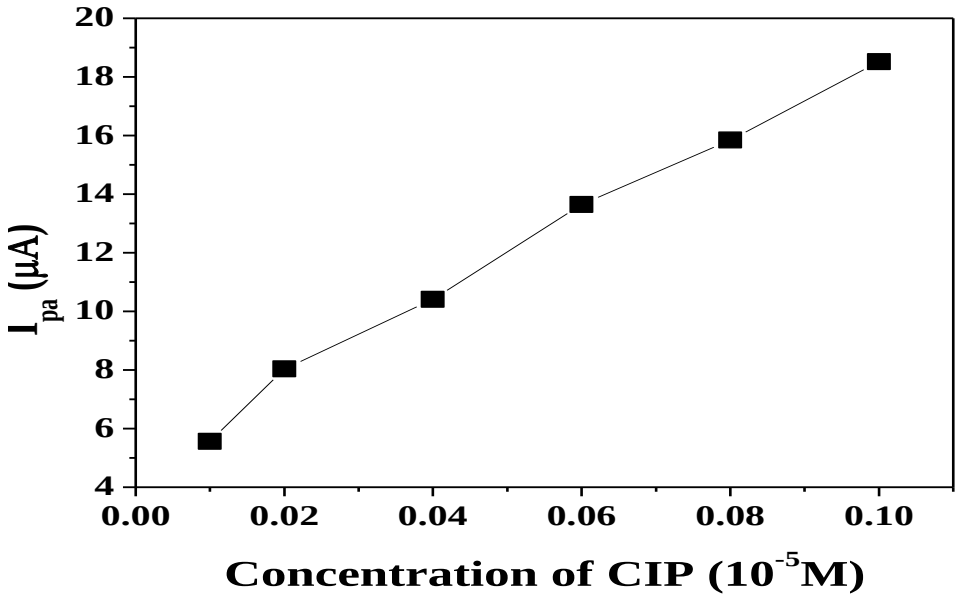

Fig. 4.10b: Plot of anodic peak current vs. CIP concentration at poly (L-Tyrosine) SnO_2 nanoparticles modified carbon paste electrode.

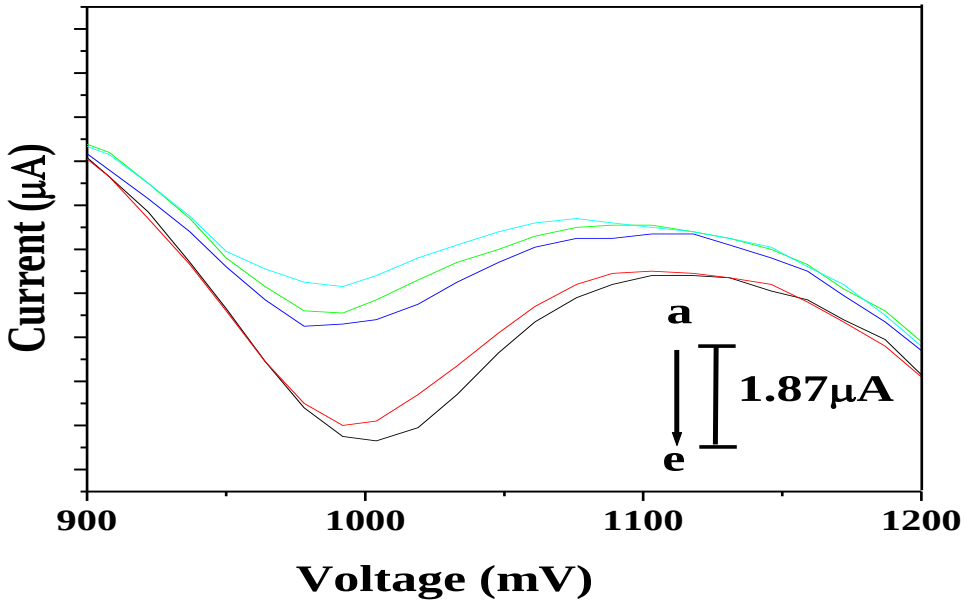

Fig. 4.11a: DPV of CIP of (a) 1×10^{-5} M, (b) 2×10^{-5} M, (c) 3×10^{-5} M, (d) 4×10^{-5} M, (e) 5×10^{-5} M at poly (L-Tyrosine) SnO_2 nanoparticles modified carbon paste electrode.

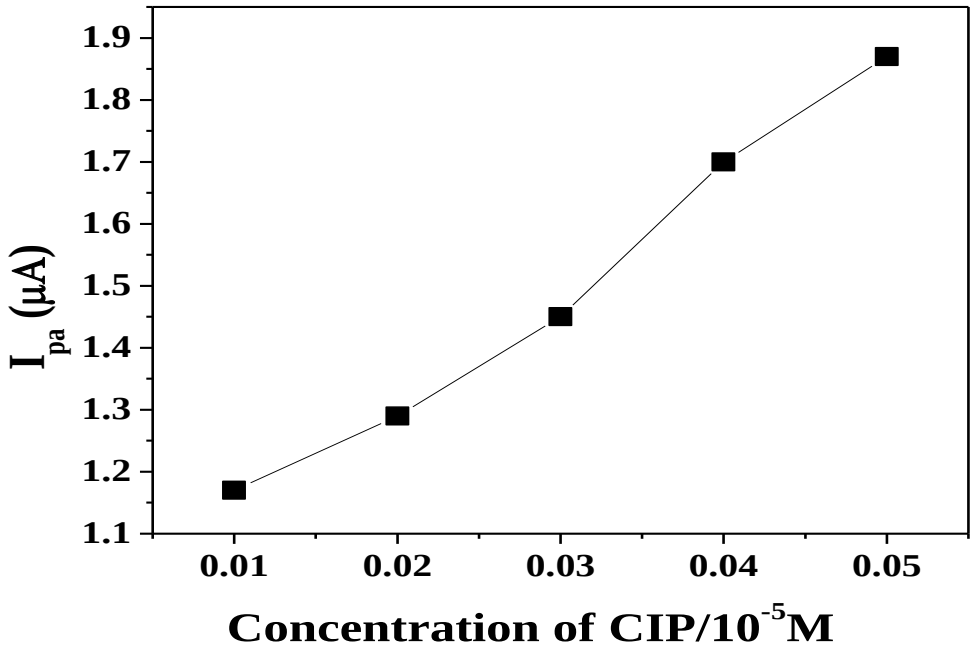

Fig. 4.11b. DPV of anodic peak current (I_{pa}) vs. concentration of CIP.

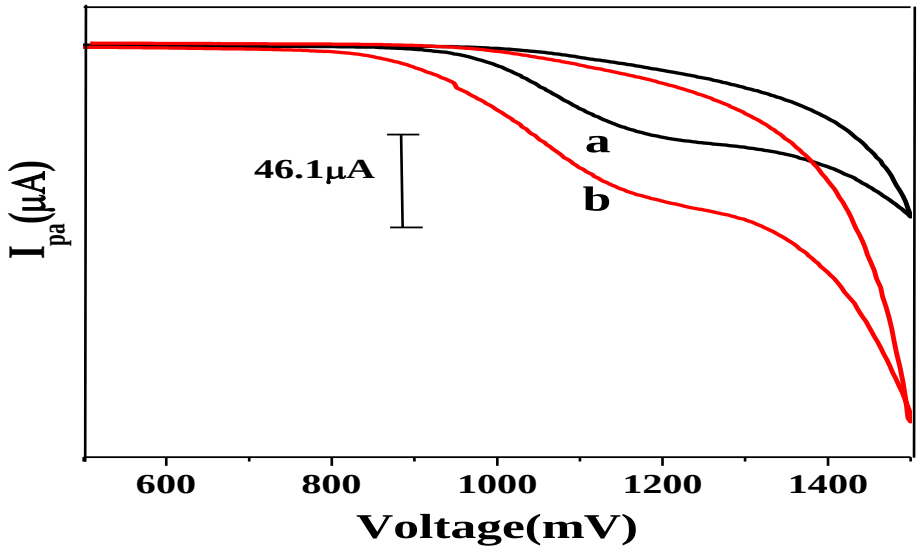

Fig. 4.12: Typical cyclic voltammograms for the determination of ciprofloxacin hydrochloride in Ciprodac tablet sample at bare carbon paste electrode (curve 'a') and at poly (L-Tyrosine) SnO_2 nanoparticles modified carbon paste electrode (curve 'b'); scan rate 50 mVs^{-1}.

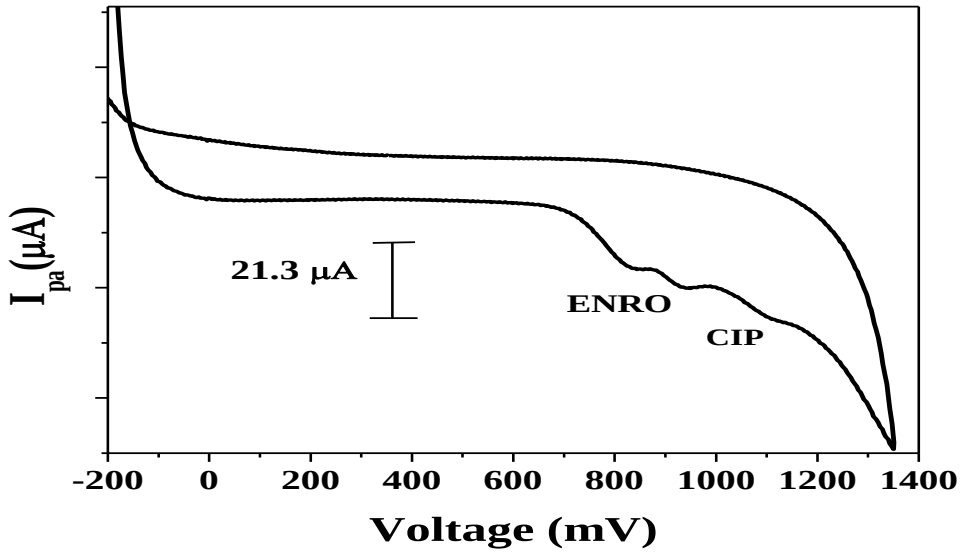

Fig. 4.13. Cyclic voltammogram obtained for oxidation of ENRO and CIP at poly (L-Tyrosine) SnO_2 nanoparticles modified carbon paste electrode with scan rate of 50 $mVs^{-}1$ in 0.2 M PBS of pH 6.5.

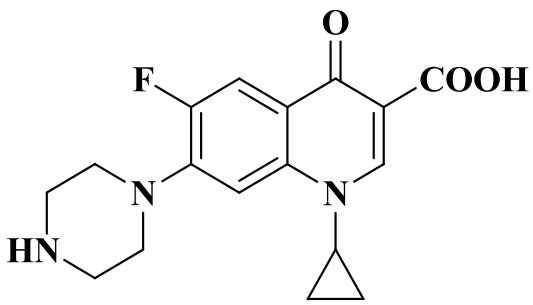

Scheme 4.1: Ciprofloxacin Hydrochloride.

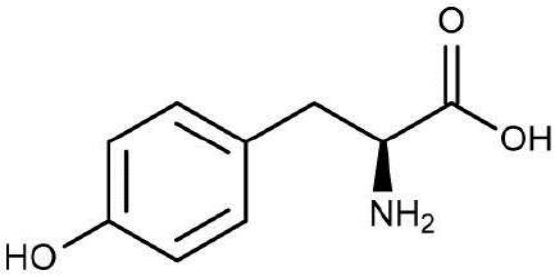

Scheme 4.2: L-Tyrosine.

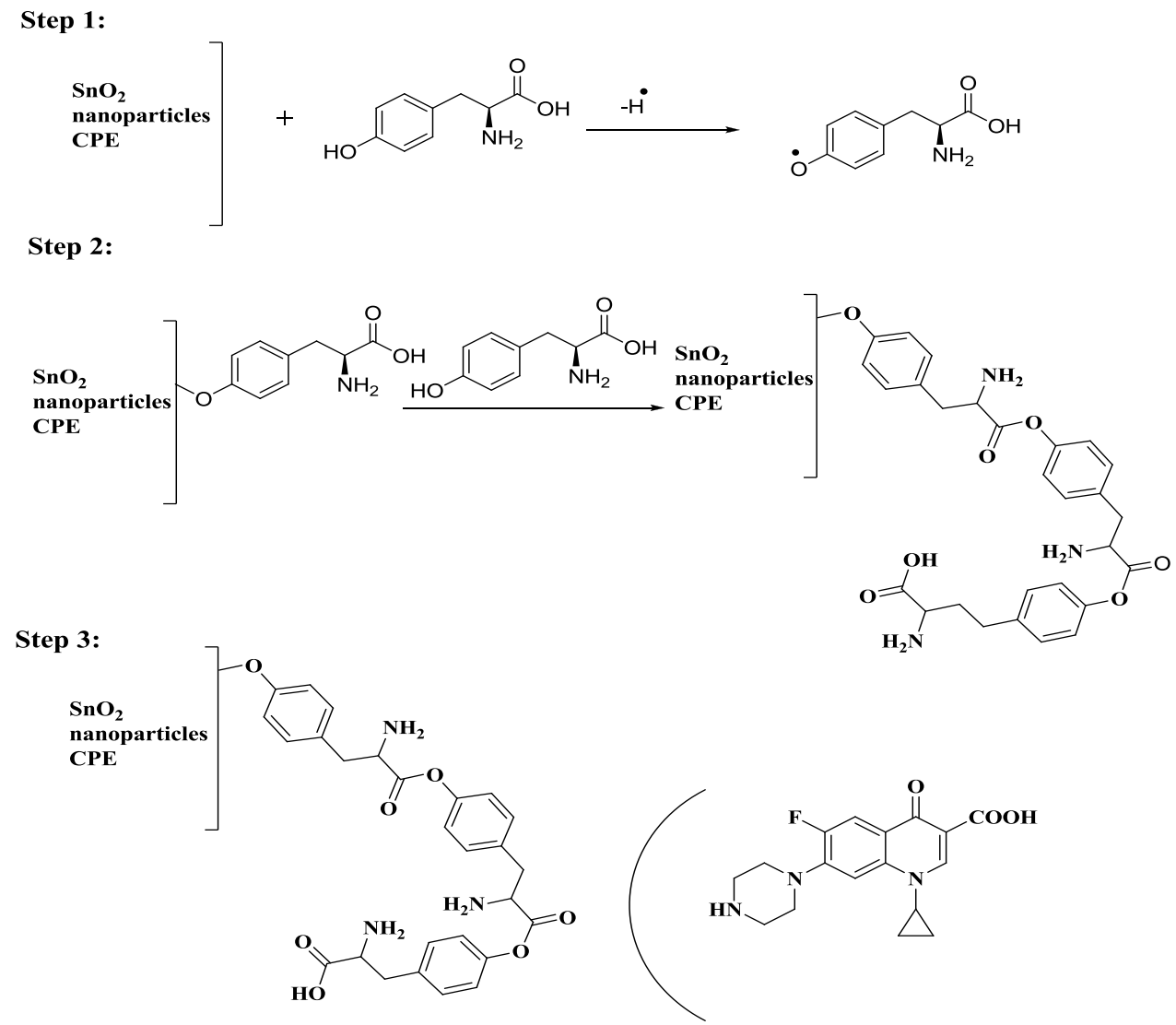

Scheme 4.3: Probable reaction mechanism of CIP.

Sl.no	Specified amount (mg)	Detected amount (mg)	Recovery%	RSD%(n=5)
1	500	497.01	99.402	0.306
2	500	501.03	100.20	
3	500	499.43	99.88	
4	500	499.02	99.80	
5	500	500.34	100.68	

Table.4.1: Cyclic voltammetric response of CIP in ciprodac tablets at poly (L-Tyrosine) SnO_2 nanoparticles modified carbon paste electrode.

Electrode	Detection limit (M)	Techniques	Reference
DNA/GC	0.117×10^{-6}	Differential pulse anodic stripping voltammetry	[13]
Hanging Mercury dropping electrode (HMDE)	7×10^{-9}	Square wave voltammetric method	[14]
Cd(II)/ Graphene modified electrode	5.9×10^{-8}	Anodic stripping voltammetry	[46]
Poly (L-Tyrosine) SnO_2 nanoparticles modified carbon paste electrode	10×10^{-9}	Cyclic voltammetry technique	Present work

Tables.4.2: Comparision of detection limit for different modified electrodes.

4.9. Reference:

[1] Bengi Uslu, Burcin Bozal, Mehmet Emin Kuscu, *The Open Chemical and Biomedical Methods Journal,* **3** (2010) 108.

[2] Yuejuan Cai ,Yuzhong Zhang, Shao Su, Shuping Li and Yonghong Ni, *Frontiers in Bioscience*, **2** (2007) 1946.

[3] Directors of the American Society of Hospital Pharmacists, Drug Information 88, Bethesda, MD, (1988) 415.

[4] World Health Organization Meeting, *Use of Quinolones in Food Animals and Potential Impact on Human Health*, Geneva, Switzerland, 1998.

[5] Zhang Zhuoyong, Li Xia, Wang Xiaoli, Chen Shilu, Song Baohua and Zhao Huichun, *Journal of rare earths*, **24** (2006) 285.

[6] Nizam Diab, Ibrahim Abu-Shqair, Radi Salim and Mohammad Al-Subu, *Int. J. Electrochem. Sci.,* **9** (2014) 1771.

[7] Ali F. Al Ghamdi, Abdulilah Dawoud Bani Yaseen, *Russian Journal of Electrochemistry,* **50** (2014) 355.

[8] Navalon, O. Ballesteros, R. Blancand and J. Vilchez, *Talanta*, **52** (2000) 845.

[9] A.C. Igboasoiyi, E.E. Attih, S.I. Ofoefule, E.D. Umoh and O.C. Udoh, *International journal of innovative research & development,* **3** (2014) 177.

[10] Qun Wang, Zhanfeng Dong, Yumin Du and John F. Kennedy, *Carbohydrate Polymers,* **69** (2007) 336.

[11] A. Dincel, A. Yildirim, F. Caglayan and A. Bozkurt, *Acta Chromatographica,* **15** (2005) 308.

[12] H. Lode, G. Hoffken, C. Prinzing, P. Glatzel and R. Wiley, *J. Clin. Chem. Biochem.*, **24** (1986) 325.

[13] N.M. Kassab, A.K. Singh, E.R. Maria and M.I. Santoro, *Brazil. J. Pharma. Sci.*, **41** (2005) 507.

[14] P. Sibinovic, A. Smelcerovic, R. Palic, S. Dordevic and V. Marinkovic, *J. Serb. Chem. Soc.*, **70** (2005) 979.

[15] Z. Vybiralova, M. Nobilis, J. Zoulora, J. Kvetina and P. Petr, *J. Pharma. Biomed. Anal.*, **37** (2005) 851.

[16] M. Kamberi, K. Tsutsumi, T. Kotegawa, K. Nakamura and S. Nakano, *Clin. Chem.*, **44** (1998) 1251.

[17] A. Navalon, O. Ballesteros, R. Blanc and J. Vilchez, *Talanta*, **52** (2000) 845.

[18] K. Basavaiah, P. Nagegowda, B.C. Somashekar and V. Ramakrishna, *Sci. Asia*, **32** (2006) 403.

[19] F.M. Abdel Gawad, Y.M. Issa, H.M. Fahmy and H.M. Hussein, *MicroChimica Acta*, **130** (1998) 35.

[20] Y.H. Diao, *Chin. J. Hosp. Pharm.*, **14** (1994) 212.

[21] A.A. Ensafi, M. Taei, T. Khayamian, F. Hasanpour, *Anal. Sci.*, **26** (2010) 803.

[22] H. Yi, C. Li, *Russ, J. Electrochem.*, **43** (2007) 1377.

[23] S. Zhang, S. Wei, *Bull. Korean Chem. Soc.*, **28** (2007) 543.

[24] P. O'Dea, A. Garcia, A. Ordieres, P. Blanco and M. Smyth, *Electroanalysis*, **2** (1990) 637.

[25] B. Uslu, B. Bozal, M. Kuscu, *Open Chem.Biomed. Meth. J.*, **3** (2010) 108.

[26] P. O'Dea, A.C. Garcíc, A.J. Ordieres, P.T. Blanco and M.R. Smyth, *Electroanal.*, **3** (1991) 337.

[27] Komorsky, S. Lovric. B. Nigovic, *J. Pharm Biomed Anal.*, **36** (2004) 81.

[28] Lidia Fotouhi, Mahnaz Alahyari, *Colloids and Surfaces B: Biointerfaces,* **81** (2010) 110.

[29] Yuejuan Cai , Yuzhong Zhang, Shao Su, Shuping Li and Yonghong Ni, *Frontiers in Bioscience*, **12** (2007) 1946.

[30] "Tyrosine". *The Columbia Electronic Encyclopedia, 6th ed*. Columbia University Press, 2007.

[31] D. Harper, "Tyrosine". *Online Etymology Dictionary*, 2001.

[32] Y. Sun, *Adv. Funct. Mater.*, **20** (2010) 3646.

[33] M.S. El-Deab, T. Ohsaka, *Angew. Chem., Int. Ed*., **45** (2006) 5963.

[34] H. B. Na, J.H. Lee, K. An, Y.I. Park, M. Park, I.S. Lee, D.H. Nam, S.T. Kim, S.H. Kim, S.W. Kim, *Angew. Chem., Int. Ed*., **46** (2007) 5397.

[35] M. Acciawi, C. Canevial, M. Mari, M. Mattoni, R. Ruffo, R. Scotti, F. Morazzoni, D. Barreca, L. Armelao and E. Tondello, *Chem Mater.*, **15** (2003) 2646.

[36] K.N. Yu, Y.H. Xiong, Y.L. Liu and C.S. Xiong, *Phys Rev B.*, **55** (1997) 2666.

[37] E. Topoglidis, Y. Astuti, F. Duriaux, M. Gratzal and J.R. Durrant, *Langmuir*, **19** (2003) 6894.

[38] Jong Hyuk Kang, Z. Jin Young Kim and Duk Young Jeon, *Journal of the Electrochemical Society*, **152** (2005) 33.

[39] M.P. Rajeeva, C.S. Naveen, Ashok R. Lamani and H.S. Jayanna, *AIP Conf.Proc*., **183** (2013) 1536.

[40] L. Patterson, *Phys. Rev. Online Arch. (Prola).*, **56** (1939) 978.

[41] M. Negahdary, S. Rad, M. Torkamani Noughabi, *Advanced Studies in Biology*, **4** (2012) 103.

[42] V. Dribs, J. Srodon, D.D. Eberl, *Reappraisal of the Kubler Index and the Scherrer Equation Clays and Clay Minerals*, **45** (1997) 461.

[43] Caro, F. Bedioui, J.H. Zagal, *Electrochim. Acta*, **47** (2002) 1489.

[44] E.J. Laviron's, *Electroanal. Chem*., **52** (1974) 355.

[45] M.P. Deepak, G.P. Mamatha, B.S. Sherigara, *Int J Phar Chem.*, **4** (2014) 122.

[46] Junshan, Young Liu, Ruizhen Li, Can Wu, Lihua Zhu and Jingdong Zhang, *Journal of electroanalytical chemistry*, **738** (2015) 123.

Chapter-5

The Simultaneous Electrochemical Determination of Dopamine and Uric acid at $Ni_{0.02}Sn_{0.98}O_2$ Nanoparticles Modified Carbon Paste Electrode by Cyclic Voltammetric Technique

Dopamine

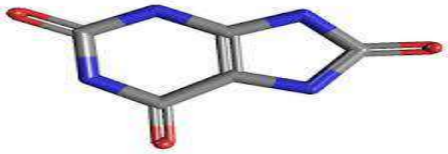

Uric acid

5.1. Introduction

Present work describes the electrochemical method using $Ni_{0.02}Sn_{0.98}O_2$ nanoparticles modified carbon paste electrode (NSNMCPE) for the determination of dopamine (DA) and uric acid (UA) simultaneously. The discussion involves the chemistry and biological relevance of DA and UA. The $Ni_{0.02}Sn_{0.98}O_2$ nanoparticles were synthesized by gel combustion method. These synthesized $Ni_{0.02}Sn_{0.98}O_2$ nanoparticles were characterized by XRD and SEM. Then the carbon paste electrode is modified with the synthesized $Ni_{0.02}Sn_{0.98}O_2$ nanoparticles by grinding method. The surface morphology of NSNMCPE was confirmed by SEM. The NSNMCPE was successfully used to study the electrochemical investigation of DA and UA in phosphate buffer solution (PBS) of pH 7.0 and pH 6.0 by cyclic voltammetric technique (CV). DA has revealed redox peaks reversibly, whereas UA has showed only oxidation peak at bare carbon paste electrode (BCPE) and NSNMCPE. The nature of voltammogram obtained at bare CPE was compared with NSNMCPE. The NSNMCPE shows good sensitivity compared to bare CPE. The low detection limit (LOD) and the low quantification limit (LOQ) of DA and UA were detected. The NSNMCPE was used for the simultaneous determination of DA and UA, the separation of the overlapping voltammograms of DA and UA at modified electrode in a mixture is successfully carried by using cyclic voltammetric technique. The proposed method was successfully applied for the determination of DA and UA due to its good sensitivity, lower detection limit and ease of preparation of the NSNMCPE allows the development of a highly sensitive voltammetric sensor for the determination of DA and UA.

5.2. Chemistry of Dopamine

Dopamine (DA), also known as "4-(2-aminoethyl) benzene-1, 2-diol"9, belongs to a member of the catecholamine family. Since the discovery of dopamine as a neurotransmitter in the late 1950s, dopamine has become the most widely studied catecholamine [1]. Dopamine plays an important role in the functions of the central nervous system, renal, hormonal, and cardiovascular systems. Its main function as a

hormone is to inhibit the release of prolactin from the anterior lobe of the pituitary. Dopamine can be supplied as a medication that acts on the sympathetic nervous system, producing effects such as increased heart rate and blood pressure. However, since dopamine cannot cross the blood-brain barrier, dopamine given as a drug does not directly affect the central nervous system. In the brain, dopamine functions as a neurotransmitter activating dopamine receptors and is produced in various areas of the brain. DA is also a neurohormone released by the hypothalamus. To increase the amount of dopamine in the brains of patients with diseases such as Parkinson's disease and Dopa-Responsive Dystonia, a synthetic precursor to dopamine such as L-DOPA (levodopa) can be given, since this will cross the blood-brain barrier.

5.2.1. Dysfunction of Dopamine

The developments of methods for measuring dopamine in biological systems are of importance for the analysis and diagnosis of neurological disorders such as Parkinson's disease. There are over 1.2 million people in the U.S. who suffer from Parkinson's disease with 50,000 new cases reported annually and is one of the most common neurological diseases in North America [2]. Numerous studies have shown that dopamine affects the brain processes that control movement, emotional response, and the ability to experience pleasure and pain. Also an imbalance of dopamine can lead to eating and sleeping disorders and additive behaviors associated with drug abuse. Therefore, there is an immediate need to develop simple and rapid methods for selectively determining dopamine in routine analysis.

5.2.2. Biological Relevance of Dopamine

Dopamine has many functions in the brain including important roles in behavior and cognition, voluntary movement, motivation, punishment and reward, inhibition of prolactin production, sleep, mood, attention, working memory, and learning. Shortage of dopamine, particularly the death of dopamine neurons in the nigrostriatal pathway causes Parkinson's disease, in which a person loses the ability to execute smooth, controlled movements. Degeneration of dopamine, decline of cognitive function, motor

symptoms, and other problems lead to decreased efficiency and function of the brain and body. This leads to a downward spiral of further decrease in efficiency and function, which results in degeneration, aging, breakdown, and death. Neurotransmission involves the conversion of an electrical impulse to a chemical event and then to another electrical event, is extremely rapid. Action potentials and neurotransmitters represents the bricks with which the internal representation of the external world is build.

5.3. Chemistry of Uric acid

Uric acid (UA) (2, 6, 8-trihydroxypurine) is the primary product of purine metabolism in the human body. It is a diprotic acid with pKa_1=5.4 and pKa_2=10.3 [3]. Thus in strong alkali at high pH it forms the dually charged full urate ion, but at biological pH it forms the singly charged hydrogen or acid urate ion as its pKa_2 is greater than the pKa_1 of carbonic acid. As its second ionization is so weak the full urate salts tend to hydrolyse back to hydrogen urate salts and free base at pH values around neutral. It is aromatic because of the purine functional group.

As a bicyclic, heterocyclic purine derivative, uric acid does not protonate in the same manner as do carboxylic acids. Thus, whereas most organic acids are deprotonated by the ionization of polar hydrogen-to-oxygen bond, usually accompanied by some form of resonance stabilization, this acid is deprotonated at a nitrogen atom and uses a tautomeric keto/hydroxy group as an electron-withdrawing group to increase the pKa_1 value. The five membered ring also possesses a keto group (in the 8 position), flanked by two secondary amino groups (in the 7 and 9 positions), and deprotonation of one of these at high pH could explain the pKa_2 and behavior as a diprotic acid [4].

5.3.1 Biological Relevance of Uric acid

UA is an important analyte in clinical field. In a healthy human being, the typical concentration of UA in urine is in millimolar range (approximately 2mM), whereas in blood it is in the micro-molar range (120–450 μM) [5, 6]. Abnormalities of

UA level indicate symptoms of several diseases, such as gout, hyperuricaemia and Leseh-Nyhan syndrome [7]. UA is the primary end product of purine metabolism. Its abnormal concentration levels will lead to several diseases such as hyperuricemia and gout. Other diseases such as leukemia and pneumonia are also associated with enhanced urate levels [8]. Uric acid is an important evolutionary significant biomolecule and it plays a vital role in adaptation of animals to completely dry terrestrial habitat. Animals like reptiles and birds are successfully adopted by conserving water by excreting its nitrogenous metabolic waste products in the form of UA [9].

5.4. Review of Electrochemistry of Dopamine and Uric acid

Extreme abnormalities of DA and UA concentrations levels may lead to several diseases and it is essential to develop a simple and rapid method for the determination of both DA and UA for routine analysis. The grinding, adsorption or coating of polymeric species or films onto the surface of conventional substrates has become a preferred approach for the construction of chemically modified electrodes (CMEs). The grinding modified electrodes have attracted great attention, because of their good stability, reproducibility and their wide applications in the fields of chemical sensors and biosensor. A variety of examples of the electrochemical determination of DA and UA along with AA have been proposed. These include a carbon paste electrode using pyrogallol red as a mediator [10], 2-Amino-5-mercapto-[1,3,4] triazole self -assembled monolayers gold electrode [11], indole-3-carboxaldehyde glassy carbon electrode [12], Lignin modified carbon paste electrode [13], p-aminobenzene sulfonic acid functionalized glassy carbon electrode [14], phosphorylated zirconia-silica composite electrode [15], 2,2'-[1,2-ethanadiylbis (nitriloethylidyne)]-bis-hydroquinone-carbon nanotube paste electrode [16].

5.5. Brief review of dopant tin (II) oxide nanoparticles

Tin oxide (SnO_2), normally known as cassiterite, is a typical wide band gap n-type semiconductor (Eg = 3.6 eV at 25°C) and one of the most widely used semiconductor oxides due to its chemical and mechanical stability [17, 18].Its high

optical transparency, electrical conductivity and chemical sensitivity make it a very attractive material for solar cells, heat mirrors, catalysis and gas-sensing applications. Tailoring the physical properties and adding new functionalities to the existing semiconductors by engineering the structure, composition, and particle/grain size are among the new approaches in advancing the current applications of semiconductor materials.

Preparation of these materials in the nanoscale size range is more interesting due to the increased surface-to-volume ratio that might affect the structural and most other physical properties. Transition-metal (TM) doping has been proposed to introduce magnetic functionality in conventional semiconductors [19, 20]. Nanoparticles of tin oxide have been synthesized through different chemical routes, such as precipitation [21, 22], sol–gel [23, 18], hydrolytic [24] and polymeric precursor [25] methods among others. In this work, we synthesize Ni-doped SnO_2 nanoparticles by gel combustion method because this method has some advantages such as precise control over the stoichiometry, high temperature synthesis, high purity and high chemical homogeneity.

In continuation of our work on the modification of carbon paste electrodes we intended for the $Ni_{0.02}Sn_{0.98}O_2$ nanoparticles as modifier and applied for the electrochemical investigation for dopamine and uric acid simultaneously.

5.6. Experimental Section

5.6.1. Reagent and Chemicals

Tin (II) chloride dehydrate ($SnCl_2.H_2O$, 99.99 %, Merck), Nitric acid (HNO_3, 70%, Merck), Citric acid ($C_6H_8O_7$, 99.5%, Merck), Nickel chloride Hexahydrate ($NiCl_2.6H_2O$), Potassium ferrocyanide $K_4[Fe(CN)_6]$ and UA solutions were prepared by dissolving in double distilled water. DA was prepared by dissolving in 0.1 M perchloric acid ($HClO_4$) solution, 0.1 M potassium chloride (KCl) was used as supporting electrolyte for all analytes. Chemicals mentioned above were all purchased from Fluka and were analytical grade.

5.6.2. Apparatus and Procedure

The electrochemical experiments were carried out using an Electroanalyser model EA-201 chemlink system. All experiments were carried out in a conventional three-electrode system. The electrode system contained a working carbon paste electrode, homemade cavity of 3mm diameter, a platinum wire as counter electrode and saturated calomel electrode as reference electrode. $Ni_{0.02}Sn_{0.98}O_2$ nanoparticles modified carbon paste electrode was prepared by grinding the 10 mg of $Ni_{0.02}Sn_{0.98}O_2$ nanoparticles with 70% graphite powder (50 µm particle size was purchased from sdfine-chem Ltd) and 30% silicon oil (Himedia) in an agate mortar by hand mixing for about 30 minute to get homogenous $Ni_{0.02}Sn_{0.98}O_2$ nanoparticles MCPE. The paste was packed into the cavity of CPE and smoothened on weighing paper. The bare CPE was prepared without adding modifier.

5.6.3. Synthesis of $Ni_{0.02}Sn_{0.98}O_2$ nanoparticles

$Ni_{0.02}Sn_{0.98}O_2$ nanoparticles were synthesized by gel combustion method. The materials used are tin (II) chloride dehydrate, 6.2 mole of nitric acid which is used as an oxidizer and mixed in an appropriate ratio to form a tin nitrate solution, then 1.5 mole of citric acid which acts as fuel and 0.02 ml Nickel chloride Hexahydrate ($NiCl_2.6H_2O$) was added to solution and the solution was heated at 90°C in a Pyrex vessel with constant stirring. When the temperature was raised to about 300°C, the polymeric precursor underwent a strong, self-sustaining combustion reaction occurs with evolution of large volume of gases and swelled into voluminous and foamy ashes. The entire combustion process occurs in a few seconds. The produced ashes were then calcined at 800°C (for 1 hour). The process was carried out, until the complete decomposition of the carbonaceous residues. Then the white powder $Ni_{0.02}Sn_{0.98}O_2$ nanoparticles were obtained [26].

5.7. Results and Discussion

5.7.1. Characterization of synthesized $Ni_{0.02}Sn_{0.98}O_2$ nanoparticles by XRD and SEM

Crystalline structure and crystallite size of $Ni_{0.02}Sn_{0.98}O_2$ nanoparticles were analyzed by Cu-K_α X-ray radiation (λ=1.5418A˚) in 2θ range from 20º to 80°, operating at 30 kV and 15 mA. The scan rate was 5°/min.). XRD patterns of $Ni_{0.02}Sn_{0.98}O_2$ nanoparticles annealed at 800°C for 1hr as shown in **Fig.5.1**, the average grain size was calculated using the Scherrer relation,

$$d = 0.89\frac{\lambda}{\beta\cos\theta} \quad \text{..... (5.1)}$$

Where d is the crystallite size, λ is the wavelength of X-rays, β is the full width of half maximum and 2θ is the diffraction peak angle [27], the (110) peak is used to calculate the crystallite sizes.

The crystallite sizes of $Ni_{0.02}Sn_{0.98}O_2$ nanoparticles are found to be 23.03 nm by using Scherer formula. The surface morphology and shape of the nanoparticles of powdered samples were investigated by scanning electron microscope (SEM) (Hitachi Model S-3200N). **Fig.5.2** shows the typical SEM image of the $Ni_{0.02}Sn_{0.98}O_2$ nanoparticles.

5.7.2. SEM Characterization of $Ni_{0.02}Sn_{0.98}O_2$ nanoparticles modified carbon paste electrode

The morphology of the CPE and NSNMCPE was characterized by scanning electron microscope (SEM) and shown in **Fig.5.3a** and **5.3b** respectively. Smooth surface was observed on bare CPE surface. In the modified electrode the formation of spindle-like nanostructures not only enlarges the surface area of the electrode, but also improves the electron transfer rate between the electrode surface and the bulk solution,

which has been confirmed by the performance of NSNMCPE in electrochemical investigation of $K_4[Fe(CN)_6]$ system.

5.7.3. Electrochemical response of potassium ferrocyanide at $Ni_{0.02}Sn_{0.98}O_2$ nanoparticles modified carbon paste electrode

Fig. 5.4 shows the electrochemical behavior of 0.1 mM potassium ferrocyanide ($K_4[Fe(CN)_6]$) in 0.1M KCl at bare carbon paste electrode (BCPE) curve 'b' and at $Ni_{0.02}Sn_{0.98}O_2$ nanoparticles modified carbon paste electrode (NSNMCPE) curve 'a' respectively. The curve 'b' shows the cathodic peak current I_{pc} 2.8 µA of E_{pc} 24.2 mV and anodic peak current I_{pa} 4.3 µA of E_{pa} 353 mV at BCPE. Whereas, for the NSNMCPE the cathodic peak current I_{pc} 15.0 of E_{pc} 54 mV and anodic peak current I_{pa} 16.3 µA of E_{pa} 291 mV has been observed. The enhancement of peak current showed excellent catalytic ability of NSNMCPE. The surface area of bare carbon paste electrode is 0.0312 cm^2, whereas the effective surface area of the modified electrode was found to be 0.0403 cm^2.

5.7.4. Electrochemical behavior of dopamine (DA) at $Ni_{0.02}Sn_{0.98}O_2$ nanoparticles modified carbon paste electrode

The electrochemical behavior of dopamine (DA) was investigated in 0.2 M phosphate buffer solution (PBS) of pH 7 at NSNMCPE using cyclic voltammetric technique. **Fig.5.5** shows cyclic voltammograms of 1 mM DA at bare CPE (curve 'b') and at NSNMCPE (curve 'a'). The curve 'c' represents the cyclic voltammogram of blank solution at NSNMCPE. **Fig.5.5** shows the confirmation of modification of bare carbon paste electrode. Above studies showed that redox peaks. The oxidation peak at 266 mV potential with peak current of 3.9 µA and reduction peak at 80 mV potential with current peak of 1.8 µA at bare CPE, whereas an oxidation peak at 257 mV potential with a peak current of 18.44 µA and reduction peak at 101 mV potential with current peak of 6.4 µA at NSNMCPE respectively in the potential range from -200 to 600 mV. The peak was observed in the reverse scan, suggesting that the electrochemical reaction is a totally quasireversible process and the redox peak at the bare CPE is broad

due to slow electron transfer, while the response was considerably improved at NSNMCPE and the peaks potentials shifted to negative direction, the shape of the peaks turns sharper and the peak current increased significantly.

5.7.5. Electrochemical behavior of uric acid (UA) at $Ni_{0.02}Sn_{0.98}O_2$ nanoparticles modified carbon paste electrode

The electrochemical behavior of UA was investigated in 0.2 M phosphate buffer solution of pH 6 at NSNMCPE using cyclic voltammetric technique. **Fig.5.6** shows cyclic voltammograms of 0.1 mM UA at bare CPE (curve 'a') and NSNMCPE (curve 'b'). The curve 'c' represents the cyclic voltammogram of blank solution at NSNMCPE. Above studies showed that only one oxidation peak at 433 mV potential with peak current of 1.18 µA at bare CPE, whereas an oxidation peak at 432 mV potential with peak current of 1.99 µA at NSNMCPE, in the potential range from 100 to 600 mV. No reduction peak was observed in the reverse scan, suggesting that the electrochemical reaction is a totally irreversible process and the oxidation peak at the NSNMCPE is broad due to slow electron transfer, while the response was considerably improved at modified electrode and the peak potentials shifted to negative direction, the shape of the peak turns sharper and the peak current increased significantly.

5.7.6. Effect of pH on DA and UA

The electro oxidation of DA was studied at 0.1 mM stock solution in 0.2 M phosphate buffer solution over pH range from 2.5 to 8.5 at a scan rate of 50 mVs^{-1} at NSNMCPE using cyclic voltammetric technique. The oxidation peak current increases with increase of pH from 2.5 to 7 and becomes maximum and peak potential shifted negatively. While pH beyond 7, a great decrease of the oxidation peak current has been observed, then it decreased gradually with the further increase in pH of the solution is shown in **Fig.5.7a** and the oxidation peak potential decrease with in increase of pH is shown in **Fig.5.7b** .The corresponding linear regression equation is

$$E_{pa}\,(mV) = 742.609 - 72.208\ pH \quad (R = 0.99687) \ldots\ldots\ldots\ldots\ldots\ldots\ldots\ldots\ldots\ldots \quad (5.2)$$

The value of this slope is in close agreement with the theoretical value of 59 mV/pH at 25^0 for a $2e^-$ transfer process. Other researchers also have reported $2e^-$ transfer oxidation process in DA [28, 29].

To study the effect of pH on UA has been studied by using 0.1 mM stock solution of UA in 0.2 M PBS in pH range from 3 to 9 at a scan rate 50 mVs^{-1} at NSNMCPE using cyclic voltammetric technique. The anodic peak current decreases with increase of pH from 3 to 5.5 and becomes maximum and peak potential shifted negatively at pH 6. While pH beyond 6, a great decrease of the oxidation peak current has been observed, then it decreased gradually with the further increase the pH of solution is shown in **Fig.5.8a** and the oxidation peak potential decrease with in increase of pH shown in **Fig.5.8b** respectively. The corresponding linear regression equation is

$$E_{pa}\,(mV) = 675.24 - 39.640\ pH \quad (R = 0.98069) \ldots\ldots\ldots\ldots\ldots\ldots\ldots\ldots \quad (5.3)$$

The negative slope of 39.640 was close to the theoretical value indicated that the electrons and protons involved in the oxidation of UA were equal (1:1).

5.7.7. Effect of scan rate on DA and UA

Useful information involving electrochemical mechanism usually can be acquired from the relationship between peak current and scan rate. Therefore, the effect of scan rates on the electrochemical response of 0.1 mM dopamine at NSNMCPE was studied at different scan rates including 25, 50, 75, 100, 125, 150, 175, 200, 225, 250, 275, 300 mVs^{-1} by CV and the cyclic voltammograms were shown in **Fig.5.9a**. As shown in **Fig.5.9b** the linear relationship with a correlation coefficient of 0.99771 obtained between the anodic peak current and square root of scan rate in the range of 25 – 300 mVs^{-1}. The corresponding linear regression equation is

$$I_{pa}\,(\mu A) = 1.303\ \nu^{1/2} + 10.856 \quad (R = 0.9977) \ldots\ldots\ldots\ldots\ldots\ldots\ldots\ldots\ldots \quad (5.4)$$

Which revealed that a diffusion controlled process occurring at $Ni_{0.02}Sn_{0.98}O_2$ nanoparticles modified carbon paste electrode. However linearity was also obtained for the plot of anodic peak current vs. the scan rate with a correlation coefficient of 0.9903 as shown in **Fig.5.9c**. The corresponding linear regression equation is given by

$$I_{pa}\,(\mu A) = 0.0560\nu + 17.632 \quad (R = 0.9903) \ldots\ldots (5.5)$$

The results suggest that the nature of electrode reaction was diffusion controlled and as a result the peak potential shifts towards positive side. The relationship between the anodic peak potential and scan rate can be explained by plotting the anodic peak potential vs. natural logarithm of scan rate **(Fig.5.9d)** by considering the relation:

$$E_{pa}\,(mV) = 0.0479 \ln\upsilon + 0.1132 \quad R= 0.98466 \ldots\ldots (5.6)$$

In addition, there was a linear relation between $\log I_{pa}$ and $\log\nu$ (**Fig.5.9e**) is corresponding to the following equation

$$\log I_{pa}\,(\mu A) = 0.265 \log\nu + 0.856 \quad (R = 0.989) \ldots\ldots (5.7)$$

The slope for the equation is 0.265, which is close to the theoretical value of 0.5 for a diffusion controlled process between scan rates 25 – 300 mVs^{-1}.

Similarly the effect of scan rates on UA has been discussed. The electrochemical response of 0.1 mM UA at NSNMCPE was studied at different scan rates including 10, 20, 30, 40, 50, 60 70, 80, 90 and 100 mVs^{-1} by CV and the cyclic voltammograms were shown in **Fig.5.10a**. As shown in **Fig.5.10b,** a linear relationship with a correlation coefficient of 0.99387 was obtained between the anodic peak current and square root of scan rate in the range of 10 – 100 mVs^{-1}. The corresponding linear regression equation is given by

$$I_{pa}\,(\mu A) = 0.4180\,\nu^{1/2} + 0.444 \quad (R = 0.9959) \ldots\ldots (5.8)$$

Which revealed that a diffusion controlled process occurring at NSNMCPE. However linearity was also obtained for the plot of scan rate vs. anodic peak current with a correlation coefficient of 0.9913 as shown in **Fig. 5.10c**. The relationship between the anodic peak potential and scan rate is explained by plotting the anodic peak potentials vs. natural logarithm of scan rate **(Fig.5.10d)** by considering the relation:

$$E_{pa}\,(mV) = 0.0184\ \ln\upsilon + 0.329 \quad R = 0.9901 \ldots\ldots\ldots\ldots\ldots\ldots\ldots\ldots \quad (5.9)$$

The linear relation between $\log I_{pa}$ and $\log\nu$ **(Fig.5.10e)** is corresponding to the following equation

$$\log I_{pa}\,(\mu A) = 0.408\ \log\nu - 0.1597 \quad (R = 0.9923) \ldots\ldots\ldots\ldots\ldots\ldots\ldots \quad (5.10)$$

The slope for the equation is 0.408, which is close to the theoretical value of 0.5 for a diffusion controlled process in scan rates 10 - 100 mVs^{-1}.

According to Laviron's theory [30], the slope is equal to $RT/\alpha n_{\alpha}F$. Then the value of αn_{α} found to be 0.4542. As for a totally quasi-reversible electrode reaction process of dopamine and irreversible electrode reaction process of uric acid. The n_{α} were calculated as 2.0238 and 1.908 respectively. Which indicated that two electrons were involved in the oxidation process of dopamine and uric acid at NSNMCPE. Since the equal number of electron and proton took part in the oxidation of dopamine and uric acid, therefore two electrons and two protons transfer were involved in the electrode reaction process. The electrochemical reaction process for dopamine and uric acid at $Ni_{0.02}Sn_{0.98}O_2$ nanoparticles modified carbon paste electrode can therefore be summarized as in **scheme 5.1**.

5.7.8. Calibration of Dopamine and Uric acid concentration

A series of dopamine and uric acid solutions of 1.0×10^{-5} to 1.0×10^{-3} M were prepared in phosphate buffer solution to investigate the relationship between the anodic peak current (I_{pa}) and concentration of dopamine and uric acid at $Ni_{0.02}Sn_{0.98}O_2$ nanoparticles modified carbon paste electrode at a scan rate of 50 mVs^{-1} by CV. The

obtained cyclic voltammogram of dopamine and uric acid were shown in **Fig.5.11a and 5.11b** respectively. A linear relationship has obtained on plotting I_{pa} vs. concentration of DA and UA which is shown in **Fig.5.12a** and **Fig.5.12b** respectively. This is explained on the basis of linear regression equations for DA and UA respectively.

I_{pa} (μA) = 18.938 C (10^{-5} M) + 0.0276 (R= 0.9971)…….. (5.11)

I_{pa} (μA) = 18.005 C (10^{-5} M) + 0.0027 (R= 0.9949)…..……..(5.12)

The limit of detection (LOD) and limit of quantification (LOQ) were 0.831 μM, 2.770 μM for DA and 1.11 μM, 3.71μM for UA respectively.

The LOD and LOQ were calculated on the peak current using the following equations are LOD= 3S/M and LOD=10S/M

Where, S is standard deviation and M is the slope of calibration plot.

5.7.9. Simultaneous determination of DA and UA at $Ni_{0.02}Sn_{0.98}O_2$ nanoparticles modified carbon paste electrode

The objective of our work was the simultaneous determination of DA and UA. **Fig.5.13** shows the cyclic voltammograms of DA and UA co-existing in phosphate buffer solution of pH 7 at the bare carbon paste electrode and $Ni_{0.02}Sn_{0.98}O_2$ nanoparticles modified carbon paste electrode. The curve 'b' shows the cyclic voltammogram of the solution containing 0.2 mM DA and 0.5 mM UA mixture at the bare carbon paste electrode. It exhibits one broad peak for both the analytes and indicates that the bare carbon paste electrode fails to separate the voltammetric signals of DA and UA. The curve 'a' of **Fig.5.13** shows the cyclic voltammogram of the oxidation of 0.2 mM DA and 0.5 mM UA mixture at $Ni_{0.02}Sn_{0.98}O_2$ nanoparticles modified carbon paste electrode. It exhibits two well-defined oxidation peaks at 270 and 315 mV potential corresponding to the oxidation of DA and UA respectively. The difference between the anodic peak potential of DA and UA was about 45 mV.

Therefore, $Ni_{0.02}Sn_{0.98}O_2$ nanoparticles modified carbon paste electrode can be effectively employed to separate DA in the presence of UA.

5.8. CONCLUSION

- The chemically modified $Ni_{0.02}Sn_{0.98}O_2$ nanoparticles modified carbon paste electrode based on grinding has been prepared for the electrochemical determination of dopamine (DA) and uric acid (UA).
- Results showed that the oxidation peak current of dopamine (DA) and uric acid (UA) was improved at $Ni_{0.02}Sn_{0.98}O_2$ nanoparticles modified carbon paste electrode.
- The electrochemical response is diffusion controlled and reversible and irreversible in nature for DA and UA respectively.
- A linear concentration range was found to occur from 1×10^{-5} to 1×10^{-3} M.
- The probable reaction mechanism involved in the oxidation of DA and UA were also proposed.

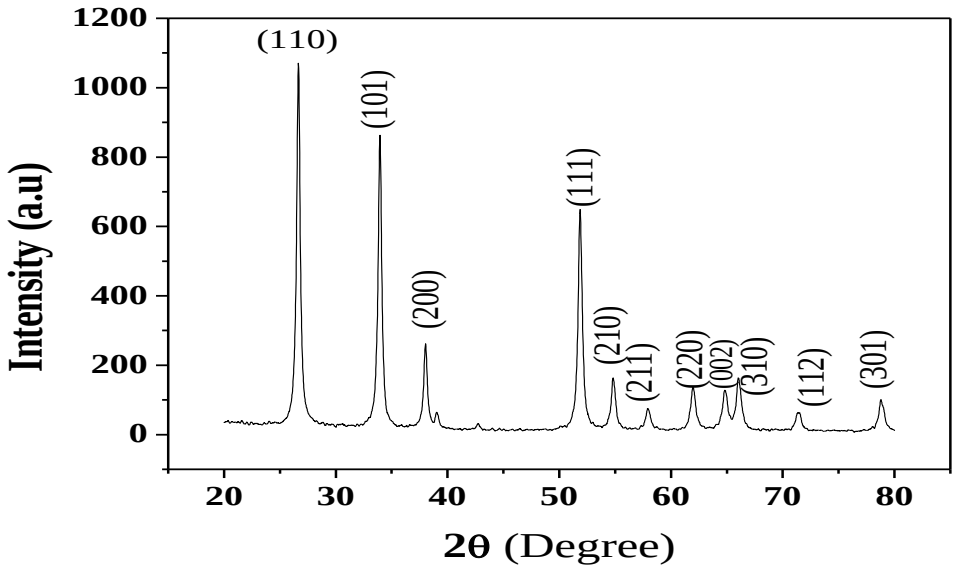

Fig. 5.1: XRD images of synthesized of $Ni_{0.02}Sn_{0.98}O_2$ nanoparticles.

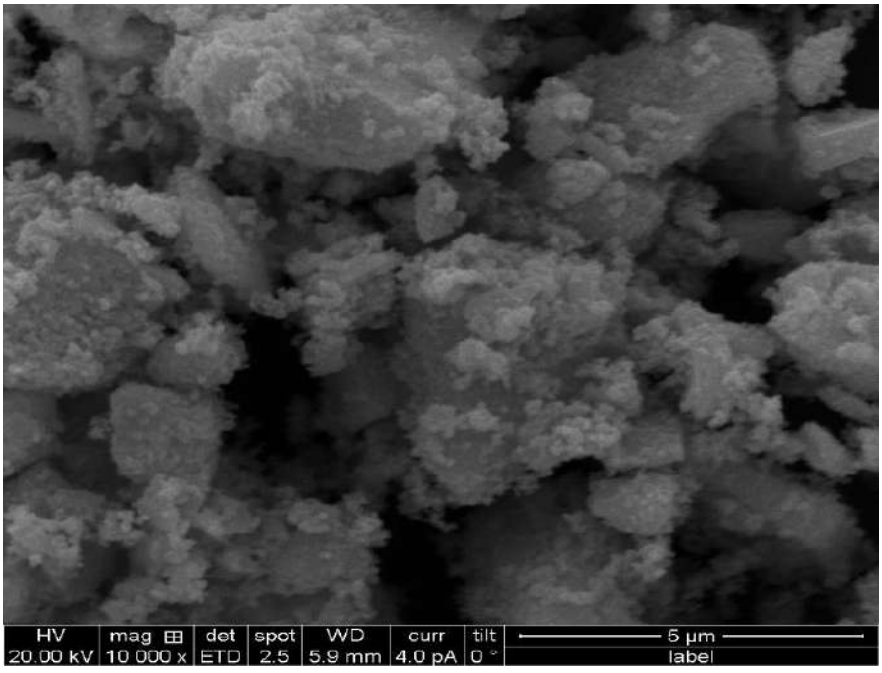

Fig. 5.2: SEM images of synthesized $Ni_{0.02}Sn_{0.98}O_2$ nanoparticles.

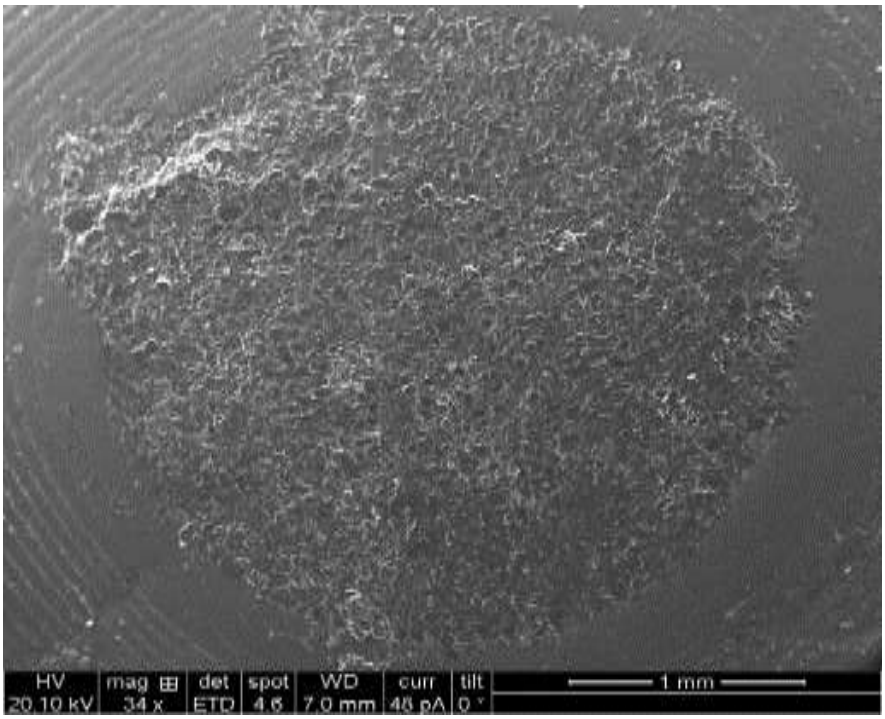

Fig. 5.3a: SEM image of bare carbon paste electrode.

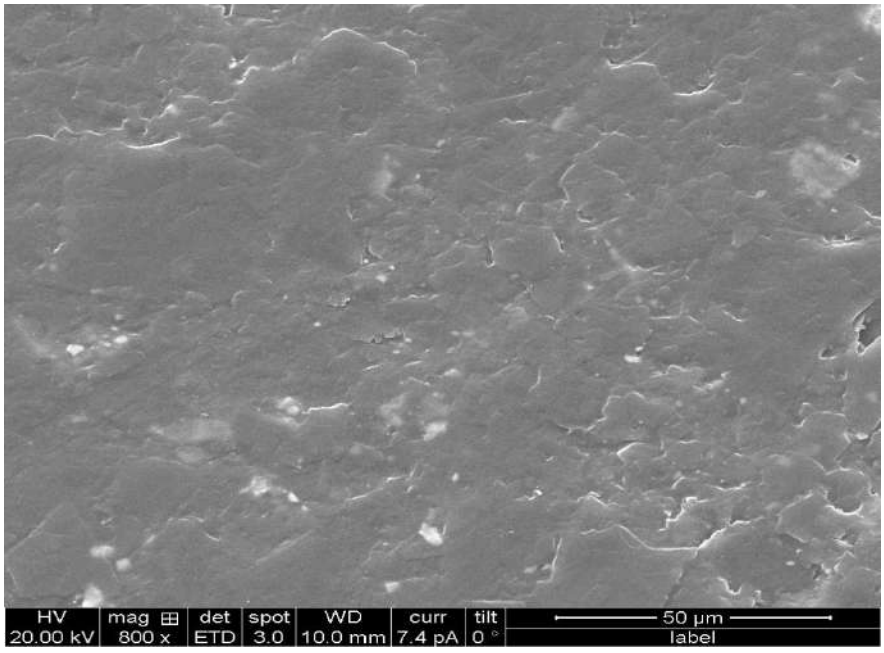

Fig. 5.3b: SEM image of $Ni_{0.02}Sn_{0.98}O_2$ nanoparticles modified carbon paste electrode.

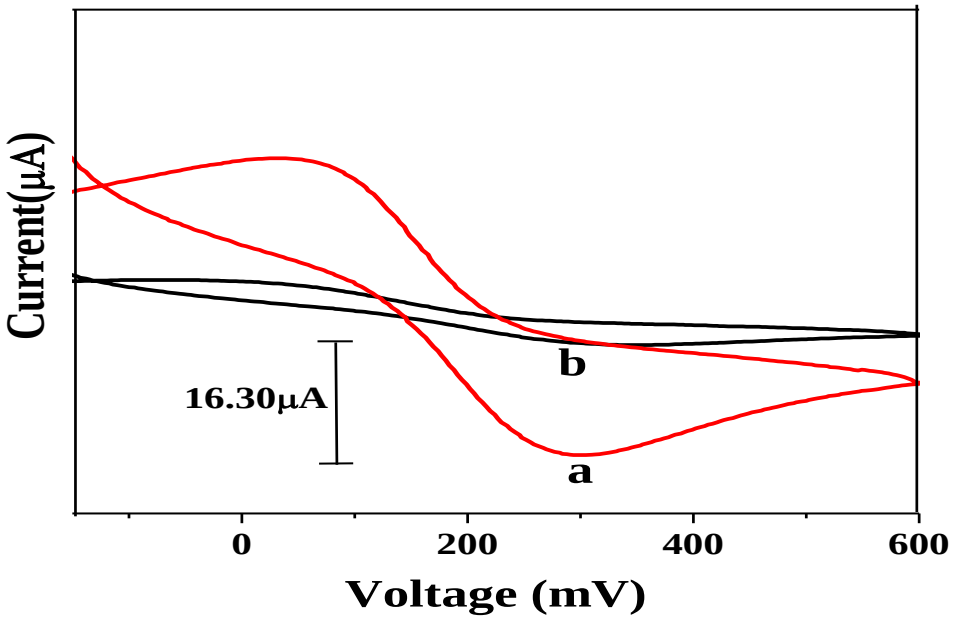

Fig. 5.4: Comparision of 0.1 mM $K_4[Fe(CN)_6]$ in 0.1 M KCl solution at $Ni_{0.02}Sn_{0.98}O_2$ nanoparticles modified carbon paste electrode (a) and bare carbon paste electrode (b).

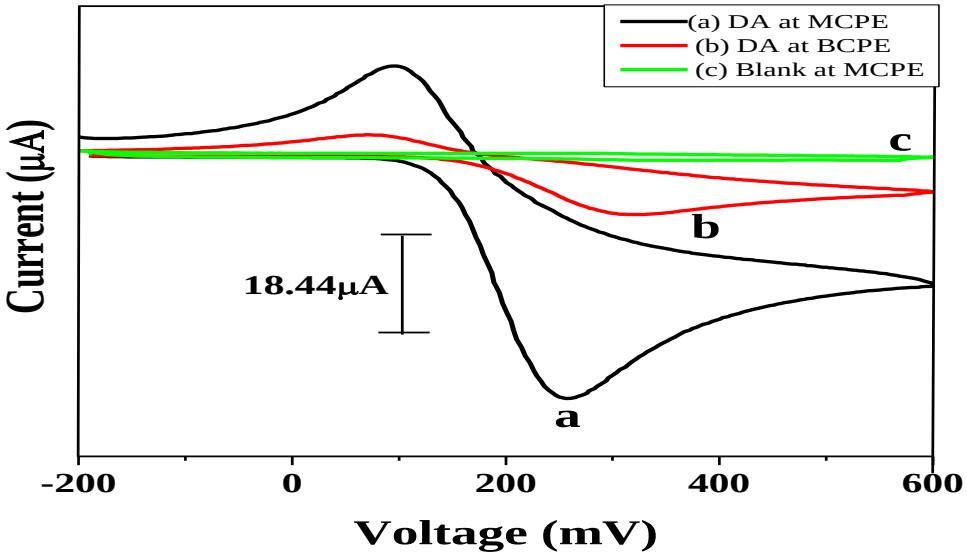

Fig. 5.5: Comparision of 1 mM DA at $Ni_{0.02}Sn_{0.98}O_2$ nanoparticles modified carbon paste electrode (a), bare carbon paste electrode (b) and blank solution in phosphate buffer at $Ni_{0.02}Sn_{0.98}O_2$ nanoparticles modified carbon paste electrode (c); pH 7, scan rate 50 mVs^{-1}.

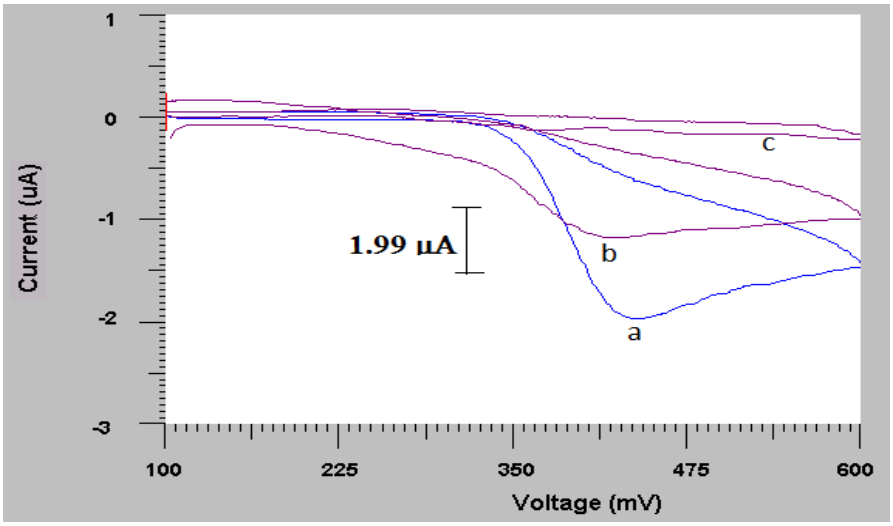

Fig. 5.6: Comparision of 0.1 mM UA at $Ni_{0.02}Sn_{0.98}O_2$ nanoparticles modified carbon paste electrode (a), bare carbon paste electrode (b) and blank solution in phosphate buffer at $Ni_{0.02}Sn_{0.98}O_2$ nanoparticles modified carbon paste electrode (c); pH 6, scan rate 10 mVs^{-1}.

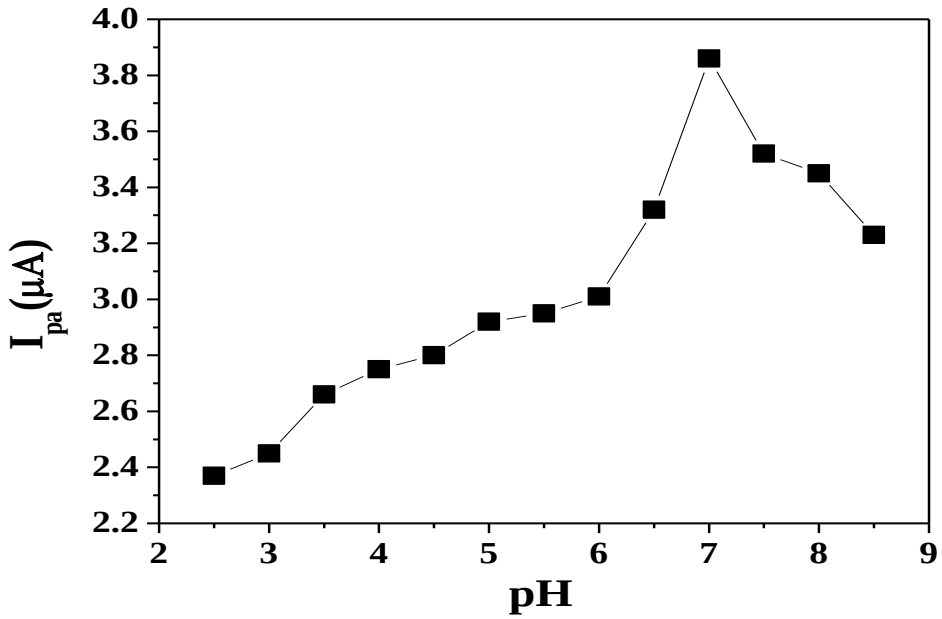

Fig. 5.7a: Plot of anodic peak current vs. pH (2.5 – 8.5) of 0.1 mM DA at $Ni_{0.02}Sn_{0.98}O_2$ nanoparticles modified carbon paste electrode.

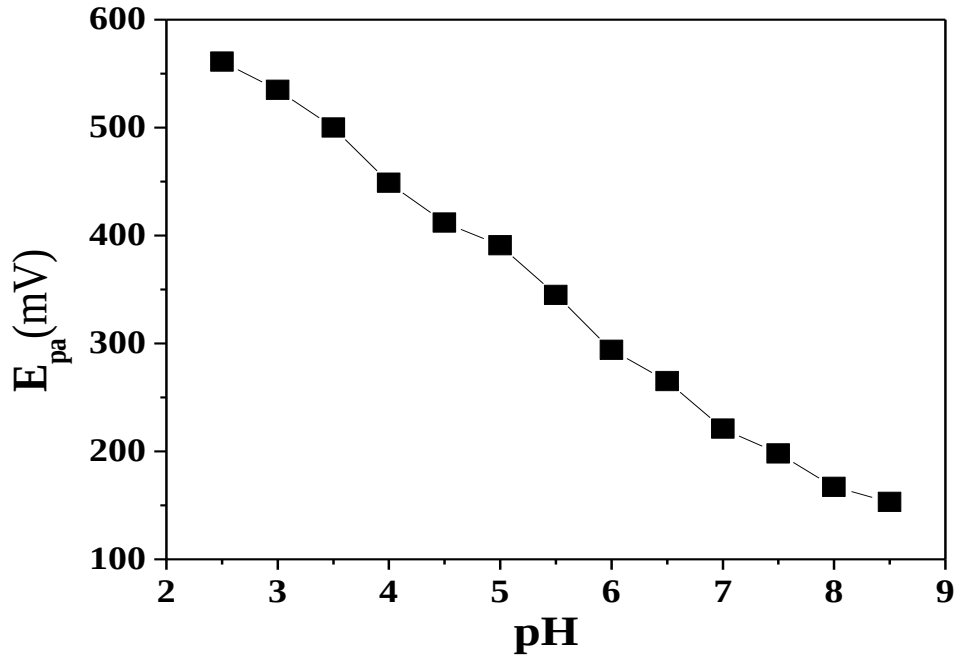

Fig. 5.7b: Plot of anodic peak potential vs. pH (2.5 – 8.5) of 0.1 mM DA at $Ni_{0.02}Sn_{0.98}O_2$ nanoparticles modified carbon paste electrode.

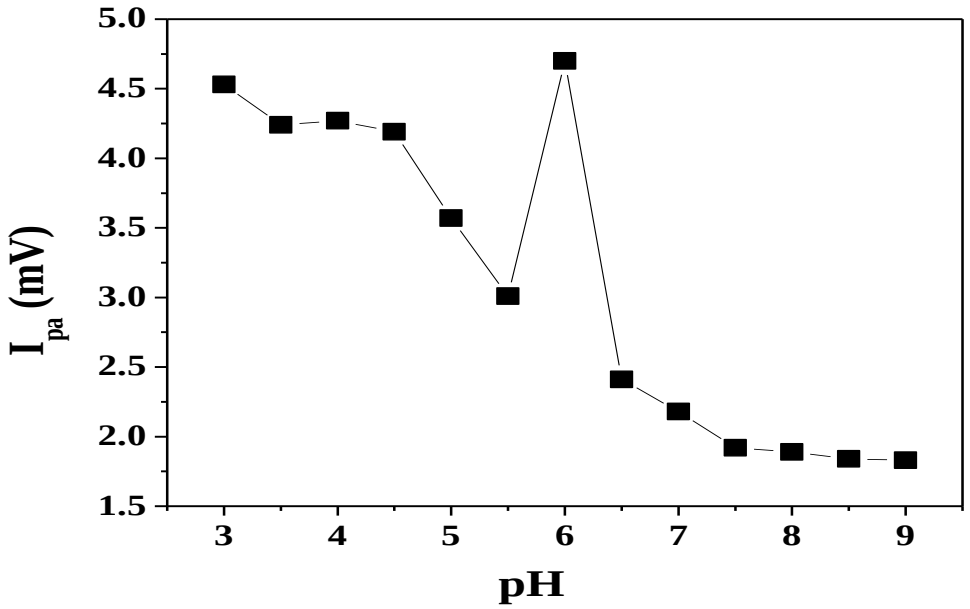

Fig. 5.8a: Plot of anodic peak current vs. pH (3–9) of 0.1 mM UA at $Ni_{0.02}Sn_{0.98}O_2$ nanoparticles modified carbon paste electrode.

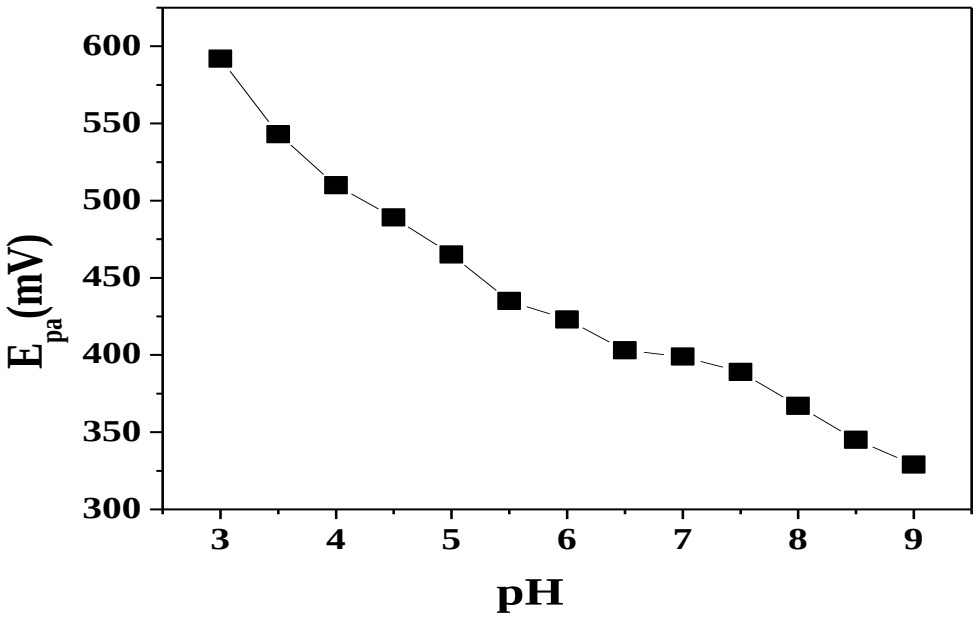

Fig. 5.8b: Plot of anodic peak potential vs. pH (3 – 9) of 0.1 mM UA at $Ni_{0.02}Sn_{0.98}O_2$ nanoparticles modified carbon paste electrode.

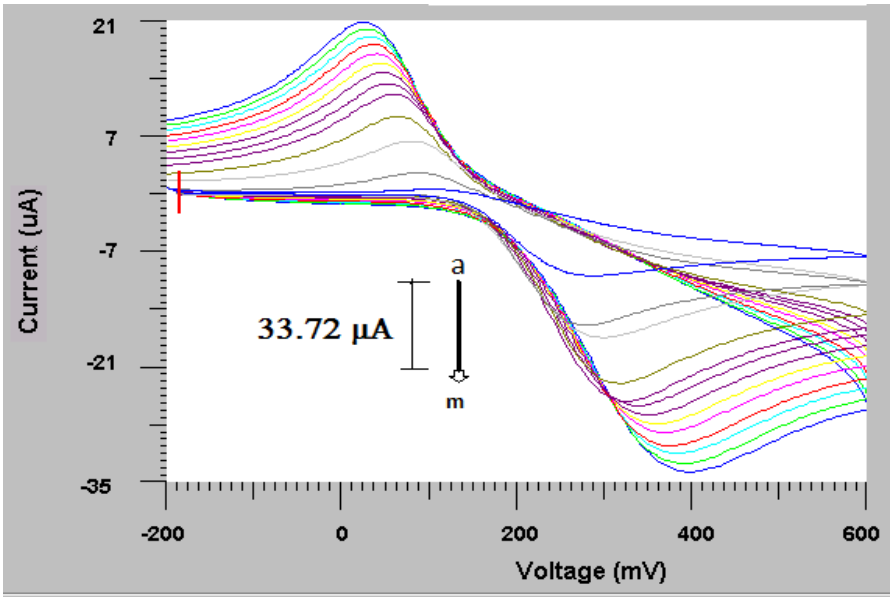

Fig. 5.9a. Cyclic voltammograms of 0.1 mM DA at $Ni_{0.02}Sn_{0.98}O_2$ modified carbon paste electrode with different scan rates (a) 25, (b) 50, (c) 75, (d) 100, (e) 125, (f) 150, (g) 175, (h) 200, (i) 225, (j) 250 and (k) 300 mVs^{-1}.

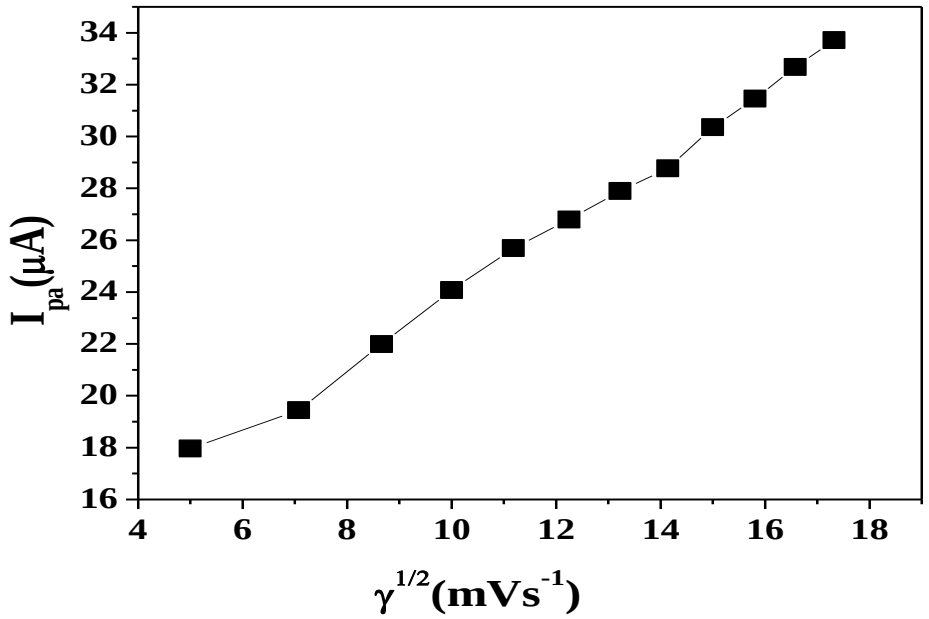

Fig. 5.9b: Plot of anodic peak current vs. square scan rates of DA at $Ni_{0.02}Sn_{0.98}O_2$ nanoparticles modified carbon paste electrode.

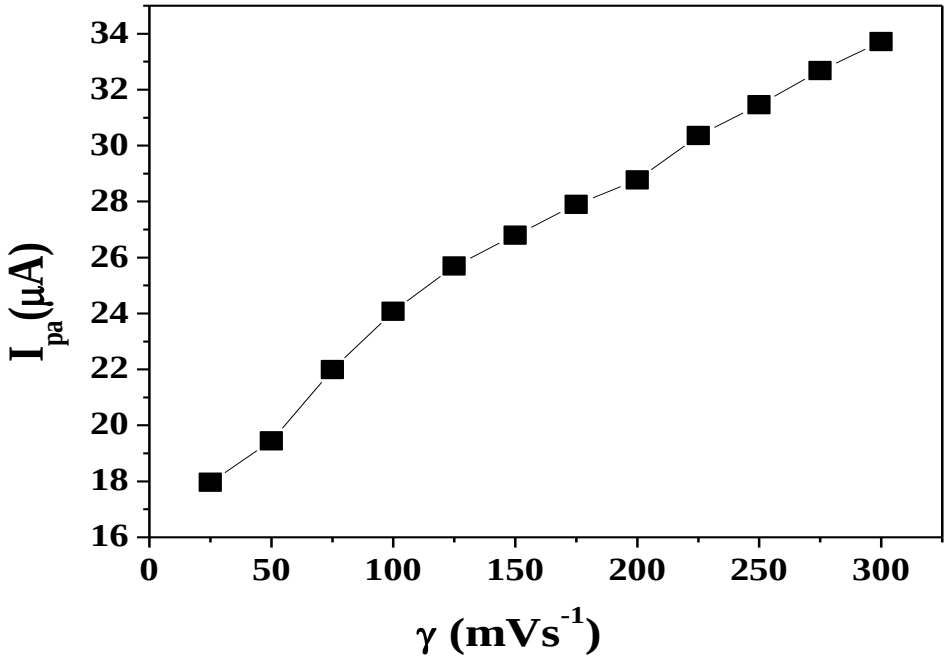

Fig. 5.9c: Plot of anodic peak current vs. scan rates of DA at $Ni_{0.02}Sn_{0.98}O_2$ nanoparticles modified carbon paste electrode.

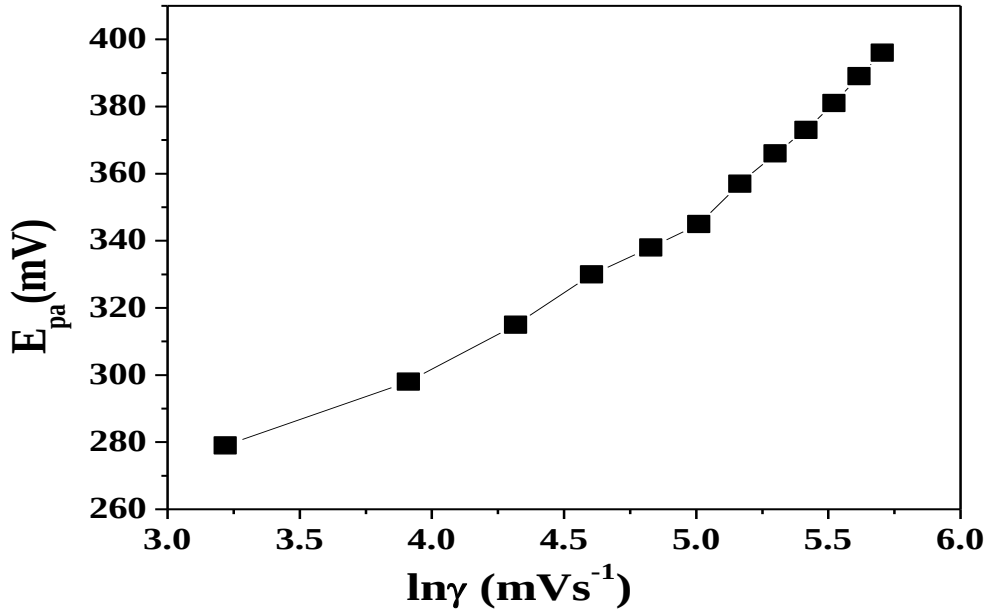

Fig. 5.9d: Plot of anodic peak potential vs. natural logarithm of scan rates of DA at $Ni_{0.02}Sn_{0.98}O_2$ nanoparticles modified carbon paste electrode.

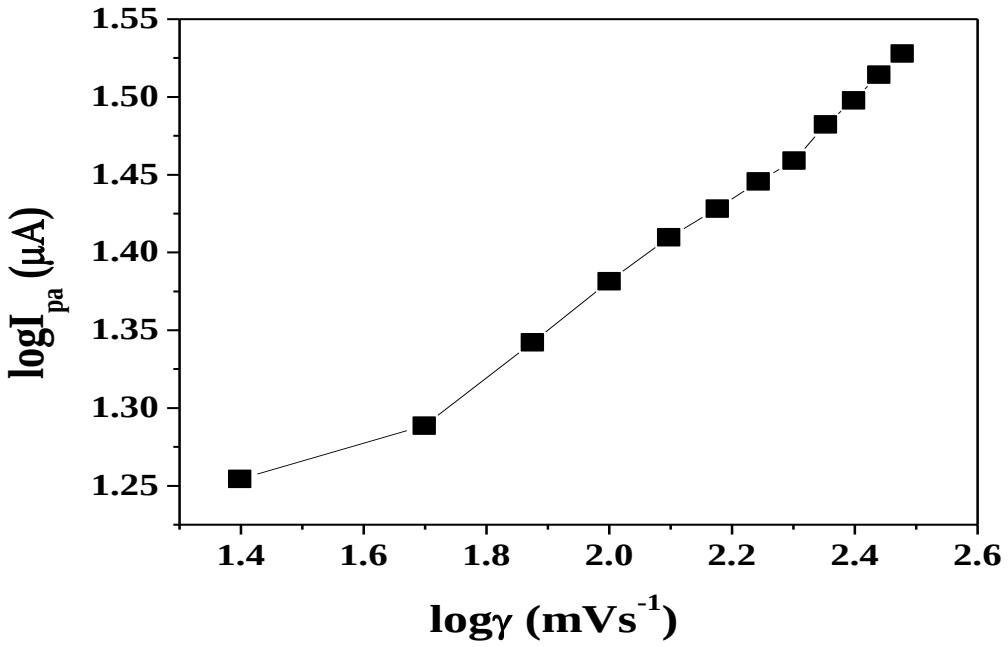

Fig. 5.9e: Plot of logarithm of anodic peak potential vs. logarithm of scan rates of DA at $Ni_{0.02}Sn_{0.98}O_2$ nanoparticles modified carbon paste electrode.

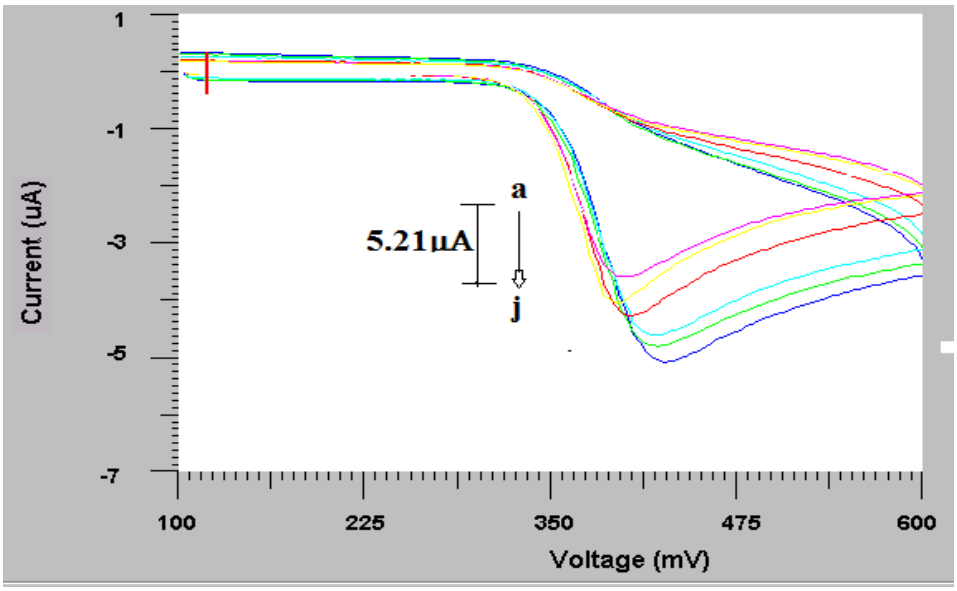

Fig. 5.10a: Cyclic voltammograms of 0.1 mM UA at $Ni_{0.02}Sn_{0.98}O_2$ nanoparticles modified carbon paste electrode with different scan rates (a) 10, (b) 20, (c) 30, (d) 40, (e) 50, (f) 60, (g) 70, (h) 80 (i) 90 and (j) 100 mVs^{-1}.

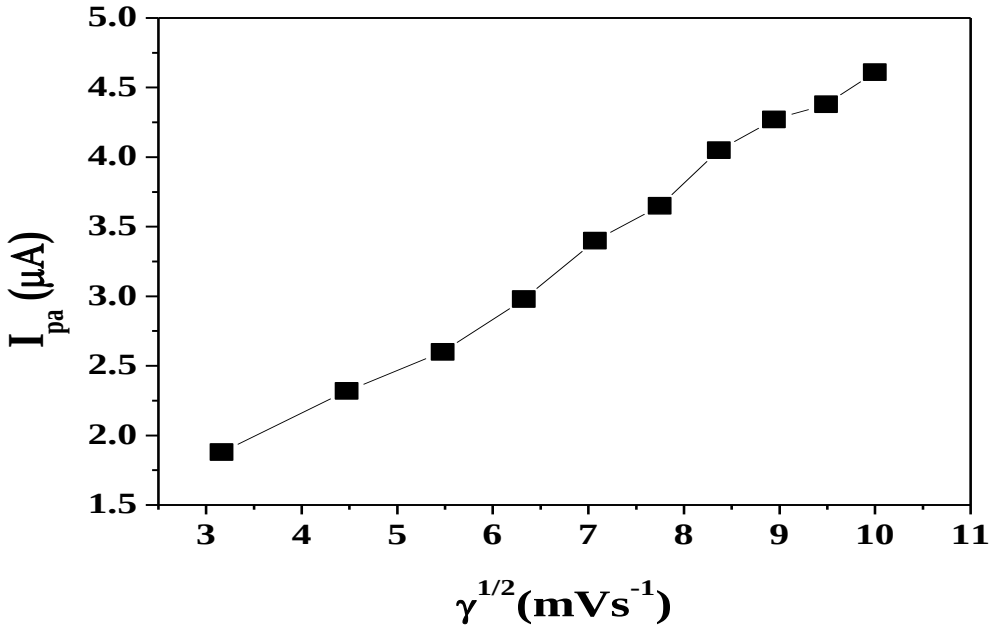

Fig. 5.10b: Plot of anodic peak current vs. square root of scan rates of UA at $Ni_{0.02}Sn_{0.98}O_2$ nanoparticles modified carbon paste electrode.

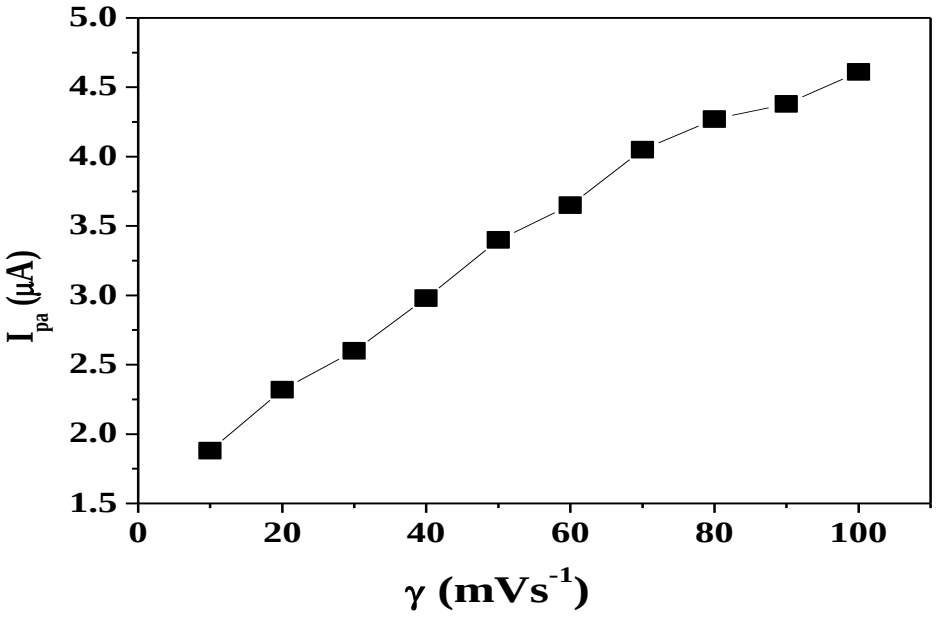

Fig. 5.10c: Plot of anodic peak current vs. scan rates of UA at $Ni_{0.02}Sn_{0.98}O_2$ nanoparticles modified carbon paste electrode.

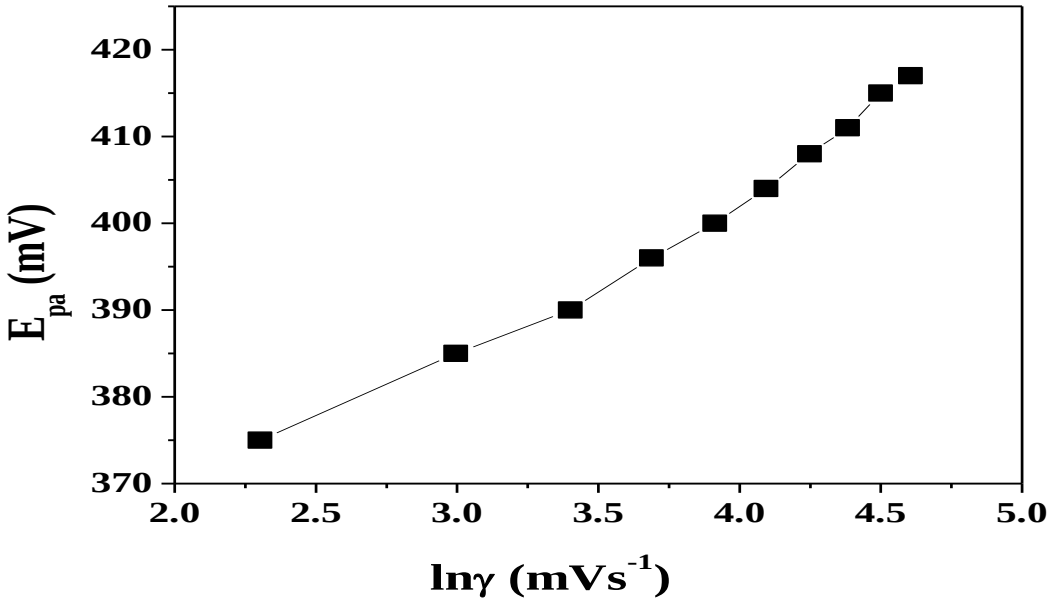

Fig. 5.10d: Plot of anodic peak potential vs. natural logarithm of scan rates of UA at $Ni_{0.02}Sn_{0.98}O_2$ nanoparticles modified carbon paste electrode.

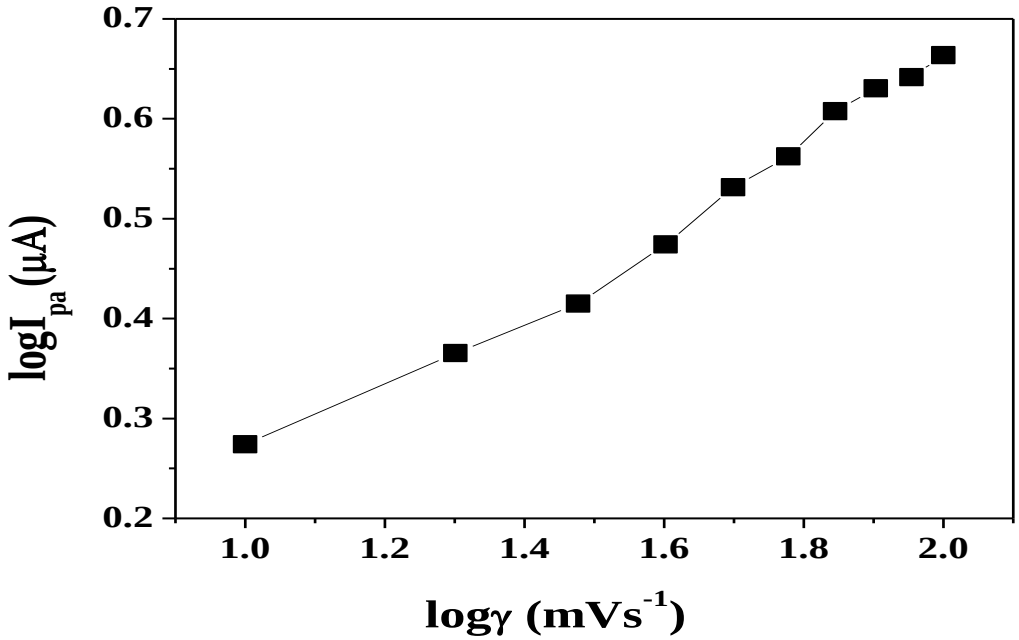

Fig. 5.10e: Plot of logarithm of anodic peak potential vs. logarithm of scan rates of UA at $Ni_{0.02}Sn_{0.98}O_2$ nanoparticles modified carbon paste electrode.

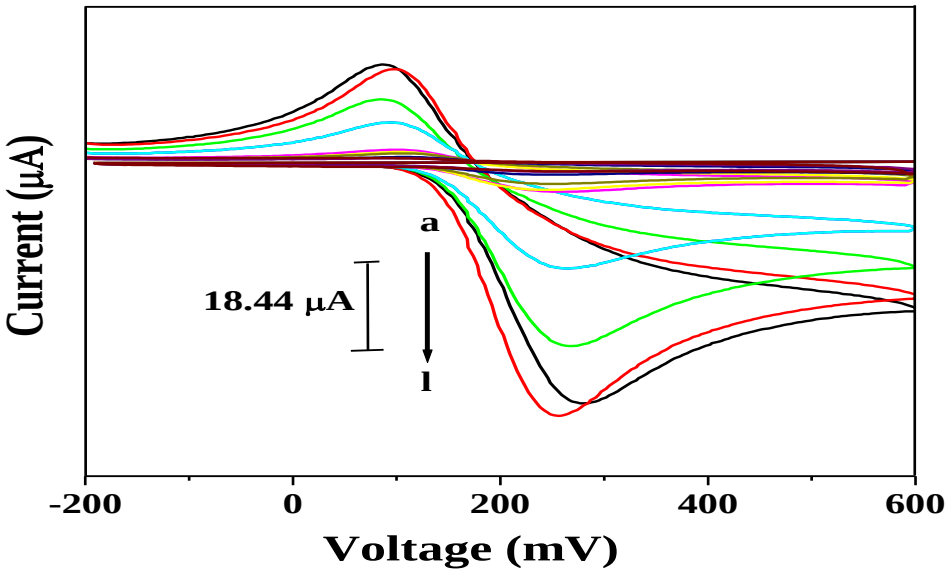

Fig. 5.11a: Effect of variation of concentration of DA (a) 1×10^{-5} M, (b) 2×10^{-5} M, (c) 4×10^{-5} M, (d) 6×10^{-5} M, (e) 8×10^{-5} M, (f) 1×10^{-4} M, (g) 2×10^{-4} M, (h) 4×10^{-4} M (j) 6×10^{-4} M (k) 8×10^{-4} M, (l) 1×10^{-4} M, on anodic peak current at $Ni_{0.02}Sn_{0.98}O_2$ nanoparticles modified carbon paste electrode; scan rate 50 mVs^{-1}.

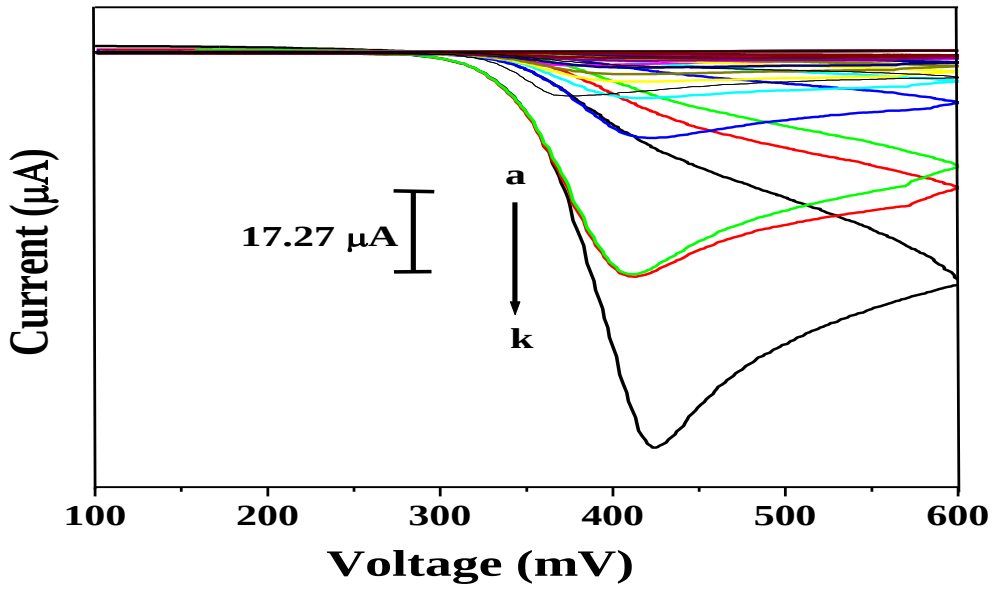

Fig. 5.11b: Effect of variation of concentration of UA (a) 1×10^{-5} M, (b) 2×10^{-5} M, (c) 4×10^{-5} M, (d) 6×10^{-5} M, (e) 8×10^{-5} M, (f) 1×10^{-4} M on anodic peak current at $Ni_{0.02}Sn_{0.98}O_2$ nanoparticles modified carbon paste electrode; scan rate 50 mVs^{-1}.

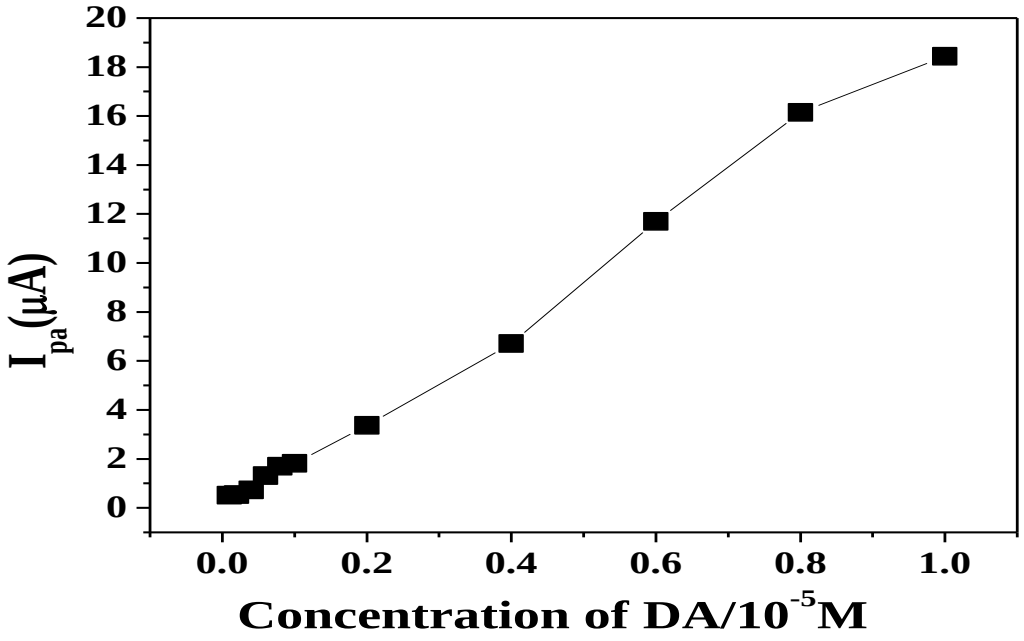

Fig.5.12a: Plot of anodic peak current vs. concentration of DA at $Ni_{0.02}Sn_{0.98}O_2$ nanoparticles modified carbon paste electrode.

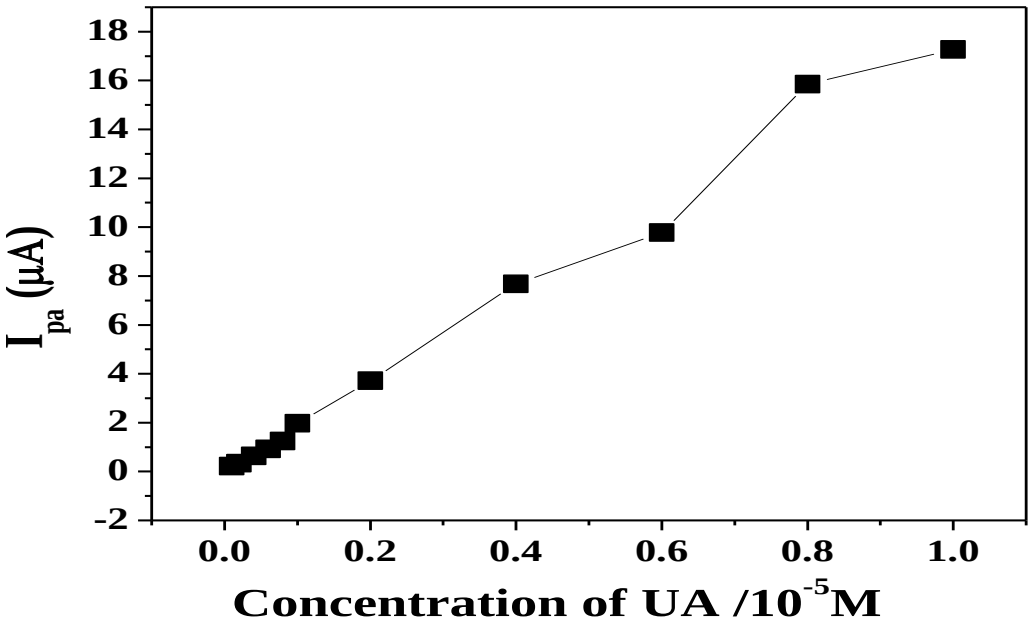

Fig. 5.12b: Plot of anodic peak current vs. concentration of UA at $Ni_{0.02}Sn_{0.98}O_2$ nanoparticles modified carbon paste electrode.

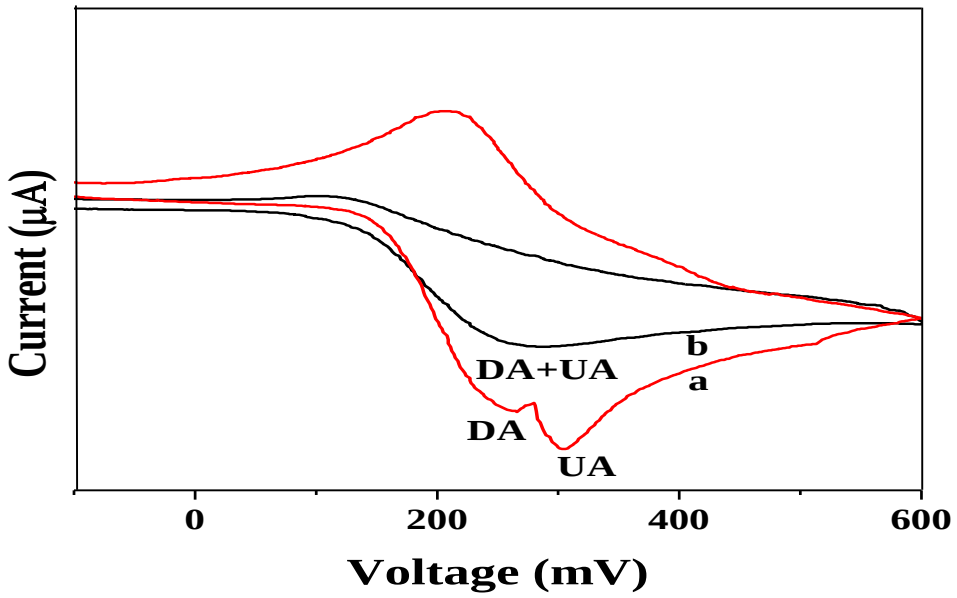

Fig. 5.13: Cyclic voltammograms at $Ni_{0.02}Sn_{0.98}O_2$ nanoparticles modified carbon paste electrode (a) and (b) bare CPE in presence of 0.5 mM DA and 0.2 mM UA in 0.2 M PBS (pH 7.0); scan rate 50 mVs^{-1}.

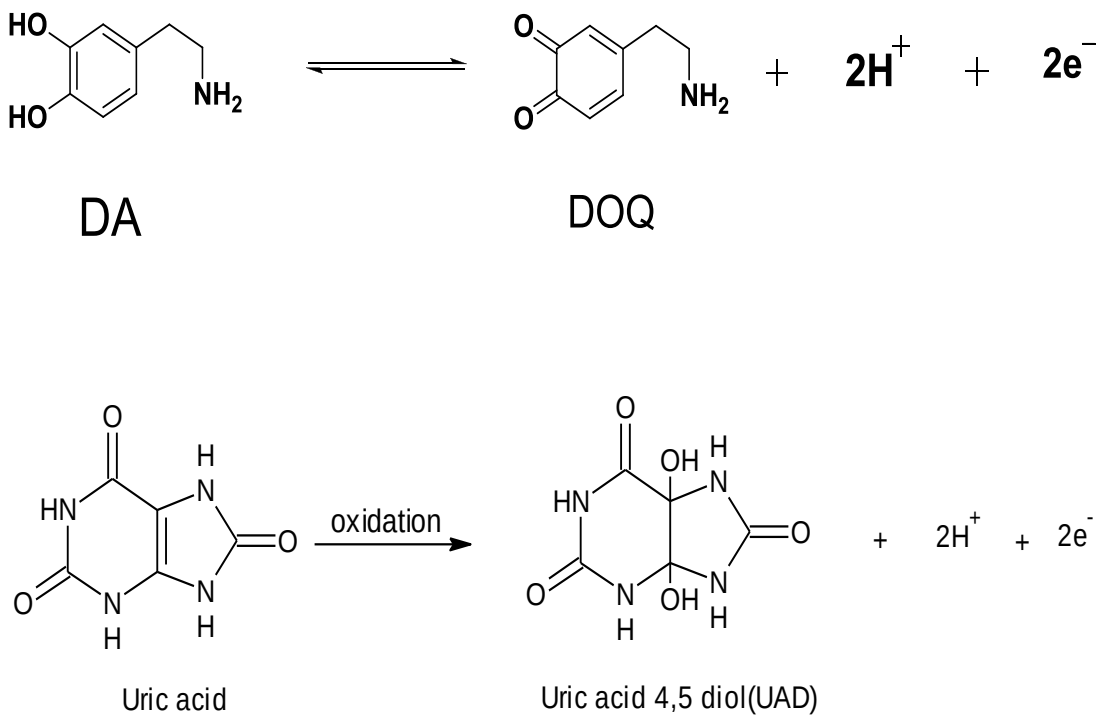

Scheme 5.1: Oxidation of DA and UA.

5.9. Reference

[1] Grace and B. Bunney, Dopamine. In *Neurotransmitter Actions in the Vertebrate Nervous System*; (Rogawski, M.; Barker, J., Eds.; Plenum Press: New York), 1985, p 285.

[2] N. Sharma, and E. Richman, *Parkinson's disease and the family: A new Guide*. (Harvard University Press), 2005.

[3] A.K. Tausche, S. Unger, K. Richter, *Der Internist.,* **47** (2006) 509.

[4] Y.C. Luo, J.S. Do, C.C. Liu, *Biosens. Bioelectron.,* **22 (**2006) 482.

[5] H. Manjunatha, D.H. Nagaraju, G.S. Suresh, T.V. Venkatesha, *Electroanalysis*, **21** (2009) 2198.

[6] S. Behera, C.R. Raj, *Biosens. Bioelectron.,* **23** (2007) 556.

[7] P. Ramesh, S. Sampath, *Electroanalysis,* **16** (2004) 866.

[8] G.G. Guilbault, *Analytical Uses of Immobilized Enzymes*, Marcel Dekker, New York, 1984.

[9] Knut Schmidt-Nielsen, *Animal physiology adaptation and environment*, Fourth edition, Cambridge University press, 1995.

[10] A.A. Ensafi, A. Arabzadeh, H. Karimi maleh, *Anal. Lett.,* **43** (2010) 1976.

[11] C.Y. Liu, L.Z. Yang, F. Song, L.Y. Jiang and G.H. Lu, *Chinese Chemical Letters*, **16** (2005) 237.

[12] D. Didem, H. Erdogan, O.S. Ali, U. Zafer, *Current Analytical Chemistry*, **6** (2010) 203.

[13] Chandrashekar C Vishwanatha, Bahaddurghatta E Kumaraswamy, K Vasantakumar Pai, *J Anal Bioanal Tech.,* **6** (2015) 5.

[14] S. Shahrokhian, H.R.Z. Mehrjardi, *Sens. Actuators B.,* **121** (2007) 530.

[15] J. Arguello, V.L. Leidens, H.A. Magosso, R.R. Ramos and Y. Gushikem, *Electrochim. Acta*, **54** (2008) 560.

[16] H. Beitollahi, M.M. Ardakani, H. Naeimi and B. Ganjipour, *J. Solid State Electrochem.*, **13** (2009) 353.

[17] L.M. Fang, X.T. Zu, Z.J. Li, S. Zhuc, C.M. Liu, W.L. Zhou and L.M. Wang, *J Alloys Compd.*, **454** (2008) 261.

[18] J. Zhang, L. Gao, *J Solid State Chem.*, **177** (2004) 1425.

[19] T. Dietl, H. Ohno, F. Matsukura, J. Cibert and D. Ferrand, *Science*, **287** (2000) 1019.

[20] H. Katayama-Yoshida, K. Sato, *J. Phys. Chem.Solids.*, **64** (2003) 1447.

[21] A.C. Bose, D. Kalpana, P. Thangadurai and S. Ramasamy, *J. Power Sources*, **107** (2002) 138.

[22] N. Segent, P. Gelin, L. Perrier, H. Praliaud and G.Thomas, *Sens. Actuators* B., **84** (2002) 176.

[23] L. Broussous, C.V. Santilli, S.H. Pulcinelli and A.F. Craievich, *J. Phys. Chem.* B., **106** (2002) 2885.

[24] Z.X. Deng, C. Wang, Y.D. Li, *J. Am. Ceram. Soc*., **85** (2002) 2837.

[25] E.R. Leite, A.P. Maciel, I.T. Weber, P.N.L. Filho, E. Longo, C.O.P. Santos, C.A. Paskocimas, Y. Maniette and W.H. Schreiner, *Adv.Mater*., **14** (2002) 905.

[26] M.P. Rajeeva, C.S. Naveen, Ashok R. Lamani and H.S. Jayanna, *AIP Conf.Proc*., **183** (2013) 1536.

[27] L. Patterson, *Phys. Rev. Online Arch. (Prola).*, **56** (1939) 978.

[28] Q.G. Von Nehring, J.W. Hightower, J.L. Anderson, *Anal. Chem.*, **58** (1986) 2777.

[29] M.P. Siswana, K.I. Ozoemena, T. Nyokong, *Electrochim. Acta*, **52** (2006) 114.

[30] E. J. Laviron's, *Electroanal. Chem*., **52** (1974) 355.

Chapter-6

Electrochemical Behavior of $Mn_{0.02}Sn_{0.980}O_2$ Nanoparticles Modified Carbon Paste Electrode and Its Application for the Determination of Dopamine, Uric acid and Ascorbic acid

Dopamine

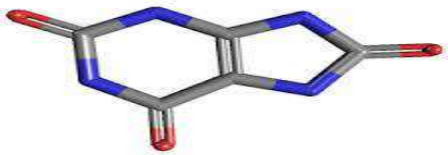

Uric acid

Ascorbic acid

6.1. Introduction

This chapter involves the synthesis of $Mn_{0.02}Sn_{0.98}O_2$ nanoparticles by gel combustion method. The synthesized $Mn_{0.02}Sn_{0.980}O_2$ nanoparticles were characterized by XRD and SEM. $Mn_{0.02}Sn_{0.980}O_2$ nanoparticles modified carbon paste electrode (MSNMCPE) was developed by known procedure. The surface morphology of MSNMCPE was confirmed by SEM. The determination of dopamine (DA), uric acid (UA) and ascorbic acid (AA) has been studied at MSNMCPE by cyclic voltammetric technique in 0.1 M phosphate buffer solution of pH 7.0, pH 6.5 and pH 5.5 respectively. The discussion involves the chemistry, biological relevance of DA, UA, AA and their redox behavior at bare carbon paste electrode (BCPE) and MSNMCPE. The effect of pH, concentration, and scan rate were studied. The MSNMCPE showed very good sensitivity for DA, UA and AA compare to bare CPE. The results suggest that the nature of electrode reaction was diffusion controlled at both bare CPE and MSNMCPE. The low detection limit (LOD) and low quantification limit (LOQ) of DA, UA, AA were detected. The simultaneous determination of dopamine, uric acid and ascorbic acid, uric acid were carried out by both cyclic voltammetric and differential pulse voltammetric techniques. The preparation of the modified electrode was easy, renewed by simple polishing gives very good reproducibility, high stability in its voltammetric response and low detection limit for DA, UA and AA.

6.2. Chemistry and Biological Relevance of Dopamine and Uric acid

The chemistry and biological relevance of dopamine has been explained in details in chapter 5 section 5.2. In this chapter the chemistry of uric acid and its biological relevance has been explained. Uric acid (UA) (2, 6, 8-trihydroxypurine) is the primary product of purine metabolism in the human body. It is a diprotic acid with pKa_1=5.4 and pKa_2=10.3 [1]. Thus in strong alkali at high pH it forms the dually charged full urate ion, but at biological pH it forms the singly charged hydrogen or acid urate ion as its pKa_2 is greater than the pKa_1 of carbonic acid. As its second ionization is so weak the

full urate salts tend to hydrolyse back to hydrogen urate salts and free base at pH values around neutral. It is aromatic because of the purine functional group.

As a bicyclic, heterocyclic purine derivative, uric acid does not protonate in the same manner as do carboxylic acids. Whereas most organic acids are deprotonated by the ionization of polar hydrogen-to-oxygen bond, usually accompanied by some form of resonance stabilization, this acid is deprotonated at a nitrogen atom and uses a tautomeric keto/hydroxy group as an electron-withdrawing group to increase the pKa_1 value. The five membered ring also possesses a keto group (in the 8 position), flanked by two secondary amino groups (in the 7 and 9 positions), and deprotonation of one of these at high pH could explain the pKa_2 and behavior as a diprotic acid [2].

6.2.1. Biological Relevance of Uric acid

UA is an important analyte in clinical field. In a healthy human being, the typical concentration of UA in urine is in millimolar range ($\sim$2 mM), whereas in blood it is in the micro-molar range (120–450 μM) [3, 4]. Abnormalities of UA level indicate symptoms of several diseases, such as gout, hyperuricaemia and Leseh-Nyhan syndrome [5]. UA is the primary end product of purine metabolism. Its abnormal concentration levels will lead to several diseases such as hyperuricaemia and gout. Other diseases such as leukemia and pneumonia are also associated with enhanced urate levels [6]. Uric acid is an important evolutionary significant biomolecule and it plays a vital role in adaptation of animals to completely dry terrestrial habitat. Animals like reptiles and birds are successfully adopted by conserving water by excreting its nitrogenous metabolic waste products in the form of UA [7].

6.3. Chemistry of Ascorbic acid.

Ascorbic acid (AA) is a naturally occurring organic compound with antioxidant properties. It is a white solid, but impure samples can appear yellowish. It dissolves well in water to give mildly acidic solutions. Ascorbic acid is one form ("vitamer") of vitamin C. It was originally called L-hexuronic acid, but, when it was found to have

vitamin C activity in animals ("vitamin C" being defined as a vitamin activity, not then a specific substance), the suggestion was made to rename it. The new name, ascorbic acid, is derived from *a*-(meaning "no") and *scorbutus* (scurvy), the disease caused by a deficiency of vitamin C. Because it is derived from glucose, many non-human animals are able to produce it, but humans require it as part of their nutrition. Other vertebrates which lack the ability to produce ascorbic acid include some primates, guinea pigs, teleost fishes, bats, and some birds, all of which require it as a dietary micronutrient (that is, in vitamin form) [8].

Ascorbic acid (AA) is partially ionized at physiological pH, contains two acid-ionized groups (pK_a 4.04 and 11.34). Though stable to air and light when dry, in aqueous solution it is powerful reducing agent, with redox potential of about 0.05 V at 30^{o}C and pH 7.4. It readily undergoes reversible oxidation to dehydroascorbic acid.

6.3.1. Biological Relevance of Ascorbic acid

Ascorbic acid or vitamin C is a common enzymatic cofactor in mammals used in the synthesis of collagen. Ascorbate is a powerful reducing agent capable of rapidly scavenging a number of reactive oxygen species (ROS). Freshwater teleost fishes also require dietary vitamin C in their diet or they will get scurvy. The most widely recognized symptoms of vitamin C deficiency in fishes are scoliosis, lordosis and dark skin coloration. Freshwater salmonids also show impaired collagen formation, internal/fin hemorrhage, spinal curvature and increased mortality. If these fishes are housed in seawater with algae and phytoplankton, then vitamin supplementation seems to be less important, it is presumed because of the availability of other, more ancient, antioxidants in natural marine environment [9]. The hydroxylation of proline and lysine in procollagen is carried out by the enzyme prolyl hydroxylase using ascorbic acid as a cofactor. The natural form of the vitamin is the L-isomer. Ascorbic acid plays an important role as a component of enzymes involved in the synthesis of collagen and carnitine; however, its most vital role is as a water-soluble vitamin in the human body [10, 11]. Ascorbic acid is a powerful antioxidant because it can donate a hydrogen atom and form a relatively stable ascorbyl free radical. As a scavenger of reactive oxygen and

nitrogen oxide species, ascorbic acid has been shown to be effective against the superoxide radical ion, hydrogen peroxide, the hydroxyl radical and singlet oxygen [12]. Ascorbic acid protects folic acid reductase, which converts folic acid to folinic acid, and may help release free folic acid from its conjugates in food. Ascorbic acid facilitates the absorption of iron. It helps maintain elasticity of the skin aids the absorption of iron and improves resistance to infection, treatment of scurvy and may prevent the occurrence and development of cancer.

6.4. Review of Cyclic Voltammetry of Dopamine, Uric acid and Ascorbic acid

In recent years the designing, fabrication and application of novel electrochemical sensor has been of considerable interest [13]. Particularly the development of voltammetric sensors for the determination of secretion neurotransmitters, such as dopamine (DA) and other catechol amines, has received a lot of interest. Dopamine (DA) is one of the excitatory neurotransmitters that play an important role in several physiological events. It is involved in the functioning of renal, cardiovascular, hormonal and nervous systems. DA is also involved in neurological diseases such as Parkinson's [14], Alzheimer's disease [15] and Schizophrenia [16]. It has been also suggested that DA plays a role in drug addiction [17 - 20] and some manifestation of HIV [21, 22]. A major problem in DA determination is the resolution between DA and coexisting species such as uric acid (UA) and ascorbic acid (AA). UA is a primary product of purine metabolism in the human body [23]. Its abnormal concentration level causes many diseases, such as gout, hyperuricaemia and Lesch-Nyan disease [24]. Therefore, the research of UA determination is of great importance in reality [25]. AA is a water soluble vitamin, and is a compound that takes part in many important life processes. It is one of the most important vitamins, due to its antioxidant and pH regulator properties often being added to various food products and pharmaceuticals [26]. UA and AA are both present in biological fluids such as blood and urine [27].

As reported, the concentration of AA is generally much higher than that of DA (100 to 1000 times) [28]. At traditional electrodes, UA and AA are oxidized at potentials close to that of DA, resulting in an overlapping voltammetric response [29 - 31]. Moreover, the unmodified electrodes very often suffer from the fouling effect due to the accumulation of oxidized products on the electrode surface, which results in rather poor selectivity and sensitivity in addition, oxidation of DA at the electrode surface in the presence of AA results in a homogeneous catalytic oxidation of AA. The regenerated DA returns to the electrode, resulting in an enhanced current [32]. Therefore, improvement of the selectivity of DA monitoring techniques has been the focus of much research, and simultaneous detection of neurotransmitters and coexisting species, especially AA and UA, is a problem of critical importance not only in the field of biomedical chemistry and neurochemistry but also in diagnostic and pathological research.

Recent reports using polymer films [33 - 40] have received extensive interest due to wide application in the fields of chemical sensors and biosensors [43 - 44]. In addition there were reports of using CTAB [45], luminol and 3, 4-ethylenedioxythiophene monomers [46], (3-(5-chloro-2-hydroxyphenylazo)-4, 5-dihydroxynaphthalene-2, 7-disulfonic acid) [47], tetrabromo-p-benzoquinone [48], Lignin [49], carbon nanotubes-ionic liquid gel [50], Evans Blue [51], carbon ionic liquid [52], acid chrome blue K [53], palladium nanoparticle-loaded carbon [54].

Nano sized material such as gold, metal oxide nanoparticles and carbon nanotubes have been received a lot of attention in electrochemical studies and widely used in preparation of modified electrodes for the application as biosensors because their large surface area high thermal and chemical stability, tunable porosity and excellent biocompatibility [55 - 60].

In this work carbon paste electrode is modified with $Mn_{0.02}Sn_{0.98}O_2$ nanoparticles and applied for the electrochemical investigation for dopamine, uric acid, Ascorbic acid.

6.5. Experimental Section

6.5.1. Reagent and Chemicals

Tin (II) chloride dehydrate ($SnCl_2.H_2O$, 99.99 %, Merck), Nitric acid (HNO_3, 70 %, Merck), Citric acid ($C_6H_8O_7$, 99.5%, Merck), Manganese Chloride Hexahydrate ($MgCl_2.6H_2O$), Potassium ferrocyanide $K_4[Fe(CN)_6]$, UA and AA solutions were prepared by dissolving in double distilled water. DA was prepared by dissolving in 0.1 M per chloric acid ($HClO_4$) solution, 0.1 M potassium chloride (KCl) was used as supporting electrolyte for all analytes. Chemicals mentioned above were all purchased from Fluka and were analytical grade.

6.5.2. Apparatus and Procedure

The electrochemical experiments were carried out using an Electroanalyser model EA-201 chemlink system. All experiments were carried out in a conventional three-electrode system. The electrode system contained a carbon paste electrode as working electrode, a platinum wire as counter electrode and saturated calomel electrode as reference electrode.$Mn_{0.02}Sn_{0.98}O_2$ nanoparticles modified carbon paste electrode was prepared by grinding the 10 mg of $Mn_{0.02}Sn_{0.98}O_2$ nanoparticles with 70% graphite powder (50 µm particle size was purchased from sdfine - chem Ltd) and 30% silicon oil (Himedia) in an agate mortar by hand mixing for about 30 minute to get homogenous $Mn_{0.02}Sn_{0.98}O_2$ nanoparticles modified carbon paste electrode. The paste was packed into the cavity of CPE and smoothened on weighing paper. The bare CPE was prepared without adding modifier.

6.5.3. Synthesis of $Mn_{0.02}Sn_{0.98}O_2$ nanoparticles

$Mn_{0.02}Sn_{0.98}O_2$ nanoparticles were synthesized by gel combustion method. The materials used are tin (II) chloride dehydrate, 6.2 mole of nitric acid which is used as an oxidizer and mixed in an appropriate ratio to form a tin nitrate solution, then 1.5 mole of citric acid which acts as fuel and 0.02 ml Manganese chloride Hexahydrate ($MgCl_2.6H_2O$) was added to solution and solution was heated at 90°C in a pyrex vessel

with constant stirring. When the temperature was raised to about 300°C, the polymeric precursor underwent a strong, self-sustaining combustion reaction occurs with evolution of large volume of gases and swelled into voluminous and foamy ashes. The entire combustion process occurs in a few seconds. The produced ashes were then calcined at 800°C (for 1 hour). The process was carried out, until the complete decomposition of the carbonaceous residues. Then the white powder $Mn_{0.02}Sn_{0.98}O_2$ nanoparticles was obtained [61].

6.6. Results And Discussion

6.6.1. Characterization of synthesized $Mn_{0.02}Sn_{0.98}O_2$ nanoparticles by XRD and SEM

Crystalline structure and crystallite size of $Mn_{0.02}Sn_{0.98}O_2$ nanoparticles were analyzed by Cu-K_α X-ray radiation (λ=1.5418A˚) in 2θ range from 20º to 80° operating at 30 kV and 15 mA. The scan rate was 5°/min.). XRD patterns of $Mn_{0.02}Sn_{0.98}O_2$ nanoparticles annealed at 800°C for 1hr as shown in **Fig. 6.1**, the average grain size was calculated using the Scherrer relation,

$$d = 0.89\frac{\lambda}{\beta\cos\theta} \quad \ldots\ldots\ldots\ldots\ldots\ldots\ldots\ldots\ldots\ldots\ldots\ldots\ldots\ldots \quad (6.1)$$

Where d is the crystallite size, λ is the wavelength of X-rays, β is the full width of half maximum and 2θ is the diffraction peak angle [62],

The crystallite sizes of $Mn_{0.02}Sn_{0.98}O_2$ nanoparticles are found to be 23.03 nm by using Scherrer formula. The surface morphology and shape of the nanoparticles of powdered samples were investigated by scanning electron microscope (SEM) (Hitachi Model S-3200N). **Fig.6.2** shows the typical SEM image of the $Mn_{0.02}Sn_{0.98}O_2$ nanoparticles.

6.6.2. SEM Characterization of $Mn_{0.02}Sn_{0.98}O_2$ nanoparticles modified carbon paste electrode(MSNMCPE)

The morphology of the CPE and MSNMCPE was characterized by scanning electron microscope (SEM) and shown in **Fig.6.3a** and **6.3b** respectively. Smooth surface was observed on bare CPE surface. In the modified electrode the formation of spindle-like nanostructures not only enlarges the surface area of the electrode, but also improves the electron transfer rate between the electrode surface and the bulk solution, which has been confirmed by the performance of MSNMCPE in electrochemical investigation of $K_4[Fe(CN)_6]$ system.

6.6.3. Electrochemical response of $K_4[Fe(CN)_6]$ at $Mn_{0.02}Sn_{0.98}O_2$ nanoparticles modified carbon paste electrode

Fig. 6.4 shows the electrochemical behavior of 1mM potassium ferrocyanide ($K_4[Fe(CN)_6]$) in 1M KCl at bare carbon paste electrode (BCPE) curve 'b' and at $Mn_{0.02}Sn_{0.98}O_2$ nanoparticles modified carbon paste electrode (MSNMCPE) curve 'a' respectively. The curve 'b' shows the cathodic peak current I_{pc} 5.56 µA of E_{pc} 240 mV and anodic peak current I_{pa} 6.24 µA of E_{pa} 403 mV at BCPE. Whereas, for the MSNMCPE the cathodic peak current I_{pc} 12.61 µA of E_{pc} 253 mV and anodic peak current I_{pa} 18.61 µA of E_{pa} 334 mV has been observed. The enhancement of peak current showed excellent catalytic ability of MSNMCPE. The surface area of bare CPE is 0.027 cm^2, whereas effective surface area of the modified electrode was found to be 0.036 cm^2.

6.6.4. Electrochemical behavior of dopamine (DA) at $Mn_{0.02}Sn_{0.98}O_2$ nanoparticles modified carbon paste electrode (MSNMCPE)

The electrochemical behavior of 0.1 mM dopamine in 0.1 M phosphate buffer solution of pH 7 has been studied at MSNMCPE using cyclic voltammetric technique. The **Fig.6.5** shows the cyclic voltammograms of 0.1 mM DA at bare CPE (curve 'b') and at MSNMCPE (curve 'a'). The curve 'c' represents the cyclic voltammogram of

blank solution at MSNMCPE. Which confirms the modification of bare CPE. Above studies showed that redox behavior of DA. The peak potentials E_{pa} and E_{pc} were found to be 272 and 80 mV with peak current I_{pa} and I_{pc} of 2.05 µA and 0.9 µA respectively at bare CPE, whereas peak potentials E_{pa} and E_{pc} were found to be 257 mV and at 101 mV with peak currents I_{pa} 5.63 µA and I_{pc} 2.27 µA at respectively at MSNMCPE in the potential range from -200 to 600 mV. The peak was observed in the reverse scan, suggesting that the electrochemical reaction is a totally quasireversible process and the redox peak at the bare CPE is broad due to slow electron transfer, while the response was considerably improved at MSNMCPE and the peaks potentials shifted to negative direction, the shape of the peaks turns sharper and the peak current increased significantly.

6.6.5. Electrochemical behavior of uric acid (UA) at $Mn_{0.02}Sn_{0.98}O_2$ nanoparticles modified carbon paste electrode

The electrochemical behavior of UA was investigated in 0.1 M phosphate buffer solution of pH 6.5 at MSNMCPE using cyclic voltammetric technique. **Fig. 6.6** shows cyclic voltammograms of 0.1 mM UA at bare carbon paste electrode (BCPE) (curve 'b') and at MSNMCPE (curve 'a'). The curve 'c' represents the cyclic voltammogram of blank solution at MSNMCPE, which confirms the modification of bare CPE. Above studies showed that only one oxidation peak at 442 mV with peak current of 1.12 µA at bare CPE, whereas an oxidation peak at 384 mV with peak current of 4.69 µA at MSNMCPE in the potential range from 100 to 600 mV. No reduction peak was observed in the reverse scan suggesting that the electrochemical reaction is a totally irreversible process and the oxidation peak at the MSNMCPE is broad due to slow electron transfer, while the response was considerably improved at modified electrode and the peak potentials shifted to negative direction, the shape of the peak turns sharper and the peak current increased significantly.

6.6.6. Electrochemical behavior of ascorbic acid (AA) at $Mn_{0.02}Sn_{0.98}O_2$ nanoparticles modified carbon paste electrode

The Ascorbic acid (AA) was investigated in 0.1 M phosphate buffer solution of pH 5.5 at MSNMCPE using cyclic voltammetric technique. **Fig. 6.7** shows cyclic voltammograms of 0.1 mM AA at bare CPE (curve 'b') and at MSNMCPE (curve 'a') also at MSNMCPE in blank solution (curve 'c'), which shows the conformation of modification of bare CPE. Above studies showed that only one oxidation peak potential at 412 mV with peak current of 5.12 µA at bare CPE, whereas an oxidation peak potential at 334 mV with peak current of 28.55 µA at MSNMCPE in the potential range from -200 to 600 mV. No reduction peak was observed in the reverse scan, suggesting that the electrochemical reaction is a totally irreversible process and the oxidation peak current at MSNMCPE.

6.6.7. Effect of pH on DA, UA and AA

The electro oxidation of DA was studied at 0.1 mM stock solution over pH range from 4 to 9 using 0.1 M phosphate buffer solution (PBS) at a scan rate 50 mVs^{-1} at MSNMCPE by cyclic voltammetric technique. The oxidation peak current increases with increase of pH from 4 to 7 and becomes maximum and peak potential shifted negatively. While pH beyond 7, a great decrease of the anodic peak current could be observed, then it decreased gradually with the further increase in pH of the solution is shown in **Fig. 6.7a** and the anodic peak potential decreases with increase in pH of the solution shown in **Fig. 6.7b** .The corresponding linear regression equation is

$$E_{pa}\ (mV) = 829.436 - 74.836pH \quad (R = 0.99687) \ldots\ldots\ldots\ldots\ldots\ldots \quad (6.2)$$

The value of this slope is in close agreement with the theoretical value of 59 mV/pH at 25^0 for a $2e^-$ transfer process. Other researchers also have reported $2e^-$ transfer oxidation process in DA [63, 64].

The effect of pH on UA has been studied by using the 0.1 mM stock solution of UA in 0.1 M PBS in the pH range from 2.5 to 9 at a scan rate of 50 mVs^{-1} at

MSNMCPE using cyclic voltammetric technique. The anodic peak current decreases with increase of pH from 2.5 to 6.5 and becomes maximum and peak potential shifted negatively at pH 6.5. While pH beyond 6.5, a great decrease of the oxidation peak current could be observed, then it decreased gradually with the further increase in the pH of solution is shown in **Fig.6.8a** and the oxidation peak potential decrease with increase in the pH as shown in **Fig.6.8b**.The corresponding linear regression equation is

$$E_{pa}\,(mV) = 670.47 - 38.052\ pH \quad R = 0.9582 \ldots\ldots\ldots\ldots\ldots\ldots \quad (6.3)$$

The negative slope of 38.640 was close to the theoretical value indicated that the electrons and protons involved in the oxidation of UA were equal (1:1).

Similarly, the effect of pH on electro oxidation of AA of 0.1 mM stock solution in 0.1 M PBS in pH range from 3 to 9 at a scan rate 50 mVs^{-1} at MSNMCPE using cyclic voltammetric technique has been studied. The anodic peak current decreases with increase of pH from 3 to 5.5 and becomes maximum and peak potential shifted negatively at pH 5.5. While pH beyond 5.5, a great decrease of the oxidation peak current could be observed, then it decreased gradually with the further increasing the pH of solution is shown in **Fig. 6.9a** and the oxidation peak potential decrease with increase in the pH is shown in **Fig. 6.9b** the relationship between the anodic peak potential and pH is explained with the following equation.

$$E_{pa}\,(mV) = 521.10 - 31.04\ pH \quad R = 0.9050 \ldots\ldots\ldots\ldots\ldots\ldots \quad (6.4)$$

The negative slope of 31.04 was close to the theoretical value indicated that the electrons and protons involved in the oxidation of AA.

6.6.8. Effect of scan rate on DA, UA and AA

The effect of scan rates on the electrochemical response of 0.1 mM DA in 0.1 M PBS at MSNMCPE was studied at different scan rates including 25, 50, 75, 100, 125, 150, 175, 200 mVs^{-1} by CV and the cyclic voltammograms were shown in **Fig. 6.10a**. The **Fig. 6.10b** shows the linear relationship between the peak current and square root

of scan rate with a correlation coefficient of 0.9977 obtained between the anodic peak current and square root of scan rate in the range of 25 – 200 mVs^{-1}. The corresponding linear regression equation is

$$I_{pa}\,(\mu A) = 0.7624\ \nu^{1/2} + 1.8863 \quad R = 0.9862 \ldots\ldots (6.5)$$

Which revealed that a diffusion controlled process occurring at MSNMCPE. However linearity was also obtained for the plot of anodic peak current vs. the scan rate with a correlation coefficient of 0.9903 shown in **Fig. 6.10c** and the corresponding linear regression equation is given by

$$I_{pa}\,(\mu A) = 0.03952\ \nu + 5.2103 \quad R = 0.99692 \ldots\ldots (6.6)$$

The results suggest that the nature of electrode reaction is diffusion controlled and as a result the peak potential shifts towards positive side. The relationship between the anodic peak potential and scan rate is explained by plotting of the anodic peak potential vs. natural logarithm scan rate **(Fig. 6.10d)** by considering the relation:

$$E_{pa}\,(mV) = 0.02830\ \ln\upsilon + 0.1132 \quad R = 0.9978 \ldots\ldots (6.7)$$

In addition, there was a linear relation between $\log I_{pa}$ and $\log\nu$ (**Fig. 6.10e**) is corresponding to the following equation.

$$\log I_{pa}\,(\mu A) = 0.3649\ \log\nu + 0.256 \quad (R = 0.9838) \ldots\ldots (6.8)$$

The slope for the equation is 0.364, which is close to the theoretical value of 0.5 for a diffusion controlled process between scan rates 25 – 200 mVs^{-1}.

To study the effect of scan rate on UA, 0.1 mM UA in 0.1 M PBS was studied for different scan rates from 10 to 150 mVs^{-1} at MSNMCPE by CV and the cyclic voltammograms were shown in **Fig. 6.11a**. The **Fig. 6.11b** shows linear relationship between peak current and square root of scan rate with a correlation coefficient of 0.9959 obtained between anodic peak current and square root of scan rate in the range of 10 – 150 mVs^{-1}.The corresponding linear regression equation is

$$I_{pa}\,(\mu A) = 0.9864\ \nu^{1/2} + 0.7314 \quad R = 0.9960 \ldots\ldots\ldots\ldots\ldots\ldots\ldots\ldots \quad (6.9)$$

Which revealed that a diffusion controlled process occurring at MSNMCPE. The linearity was also obtained for the plot of anodic peak current of vs. scan rate with a correlation coefficient of 0.9953 shown in **Fig. 6.11c**. The relationship between the anodic peak potential and scan rate is explained by plotting of the anodic peak potentials vs. natural logarithm of scan rate **(Fig. 6.11d)** by considering the relation:

$$E_{pa}\,(mV) = 0.0166\ \ln\upsilon + 0.3360, \quad R = 0.9915 \ldots\ldots\ldots\ldots\ldots\ldots \quad (6.10)$$

The linear relation between $\log I_{pa}$ and $\log\nu$ (**Fig.6.11e**) is corresponding to the following equation

$$\log I_{pa}\,(\mu A) = 0.425\ \log\nu - 0.1713 \quad (R = 0.9919) \ldots\ldots\ldots\ldots\ldots\ldots \quad (6.11)$$

The slope for the equation is 0.425, which is close to the theoretical value of 0.5 for a diffusion controlled process between scan rates 10 - 150 mVs^{-1}.

Similarly, the effect of scan rate on 0.1 mM AA for different scan rates 10, 20, 30, 40, 50, 60 70, 80, 90 and 100 mVs^{-1} at MSNMCPE has been studied by CV and the corresponding cyclic voltammograms were shown in **Fig. 6.12a**. The **Fig. 6.12b** shows the linear relationship between the peak current and square root of scan rate with a correlation coefficient of 0.9959 obtained between the anodic peak current and square root of scan rate in the range of 10 – 100 mVs^{-1} .The corresponding linear regression equation is

$$I_{pa}\,(\mu A) = 0.9864\ \nu^{1/2} + 0.7314 \quad R = 0.99608 \ldots\ldots\ldots\ldots\ldots\ldots \quad (6.12)$$

Which revealed that a diffusion controlled process occurring at the MSNMCPE. The linearity was also obtained for the plot of scan rate vs. the anodic peak current with a correlation coefficient of 0.9953 shown in **Fig. 6.12c**. The relationship between the anodic peak potential and scan rate is explained by plotting of anodic peak potentials vs. natural logarithm of scan rate **(Fig. 6.12d)** by considering the relation:

$$E_{pa}\,(mV) = 0.0166\ \ln\upsilon + 0.3360 \quad R = 0.9915 \ldots\ldots\ldots\ldots\ldots\ldots\ldots\ldots \quad (6.13)$$

The linear relation between $\log I_{pa}$ and $\log\nu$ (**Fig. 6.12e**) is corresponding to the following equation

$$\log I_{pa} = 0.425\ \log\nu - 0.1713 \quad R = 0.9919 \ldots\ldots\ldots\ldots\ldots\ldots\ldots\ldots \quad (6.14)$$

The slope for the equation is 0.425, which is close to the theoretical value of 0.5 for a diffusion controlled process between scan rates 10 - 100 mVs^{-1}.

According to Laviron's theory [65], the slope is equal to $RT/\alpha n_{\alpha}F$. Then the value of αn_{α} was found to 0.4542. As for a totally quasi-reversible electrode reaction process of dopamine and irreversible electrode reaction process of uric acid and ascorbic acid. The n_{α} was calculated as 1.73, 2.4708 and 1.709 respectively, which indicated that two electrons were involved in the oxidation process of dopamine, uric acid and ascorbic acid at MSNMCPE. Since the equal number of electron and proton took part in the oxidation of dopamine, uric acid and ascorbic acid therefore two electrons and two protons transfer were involved in the electrode reaction process. The electrochemical reaction process for dopamine, uric acid and ascorbic acid at MSNMCPE is summarized in **scheme 6.1**.

6.6.9. Calibration of Dopamine, Uric acid and Ascorbic acid concentration:

A series of dopamine, uric acid and ascorbic acid solutions of range 1.0×10^{-5} to 1.0×10^{-3} M were prepared in PBS to investigate the relationship between the anodic peak current (I_{pa}) and concentration of dopamine, uric acid, ascorbic acid at $Mn_{0.02}Sn_{0.98}O_2$ nanoparticles modified carbon paste electrode at a scan rate of 25, 10 and 10 mVs^{-1} by cyclic voltammetry. The obtained cyclic voltammograms of DA, UA and AA were shown in **Fig. 6.13a, 6.13b and 6.13c** respectively. A linear relationship has obtained on plotting I_{pa} versus concentration of DA, UA and AA which is shown in **Fig. 6.14a, 6.14b and 6.14c** respectively, this is explained on the basis of linear regression equations for DA, UA and AA respectively were expressed as

I_{pa} (µA) = 32.341 C (10^{-5} M) + 2.0089 R= 0.993…….. (6.15)

I_{pa} (µA) = 38.505 C (10^{-5} M) + 0.5114 R= 0.9970……..... (6.16)

I_{pa} (µA) = 29.239 C (10^{-5} M) + 0.0497 R= 0.9970…… (6.17)

The limit of detection (LOD) and limit of quantification (LOQ) were 1.316 µM, 4.389 µM for DA, 0.848 µM, 2.82 µM for UA and 0.965 µM, 3.216 µM for AA.

The LOD and LOQ were calculated on the peak current using the following equation:

LOD= 3S/M, LOD=10S/M

Where, S is standard deviation and M is the slope of calibration plot.

6.6.10. Simultaneous determination of DA, UA and UA, AA at $Mn_{0.02}Sn_{0.98}O_2$ nanoparticles modified carbon paste electrode by cyclic voltammetry

Simultaneous determination of DA, UA and AA, UA in 0.1 M PBS of pH 7 and pH 5.5 carried at bare and MSNMCPE. The corresponding cyclic voltammograms are showed in **Fig.6.15a and Fig 6.15b** respectively. In the **Fig.6.15a** the curve 'b' exhibits one broad peak for the solution containing 0.5 mM DA and 0.2 mM UA mixture at bare CPE, which indicates that the bare CPE fails to separate the voltammetric signals of DA and UA. Whereas the curve 'a' exhibits two well defined oxidation peaks at potentials at 272 and 354 mV for 0.5 mM DA and 0.2 mM UA at modified carbon paste electrode indicating the efficiency of the modified electrode. Thus MSNMCPE can be effectively employed to separate DA and UA. Similarly in **Fig. 6.15b** the curve 'b' exhibits one broad peak for the solution containing 1 mM AA and 0.2 mM UA mixture at bare CPE. The curve 'a' exhibits two oxidation peaks at potentials 367 and 486 mV for AA and UA respectively at modified carbon paste electrode indicating the efficiency of modified electrode in separating the voltammetric signals AA and UA respectively. Thus MSNMCPE can be effectively employed to separate DA, UA and AA, UA.

6.6.11. Resolution of DA, UA and AA, UA by differential pulse voltammetry (DPV).

Differential pulse voltammetry (DPV) was used to investigate the possibility of MSNMCPE for the simultaneous determination of DA, UA and AA, UA. The modified electrode separates DA, UA and AA, UA mixture. As the concentration of mixture increases, current also increases which shown in **Fig. 6.16a & Fig. 6.16b.**

6.6.12. Simultaneous determination of DA, UA and AA by differential pulse voltammetry (DPV).

The simultaneous determination of DA, UA and AA at MSNMCPE was also examined by differential pulse voltammetry. **Fig.6.17** shows the differential pulse voltammograms of mixed solution of 0.5 mM DA, 0.2 mM UA and 1mM AA of pH 5.5. The curve exhibits three oxidation peaks at potentials 492, 524, 279 mV for AA, DA and UA respectively. This suggests that the MSNMCPE can be effectively employed to separate DA, UA and AA.

6.7. CONCLUSION

- In this work, $Mn_{0.02}Sn_{0.98}O_2$ nanoparticles modified CPE was fabricated and the characteristics of the electrode is studied.
- The present work has indicated that $Mn_{0.02}Sn_{0.98}O_2$ nanoparticles modified carbon paste electrode improved the electrochemical activities towards the oxidation of DA, UA and AA.
- Large peak separation allows the modified electrode for the simultaneous determination of DA, UA in the PBS of pH 7.0 and AA, UA in PBS of pH 5.5 by CV and DPV techniques.
- Linear calibration plots for the oxidation of DA, UA and AA were obtained in the range of 1×10^{-5} M to 1×10^{-3} M.

- The detection limits (LOD) of DA, UA and AA at $Mn_{0.02}Sn_{0.98}O_2$ nanoparticles modified carbon paste electrode were found to be 1.316, 0.848, 0.965 µM respectively.

- The proposed method has been practically and successfully applied for the simultaneous determination of DA, UA and AA.

- Due to its good stability and reproducibility the $Mn_{0.02}Sn_{0.98}O_2$ nanoparticles modified carbon paste electrode can be used for the simultaneous measurement of DA, UA and AA.

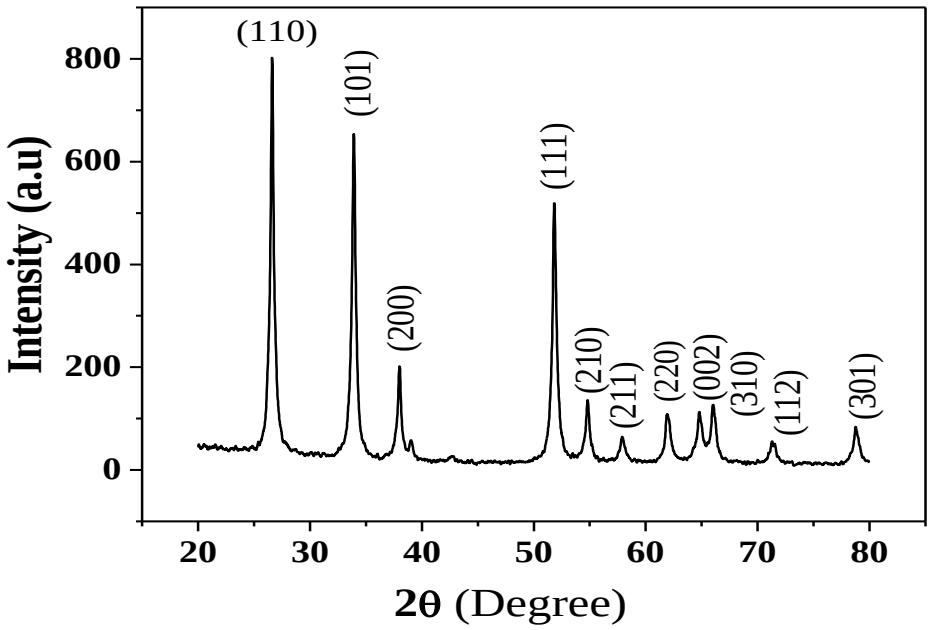

Fig. 6.1: XRD images of synthesized of $Mn_{0.02}Sn_{0.98}O_2$ nanoparticles.

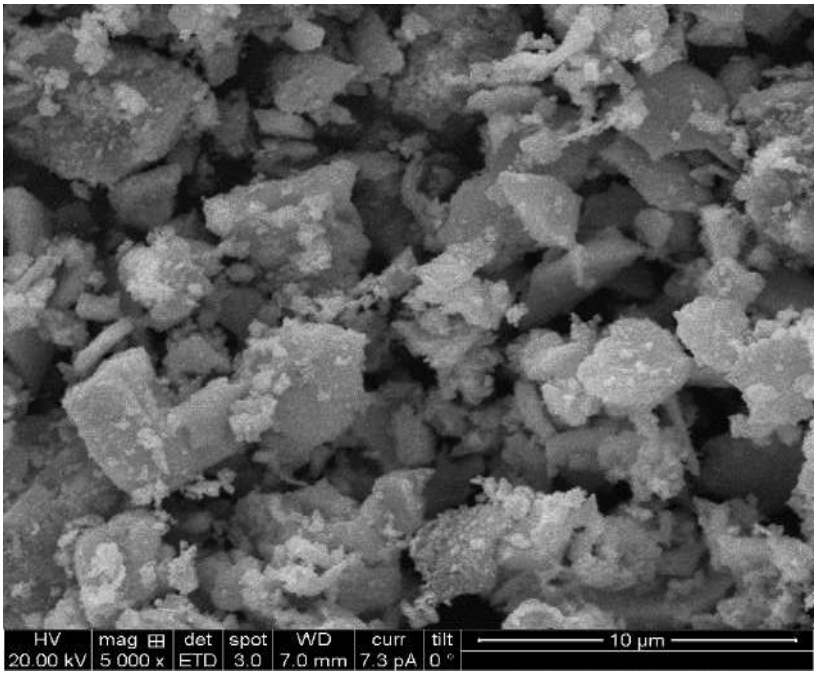

Fig. 6.2: SEM images of synthesized $Mn_{0.02}Sn_{0.98}O_2$ nanoparticles.

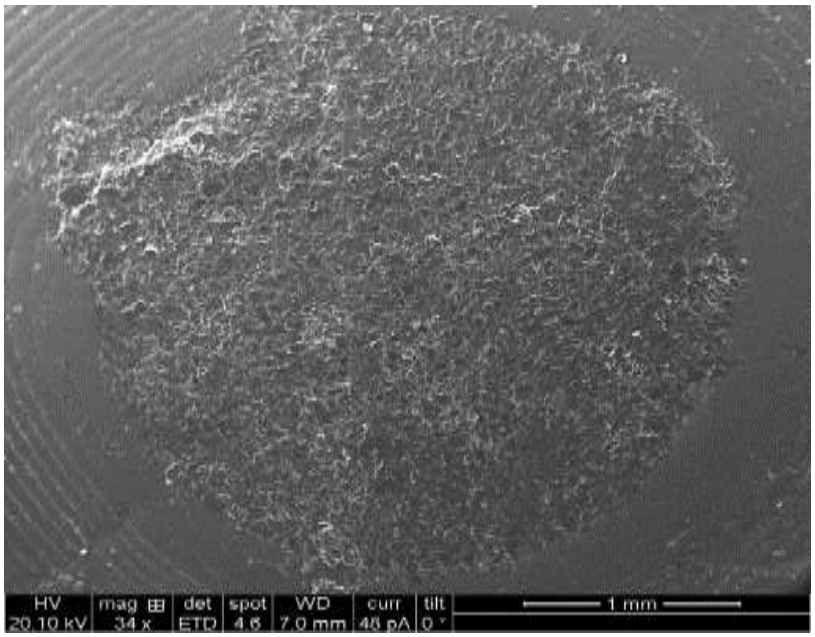

Fig. 6.3a: SEM image of bare carbon paste electrode.

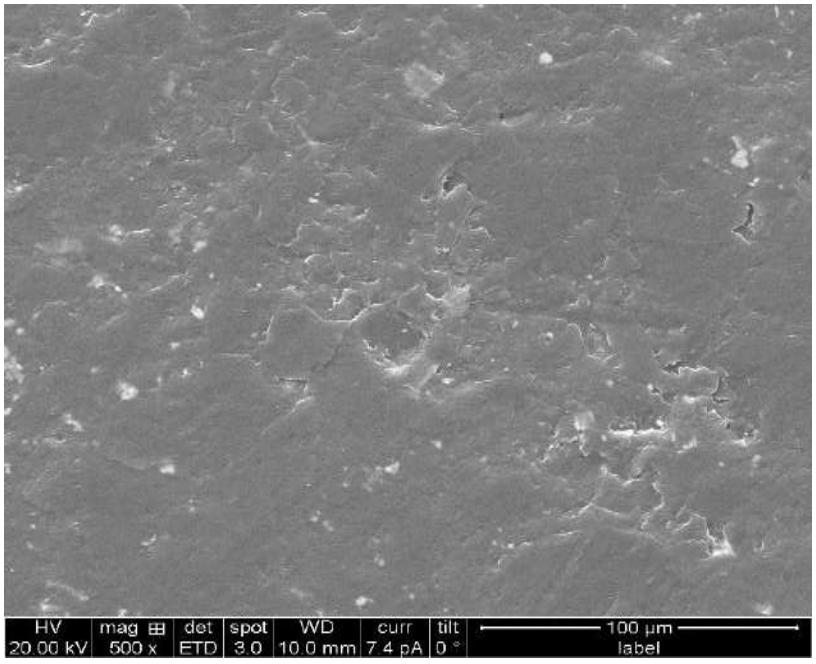

Fig. 6.3b: SEM image of $Mn_{0.02}Sn_{0.98}O_2$ nanoparticles modified carbon paste electrode.

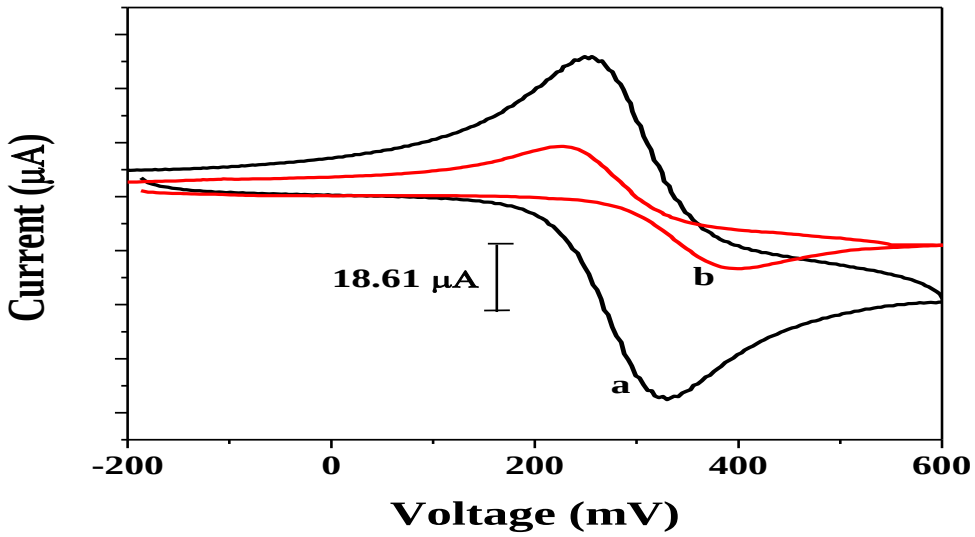

Fig. 6.4: Comparision of 0.1 mM $K_4[Fe(CN)_6]$ in 0.1M KCl solution at $Mn_{0.02}Sn_{0.98}O_2$ nanoparticles modified carbon paste electrode (a) and bare carbon paste electrode (b).

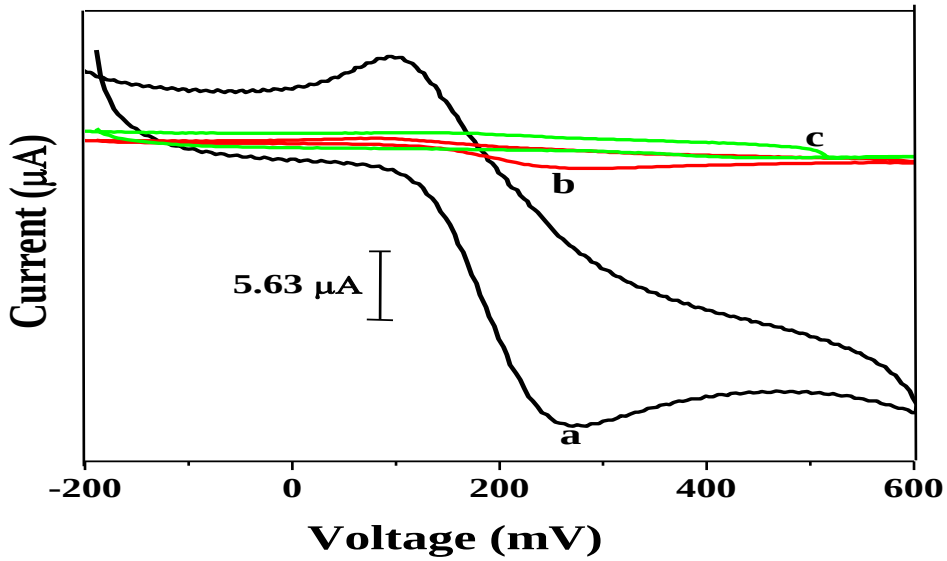

Fig. 6.5: Comparision of 0.1 mM DA at $Mn_{0.02}Sn_{0.98}O_2$ nanoparticles modified carbon paste electrode (a), bare carbon paste electrode (b) and blank solution in 0.1 M phosphate buffer at $Mn_{0.02}Sn_{0.98}O_2$ nanoparticles modified carbon paste electrode (c); pH 7, scan rate 25 mVs^{-1}.

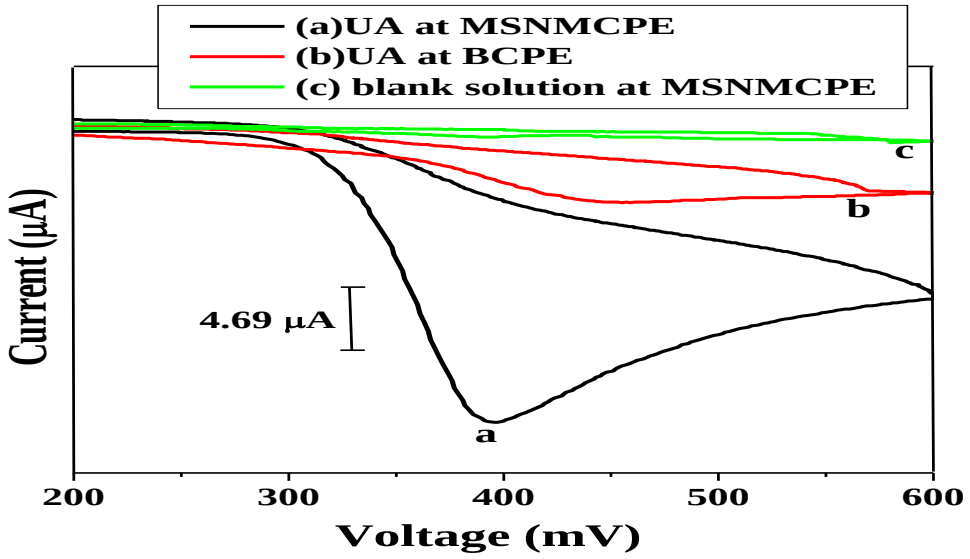

Fig. 6.6: Comparision of 0.1 mM UA at $Mn_{0.02}Sn_{0.98}O_2$ nanoparticles modified carbon paste electrode (a), bare carbon paste electrode (b) and blank solution in phosphate buffer solution at $Mn_{0.02}Sn_{0.98}O_2$ nanoparticles modified carbon paste electrode (c); pH 6.5, scan rate 10 mVs^{-1}.

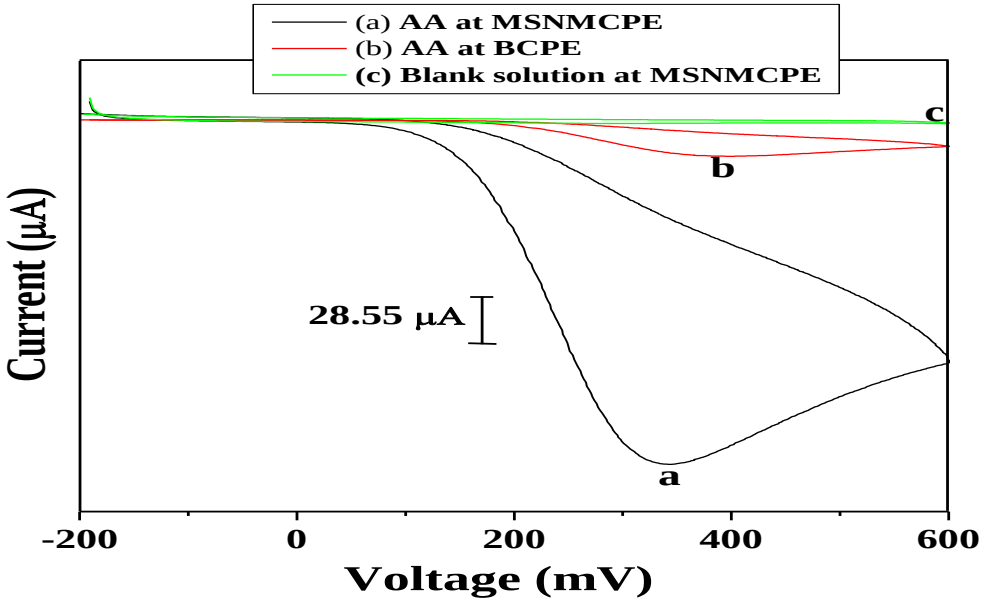

Fig. 6.6: Comparision of 1 mM AA at $Mn_{0.02}Sn_{0.98}O_2$ nanoparticles modified carbon paste electrode (a), bare carbon paste electrode (b) and blank solution in 0.1 M phosphate buffer at $Mn_{0.02}Sn_{0.98}O_2$ nanoparticles modified carbon paste electrode (c); pH 5.5, scan rate 10 mVs^{-1}.

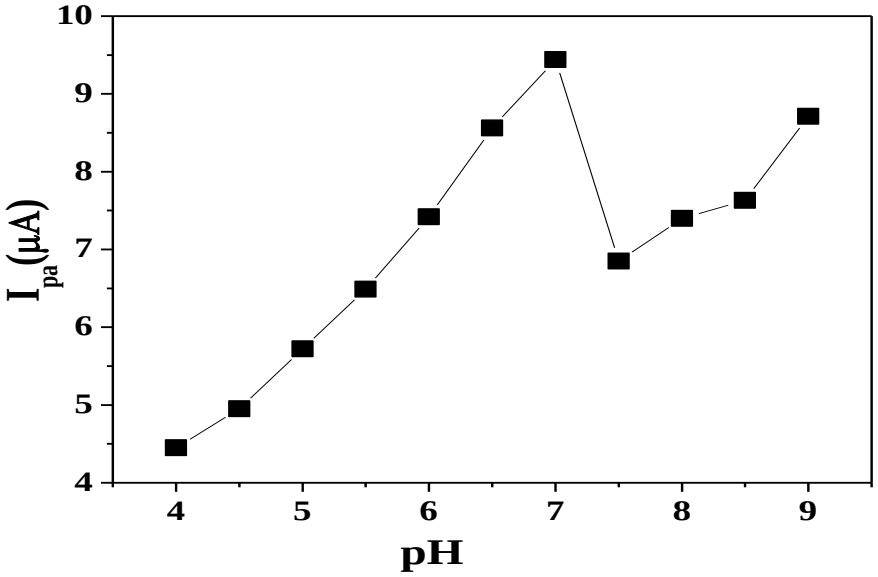

Fig. 6.7a: Plot of anodic peak current vs. pH (4 – 9) of 0.1 mM DA at $Mn_{0.02}Sn_{0.98}O_2$ nanoparticles modified carbon paste electrode.

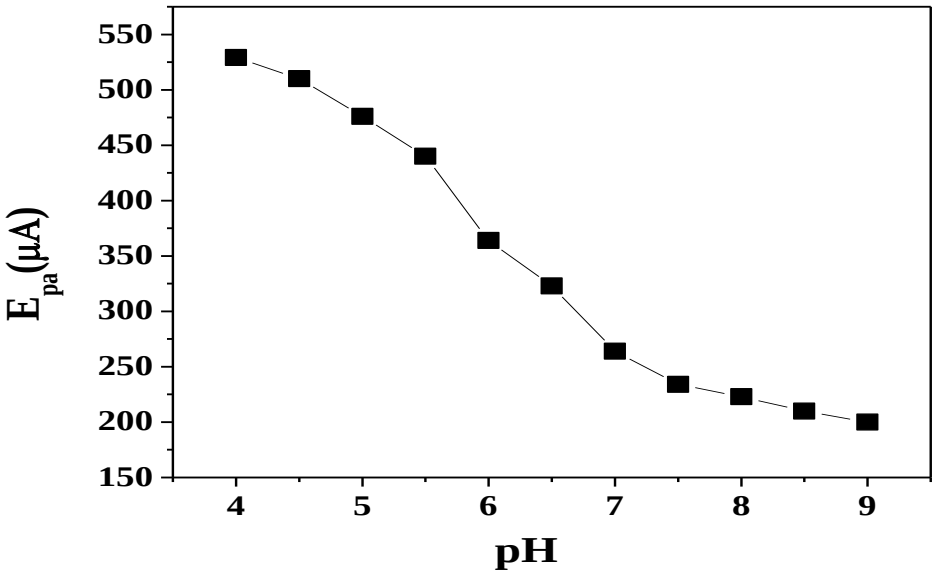

Fig. 6.7b: Plot of anodic peak potential vs. pH (4 – 9) of 0.1 mM DA at $Mn_{0.02}Sn_{0.98}O_2$ nanoparticles modified carbon paste electrode.

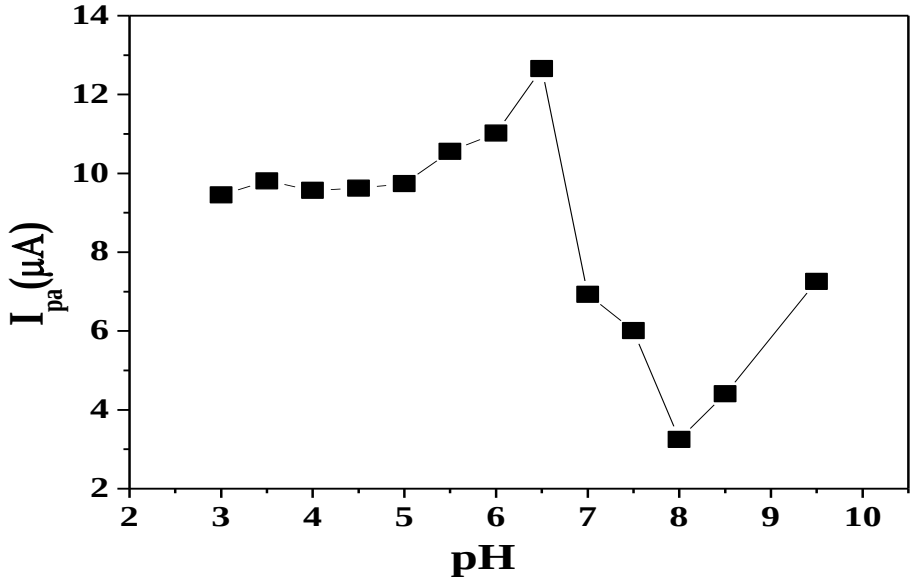

Fig. 6.8a: Plot of anodic peak current vs. pH (3 – 9.5) of 0.1 mM UA at $Mn_{0.02}Sn_{0.98}O_2$ nanoparticles modified carbon paste electrode.

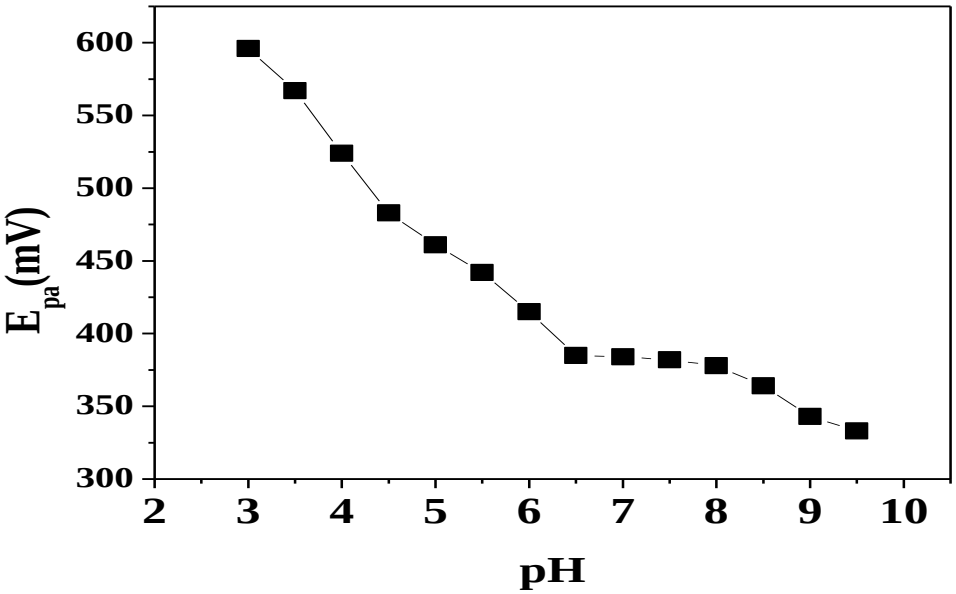

Fig. 6.8b: Plot of anodic peak potential vs. pH (3 – 9.5) of 0.1 mM UA at $Mn_{0.02}Sn_{0.98}O_2$ nanoparticles modified carbon paste electrode.

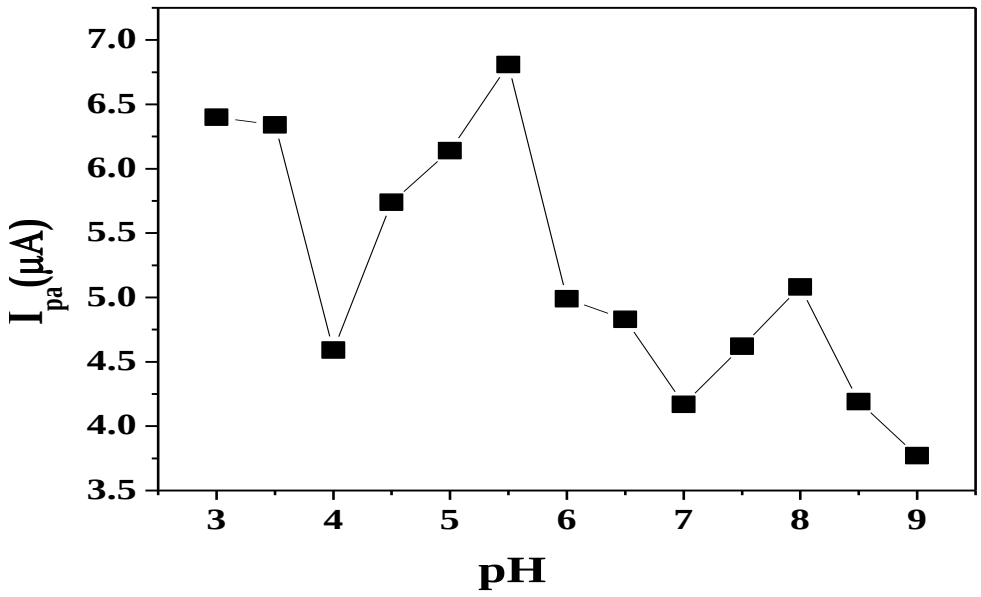

Fig. 6.9a: Plot of anodic peak current vs. pH (3 – 9) of 0.1 mM AA at $Mn_{0.02}Sn_{0.98}O_2$ nanoparticles modified carbon paste electrode.

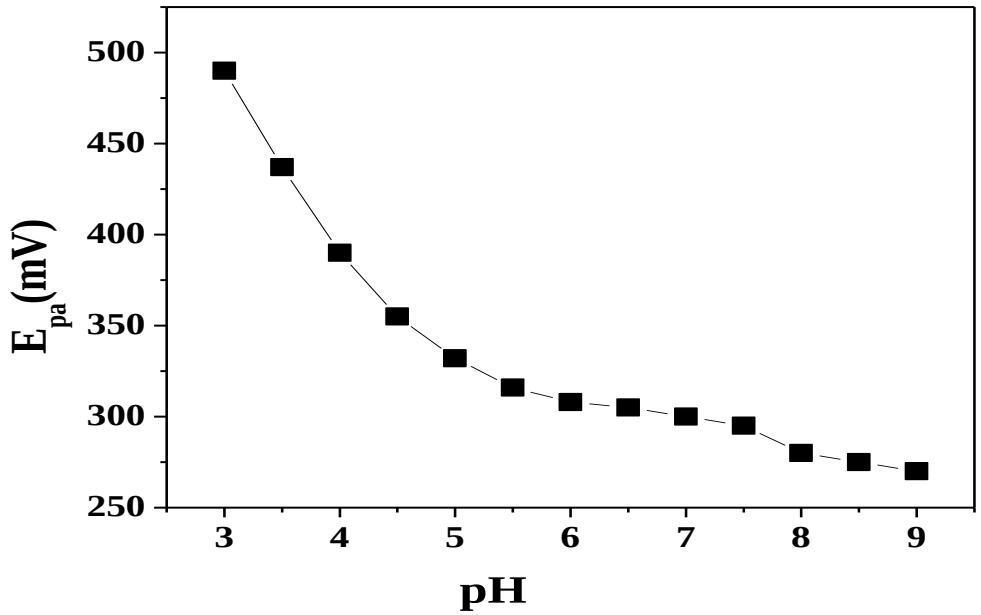

Fig .6.9b: Plot of anodic peak potential vs. pH (3 – 9) of 0.1 mM AA at $Mn_{0.02}Sn_{0.98}O_2$ nanoparticles modified carbon paste electrode.

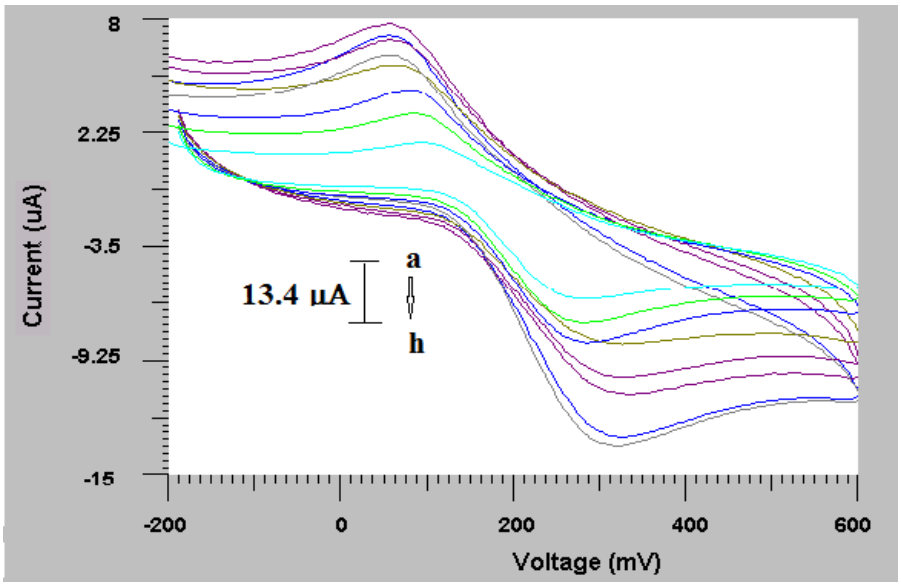

Fig. 6.10a: Cyclic voltammogram of 0.1 mM DA at $Mn_{0.02}Sn_{0.98}O_2$ nanoparticles modified carbon paste electrode with different scan rates (a) 25, (b) 50, (c) 75, (d) 100, (e) 125, (f) 150, (g) 175, (h) 200 mVs^{-1}.

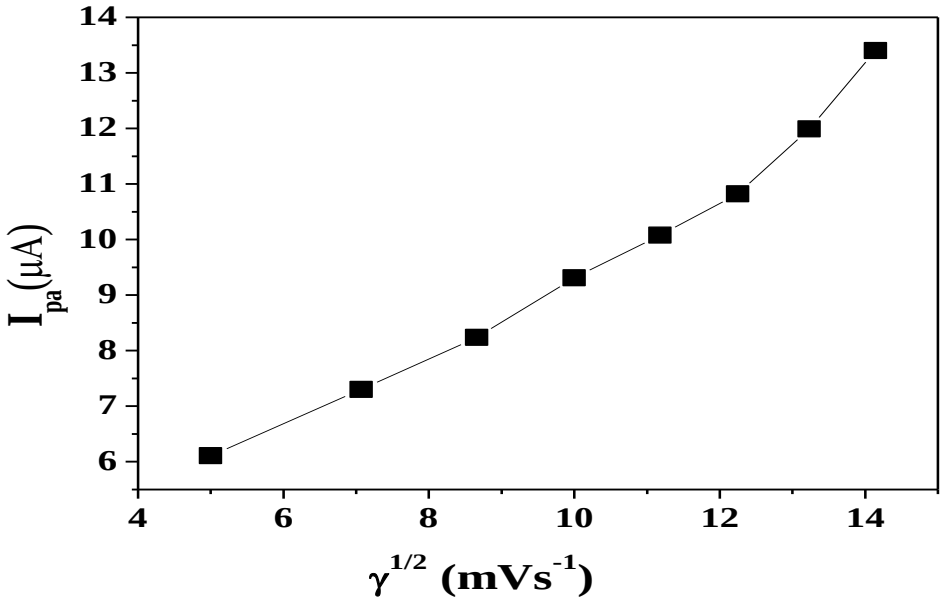

Fig.6.10b: Plot of anodic peak current vs. square root of scan rates of DA at $Mn_{0.02}Sn_{0.98}O_2$ nanoparticles modified carbon paste electrode.

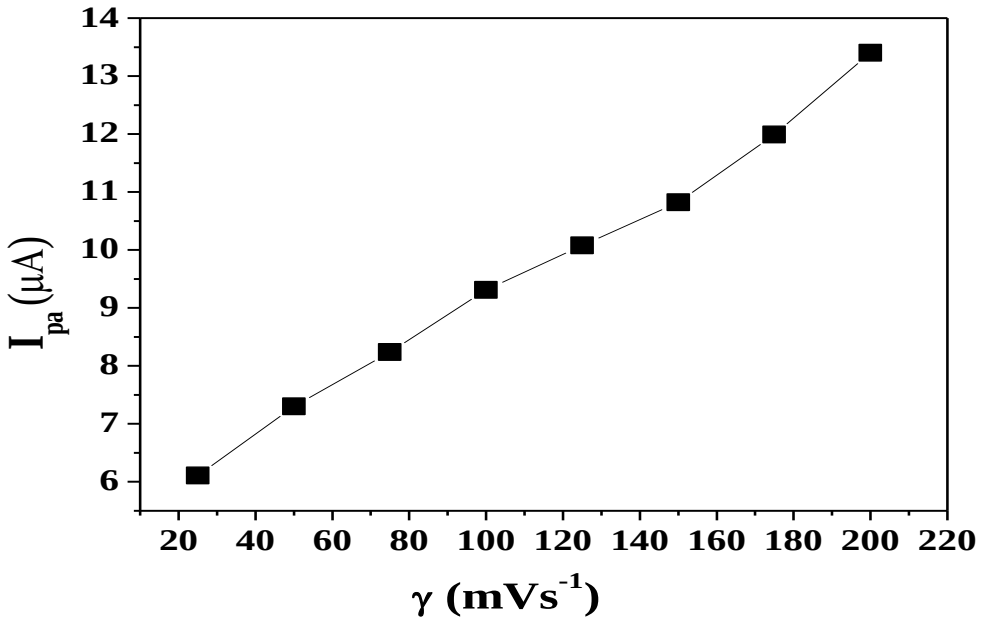

Fig.6.10c: Plot of anodic peak current vs. scan rates of DA at $Mn_{0.02}Sn_{0.98}O_2$ nanoparticles modified carbon paste electrode.

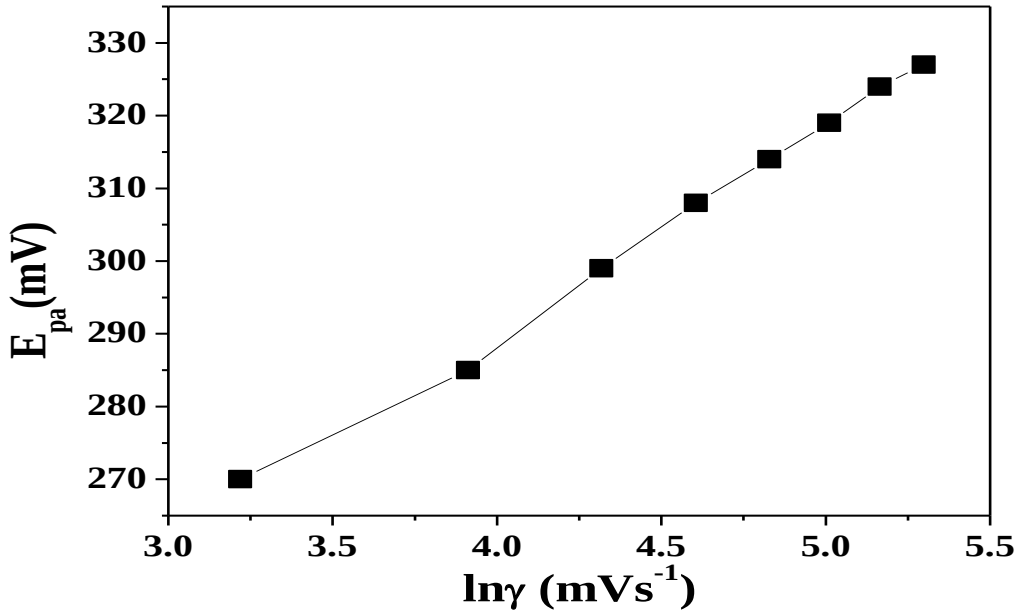

Fig. 6.10d: Plot of anodic peak potential vs. natural logarithm of scan rates of DA at $Mn_{0.02}Sn_{0.98}O_2$ nanoparticles modified carbon paste electrode.

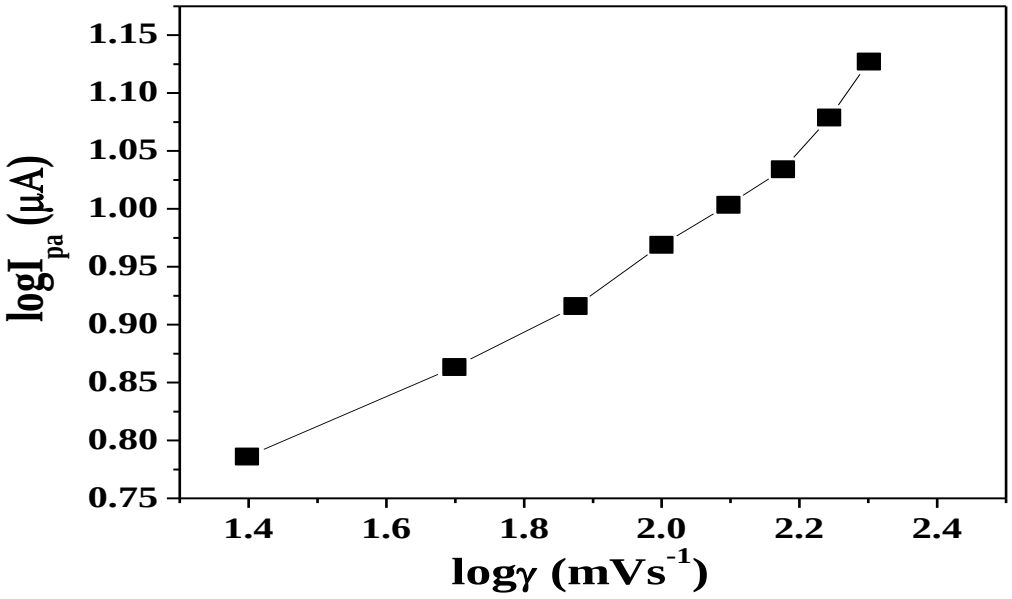

Fig. 6.10e: Plot of logarithm of anodic peak potential vs. logarithm of scan rates of DA at $Mn_{0.02}Sn_{0.98}O_2$ nanoparticles modified carbon paste electrode.

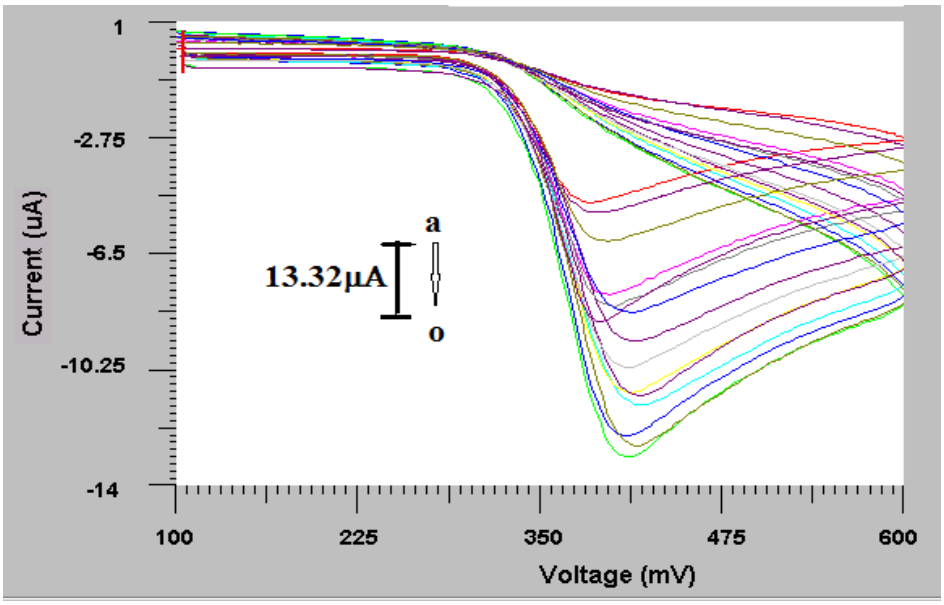

Fig. 6.11a: Cyclic voltammograms of 0.1 mM UA at $Mn_{0.02}Sn_{0.98}O_2$ nanoparticles modified carbon paste electrode with different scan rates (a) 10, (b) 20, (c) 30, (d) 40, (e) 50, (f) 60, (g) 70, (h) 80, (i) 90, (j) 100 (k) 110 (l) 120 (m) 130 (n) 140 (o) 150 mVs^{-1}.

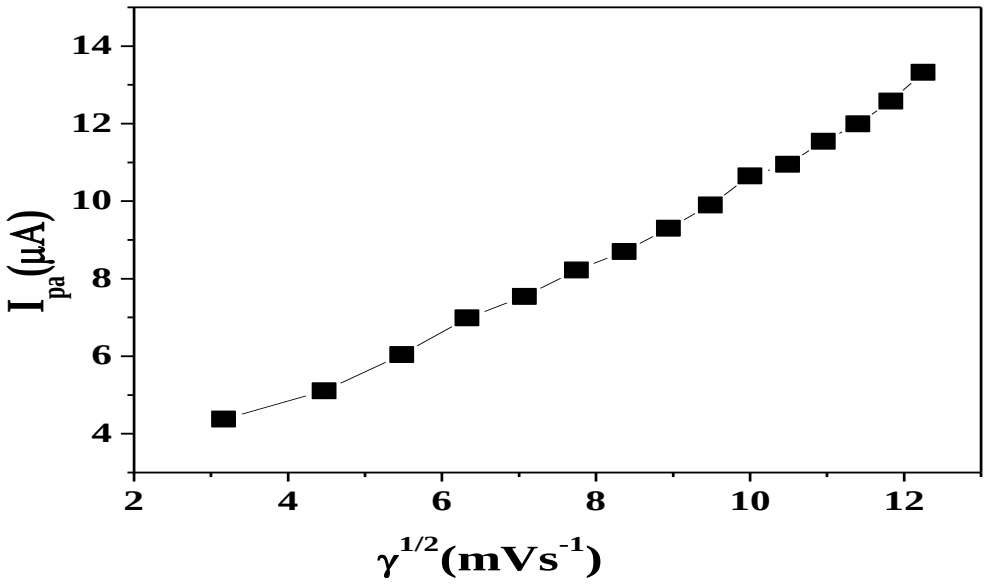

Fig. 6.11b: Plot of anodic peak current vs. square root of scan rates of UA at $Mn_{0.02}Sn_{0.98}O_2$ nanoparticles modified carbon paste electrode.

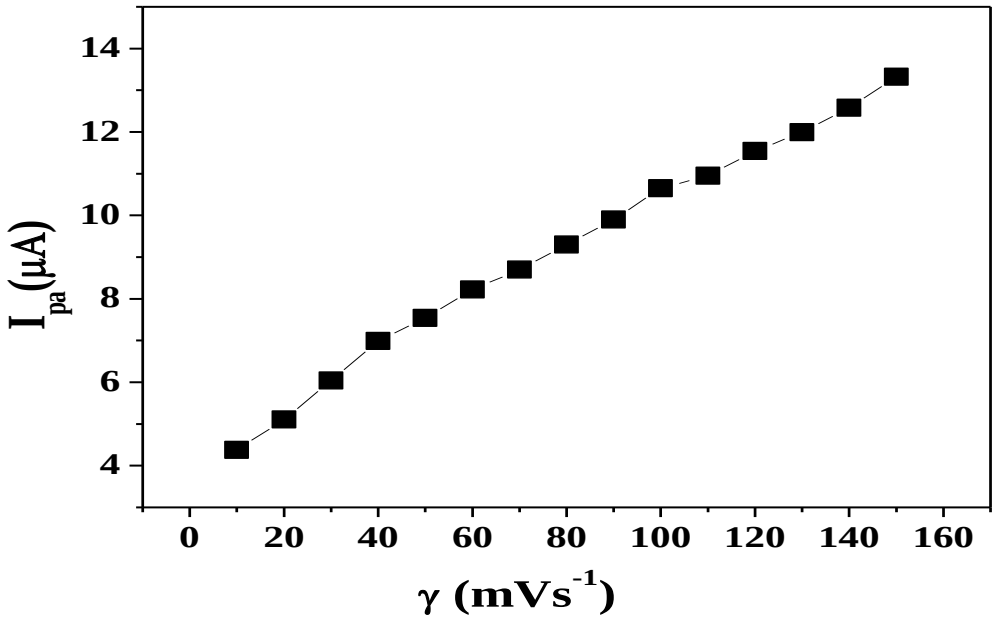

Fig. 6.11c: Plot of anodic peak current vs. scan rates of UA at $Mn_{0.02}Sn_{0.98}O_2$ nanoparticles modified carbon paste electrode.

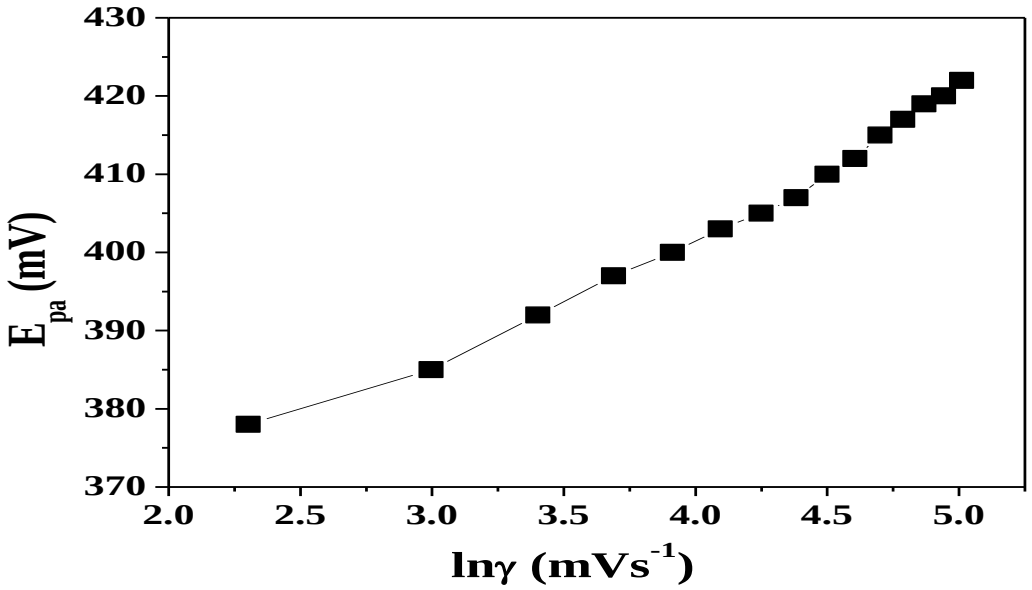

Fig. 6.11d: Plot of anodic peak potential vs. natural logarithm of scan rates of UA at $Mn_{0.02}Sn_{0.98}O_2$ nanoparticles modified carbon paste electrode.

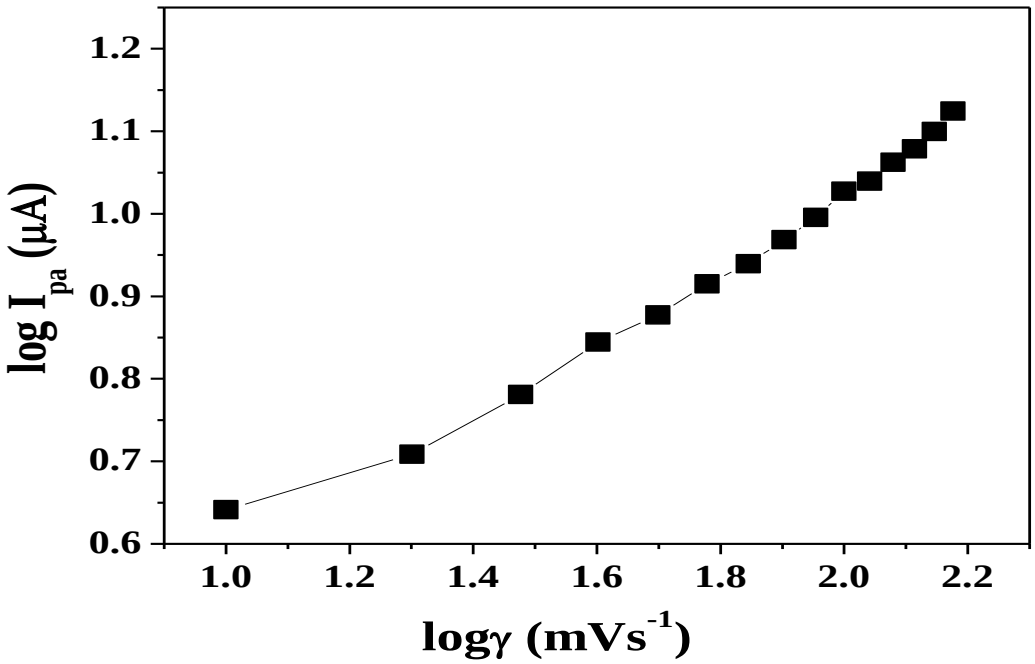

Fig. 6.11e: Plot of logarithm of anodic peak potential vs. logarithm of scan rates of UA at $Mn_{0.02}Sn_{0.98}O_2$ nanoparticles modified carbon paste electrode.

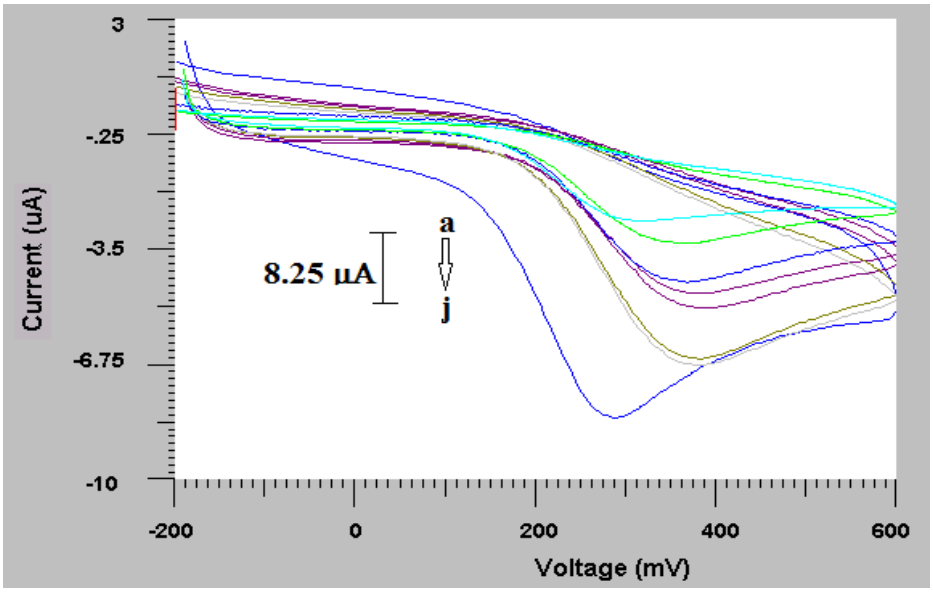

Fig. 6.12a: Cyclic voltammograms of 0.1 mM AA at $Mn_{0.02}Sn_{0.98}O_2$ nanoparticles modified carbon paste electrode with different scan rates (a) 10, (b) 20, (c) 30, (d) 40, (e) 50, (f) 60, (g) 70, (h) 80, (i) 90, (j) 100 mVs^{-1}.

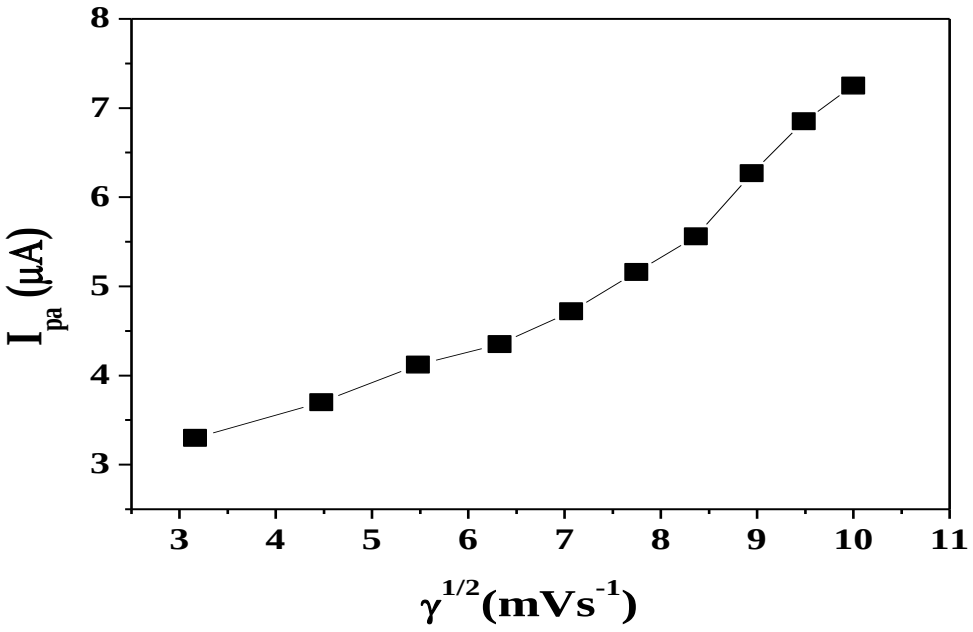

Fig. 6.12b: Plot of anodic peak current vs. square root of scan rates of AA at $Mn_{0.02}Sn_{0.98}O_2$ nanoparticles modified carbon paste electrode.

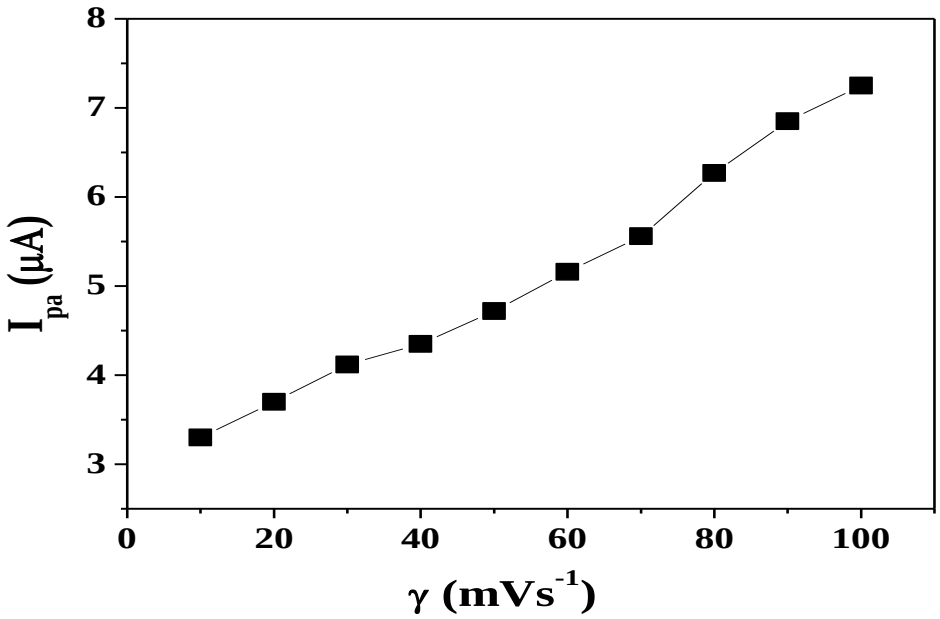

Fig. 6.12c: Plot of anodic peak current vs. scan rates of AA at $Mn_{0.02}Sn_{0.98}O_2$ nanoparticles modified carbon paste electrode.

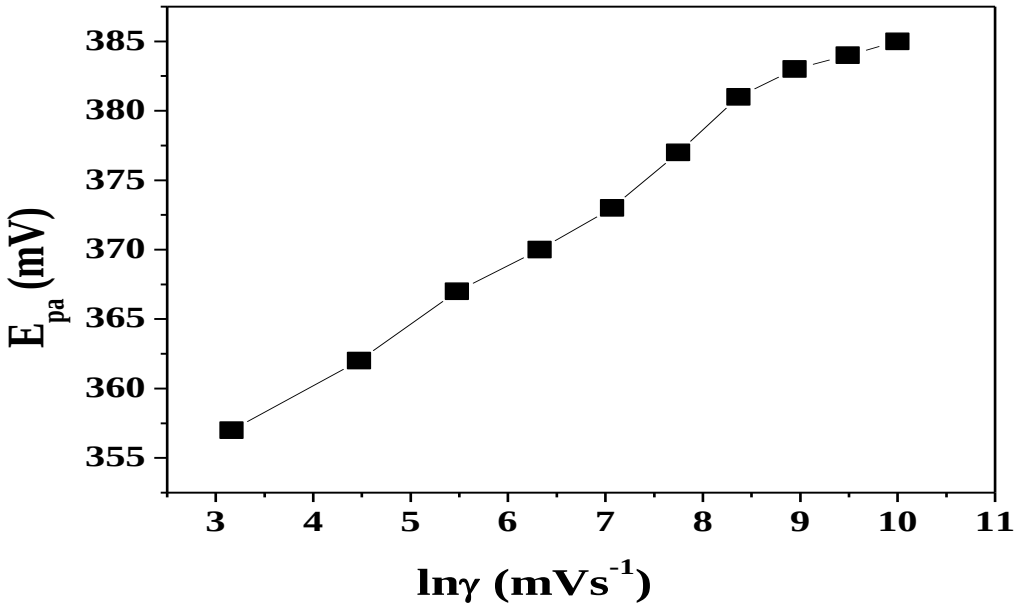

Fig. 6.12d: Plot of anodic peak potential vs. natural logarithm of scan rates of AA at $Mn_{0.02}Sn_{0.98}O_2$ nanoparticles modified carbon paste electrode.

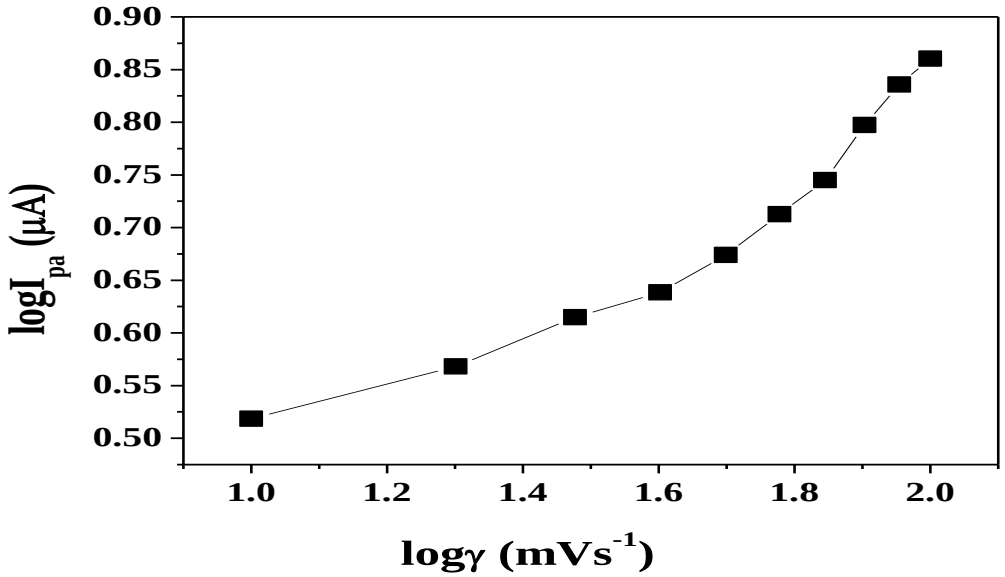

Fig. 6.12e: Plot of logarithm of anodic peak potential vs. logarithm of scan rates of AA at $Mn_{0.02}Sn_{0.98}O_2$ nanoparticles modified carbon paste electrode.

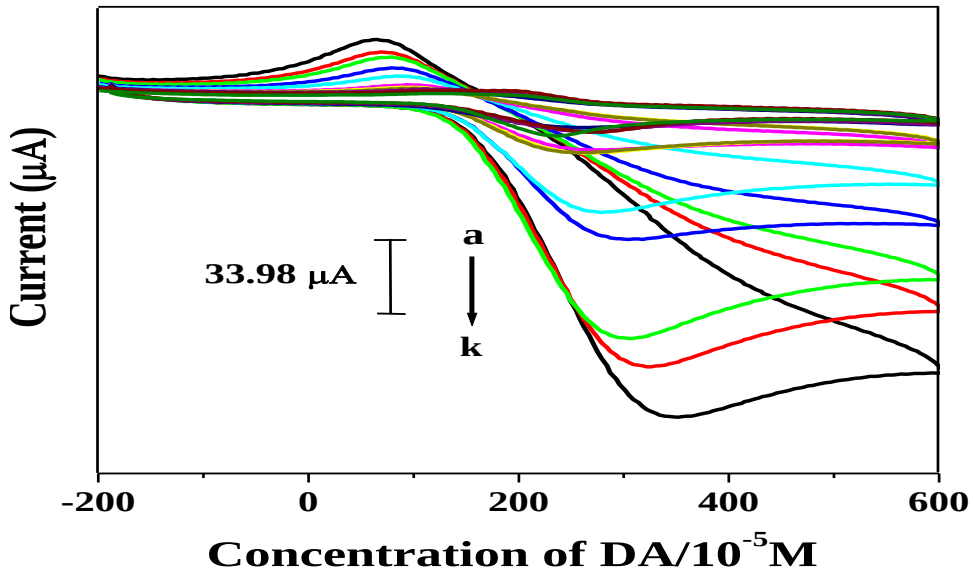

Fig. 6.13a: Effect of variation of concentration of DA (a) 1×10^{-5} M, (b) 2×10^{-5} M, (c) 4×10^{-5} M, (d) 6×10^{-5} M, (e) 8×10^{-5} M, (f) 1×10^{-4} M, (g) 2×10^{-4} M, (h) 4×10^{-4} M (i) 6×10^{-4} M, (j) 8×10^{-4} M, (k) 1×10^{-3} M on anodic peak current at $Mn_{0.02}Sn_{0.98}O_2$ nanoparticles modified carbon paste electrode; scan rate 25 mVs^{-1}.

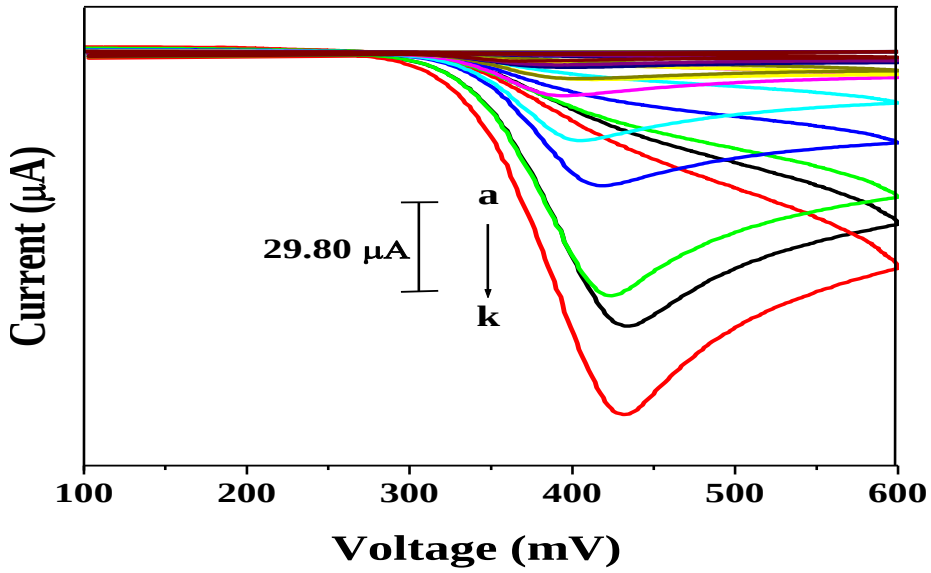

Fig. 6.13b: Effect of variation of concentration of UA (a) 1×10^{-5} M, (b) 2×10^{-5} M, (c) 4×10^{-5} M, (d) 6×10^{-5} M, (e) 8×10^{-5} M, (f) 1×10^{-4} M, (g) 2×10^{-4} M, (h) 4×10^{-4} M, (i) 6×10^{-4} M, (j) 8×10^{-4} M, (k) 1×10^{-3} M on anodic peak current at $Mn_{0.02}Sn_{0.98}O_2$ nanoparticles modified carbon paste electrode; scan rate 10 mVs^{-1}.

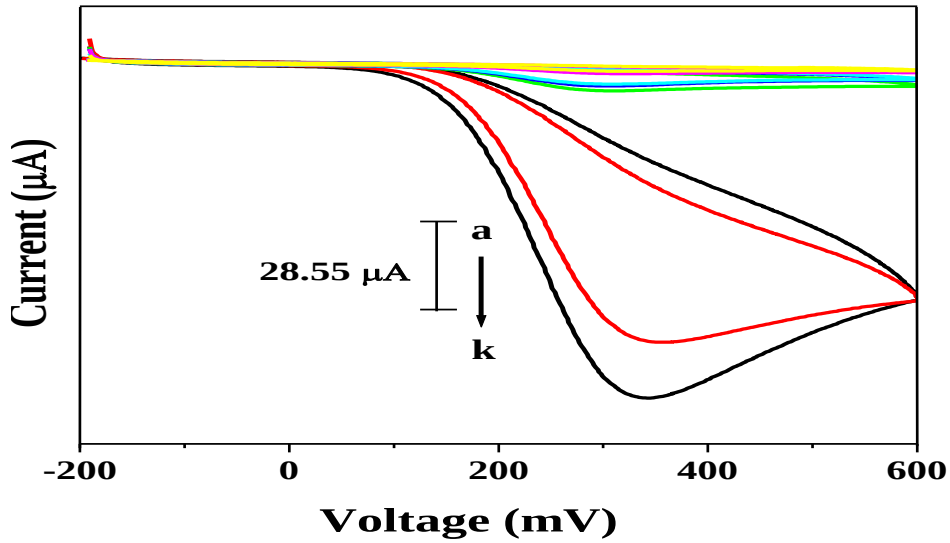

Fig. 6.13c: Effect of variation of concentration of AA (a) 1×10^{-5} M, (b) 2×10^{-5} M, (c) 4×10^{-5} M, (d) 6×10^{-5} M, (e) 8×10^{-5} M, (f) 1×10^{-4} M, (g) 2×10^{-4} M, (h) 4×10^{-4} M (i) 6×10^{-4} M, (j) 8×10^{-4} M (k) 1×10^{-3} M on anodic peak current at $Mn_{0.02}Sn_{0.98}O_2$ nanoparticles modified carbon paste electrode; scan rate 10 mVs^{-1}.

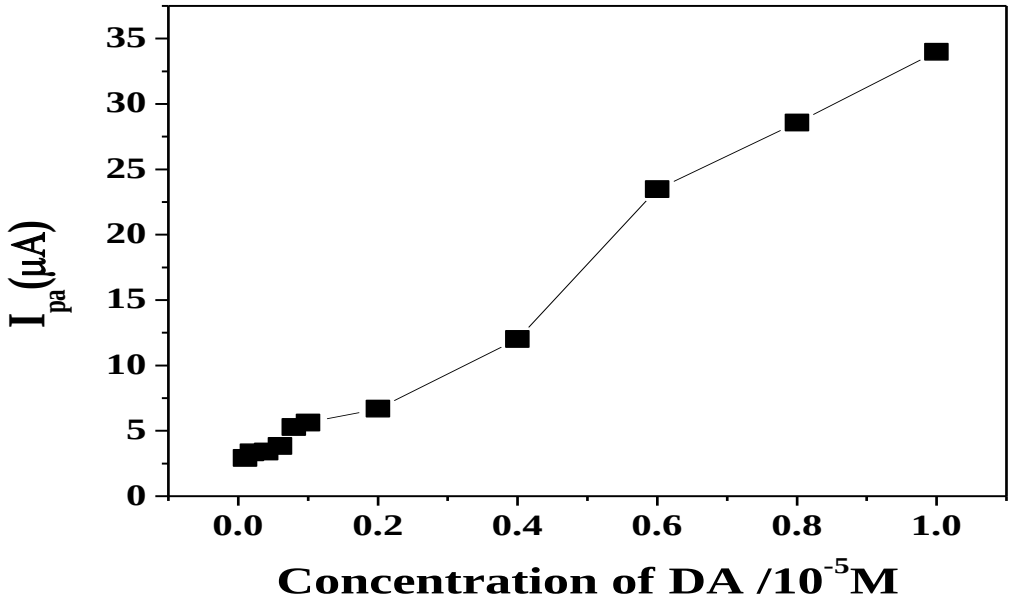

Fig. 6.14a: Plot of anodic peak current vs. concentration of DA at $Mn_{0.02}Sn_{0.98}O_2$ nanoparticles modified carbon paste electrode.

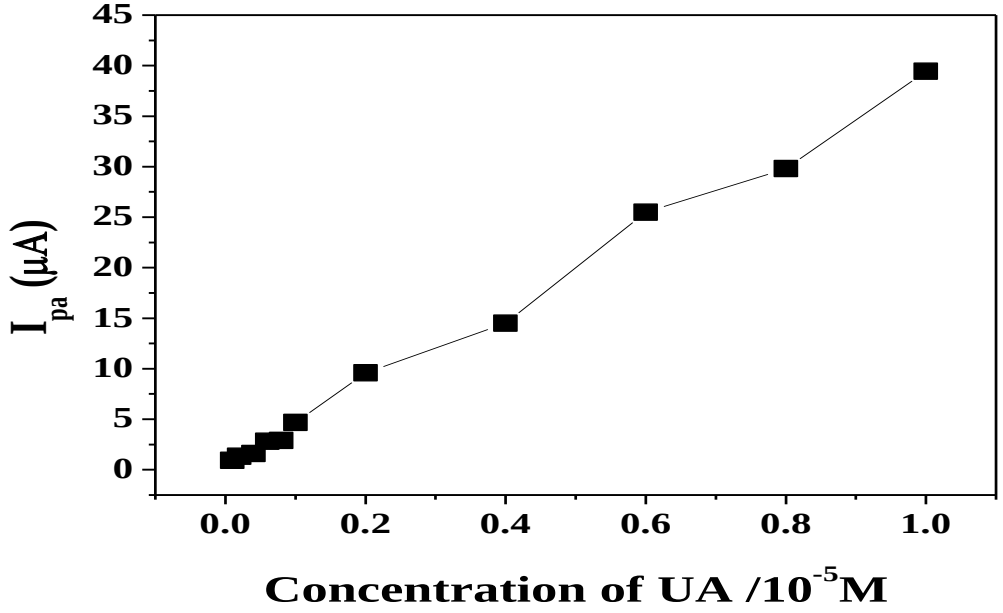

Fig. 6.14b: Plot of anodic peak current vs. concentration of UA at $Mn_{0.02}Sn_{0.98}O_2$ nanoparticles modified carbon paste electrode.

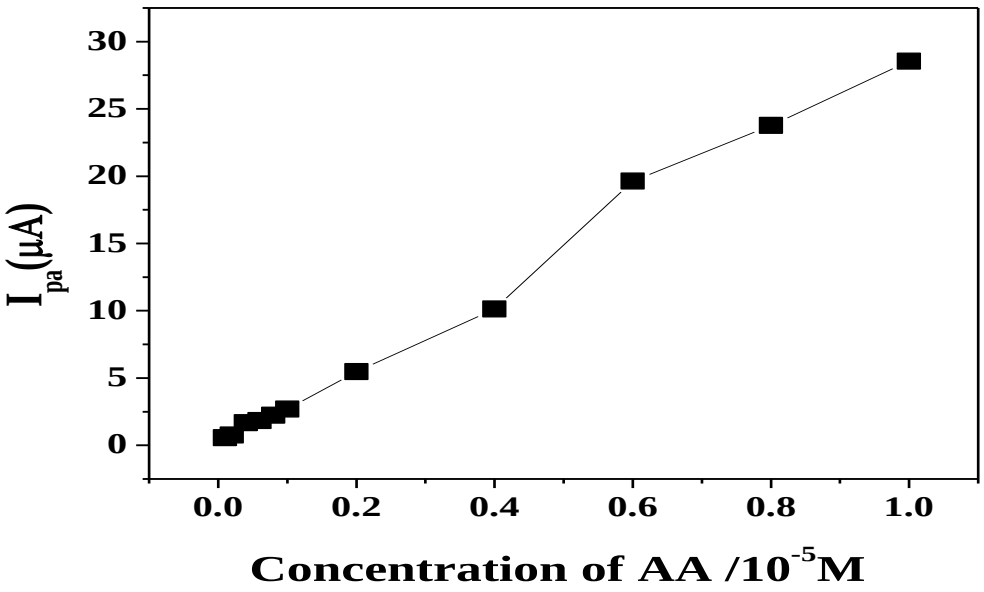

Fig. 6.14c: Plot of anodic peak current vs. concentration of AA at $Mn_{0.02}Sn_{0.98}O_2$ nanoparticles modified carbon paste electrode.

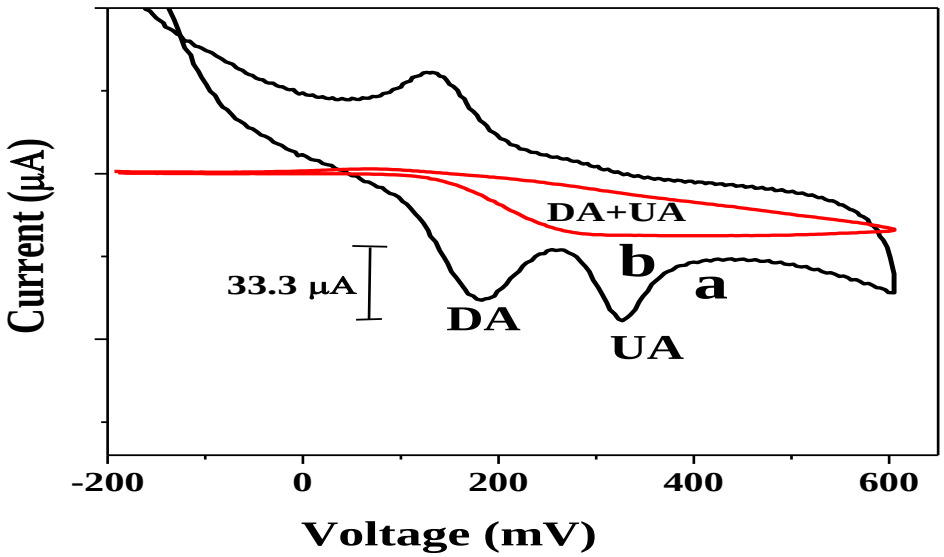

Fig. 6.15a: Cyclic voltammograms at $Mn_{0.02}Sn_{0.98}O_2$ nanoparticles modified carbon paste electrode (a) and bare carbon paste electrode (b) in presence of 0.5 mM DA and 0.2 mM UA in 0.1 M PBS of pH 7; scan rate 25 mVs^{-1}.

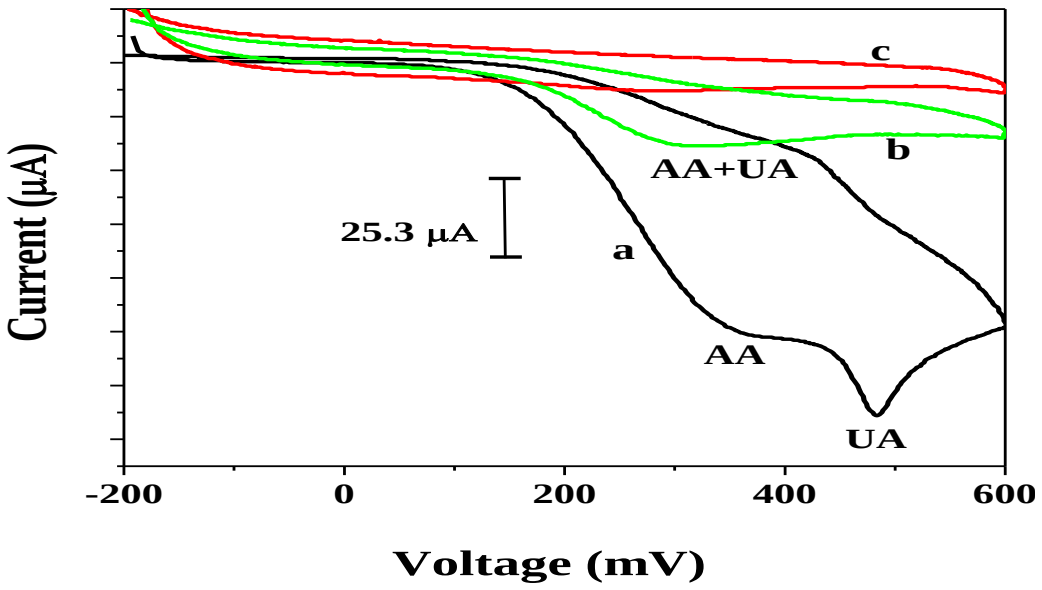

Fig. 6.15b: Cyclic voltammograms at $Mn_{0.02}Sn_{0.98}O_2$ nanoparticles modified carbon paste electrode (a), bare carbon paste electrode (b) in presence of 1 mM AA and 0.2 mM UA and blank solution in 0.1 M PBS at $Mn_{0.02}Sn_{0.98}O_2$ nanoparticles modified carbon paste electrode; pH 5.5, scan rate 10 mVs^{-1}.

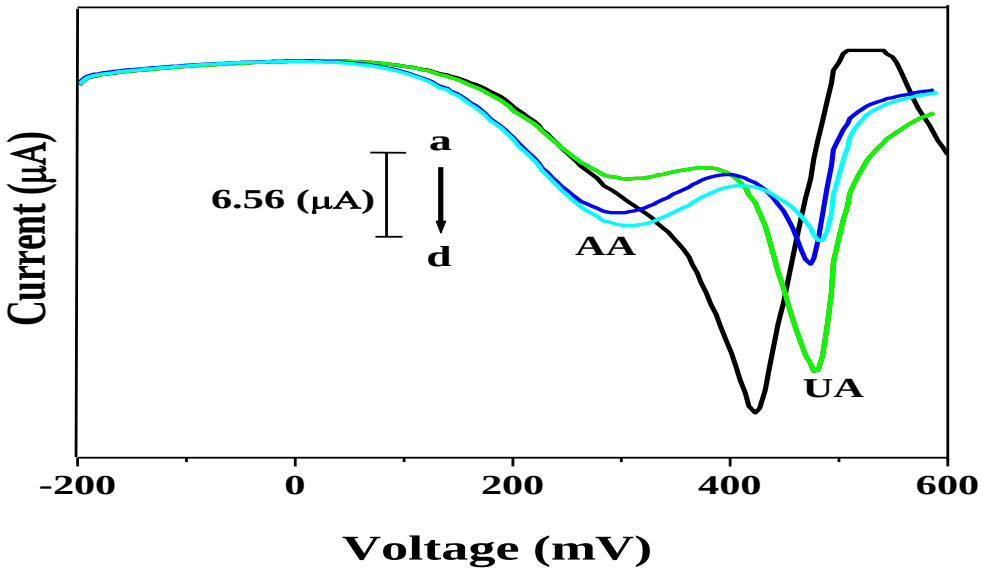

Fig. 6.16a: Differential pulse voltammograms of AA and UA at $Mn_{0.02}Sn_{0.98}O_2$ nanoparticles modified carbon paste electrode at pH 5.5 in PBS with scan rate 10 mVs^{-1}. (a) 0.5 mM UA + 0.2 (a), 0.4 (b), 0.6 (c) and 0.8 mM AA(d).

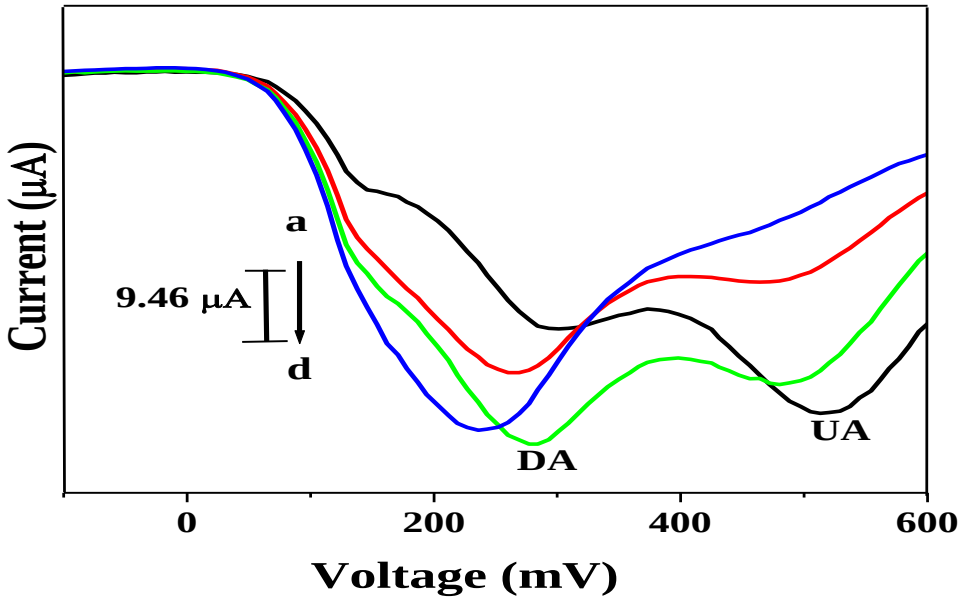

Fig. 6.16b: Differential pulse voltammograms of DA and UA at $Mn_{0.02}Sn_{0.98}O_2$ nanoparticles modified carbon paste electrode in pH 7.0 PBS with the scan rate 25 mVs^{-1}, 0.5 mM DA + 0.1 (a), 0.2 (b), 0.3 (c) and 0.4 mM UA(d).

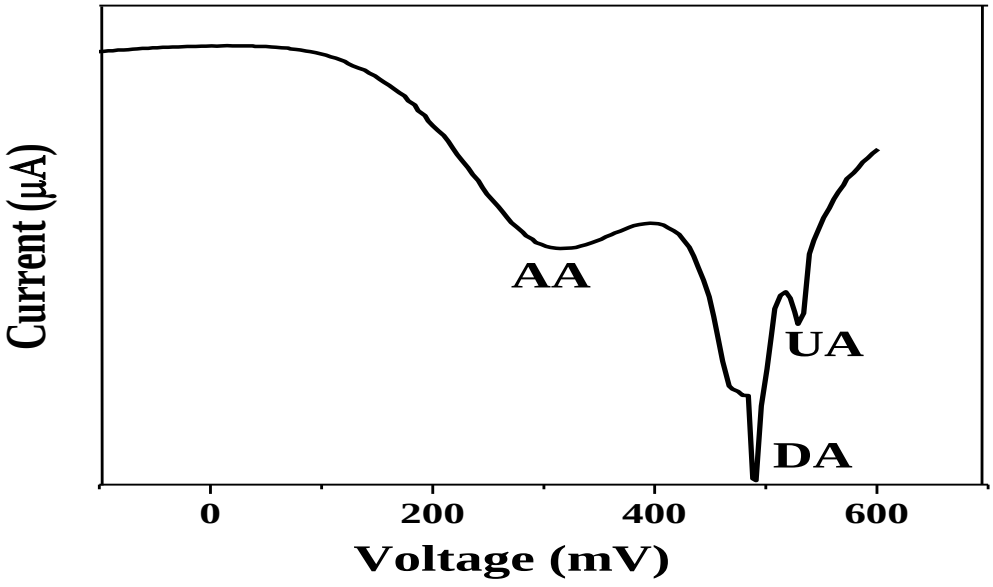

Fig. 6.17: Differential pulse voltammograms of 0.2 mM AA and 0.5 mM DA in presence of 1mM UA at $Mn_{0.02}Sn_{0.98}O_2$ nanoparticles modified carbon paste electrode with scan rate 25 mVs^{-1}.

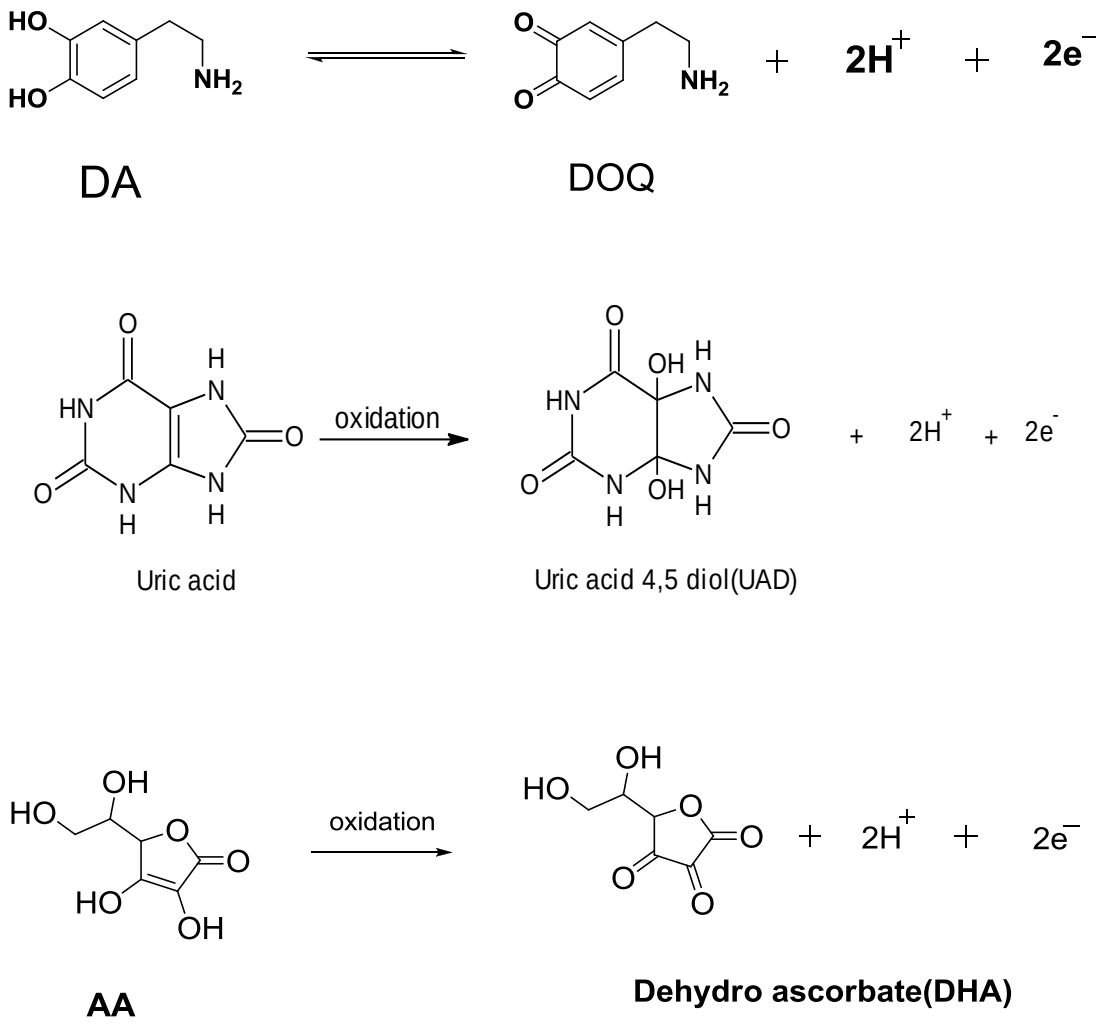

Scheme 6.1: Probable oxidation of DA, UA and AA.

6.8. Reference:

[1] A.K. Tausche, S. Unger, K. Richter, *Der Internist.,* **47** (2006) 509.

[2] Y.C. Luo, J.S. Do, C.C. Liu, *Biosens. Bioelectron.,* **22 (**2006) 482.

[3] H. Manjunatha, D.H. Nagaraju, G.S. Suresh and T.V. Venkatesha, *Electroanalysis,* **21** (2009) 2198.

[4] S. Behera, C.R. Raj, *Biosens. Bioelectron.,* **23** (2007) 556.

[5] P. Ramesh, S. Sampath, *Electroanalysis,* **16** (2004) 866.

[6] G.G. Guilbault, *Analytical Uses of Immobilized Enzymes,* Marcel Dekker, New York, 1984.

[7] Knut Schmidt-Nielsen, *Animal physiology adaptation and environmen*t, Fourth edition, Cambridge University press, 1995.

[8] M.Y. Lachapelle, G. Rouyn, *Genetica,* **139** (2010) 199.

[9] L.J. Hardie, T.C. Fletcher, C.J. Secombes, *Aquaculture,* **95** (1991) 201.

[10] H. Sies, W. Stahl, *Am. J. Clin. Nutr.,* **62** (1995) 1315S.

[11] M. Levine K.R. Dhariwal, R.W. Welch, Y. Wang and J.B. Park, *Am J Clin Nutr.,* **62 (**1995) 1347S.

[12] P. Weber, A. Bendich, Schalch, *Int. J. Vit. Nutr. Res.,* **66** (1996) 19.

[13] R.M. Wightman, L.J. May, A.C. Michael, *Anal. Chem.,* **60** (1988) 769A.

[14] S. Marceglia, G. Foffani, A. Bianchi, G. Baselli, F. Tamma, M. Egidi and A. Priori, *J. Physiol.*, **571** (2006) 579.

[15] N. Kemppainen, P. Marjamaki, M. Route, J. Rinne, *J. Neural. Transm.,* **108** (2001) 827.

[16] L. Schwieler, G. Engberg, S. Erhardt, *Synapse,* **52** (2004) 114.

[17] J. Berke, S. Hyman, *Neuron,* **25** (2000) 515.

[18] G. Di Chiara, V. Bassareo, S. Fenu, M. De Luca, L. Spina, C. Cadoni, E. Acais, E. Carbons, V. A. Valentine and D. Lecca, *Neuropharmacology*, **47** (2004) 227.

[19] I. Franken, J. Booij, W. van den Brink, *Eur. J. Pharmacol.,* **526** (2005) 199.

[20] M. Heien, A. Khan, J. Ariansen, J. Cheer, P. Phillips, K. Wassum and M. Wightman, *Proc Natl Acad. Sci.,***102** (2005) 10023.

[21] O. Rohr, B. Sawaya, D. Lecestre, D. Aunis and E. Schaeffer, *Nucleic Acids Res.,* **27** (1999) 3291.

[22] C. Scheller, S. Sapper, C. Jessy, V. termeulen, P. Riederer and E. Koutsilieri, *J. Neural Transm.,* **107** (2000) 1483.

[23] J. Premkumar, S.B. Khoo, *J. Electroana. Chem.*, **576** (2005) 105.

[24] C.R. Raj, F. Kitamura, T. Ohsaka, *Analyst,* **9** (2002) 1155.

[25] Lin Mei Niu, Hong Dun Loud, Nian Bing Li, *Instrumentation science and Technology*, **35** (2007) 59.

[26] J.B. Raoof, Ojani, A. Kiani, *J. Electroanal.Chem.,* **515** (2001) 45.

[27] Zhongua Wang, Yiming Wang, Guoan Luo, *Analyst*, **127** (2002) 1353.

[28] R.M. Wightman, L.J May, A.C. Michael, *Anal.Chem.,* **60** (1988) 769A.

[29] F. Gonon, M. Buda, R. Cespuglio, M. Jouvet and J.F. Pujol, *Nature,* **286** (1980) 902.

[30] R.D. O'Neill, *Analyst*, **119** (1994) 767.

[31] A. Salimi, H. Mam-Khezri, R. Hallaj, *Talanta*, **70** (2006) 823.

[32] M.A. Dayton, A.G. Ewing, R.M. Wightman, *Anal. Chem.*, **52** (1980) 2392.

[33] A. Balamurugan, S.M. Chen, *Anal. Chi. Acta*, **596** (2007) 92.

[34] Y.X. Li, X.Q. Lin, *Sens. Actuators B.*, **115** (2006) 134.

[35] L.Q. Lin, J.H. Chen, H. Yao, Y.Z. Chen, Y.J. Zheng and X.H. Lin, *Bioelectrochemistry*,**73** (2008) 11.

[36] Y.F. Zhao, Y.Q. Gao, D.P. Zhan, H. Liu, Q. Zhao, Y. Kou, Y.H. Shao, M.X. Li, Q.K. Zhuang and Z.W. Zhu, *Talanta*, **66** (2005) 51.

[37] H. Yao, Y.Y. Sun, X.H. Lin, Y.H. Tang and L.Y. Huang, *Electrochim. Acta*, **52** (2007) 6165.

[38] X.H. Lin, Q. Zhuang, J.H. Chen, S.B. Zhang and Y.J. Zheng, *Sens. Actuators B.*, **125** (2007) 240.

[39] Y.Z. Zhao, L.J. Zhang, S.L. Chen, S.Y. Dong and X.H. Zheng, *Chinese. Chem. Lett.*, **20** (2009) 217.

[40] R. Zhang, G.D. Jin, D. Chen and X.Y. Hu, *Sens. Actuators B.*, **138** (2009) 174.

[41] K.M. Manesh, P. Santhosh, A. Gopalan and K.P. Lee, *Talanta*, **75** (2008) 1307.

[42] W.Y. Su, S.H. Cheng, *Electrochem. Commun.*, **10** (2008) 899.

[43] W. Zheng, J. Li, Y.F. Zheng, *Biosensor. Bioelectron.*, **23** (2008) 1562.

[44] A. Liu, S.B. Zhang, W. Chen, X.H. Lin and X.H. Xia, *Biosensor. Bioelectron.*, **23** (2008) 1488.

[45] S. Sharath Shankar, B.E. Kumara Swamy, Umesh Chandra, J.G. Manjunatha and B.S. Sherigara, *Int. J. Electrochem. Sci.,* **4** (2009) 592.

[46] Kuo-Chiang Lin, Chain-Yu Yin, Shen-Ming Chen, *Int. J. Electrochem. Sci*., **6** (2011) 3951.

[47] Ali A. Ensafi, M. Taei, T. Khayamian, *Journal of Electroanalytical Chemistry*, **633** (2009) 212.

[48] H.R. Zare, N. Nasirizadeh, M. Mazloum Ardakani, *Journal of Electroanalytical Chemistry*, **577** (2005) 25.

[49] Chandrashekar C. Vishwanatha, Bahaddurghatta E. Kumara Swamy, K. Vasantakumar Pai, *J Anal Bioanal Tech.*, **6** (2015) 1.

[50] Yifang Zhao, Yuqian Gao, Dodging Zhan, Hui Liu, Qiang Zhao, Yuan Kou, Yuanhua Shao, Magician Li, Qiankun Zhuang and Zhiwei Zhu, *Talanta*, **66** (2005) 51.

[51] Lying Lin, Jinghua Chen, Hong Yao, Yuanzhong Chen, Yanjie Zheng, Xinhua Lin, *Bioelectrochemistry*, **73** (2008) 11.

[52] Afsaneh Safaris, Nitrous Maleki, Imran Moradlou, Arriba Tajabadi, *Analytical Biochemistry*, **359** (2006) 224.

[53] Rui Zhang, Gen-Di Jin, Da Chen, Xiao-Ya Hu, *Sensors and Actuators B*, **138** (2009) 174.

[54] Jianshe Huanga, Yang Liua, Haoqing Houb and Tianyan Youa, *Biosensors and Bioelectronics*, **24** (2008) 632.

[55] W. Sun, Z. Zhai, D. Wang, S. Liu and K. Jiao, *Bioelectrochem.*, **74** (2009) 295.

[56] J. Tashkhourian, M.R. Hormozi Nazca, J. khodavesi and S. Javadi, *J. Electroanal.Chem*., **633** (2009) 85.

[57] D. Ragupathy, A.I. Gopalana, K.P. Lee, *Sens. Actu B.*, **143** (2010) 696.

[58] Y. Wei, M. Li, S. Jiao, Q. Huang, G. Wang and B. Fang, *Electochim. Acta*, **52** (2006) 766.

[59] J. Li, X.Q. Lin, *Anal Chem Acta*, 596 (2007) 222.

[60] J. Eriksson, V. Khranovskyy, F. Soderlind, P.O. Kall, R. Yakimova and A.L. Septz, *Sens Actu.*, **37** (2009) 94.

[61] M.P. Rajeeva, C.S. Naveen, Ashok R. Leman and H.S. Jayanna, *AIP Conf. Proc*., **183** (2013) 1536.

[62] L. Patterson, *Phys. Rev. Online Arch. (Prola).*, **56** (1939) 978.

[63] Q.G. Von. Nehring, J.W. Hightower and J.L. Anderson, *Anal. Chem.*, **58** (1986) 2777.

[64] M.P. Siswana, K.I. Ozoemena, T. Nyokong, *Electrochim. Acta,* **52** (2006) 114.

[65] E.J. Laviron's, *Electroanal. Chem*., **52** (1974) 355.

Chapter-7

PART-A

Simultaneous Determination of Ciprofloxacin Hydrochloride and Enrofloxacin at Poly (Furosemide) Modified Carbon Paste Electrode by Cyclic Voltammetry

Ciprofloxacin Hydrochloride

Enrofloxacin

7.1. Introduction:

In this chapter, a poly (furosemide) modified carbon paste electrode (PFMCPE) was used for the sensitive voltammetric determination of ciprofloxacin hydrochloride (CIP) and Enrofloxacin (ENRO). The surface morphology of PFMCPE was characterized by SEM. The discussions involves the chemistry, biological relevance of CIP and ENRO and their oxidation behaviors in phosphate buffer solution at PFMCPE. It was found that the electrochemical behavior of the polymer film modified electrode depended on the film thickness of the polymer film. The electrochemical response of CIP and ENRO were investigated by cyclic voltammetric (CV) and differential voltammetric techniques (DPV). The effect of pH, concentration and sweep rate has been studied. The modified electrode was used for the simultaneous determination of CIP and ENRO in the phosphate buffer solution of pH 7.2. The linear relationship was obtained between the anodic peak current (I_{pa}) and concentration of ENRO and CIP in the range of 8×10^{-5} M to 1×10^{-3} M with correlation coefficient of 0.993, 0.9915 respectively. The low detection limit (LOD) and low quantification limit (LOQ) of ENRO and CIP were detected. This modified electrode was successfully used for the simultaneous determination of CIP and ENRO by resolving the overlapped voltammetric peaks by using cyclic voltammetry. The modified electrode showed high sensitivity, detection limit, high reproducibility, easy preparation and regeneration of the electrode surface.

7.2. Chemistry and Biological Relevance of Ciprofloxacin Hydrochloride and Enrofloxacin

The chemistry and biological relevance of ciprofloxacin hydrochloride has been explained in details in chapter 4 section 4.2. In this work, two important fluoroquinolones, namely Enrofloxacin (1-cyclopropyl-7-(4-ethyl-1-piperazinyl)-6-fluoro-1,4-dihydro- 4-oxo-3-quinolonecarboxylic acid) and ciprofloxacin (1-cyclopropyl-7-(1-piperazinyl)-6-fluoro-1,4-dihydro-4-oxo-3-quinolinecarboxylic acid), were investigated and quantitatively analyzed by voltammetric methods. In several

animal species, including pigs, Enrofloxacin (ENRO) is de-ethylated to its primary metabolite, ciprofloxacin (CIPRO) [1] and both ENRO and CIPRO are found in the bile and urine of animals receiving ENRO [2].

ENRO has been historically used as veterinary medicine for treatment of gastrointestinal and respiratory infections in several animal species, including pigs cursing diseases caused by gram-positive and negative bacteria. Enrofloxacin is used to prevent and treat pneumonia and E.coli bacterial diarrhea syndrome in cows and pigs. Due to these many problems, a lot of researchers have been carried out to remove antibiotics.

7.3. Review of electrochemistry of Ciprofloxacin Hydrochloride and Enrofloxacin

Several analytical techniques have been used for the determination of ENRO and CIPRO including liquid chromatography [3-6], capillary electrophoresis with diode array detection [7] and molecularly imprinted matrix solid-phase dispersion [8]. Electrochemical methods, such as polarography and voltammetry, have high sensitivity and are widely used in many areas of analytical chemistry. Recently, cathodic adsorptive stripping voltammetry on a static mercury drop electrode and principal-component regression have been applied for the determination of ENRO in the presence of CIPRO [9] at trace levels. However, the linear dynamic range of the method is too narrow, and the toxicity of mercury (as an electrode) has caused its application in routine laboratories to decline. At more negative potentials, many biological compounds are adsorbed on the surface of the Hg-electrode, diminishing the selectivity of the method [9].The linear sweep voltammetry (LSV) used for the first time with a multiwall carbon nanotubes/glassy carbon electrode (MWCNT/GCE) for the determination of ENRO or CIPRO has been studied by Ali A. Ensafi et al., [10].

In this work, cyclic voltammetry (CV) and differential pulse voltammetric (DPV) techniques were used for poly (FUR) modified carbon paste electrode which provides a sensitive method for the determination of ENRO and CIP simultaneously.

7.4. Experimental section

7.4.1. Reagents

Ciprofloxacin Hydrochloride, Enrofloxacin and Furosemide were purchased from Merck, Himedia chemicals and all other chemicals were of analytical grade. The electropolymerisation of furosemide was performed in 0.1 M phosphate buffer solution. The phosphate buffer solution was prepared from KH_2PO_4 and K_2HPO_4 and the pH was adjusted with 0.1N NaOH solution. The 10 mM stock solution of CIP was prepared by dissolving in water and ENRO dissolving in 0.1N acetic acid respectively. Other chemicals used were of analytical grade except for spectroscopically pure graphite powder. All solutions were prepared with doubly distilled water.

7.4.2. Apparatus

Electrochemical measurements were carried out with a model-201 electrochemical analyzer (EA-201 chemlink systems) in a conventional three-electrode system. The working electrode was carbon paste electrode, having cavity of 3 mm diameter. The counter electrode was platinum electrode with a saturated calomel electrode (SCE) as a standard reference electrode for completing the circuit.

7.4.3. Preparation of bare carbon paste electrode

The bare carbon paste electrode was prepared by hand mixing of graphite powder 70% and silicon oil 30% in an agate mortar for about 30 min to get homogenous carbon paste. The paste was then packed into the cavity of a Teflon tube electrode (3 mm diameter). Before measurement, the modified electrode was smoothened on a piece of transparent paper to get a uniform, smooth and fresh surface.

7.4.4. Preparation of poly (furosemide) modified carbon paste electrode (PFMCPE)

Electrochemical polymerization process of furosemide (FUR) has been carried by using cyclic voltammetric in potential range -200 to 1400 mV at scan rate of 50 mVs^{-1} in phosphate buffer solution (PBS) of pH 4.5. The monomer concentration was usually 1 mM. After 10 cycles, the surface of the electrode was washed with doubly distilled water to remove the physically adsorbed material. This modified electrode was immersed in PBS and electrochemical determination of CIP and ENRO was carried out in a voltammetric cell in the potential range from -200 mV to 1400 mV. The same procedure was applied for all the sample analysis and all electrochemical measurements were carried out at room temperature.

7.5. Result and Discussion

7.5.1. Electropolymerisation of Furosemide on a carbon paste electrode

Electrochemical polymerization process has been carried out for furosemide (FUR) by using carbon paste electrode modified with electropolymerised film of furosemide. A solution of monomer furosemide is oxidized to an activated form that polymerizes to form a polymer film directly on the electrode surface. This procedure results in few pinholes since polymerization would be accentuated at exposed (pinholes) sites at the electrode surface. Electro catalysis at a modified electrode is usually an electron transfer reaction between the electrode and solution substrate which, when mediated by an immobilized redox couple (i.e., the mediator) proceeds at a lower over potential and enhances the peak current. Electropolymerisation of furosemide was fabricated in 0.1 M phosphate buffer solution containing 1 mM furosemide on CPE. The film was grown on CPE by cyclic voltammetric scans between -200 to 1400 mV. The optimized scan number under the experimental conditions was determined as 10 for reaching the steady response. As shown in **Fig. 7.1,** in the first cycle, with the potential scanning from -200 to 1400 mV the two anodic peaks were observed at 885 & 1091 mV corresponding to the oxidation of Furosemide (FUR). The peak descended gradually

with the increase in cyclic time; such decrease indicates the poly (FUR) membrane forming and depositing on the surface of the carbon paste electrode by electropolymerisation. FUR was oxidized to free radical at the surface of carbon paste electrode rapidly resulting in the possible structure of electropolymerised poly (FUR). After polymerization the poly (FUR) modified carbon paste electrode was carefully rinsed with distilled water to remove the physically adsorbed material. Then the film electrode was transferred to an electrochemical cell and cyclic voltammetric sweeps were carried out to obtain electrochemical steady state.

7.5.2. Effect of the poly (FUR) film thickness on the electrochemical response of Ciprofloxacin hydrochloride (CIP) and Enrofloxacin (ENRO)

The thickness of poly (FUR) film could be controlled by the cyclic number of voltammetric scans during the electrochemical modification. The effect of the thickness of poly (FUR) film on the electrochemical response was investigated by cyclic voltammetric technique. The anodic peak current (I_{pa}) response of poly (FUR) films increase gradually as the number of cycles increases during film formation from 5 to 10 cycles. Afterwards I_{pa} starts to decrease by increasing the number of cycles which was examined up to 30 cycles **(Fig. 7.1a),** In order to obtain better oxidation peaks and higher sensitivity of current for the electrochemical response of CIP and ENRO. 10 scans were chosen to control the thickness of the poly (FUR) film.

7.5.3. SEM Characterization of poly (FUR) modified carbon paste electrode (PFMCPE)

Fig. 7.2a and **Fig. 7.2b** explain the surface morphology of bare carbon paste electrode (BCPE) and modified carbon paste electrode respectively using scanning electron microscope (SEM). The surface of bare CPE was formed by irregularly shaped micrometer-sized flakes of graphite. Whereas modified electrode had a typical uniform arrangement of on the surface of PFMCPE [11].

7.5.4. Electrochemical investigation of potassium ferrocyanide at poly (FUR) modified carbon paste electrode (PFMCPE)

The electrochemical response of 1mM $K_4[Fe(CN)_6]$ in 1 M KCl at bare CPE and poly (FUR) modified carbon paste electrode (PFMCPE) are shown in the **Fig 7.3.** The cyclic voltammograms of $K_4[Fe(CN)_6]$ at PFMCPE (curve 'a') showed that the redox peak current increased than that of bare CPE (curve 'b'). At the bare CPE the cyclic voltammograms of $K_4[Fe(CN)_6]$ showed a pair of redox peaks, anodic peak potential E_{pa} at 245 mV with peak current I_{pa} 6.45 µA and the cathodic peak potential E_{pc} at 124 mV with peak current I_{pc} 6.23. Whereas for poly (FUR) modified carbon paste electrode a pair of redox peaks of $K_4[Fe(CN)_6]$ were observed with greatly increase of the peak current. The anodic peak potential E_{pa} at 263 mV with peak current of 24.93 µA and the cathodic peak potential E_{pc} at 182 mV with peak current of 18.59 µA respectively. The results of the enhancement of peak current showed excellent catalytic ability of poly (FUR) modified carbon paste electrode. The bare Caron paste electrode is 0.024 cm^2, whereas the effective area of the modified electrode was found to be 0.032 cm^2.

7.5.5. Electrochemical response of ciprofloxacin hydrochloride (CIP) at poly (FUR) modified carbon paste electrode:

Ciprofloxacin hydrochloride (CIP) was investigated in 0.1 M phosphate buffer solution of pH 4.5 at PFMCPE using cyclic voltammetric technique. **Fig. 7.4** shows cyclic voltammograms of 0.1mM CIP at bare carbon paste electrode (curve 'b') and at PFMCPE. Curve 'c' represent cyclic voltammograms of blank solution at PFMCPE. Above studies showed that one oxidation peak at 1090 mV potential with peak current 12.41 µA at bare CPE , whereas an oxidation peak at 1063 mV potential with peak current of 41.6 µA at poly (FUR) modified carbon paste electrode in the potential range from 500 to 1400 mV. The peak was observed in the irreverse scan, suggesting that the electrochemical reaction is a totally irreversible process.

7.5.6. Electrochemical response of Enrofloxacin (ENRO) at poly (FUR) modified carbon paste electrode

Fig.7.5 shows cyclic voltammograms of 0.1 mM ENRO at bare carbon paste electrode (curve 'b') and at PFMCPE (curve 'a'). The curve 'c' represents cyclic voltammograms of blank solution at PFMCPE. Two oxidation peaks at 891 and 1123 mV potential with a peak current 14.4 and 27.4 µA respectively at bare CPE, whereas two oxidation peaks at 891 and 1113 mV potential with peak current of 44.3 and 67.4 µA respectively at PFMCPE. The curve 'c' represent cyclic voltammograms of blank solution at PFMCPE in the potential range from -200 to 1400 mV. No reduction peak was observed in the reverse scan, suggesting that the electrochemical reaction is a totally irreversible process.

7.5.7. Effect of pH on CIP and ENRO

To optimize the electrochemical response of modified carbon paste electrode for the oxidation of CIP, the effect of pH on the electrode response was studied. As the pH increase from 2 to 9, the anodic peak current shifted towards the negative side the well oxidation peak arrived at pH 4.5 **(Fig.7.6a)** and value of slope obtained was 42.23 mV/pH **(Fig.7.6b)**.The plot of E_{pa} versus pH clearly indicates that the catalytic peak shift to a more negative potential with increasing the pH.

To study effect of pH on ENRO, the electro oxidation of ENRO of 0.1 mM stock solution in 0.1 M PBS over pH range from 2 to 8.5 at a scan rate of 50 mVs^{-1} at PFMCPE using cyclic voltammetric technique has been studied. The anodic peak current decreases with increase of pH from 2 to 7 and becomes maximum and peak potential shifted negatively at pH 7. While pH beyond 7, a great decrease of the oxidation peak current could be observed, then it decreased gradually with the further increase in pH of the solution as shown in **Fig.7.7.**

7.5.8. Effect of scan rate on CIP and ENRO

The effect of scan rates on the electrochemical response of CIP at poly (FUR) modified carbon paste electrode was studied and the cyclic voltammograms are shown in **Fig.7.8a**. It was found that with the increase of the scan rate, oxidation peak current increased gradually and the oxidation peak potential shifted towards more positive potential. A linear relationship of anodic peak current versus scan rate in the range from 10 to 150 mVs^{-1} with correlation coefficient of 0.9926 is shown in **Fig.7.8b.** However, the linear relationship with a correlation coefficient of 0.9837 obtained between the anodic peak current and square root of scan rate in **Fig.7.8c** with the linear regression equation is given by

$$I_{pa}\,(\mu A) = 0.0128\ \nu^{1/2} + 17.380 \quad R = 0.9823 \ldots\ldots\ldots\ldots\ldots\ldots\ldots\ldots\ (7.1)$$

Which revealed that a diffusion controlled process occurring at poly (FUR) modified carbon paste electrode.

According to Randles Sevick's equation, increase in the scan rate increase the peak current. Poly (FUR) modified carbon paste electrode showed increase in the peak current with increase in the scan rate from 10 to 100 mVs^{-1} in the presence of 0.1 mM ENRO in 0.1 M phosphate buffer solution of pH 7. The plot of anodic peak current against scan rate is shown in **Fig. 7.9a**. The corresponding linear regression equation is

$$I_{pa}\,(\mu A) = 0.912\ \nu + 22.68 \quad R = 0.9957 \ldots\ldots\ldots\ldots\ldots\ldots\ldots\ldots\ (7.2)$$

As shown in **Fig.7.9b** the linear relationship with a correlation coefficient of 0.9837 obtained between the anodic peak current and square root of scan rate in the range of 10 - 100 mVs^{-1}. The corresponding linear regression equation is

$$I_{pa}\,(\mu A) = 0.12051\ \nu^{1/2} + 12.787 \quad R = 0.9837 \ldots\ldots\ldots\ldots\ldots\ldots\ldots\ (7.3)$$

Which revealed that a diffusion controlled process occurring at poly (FUR) modified carbon paste electrode.

According to Laviron's theory [12], the slope is equal to $RT/\alpha n_\alpha F$. Then the value of αn_α was found to be 0.4542. For a totally irreversible electrode reaction process of CIP and ENRO the n_α was calculated as 1.646 and 1.705 respectively. Which indicated that two electrons were involved in the oxidation process of CIP and ENRO at poly (FUR) modified carbon paste electrode. The electrochemical reaction process for CIP and ENRO at poly (FUR) modified carbon paste electrode can therefore be summarized as in **scheme 7.1**.

7.5.9. Effect of Ciprofloxacin Hydrochloride and Enrofloxacin concentration at poly (FUR) modified carbon paste electrode (PFMCPE)

The effect of concentration of CIP and ENRO were studied at poly (FUR) modified carbon paste electrode in 0.1 M phosphate buffer solution of pH 6 and pH 7.2 with scan rate of 10 mVs^{-1} and 50 mVs^{-1} respectively by CV. The anodic peak current of CIP and ENRO increase with increase in concentration as shown in **Fig. 7.10a** and **Fig. 7.10b**. The plot of anodic peak current vs. concentration showed that concentration is proportional to electrochemical peak current is shown in **Fig.7.11a** and **Fig.7.11b**, a linear concentration range was found to occur from 8×10^{-5} to 1.0×10^{-3} M and can be described by the linear regression equations for CIP and ENRO respectively were expressed as:

I_{pa} (µA) = 94.794 C (10^{-5} M) + 32.379 R= 0.9915…….. (7.3)

I_{pa} (µA) = 39.108 C (10^{-5} M) + 35.108 R= 0.9936……. (7.4)

The limit of detection (LOD) and limit of quantification (LOQ) were 1.508, 4.526 µM for CIP and 1.335, 4.451µM for ENRO.

The LOD and LOQ were calculated on the peak current using the following equation:

LOD= 3S/M and LOD=10S/M

Where, S is standard deviation and M is the slope of calibration plot.

7.5.10. Simultaneous detection of ENRO and CIP at ploy (FUR) modified carbon paste electrode (PFMCPE)

In order to examine the sensitivity and selectivity of poly (FUR) modified carbon paste electrode the electrochemical behavior of a mixture of 0.1 mM ENRO and 0.5 mM CIP in 0.1M PBS of pH.7.2 was investigated using cyclic voltammetry. **Fig.7.12** shows the cyclic voltammograms obtained for ENRO and CIP coexisting at bare CPE and at PFMCPE. At bare CPE curve 'b' shows unable to separate the voltammetric signals of ENRO and CIP. Only broad voltammetric signals for ENRO and CIP were observed at approximately 1008 mV. Therefore it is impossible to use bare electrode for the voltammetric determination of CIP in the presence of ENRO. For the PFMCPE voltammetric signals are resolved into three peaks potentials at 840 and 970 mV for ENRO and at 1144 mV for CIP are observed (Curve 'a'). This is because ENRO exist as anionic form in pH 7.2, phosphate buffer solution and hence the electrostatic repulsion between the ENRO anions and the negatively charged groups on the electrode surface retarded the electron transfer and shifted the oxidation potential of ENRO towards more negative value so that the oxidation peak of CIP could be separated from that of ENRO. The ENRO is readily oxidized well before the oxidation potential reached, so the catalytic oxidation of ENRO is possible at the PFMCPE. The separation between the oxidation peaks of CIP and ENRO was 189 mV. Therefore the simultaneous determination of CIP and ENRO at poly (FUR) modified carbon paste electrode is possible.

7.6. CONCLUSION

- This modified electrode exhibited high electrocatalytic activities towards the oxidation of CIP and ENRO by significantly increasing their oxidation over potentials and enhancing the peak currents.

- The electrochemical response is diffusion controlled and irreversible in nature for CIP and ENRO respectively.

- The probable reaction mechanism involved in the oxidation of CIP and ENRO were also proposed.

- Peak separation between CIP and ENRO could be obtained using cyclic voltammetry, indicating that the poly (FUR) modified carbon paste electrode facilitated their simultaneous determination. This electrochemical sensor showed excellent selectivity and high sensitivity.

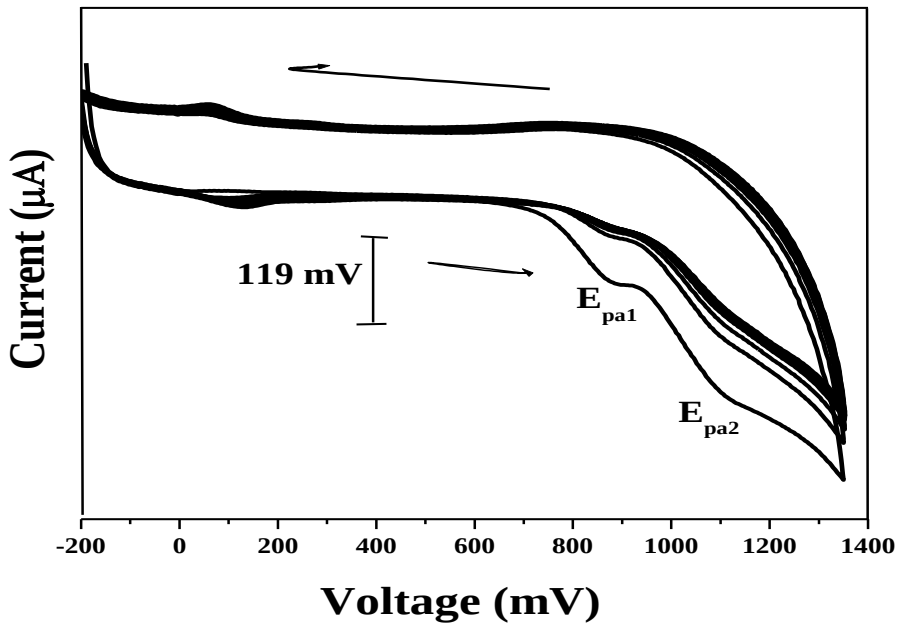

Fig. 7.1: Cyclic voltammograms for the electro polymerization of 1 mM of FUR 0.1 M phosphate buffer solution on CPE, - 200 to 1400 mV, Scan rate 50 mVs^{-1}.

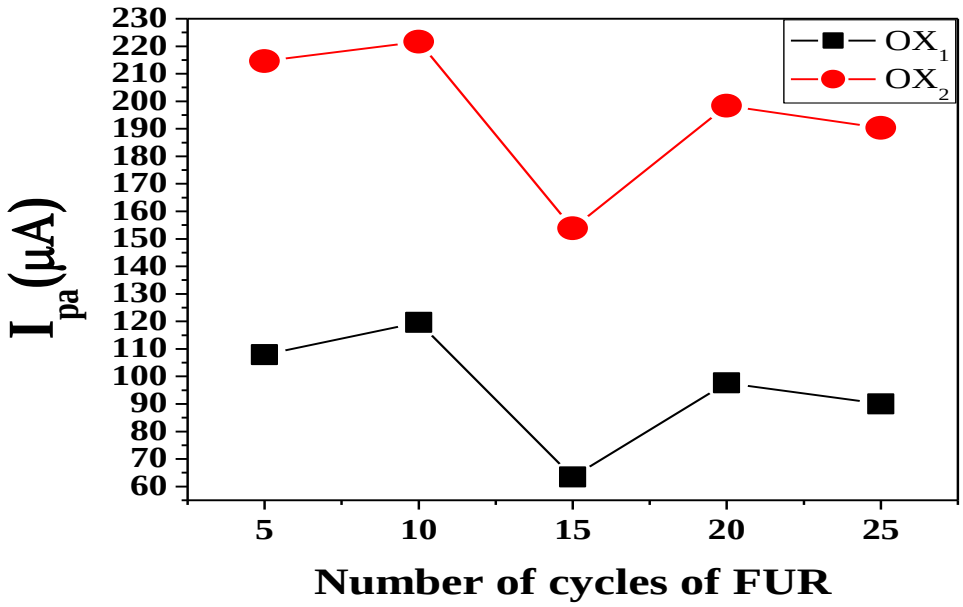

Fig. 7.1a: Anodic peak current v/s. number of cycles of FUR.

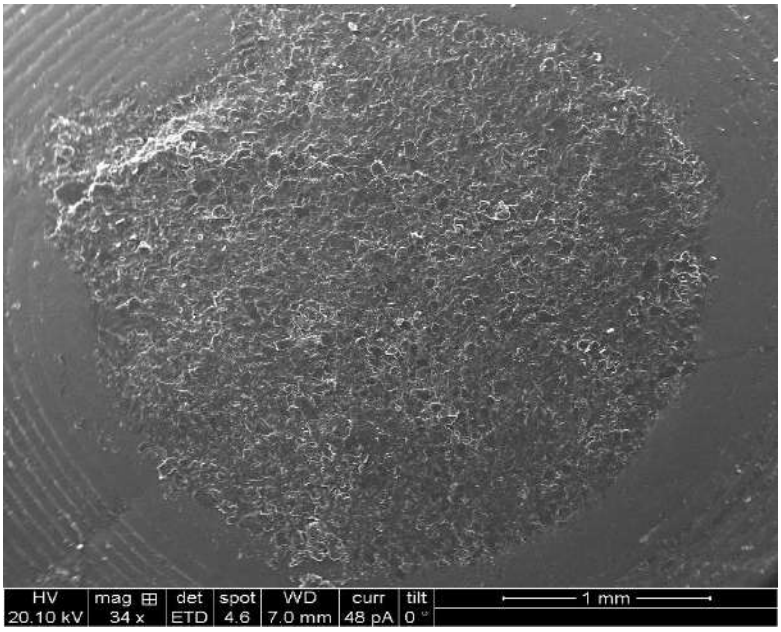

Fig.7.2a: SEM images of bare carbon paste electrode.

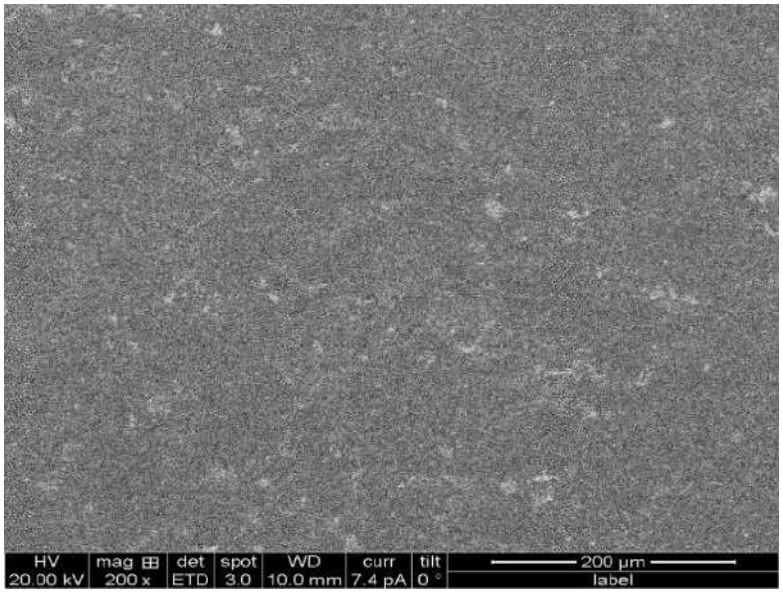

Fig.7.2b: SEM images of poly (FUR) modified carbon paste electrode.

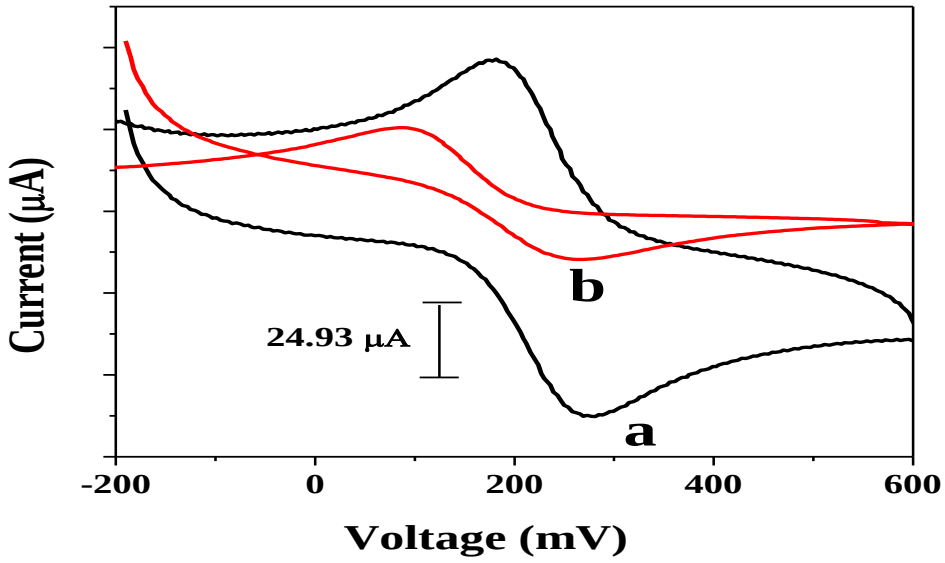

Fig. 7.3: Comparison of 1 mM $K_4[Fe(CN)_6]$ in 1 M KCl solution at poly (FUR) modified carbon paste electrode (a) and at bare carbon paste electrode (b).

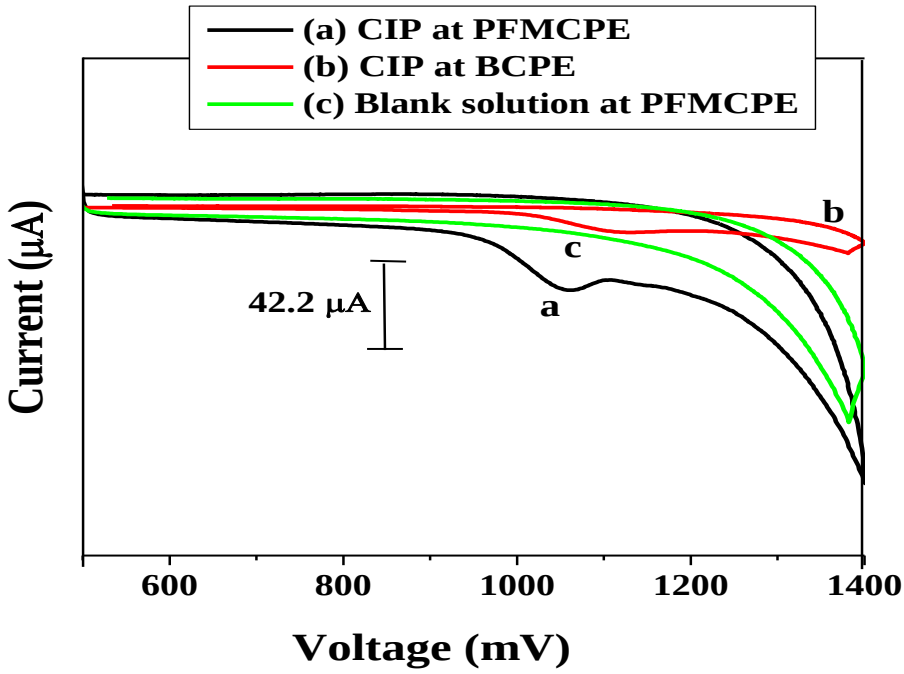

Fig. 7.4: Comparision of 0.1 mM CIP at poly (FUR) modified carbon paste electrode (a), bare carbon paste electrode (b) and blank solution in 0.1M phosphate buffer at poly (FUR) modified carbon paste electrode (c), scan rate of 10 mVs^{-1}.

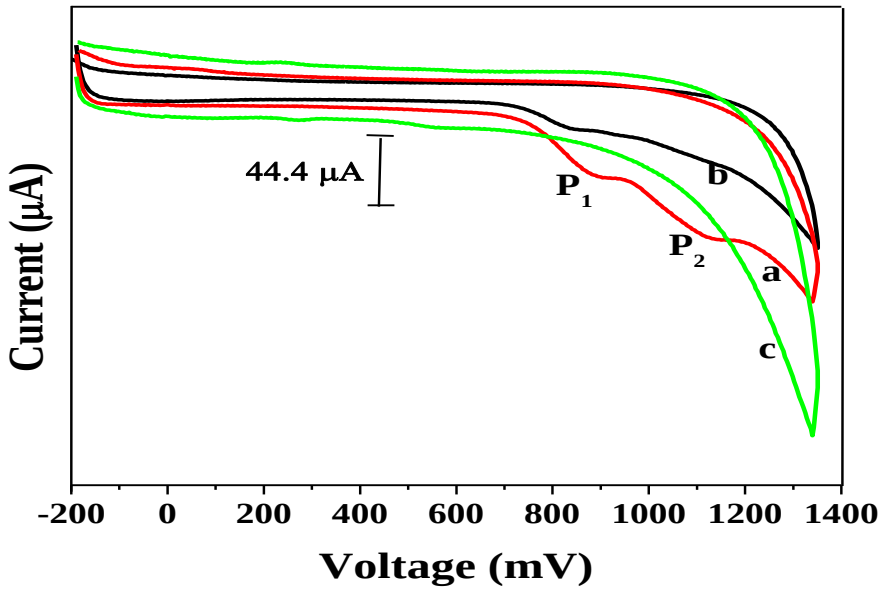

Fig. 7.5: Comparision of 0.1 mM ENRO at poly (FUR) modified carbon paste electrode (a), bare CPE (b) and blank solution in 0.1 M phosphate buffer at poly (FUR) modified carbon paste electrode (c), scan rate 50 mVs^{-1}.

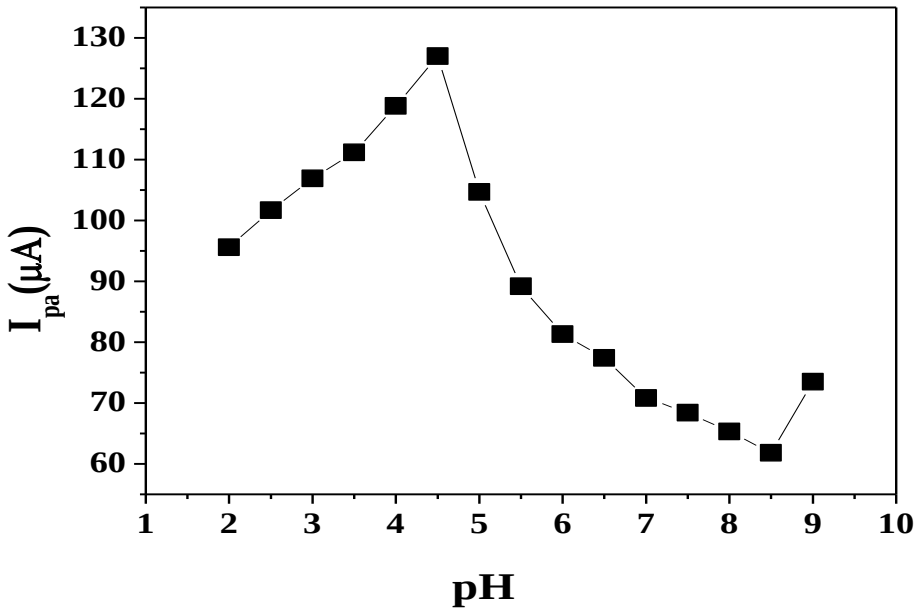

Fig. 7.6a: Plot of anodic peak current vs. pH (2 - 9) of 0.1 mM CIP at the poly (FUR) modified carbon paste electrode.

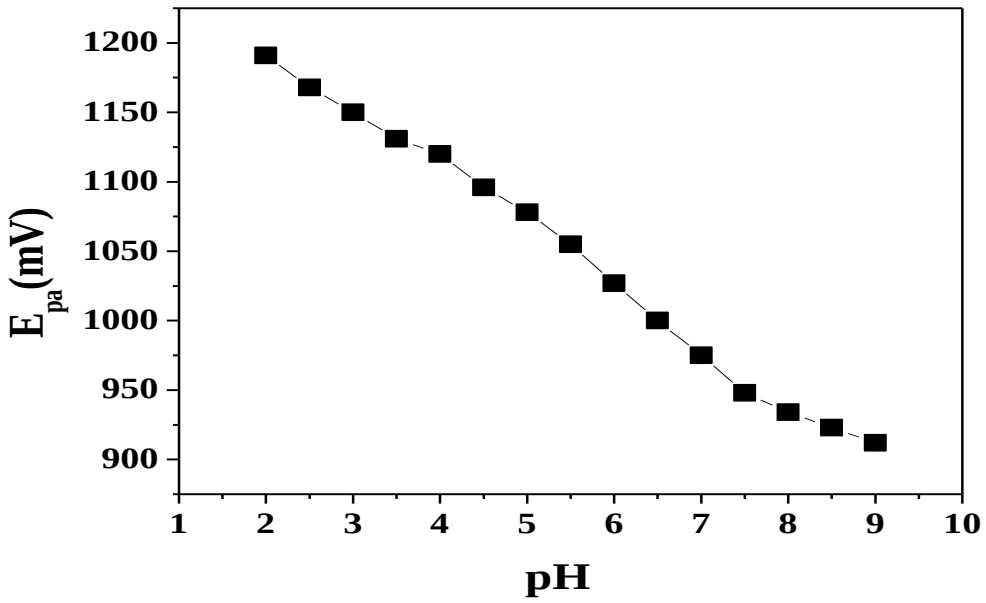

Fig. 7.6b: Plot of anodic peak potential vs. pH (2 – 9) of 0.1 mM CIP at poly (FUR) modified carbon paste electrode.

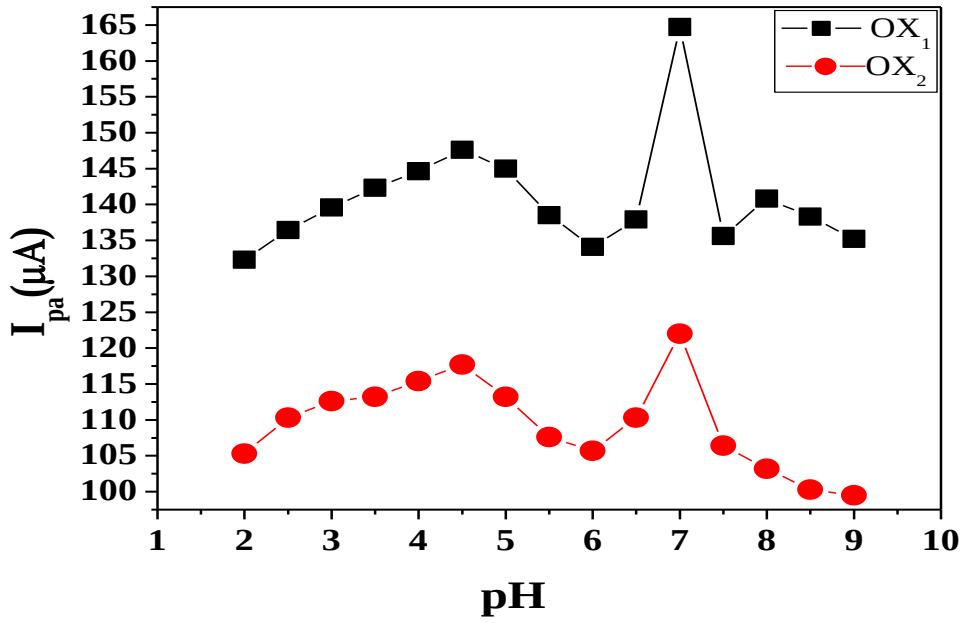

Fig. 7.7: Plot of anodic peak current vs. pH (2 - 9) of 0.1 mM ENRO at poly (FUR) modified carbon paste electrode.

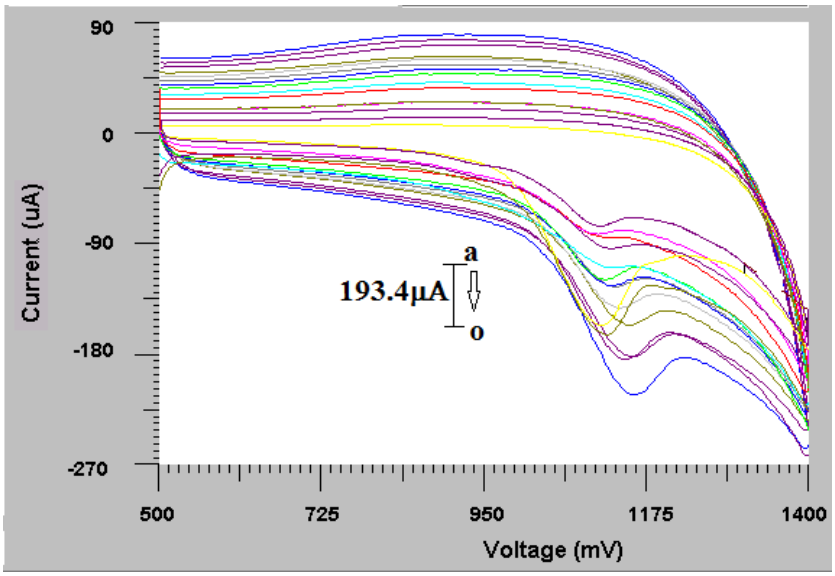

Fig. 7.8a: Cyclic voltammograms of 0.1 mM CIP at poly (FUR) modified carbon paste electrode with different scan rates (a) 10, (b) 20, (c) 30, (d) 40, (e) 50, (f) 60, (g) 70, (h) 80, (i) 90, (j) 100 (k) 110 (l) 120 (m) 130 (n) 140 (o) 150 mVs^{-1}.

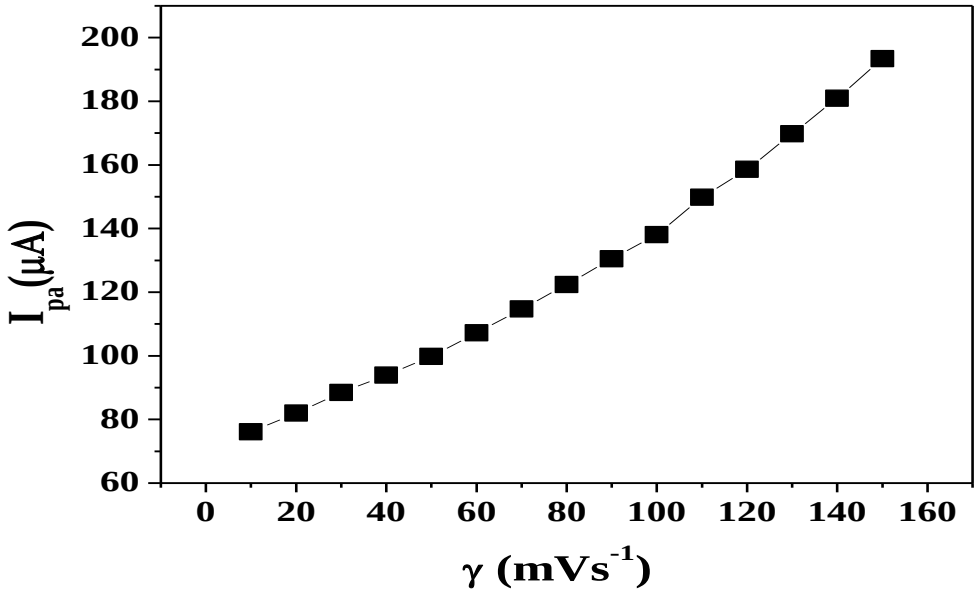

Fig. 7.8b: Plot of anodic peak current vs. scan rates of CIP at poly (FUR) modified carbon paste electrode

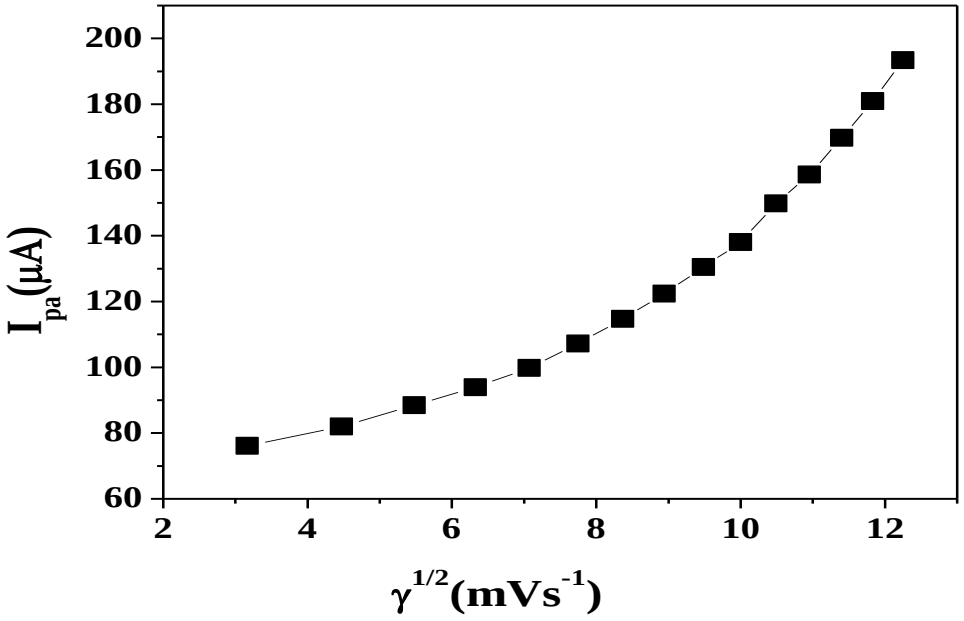

Fig. 7.8c: Plot of anodic peak current vs. square root of scan rates of CIP at poly (FUR) modified carbon paste electrode.

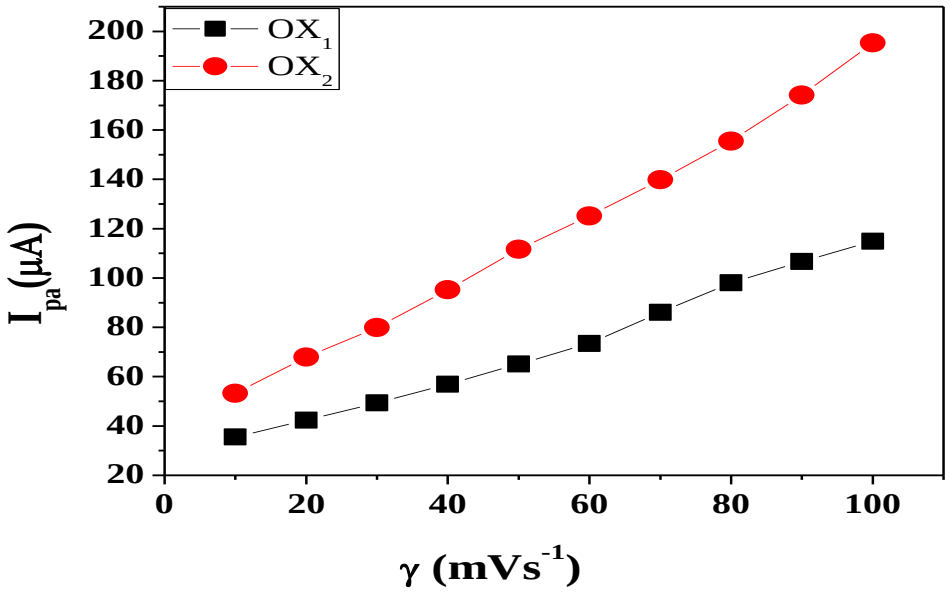

Fig. 7.9a: Plot of anodic peak current vs. scan rates of ENRO at poly (FUR) modified carbon paste electrode.

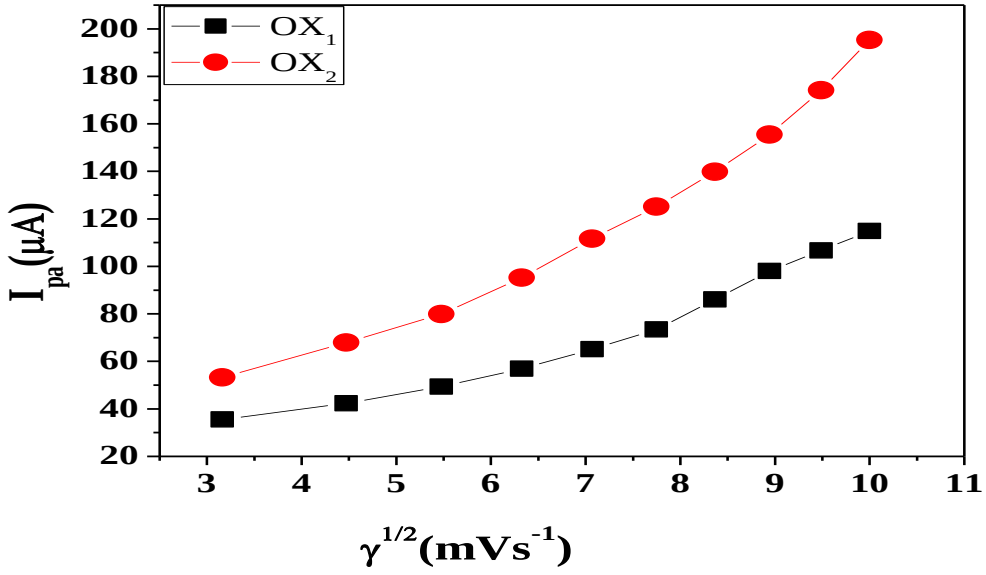

Fig. 7.9b: Plot of anodic peak current vs. square root of scan rates of ENRO at poly (FUR) modified carbon paste electrode.

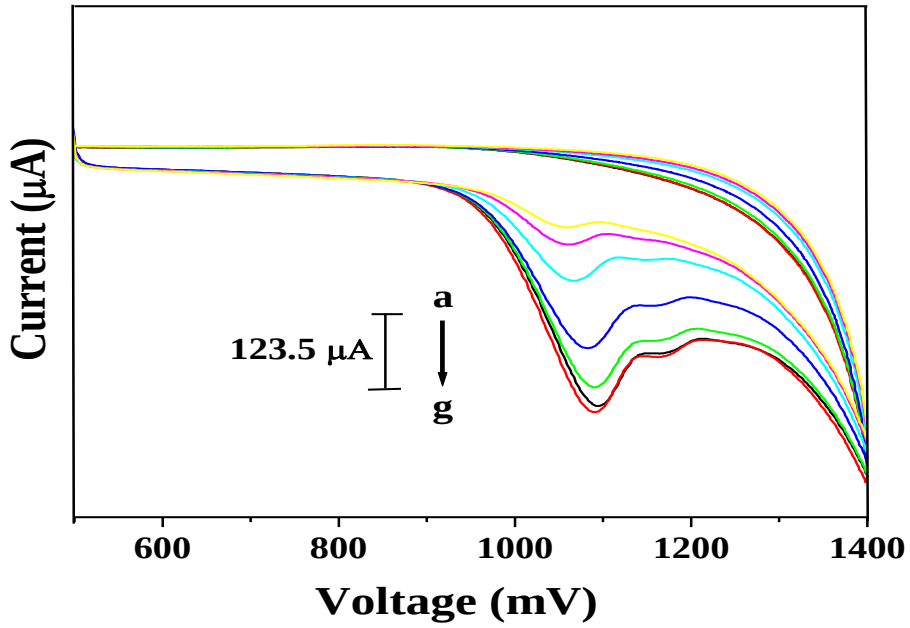

Fig. 7.10a: Effect of variation of concentration of CIP (a) 8×10^{-4} M, (b) 1×10^{-4} M, (c) 2×10^{-4} M, (d) 4×10^{-4} M, (e) 6×10^{-4} M, (f) 8×10^{-4} M, (g) 1×10^{-3} M on anodic peak current at poly (FUR) modified carbon paste electrode; scan rate 10 mVs^{-1}.

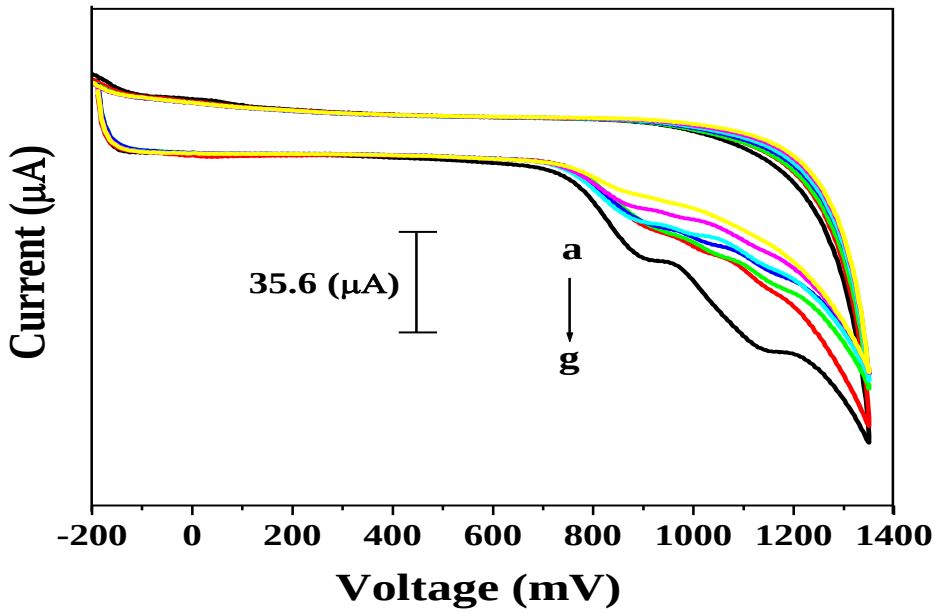

Fig. 7.10b: Effect of variation of concentration of ENRO (a) 8×10^{-4} M, (b) 1×10^{-4} M, (c) 2×10^{-4} M, (d) 4×10^{-4} M, (e) 6×10^{-4} M, (f) 8×10^{-4} M, (g) 1×10^{-3} M on anodic peak current at poly (FUR) modified carbon paste electrode; scan rate 50 mVs^{-1}.

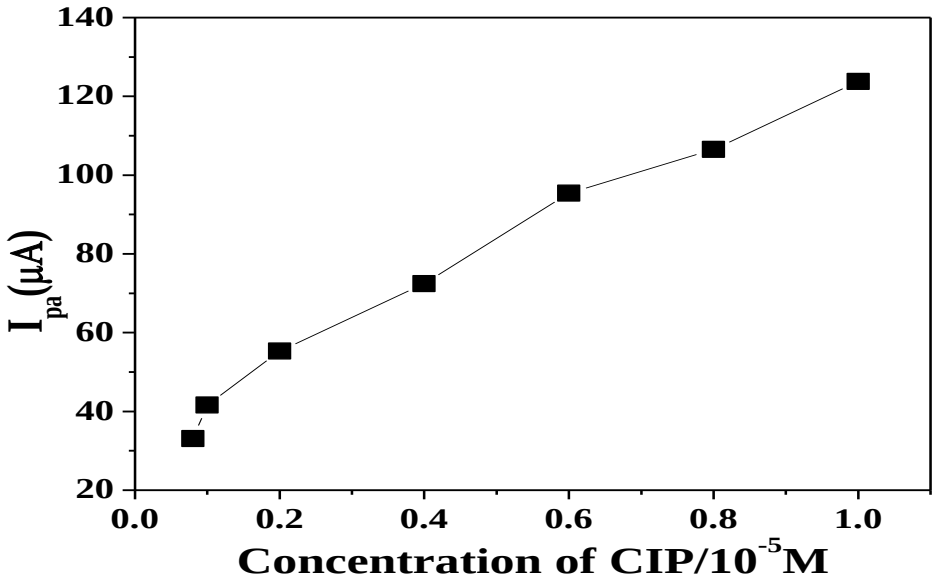

Fig. 7.11a: Plot of anodic peak current vs. CIP concentration at poly (FUR) modified carbon paste electrode.

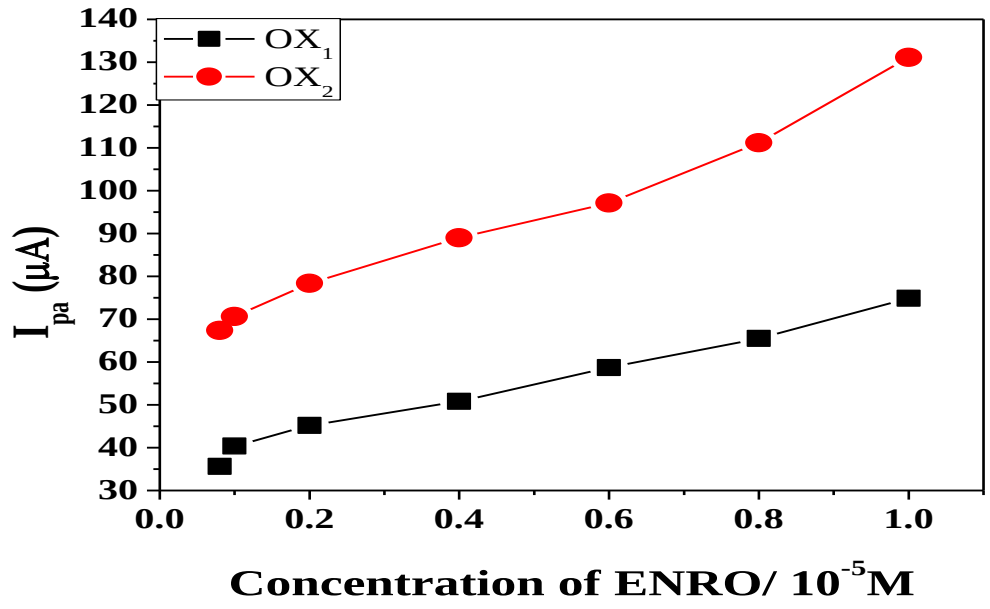

Fig. 7.11b: Plot of anodic peak current vs. ENRO concentration at poly (FUR) modified carbon paste electrode.

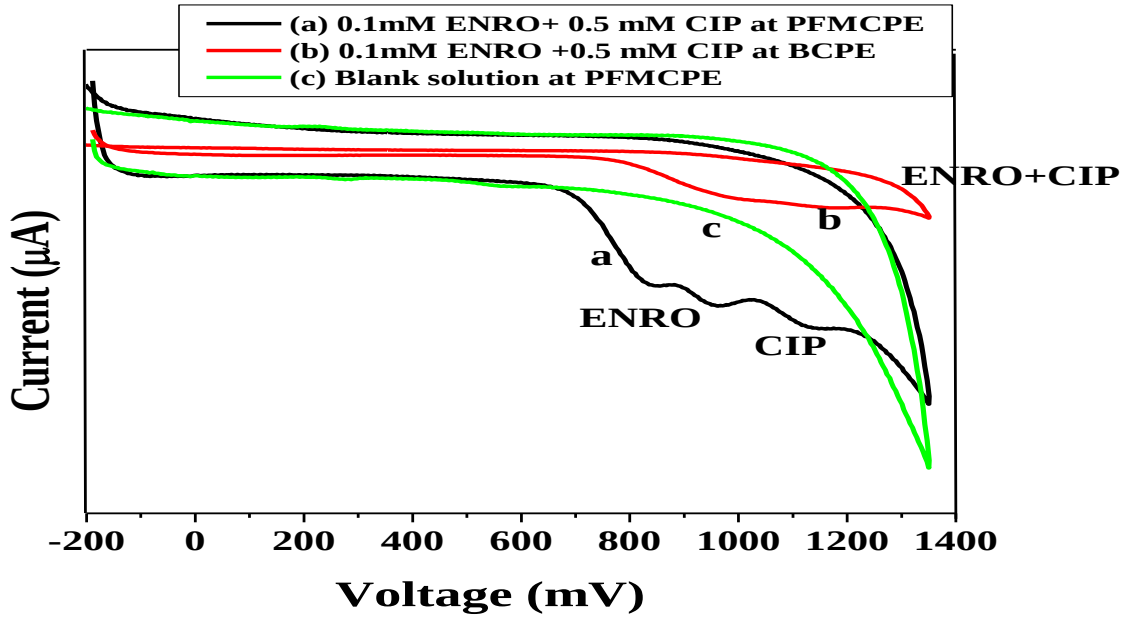

Fig.7.12: Cyclic voltammograms at poly (FUR) modified carbon paste electrode (a), bare carbon paste electrode (b) in presence of 0.1 mM ENRO and 0.5 mM CIP, blank solution in 0.1 M PBS at poly (FUR) modified carbon paste electrode (c); pH 7.2, scan rate 50 mVs^{-1}.

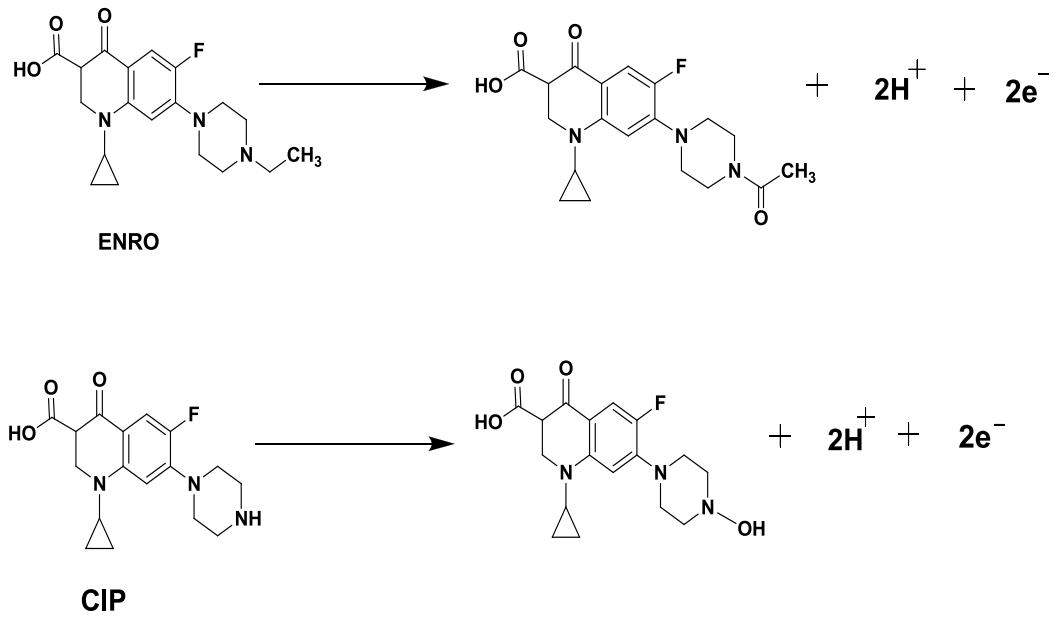

Scheme 7.1: Probable oxidation mechanism of ENRO and CIP

7.7. References

[1] J.C. Yorke, P. Froc, *J. Chromatogr. A.*, 882 (2000) 63.

[2] K. Tyczkowska, K.M. Hedeen, D.P. Aucoin and A.L. Aronson, *J. Chromatogr*., 493 (1989) 337.

[3] M.A. Garcia, C. Solans, J.J. Aramayona, S. Rueda, M.A. Bregante and A. de Jong, *Biomed. Chromatogr*., **13** *(*1999) 350.

[4] J. Sunderland, A.M. Lovering, C.M. Tobin, A.P. McGowan, J.M. Roe and A.A. Delsol, *Int. J. Antimicrob. Agents*, **23** (2004) 390.

[5] M.A. Garcia, C. Solans, E. Hernandez, M. Puig and M.A. Bregante, *J. Chromatogr., A*, **54** (2001) 191.

[6] S. Bailac, O. Ballesteros, E. Jiménez-Lozano, D. Barrón, V. Sanz - Nebot, A. Navalón, J. L. Vílchez and J. Barbosa, *J. Chromatogr. A.*, **1029** (2004) 145.

[7] H.W. Sun, P. He, Y.K. Lv and S.X. Liang, *J. Chromatogr. B.*, **852** (2007) 145.

[8] H. Sun, F. Qiao, G. Liu and S. Liang, *Anal. Chim. Acta*, **625** (2008) 154.

[9] A. Navalón, R. Blanc, L. Reyes, N. Navas and J.L. Vílchez, *Anal. Chim. Acta*, **454** (2008) 83.

[10] Ali A. Ensafi, M. Taei, T. Khayamian and F. Hasanpour, *Analytical sciences*, **26** (2010) 803.

[11] C.A. Caro, F. Bedioui, J.H. Zagal, *Electrochim. Acta*, **47** (2002) 1489.

[12] E.J. Laviron's, *Electroanal. Chem.*, **52** *(*1974) 355.

Chapter-7

PART - B

Electrochemical Investigation of Uric acid at Poly (Isoniazid) film Modified Carbon Paste Electrode

Uric acid

7.8. Introduction

In this chapter the determination of uric acid in 0.2 M phosphate buffer solution of pH 5 at poly (Isoniazid) film modified carbon paste electrode (PINHMCPE) by cyclic voltammetry has been carried out. The discussion involves the chemistry and biological relevance of uric acid (UA). The carbon paste electrode (CPE) was modified by isoniazid. The surface morphology of PINHMCPE was studied by scanning electron microscope (SEM). PINHMCPE showed very good sensitivity for uric acid compared to bare carbon paste electrode (BCPE). The effect of pH, scan rate, concentration of UA at PINHMCPE was studied. The oxidation of peak current is a linear dependence on UA concentration from 0.01 mM to 1 mM with correlation coefficient of 0.99442. The low detection limit (LOD) and low detection quantification (LOQ) were found to be 1.173 µm and 3.910 µm. The preparation of the modified electrode is easy and renewed by simple polishing gives very good reproducibility, high stability in its voltammetric response and low detection limit for UA.

7.9. Chemistry and Biological Relevance of Uric acid

Uric acid (UA) (2, 6, 8-trihydroxypurine) **(Scheme. 7.8)** is the primary product of purine metabolism in the human body. The chemistry and biological relevance of UA has been explained in detail in chapter 6 section 6.2.

7.10. Review of Electrochemistry of Uric acid

Extreme abnormalities of UA concentration levels may lead to several diseases and it is essential to develop a simple and rapid method for the determination of UA for routine analysis. In recent years polymer film-modified electrodes have attracted great attention, because of their good stability, reproducibility and their wide applications in the fields of chemical sensors and biosensors [1 - 4]. When polymer modified electrodes (PMEs) were used, carbon-base electrodes have been primarily used compared to metal electrodes due to its biocompatibility with tissue, having low residual current over a

wide potential range and minimal propensity to show a deteriorated response as a result of electrode fouling up to now different methodologies have been used to prepare polymeric film-modified electrodes. Among them electropolymerisation yields a modified electrode with a three-dimensional distribution of mediators. This type of electrodes enhances the sensitivity and improves the catalytic activity than monolayers.

The designing, fabrication and application of sensitive and selective electrochemical sensors are considerable interest in recent years. Fu Yong Zhao *et al.,* [5] studied a simple, fast, precise and eco-friendly analytical method for the determination of uric acid (UA) in human urine by ion chromatography (IC) was established. Hairul Hisham Hamzah *et al.,* [6] studied a simple spectrophotometric method. R.R. Marquardt *et al.,* [7] studied a high-performance liquid chromatographic assay for uric acid in excreta and tissue samples. The levels of uric acid in different biological matrices such as urine and serum have been determined by numerous standard analytical methods such as reversed phase liquid chromatography [8], potentiometric enzyme electrode [9] and flow injection analysis system with tubular amperometric detector [10]. Shengf Wang *et al.,* [11] have reported a carbon-coated iron nanoparticles (CIN, a new style fullerenes related nanomaterial) modified glassy carbon electrode (CIN/GCE) for the determination of uric acid (UA). Murat sadikoglu *et al.,* [12] have prepared a stable modified glassy carbon electrode based on poly (*p*-aminobenzene sulfonic acid) (*p*-ABSA) film by electrochemical polymerization technique in phosphate buffer solution (PBS) (pH 7.0) and its electrochemical behavior were studied by cyclic voltammetry (CV).

Isoniazid (Laniazid, Nydrazid), also known as isonicotinylhydrazine (INH), is an organic compound that is the first-line medication in prevention and treatment of tuberculosis. Tuberculosis is one of the leading causes of death worldwide. Isonicotinic acid hydrazide (INH), or Pyridine-4-carboxylic acid hydrazide **(scheme. 7.9)**, commercially known as isoniazid (INH), is one of the most important drugs that are widely used in manufacturing pharmaceuticals and agrochemicals along with rifampicin and pyrazinamide in the chemotherapy of the disease [13, 14].

Electropolymerization is a good approach to immobilize polymers to prepare polymer modified electrodes (PMEs) as adjusting the electrochemical parameters can control film thickness, permeation and charge transport characteristics. Polymer-modified electrodes have many advantages in the detection of analytes because of their selectivity, sensitivity and homogeneity in electrochemical deposition, strong adherence to electrode surface and chemical stability of the film [15]. Selectivity of PMEs as a sensor can be attained by different mechanisms such as size exclusion [16] ion exchange [17] hydrophobicity interaction [18] and electrostatic interaction [19, 20]. Carbon paste electrodes have found widespread use in analytical voltammetry and especially carbon paste based microelectrode in brain electrochemistry [21]. The carbon paste has been widely applied in electrochemistry mainly as a substitute for noble metals because depending on the supporting electrolyte it can be used at positive and negative potentials ranging from -1.4 to 1.3 V *vs. the* saturated calomel electrode (SCE) [22, 23].

In present work, poly (INH) film modified carbon paste electrode is used for the selective detection of UA and to study the electrochemical behavior and mechanism of the oxidation of uric acid (UA).The present investigation will also throw some light on the mechanism of conversion of medicinal compounds in biological systems.

7.11. Experimental section

7.11.1.Reagents

Isoniazid (INH) and uric acid (UA) were purchased from Himedia chemicals and all other chemicals were of analytical grade. The electropolymerisation of Isoniazid was performed in 0.2 M phosphate buffer. The phosphate buffer solution was prepared from KH_2PO_4 and K_2HPO_4 and the pH was adjusted with 0.1 N NaOH solution. The stock solution of the uric acid (10 mM) was prepared by dissolving it in NaOH. Other chemicals used were of analytical grade except for spectroscopically pure graphite powder. All Solutions were prepared with doubly distilled water. Freshly prepared UA solution is used prior to measurements.

7.11.2. Apparatus

Electrochemical measurements were carried out with a model-201 electrochemical analyzer (EA-201 chemlink systems) in a conventional three-electrode system. The working electrode was carbon paste electrode, having cavity of 3 mm diameter. The counter electrode was platinum electrode with a saturated calomel electrode (SCE) as a standard reference electrode for completing the circuit.

7.11.3. Preparation of bare carbon paste electrode

The bare carbon paste electrode was prepared by hand mixing of graphite powder 70% and silicon oil 30% in an agate mortar for about 30 min to get homogenous carbon paste. The paste was then packed into the cavity of a Teflon tube electrode (3 mm diameter). Before measurement, the modified electrode was smoothened on a piece of transparent paper to get a uniform, smooth and fresh surface.

7.11.4. Preparation of the Isoniazid (INH) polymer film modified carbon paste electrode

Electrochemical polymerization of isoniazid by using cyclic voltammetric in potential range 500 to 1150 mV at scan rate of 50 mVs^{-1} in phosphate buffer solution (pH 4.0) has been carried out. The monomer concentration was usually 1 mM. After 10 cycles, the surface of the electrode was washed with doubly distilled water to remove the physically adsorbed material. This modified electrode was immersed in PBS (pH 5.0) and electrochemical determination of UA was carried out in a voltammetric cell in the potential range from 100 to 600 mV. The same procedure is applied for all the sample analysis and all electrochemical measurements were carried out at room temperature.

7.12. Result and Discussion

7.12.1. Electropolymerisation of Isoniazid on carbon paste electrode

Carbon paste electrode (CPE) is modified with electropolymerised film of isoniazid (INH). A solution of monomer isoniazid is oxidized to an activated form that polymerizes to form a polymer film directly on the electrode surface. This procedure results in few pinholes since polymerization would be accentuated at exposed (pinholes) sites at the electrode surface. Electro catalysis at a modified electrode is usually an electron transfer reaction between the electrode and solution substrate which, when mediated by an immobilized redox couple (i.e., the mediator), proceeds at a lower over potential than would otherwise occur at the bare electrode and enhances the peak current. Electropolymerisation of isoniazid was fabricated in 0.2 M phosphate buffer solution containing 1 mM isoniazid on CPE. The film was grown on CPE by cyclic voltammetric scans between 500 to 1150 mV. The optimized scan number under the experimental conditions was determined as 10 for reaching the steady response. As shown in **Fig.7.13,** in the first cycle, with the potential scanning from 500 to 1150 mV the anodic peak was observed at 1009 mv corresponding to the oxidation of isoniazid (INH). The peak descended gradually with the increase in cyclic number such decrease indicates the poly (INH) membrane forming and depositing on the surface of the CPE by electropolymerisation. Isoniazid was oxidized to free radical at the surface of CPE rapidly resulting in the possible structure of electropolymerised poly (INH). After polymerization the poly (INH) modified carbon paste electrode was carefully rinsed with distilled water to remove the physically adsorbed material. Then the film electrode was transferred to an electrochemical cell and cyclic voltammetric sweeps were carried out to obtain electrochemical steady state.

7.12.2. Effect of the poly (isoniazid) film thickness on the electrochemical response of uric acid (UA)

The thickness of poly (INH) film could be controlled by the cyclic number of voltammetric scans during the electrochemical modification. The effect of the thickness

of poly (INH) film on the electrochemical response was investigated by cyclic voltammetric technique. The anodic peak current (I_{pa}) response of poly (INH) films increase gradually as the number of cycles increases during film formation from 5 to 10 cycles. Afterwards I_{pa} starts to decrease by increasing the number of cycles which was examined up to 30 cycles **(Fig.7.13a)**. In order to obtain better oxidation peak and higher sensitivity of current for the electrochemical response of uric acid, 10 scans were chosen to control the thickness of the poly (INH) film.

7.12.3. SEM Characterization of poly (isoniazid) film modified carbon paste electrode

Fig.7.14a and **Fig.7.14b** explain the surface morphology of bare CPE and poly (INH) film modified CPE respectively using scanning electron microscope (SEM). The surface of bare CPE was formed by irregularly shaped micrometer-sized flakes of graphite. Whereas modified electrode had a typical uniform arrangement of INH molecules on the surface of CPE [24].

7.12.4. Electrochemical response of potassium ferrocyanide at poly (Isoniazid) modified carbon paste electrode

Fig.7.15 shows the cyclic voltammogram of 0.1mM $K_4[Fe(CN)_6]$ in 0.1M KCl at poly (INH) film modified carbon paste electrode (PINHMCPE). The curve 'a' showed that the redox peak current increased than that at bare carbon paste electrode (BCPE) curve 'b'. At the bare CPE the cyclic voltammograms of $K_4[Fe(CN)_6]$ showed a pair of redox peaks corresponding to the anodic peak at 357 mV potential with peak current of 5.34 µA and the cathodic peak at 284 mV potential with peak current of 3.45 µA. Whereas, poly (INH) film modified carbon paste electrode a pair of redox waves of $K_4[Fe(CN)_6]$ were observed with greatly increase of the peak current. The anodic peak potential was located at 355 mV with peak current of 9.5 µA and the cathodic peak potential at 298 mV with peak current of 6.13 µA respectively. The results of the enhancement of peak current showed excellent catalytic ability of PINHMCPE. The

surface area of bare carbon electrode is 0.0174 cm^2. Whereas effective surface area of the modified electrode was found to be 0.0219 cm^2.

7.12.5. Electrochemical behavior of uric acid at poly (isoniazid) film modified carbon paste electrode

The electrochemical behavior of uric acid (UA) was investigated in 0.2 M phosphate buffer solution of pH 5 at poly (INH) film modified carbon paste electrode (PINHMCPE) using cyclic voltammetric technique. **Fig.7.16.** shows cyclic voltammograms of 1 mM uric acid at bare CPE (curve 'b') and PINHMCPE (curve 'a') The curve 'c' represents the cyclic voltammogram of blank solution at PINHMCPE. Above studies showed that only one oxidation peak at 441 mV potential with peak current 3.28 µA at bare carbon paste electrode, whereas an oxidation peak at 428 mV potential with peak current 20.46 µA at PINHMCPE in the potential range 100 to 600 mV. No reduction peak was observed in the reverse scan, suggesting that the electrochemical reaction is a totally irreversible process and the oxidation peak at the bare CPE is broad due to slow electron transfer, while the response was considerably improved at PINHMCPE and the peak potentials shifted to negative direction, the shape of the peak turns sharper and the peak current increased significantly.

7.12.6. Effect of pH

The electro oxidation of UA was studied at 0.1 mM stock solution over pH range from 2.5 to 8 using 0.2 M phosphate buffer solution at scan rate of 50 mVs^{-1} at PINHMCPE using cyclic voltammetric technique. The oxidation peak current increases with increase of pH from 2.5 to 5 and becomes maximum and peak potential shifted negatively. While pH beyond 5 a great decrease of the oxidation peak current could be observed, then it decreased gradually with the further increase in pH of the solution. **Fig.7.17a** shows the relationship between the anodic peak current and pH of the solution. The oxidation peak potential decrease with increase of pH, **Fig.7.17b** shows the relationship between the anodic peak potential and pH of the solution. A linear

relationship was obtained between the anodic peak potential and pH of the solution in the range 2 - 8. The corresponding linear regression equation is

$$E_{pa}\ (mV) = 652.98 - 45.902\ pH \quad (R = 0.997) \ldots\ldots\ldots\ldots\ldots\ldots\ldots\ (7.10).$$

With a negative slope of 45.902 is close to the theoretical value of 59 mV/pH, which indicating that the number of electrons and protons is equal in the electrochemical oxidation of UA at poly (INH) film modified carbon paste electrode.

7.12.7.Effect of scan rate

Useful information involving electrochemical mechanism usually can be acquired from the relationship between peak current and scan rate. The effect of scan rates on the electrochemical response of 0.1 mM UA at PINHMCPE was studied at different scan rates 25, 50, 75, 100, 125,150, 175, 200, 225 and 250 mVs^{-1}. The corresponding cyclic voltammograms were shown in **Fig.7.18a**. The linearity was obtained for the plot of anodic peak current vs. scan rate with a correlation coefficient of 0.9995 shown in **Fig.7.18b**. However a linear relationship with a correlation coefficient of 0.9916 was also obtained between the anodic peak current and square root of scan rate in the range of 25 - 250 mVs^{-1} as shown in **Fig.7.18c** which indicates that the process is diffusion controlled. The relationship between the anodic peak potential and scan rate can be explained by plotting the anodic peak potentials vs. natural logarithm of scan rate **(Fig.7.18d)** by considering the relation:

$$E_{pa}\ (mV) = 0.02172\ \ln\upsilon + 0.3490 \quad R = 0.99733 \ldots\ldots\ldots\ldots\ldots\ldots\ldots\ (7.11)$$

And the relationship between the anodic peak current and scan rate can be explained by plotting the logarithm of anodic peak current vs. logarithm of scan rate **(Fig.7.18e)** by considering the relation:

$$\log I_{pa}\ (\mu A) = 0.32049\ \log\upsilon + 0.87024 \quad R = 0.9818 \ldots\ldots\ldots\ldots\ldots\ldots\ (7.12)$$

According to Laviron's theory [25] the slope is equal to $RT/\alpha n_{\alpha}F$. As for a totally irreversible electrode reaction on the basis of the above discussion, the n_{α} was

found to be 2.385, which indicated that two electrons were involved in the oxidation process of UA at PINHMCPE. Since the equal number of electron and proton took part in the oxidation of uric acid indicates two electrons and two protons transfer were involved in the electrode reaction process. The electrochemical reaction process for uric acid at PINHMCPE can therefore be summarized as in **scheme 7.10**. From the deduced mechanism of uric acid, an intermediate of a free radical was formed. It may be just the free radical polymerizes and comes into being as insoluble products that deposit on the electrode surface, which agrees with the phenomena of voltammograms recorded from multi-cycles [26].

7.12.8. Calibration of uric acid concentration

A series of uric acid solution 1×10^{-5} to 1×10^{-3} M were prepared to investigate the relationship between the anodic peak current (I_{pa}) and concentration of uric acid at PINHMCPE of a scan rate 50 mVs^{-1}. **Fig.7.19a** shows as the concentration of UA increases the anodic peak current also increases and at higher concentration of UA the potential shifts towards negative direction. The plot of anodic peak current vs. concentration shows linear **Fig.7.19b** and can be described by a linear regression equation:

I_{pa} (μA) = 18.73905 C (10^{-5} M) + 0.18307 R = 0.99442……. (7.13)

The limit of detection (LOD) and limit of quantification (LOQ) were 1.173 μM and 3.910 μM respectively for UA.

The LOD and LOQ were calculated from the peak current using the following equation:

LOD = 3S/M and LOD = 10S/M

Where S is standard deviation and M is the slope of calibration plot.

7.13. Conclusion

- In the present study, a chemically modified poly (INH) film modified carbon paste electrode based on the electropolymerisation has been prepared for the electrochemical determination of uric acid (UA).

- Results showed that the anodic peak current of uric acid (UA) was improved at poly (INH) film modified CPE. The electrochemical response is diffusion controlled and irreversible in nature.

- A linear concentration range was found to occur from 1×10^{-5} to 1×10^{-3} M.

- The probable reaction mechanism involved in the oxidation of uric acid (UA) were also proposed.

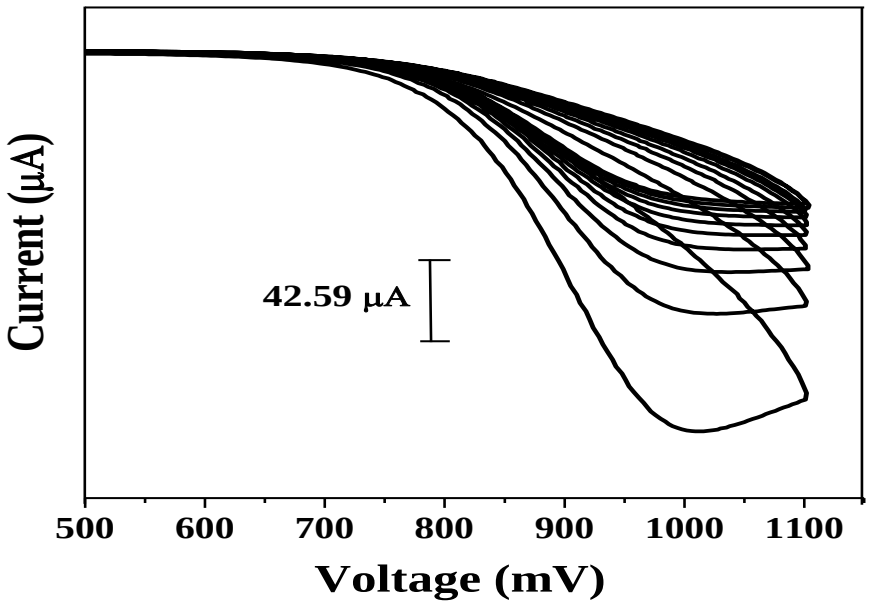

Fig. 7.13: Cyclic voltammograms for the electropolymerisation of 1 mM of isoniazid in 0.2 M phosphate buffer solution on CPE.

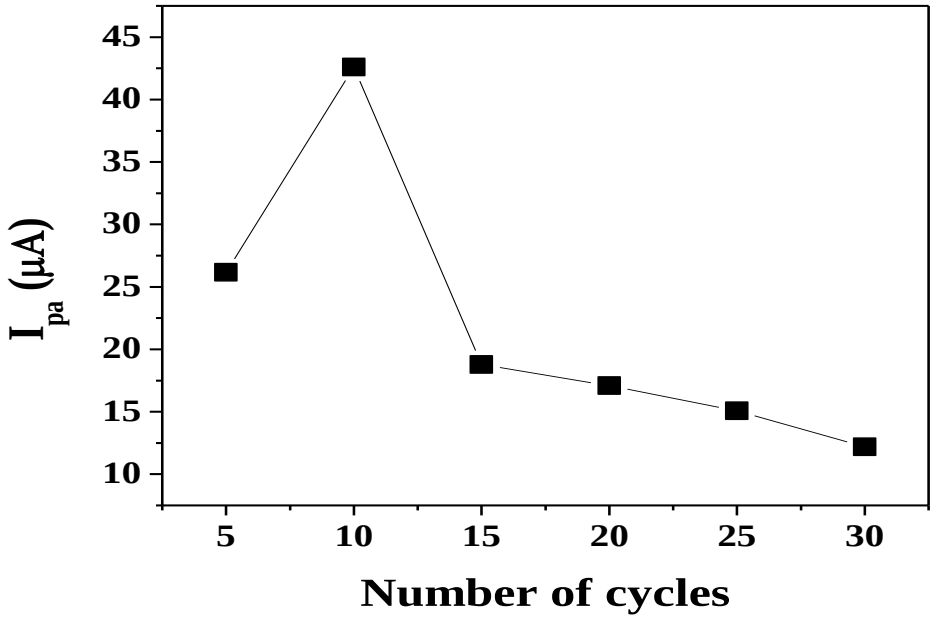

Fig. 7.13a: Anodic peak current v/s. number of cycles of isoniazid.

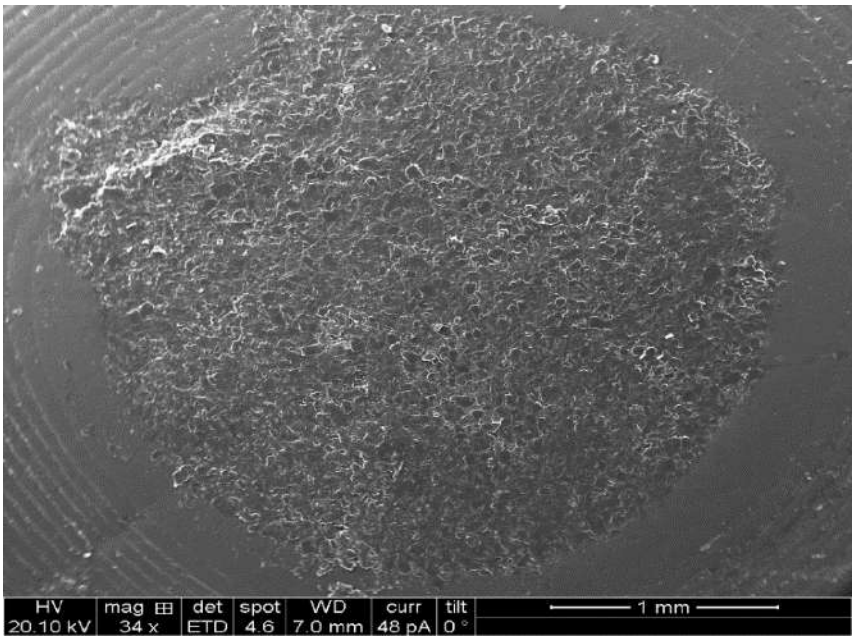

Fig. 7.14a: SEM images of bare carbon paste electrode.

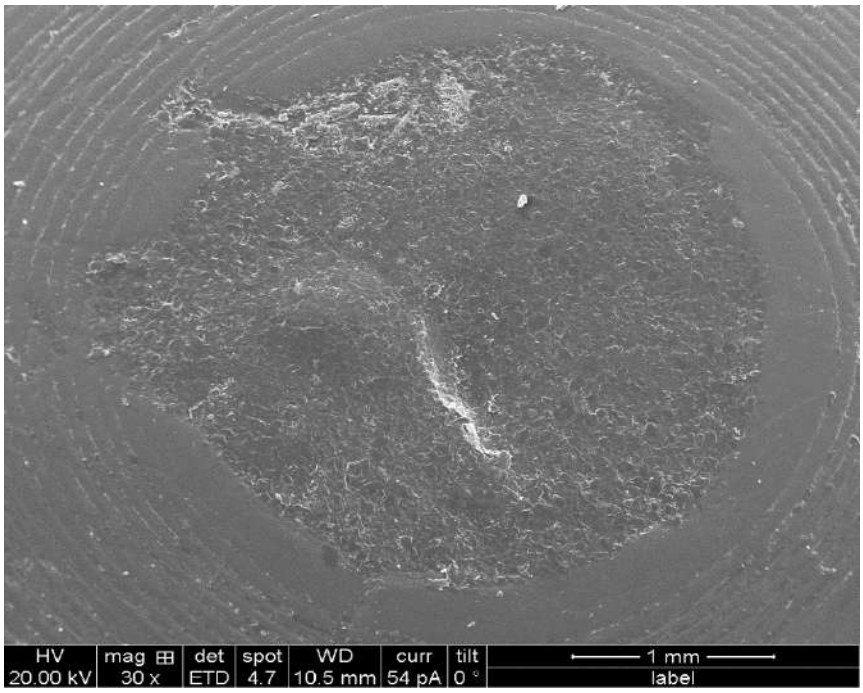

Fig. 7.14b: SEM images of poly (INH) film modified carbon paste electrode.

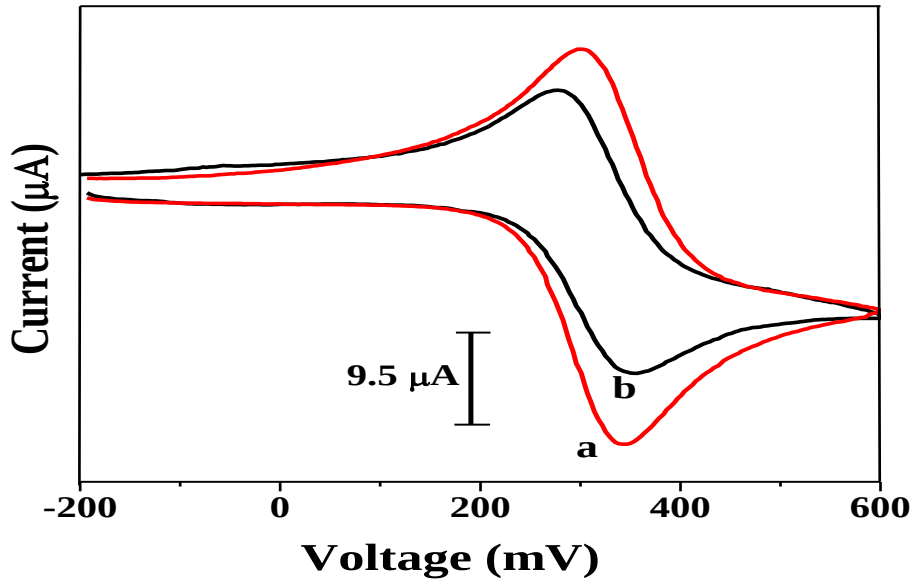

Fig. 7.15: Comparison of 0.1 mM $K_4[Fe(CN)_6]$ in 0.1 M KCl solution at poly (INH) film modified carbon paste electrode (a) and at bare carbon paste electrode (b).

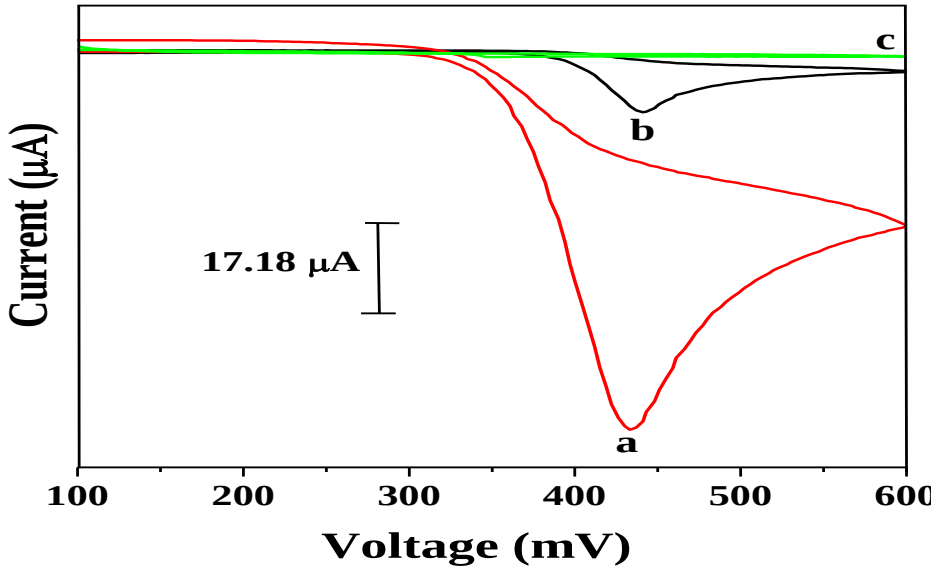

Fig. 7.16: Comparision of 1 mM UA at poly (INH) film modified carbon paste electrode (a), bare carbon paste electrode (b) and blank soluton in phosphate buffer at poly (INH) film modified carbon paste electrode (c), scan rate 50 mVs^{-1}.

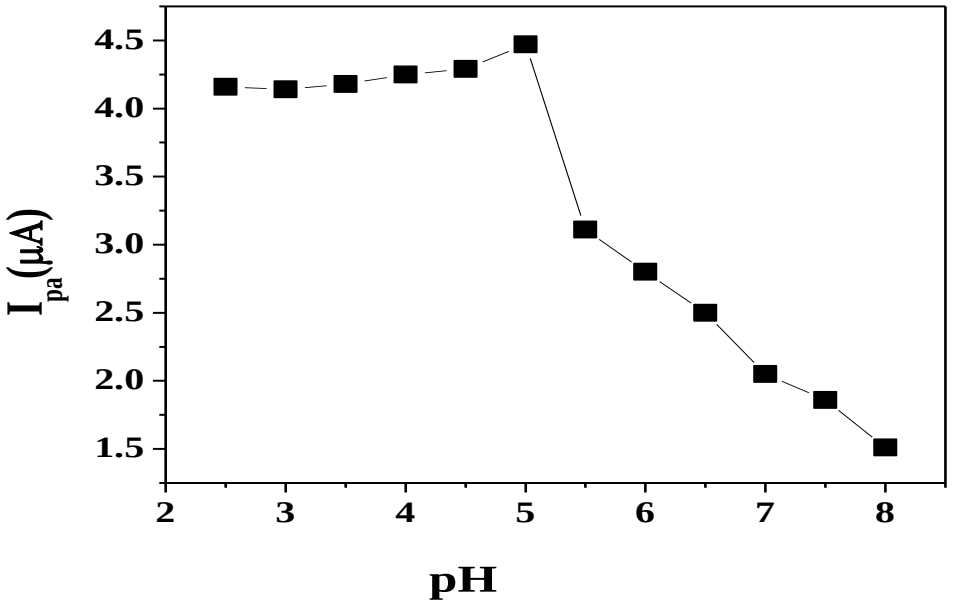

Fig. 7.17a: Plot of anodic peak current vs. pH (2.5 – 8.0) of 0.1 mM UA at poly (INH) film modified carbon paste electrode.

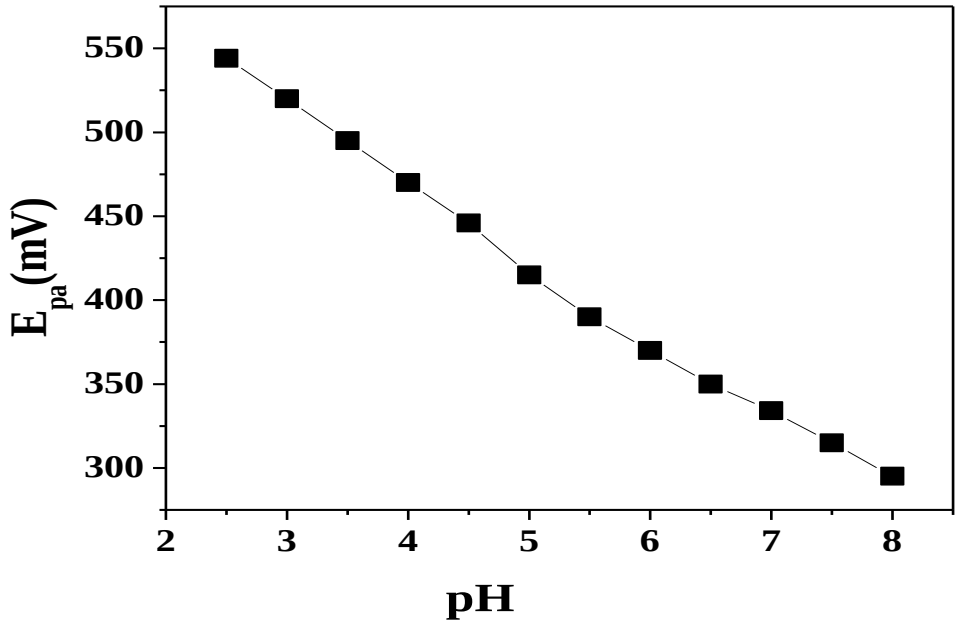

Fig. 7.17b: Plot of anodic peak potential vs. pH (2.5 – 8.0) of 0.1 mM UA at poly (INH) film modified carbon paste electrode.

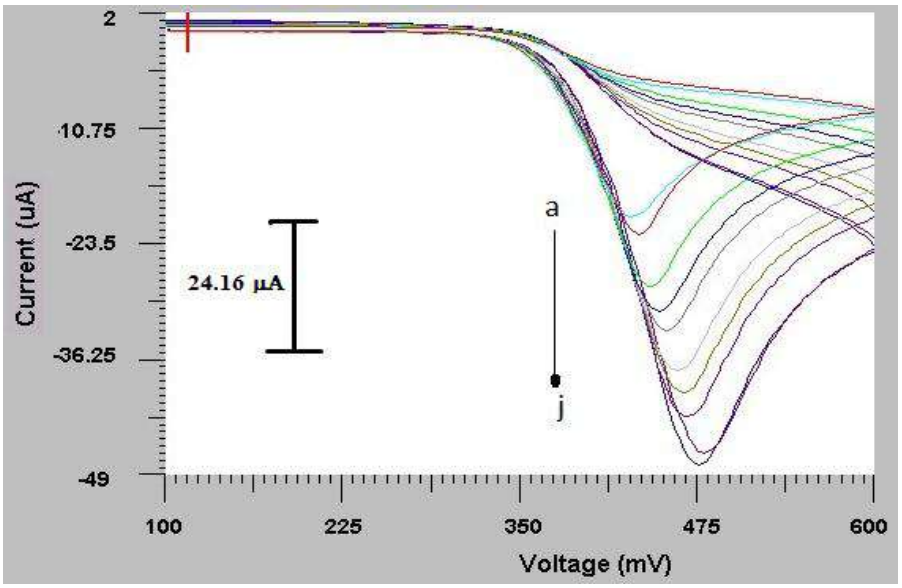

Fig. 7.18a: Cyclic voltammograms of 0.1 mM UA at poly (INH) film modified carbon paste electrode with different scan rates (a) 25, (b) 50, (c) 75, (d) 100, (e) 125, (f) 150, (g) 175, (h) 200, (i) 225, (j) 250 mVs^{-1}.

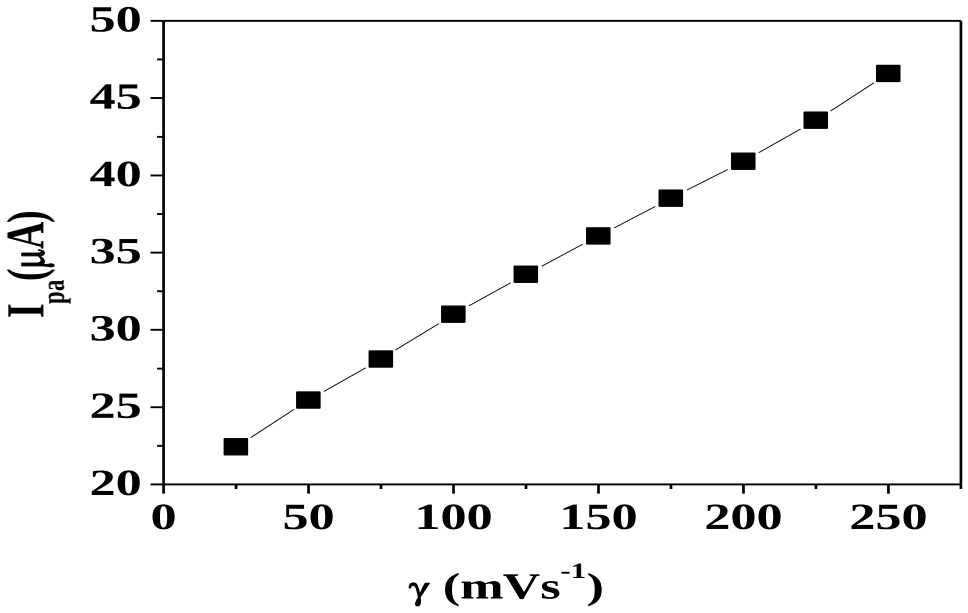

Fig. 7.18b: Plot of anodic peak current vs. scan rates of UA at poly (INH) film modified carbon paste electrode.

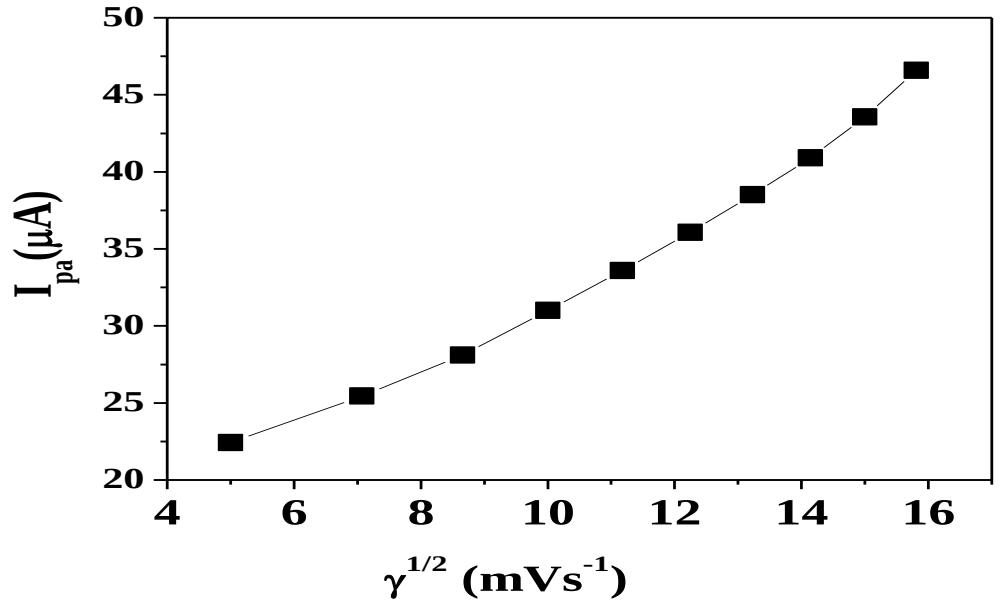

Fig. 7.18c: Plot of anodic peak current vs. square root of scan rates of UA at poly (INH) modified carbon paste electrode.

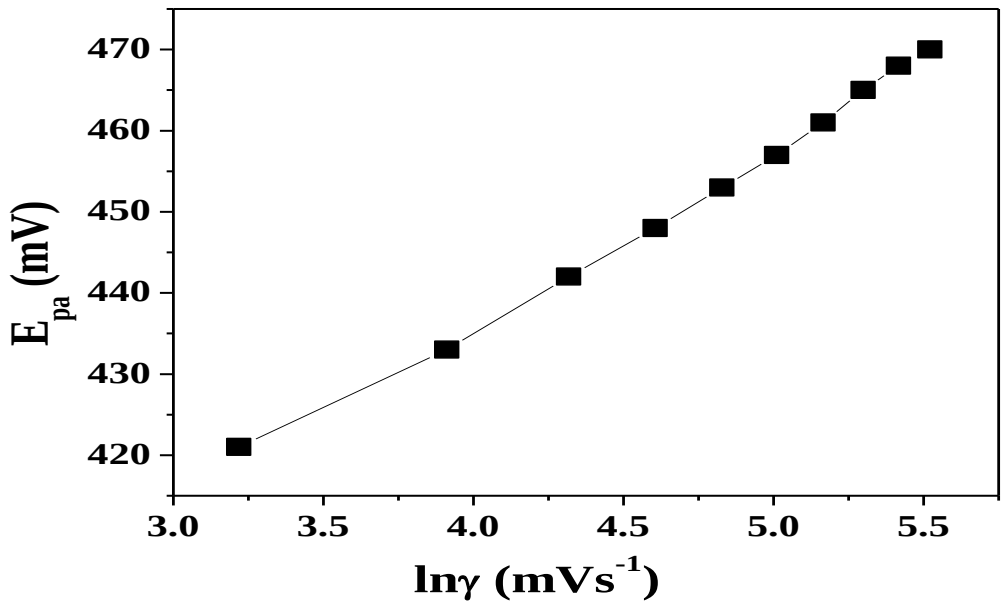

Fig. 7.18d: Plot of anodic peak potential vs. natural logarithm of scan rates of UA at poly (INH) modified carbon paste electrode.

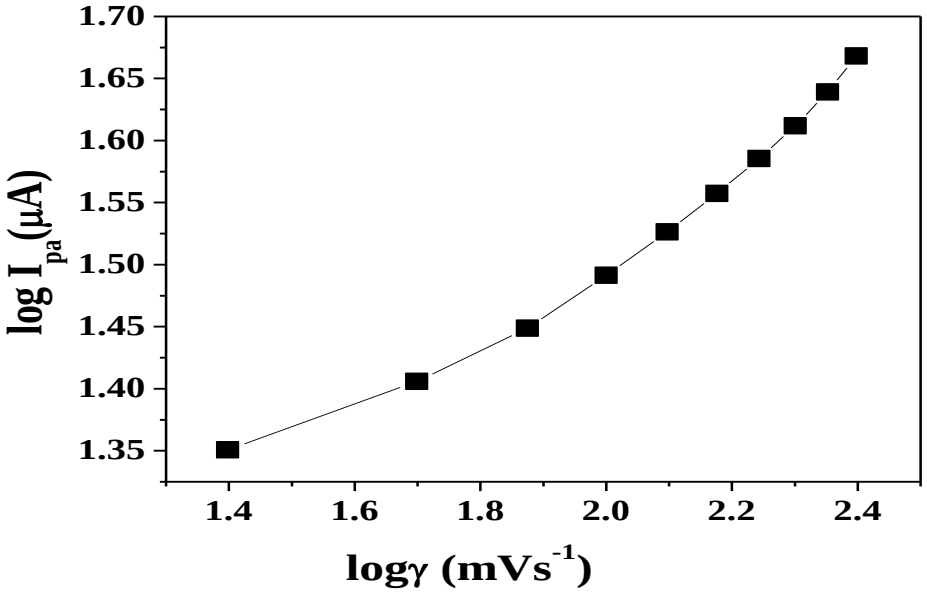

Fig. 7.18e: Plot of logarithm of anodic peak current vs. logarithm of scan rates of UA at poly (INH) film modified carbon paste electrode.

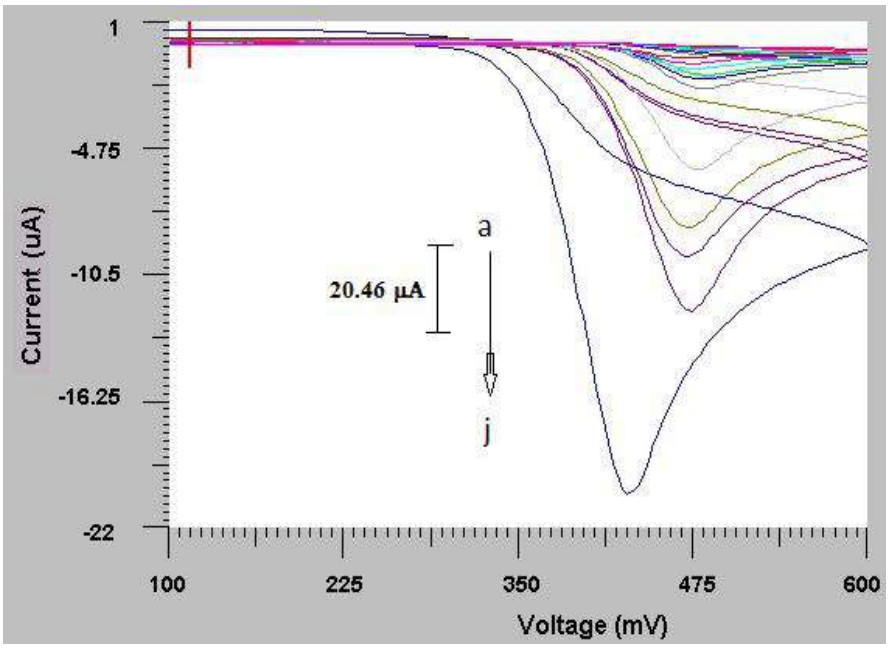

Fig. 7.19a: Effect of variation of concentration of UA (a) 1×10^{-5} M, (b) 2×10^{-5} M, (c) 4×10^{-5} M, (d) 6×10^{-5} M, (e) 8×10^{-5} M, (f) 1×10^{-4} M, (g) 2×10^{-4} M, (h) 4×10^{-4} M, (i) 6×10^{-4} M, (j) 8×10^{-4} M, (k) 1×10^{-3} M on anodic peak current at poly (INH) modified carbon paste electrode; scan rate 50 mVs^{-1}.

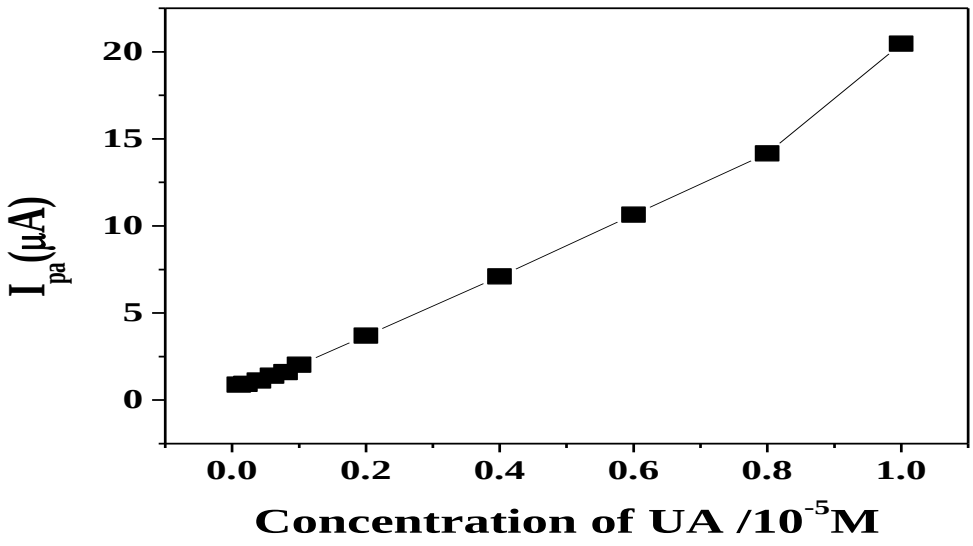

Fig. 7.19b: Plot of anodic peak current vs.UA concentration at poly (INH) film modified carbon paste electrode.

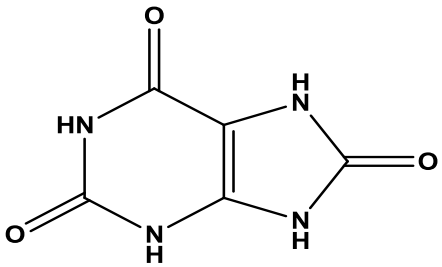

Scheme 7.8: Uric acid.

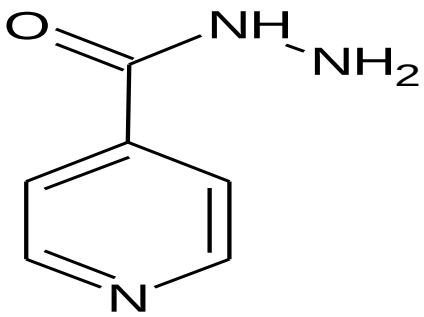

Scheme 7.9. Structure of Isoniazid.

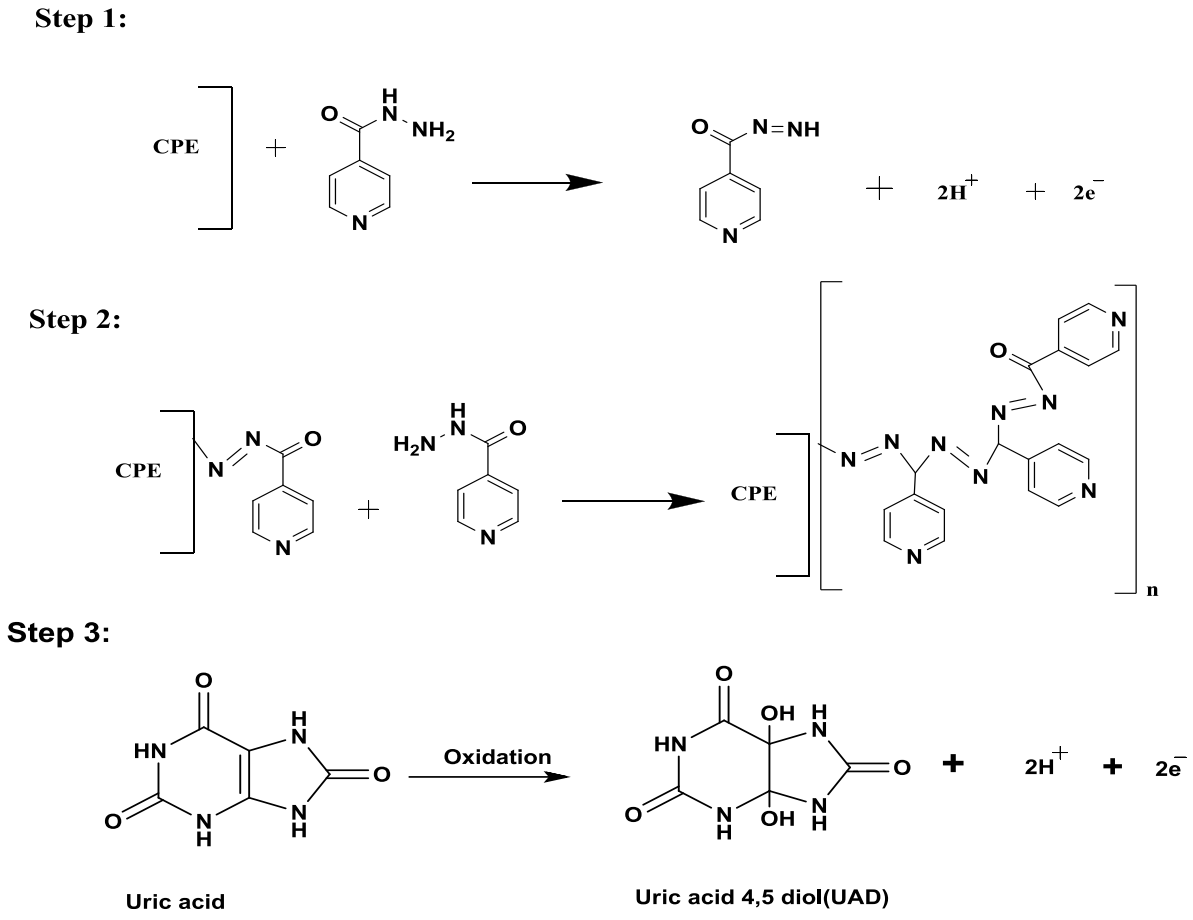

Scheme. 7.9: Probable reaction mechanism of UA on poly (INH) film modified carbon paste electrode.

7.14. References

[1] A.K. Tausche, S. Unger, K. Richter, *Der Internist.*, **47** (2006) 509.

[2] Y.C. Luo, J.S. Do, C.C. Liu, *Biosens. Bioelectron.*, **22 (**2006) 482.

[3] H. Manjunatha, D.H. Nagaraju, G.S. Suresh and T.V. Venkatesha, *Electroanalysis*, **21** (2009) 2198.

[4] S. Behera, C.R. Raj, *Biosens. Bioelectron.*, **23** (2007) 556.

[5] Fu Yong Zhao, Zong Hua Wang, Hui Wang, Rui Zhao and Ming Yu Ding, *Chinese Chemical Letters*, **22** (2011) 342.

[6] Hairul Hisham Hamzah, Zainiharyati Mohd Zain, Nor Lailatul Wahidah Musa, Yun-Chun Lin and Emma Trimbee, *J Anal Bioanal Tech.*, (2013) 2.

[7] R.R. Marquardt, A.T. Ward, L.D. Campbell, *Poult Sci*., **62** (1983) 2099.

[8] A. Hausen, D. Fuchs, K. König and H. Wachter, *Clin Chem.*, **27** (1981) 1455.

[9] T. Kawashima, G.A. Rechnitz, *Anal Chim Acta*, **83** (1976) 9.

[10] M.B.Q. Garcia, J.F.L.C. Lima, M.L. Silva and J.P. Sousa, *Portugaliae Electrochimica Acta*, **22** (2004) 249.

[11] Shengfu Wang, Qiao Xu , Guodong Liu, *Electroanalysis*, **20** (2008) 1116.

[12] Murat sadikoglu, Gamze taskin, Fatma Gül demirtas, Bedrettin selvi and Mustafa barut, *Int. J. Electrochem. Sci.*, **7** (2012) 11550.

[13] B.R. Bloom, C.J.L. Murray, *Science*, **257** (1992) 1055.

[14] M. Wilming, K. Johnsson, *Angew. Chem.*, **38** (1999) 2588.

[15] P.R. Roy, T. Okajima, T. Ohsaka. *Bioelectrochemistry*, **59** (2003) 11.

[16] Xiao-Lin Wen, Yunhua Jia, Li Yang and Zhong-Li Liu, *Talanta,* **53** (2001) 1031.

[17] E. Ekinci, G. Erdogdu, A.E. Karagozler, *J. Appl. Polym. Sci.*, **79** (2001*)* 327.

[18] M. Pontie, C. Gobin, T. Pauporte, F. Bedioui and Devynck, *J, Anal. Chim. Acta*, **411** (2000) 175.

[19] H. Zhao, Y.Z. Zhang, Z.B. Yuan, *Electroanal.*, **14** (2002) 445.

[20] H. Zhao, Y.Z. Zhang, Z.B. Yuan, *Anal. Chim. Acta,* **454** (2002) 75.

[21] R.N. Adams, *Anal.Chem.*, **48** (1976) 1128.

[22] I. Svancara, K. Vyatras, *Anal.Chim.Acta,* **273** (1993) 195.

[23] I. Svancara, M. Pravda, M. Hvizdalova, K. Vytras and Kalcher. *Electroanalysis*, **6** (1994) 663.

[24] C.A. Caro, F. Bedioui, J.H. Zagal, *Electrochim. Acta*, **47** (2002) 1489.

[25] E.J. Laviron's, *Electroanal. Chem.,* **52** *(*1974) 355.

[26] M.B. Deepa, G.P. Mamatha, Y. Arthoba Naik, B.S. Sherigara, S. Manjappa and G. Pradeep, *Int J Phar Chem.*, **2** (2012) 36.